The University Of Sheffield.

The Role of Outer Membrane Proteins of *Porphyromonas gingivalis* in Host-Pathogen Interactions

By:

Kathryn Lucy Naylor

A thesis submitted in partial fulfilment of the requirements for the degree of Doctor of Philosophy

The University of Sheffield
Faculty of Medicine, Dentistry and Health
School of Clinical Dentistry

23 / 08 / 2016

Summary

The keystone periodontal pathogen, *P. gingivalis*, is a Gram-negative oral anaerobe that is strongly implicated as the prime etiological agent in the initiation and progression of periodontal disease. *P. gingivalis* contains a plethora of virulence factors, including fimbriae, proteases, lipopolysaccharides and outer membrane proteins that contribute to the pathogenesis of the disease. The bacterium also displays the ability to interact with host cells through the adherence and invasion both *in vitro* and *in vivo*. In this thesis new light has been shed on the role of the heterotrimeric outer membrane protein A (OmpA). Through the creation of *ompA* mutants and recombinant complementation plasmids, alongside the use of standard antibiotic protection assays in an oral epithelial cell line, this research has demonstrated the importance of OmpA, specifically the OmpA2 subunit, in the invasion of the host and in the ability of the bacteria to form biofilms. Structural analysis of the protein identified extracellular loops, which when synthetic versions were applied to host cells, demonstrated successful interruption of wild-type *P. gingivalis* adherence and invasion of the host, indicating a direct interaction of OmpA2 with oral epithelial cells. In particular, this research demonstrates that OmpA2-loop 4 plays an important role in the interaction with the host through significantly increased binding to host cells when applied to fluorescent latex beads.

This work also characterised the putative periplasmic chaperone protein OmpH, identifying potential proteins that act as clients to this chaperone, including OmpA. Through the creation of an *ompH1H2* knock out mutant, enzymatic analysis of various virulence factors was assessed, demonstrating a loss of gingipain activity, whilst also identifying a loss of membrane stability through the observation of an increase in outer membrane vesicle formation. Evidence is also presented for the role of OmpH protein in chaperoning OmpA across the periplasm to the outer membrane and this work has opened up the potential for novel work identifying other clients of this chaperone system.

Overall, the work in this thesis has demonstrated that the OmpA protein, specifically OmpA2, is directly involved in the interaction with host oral epithelial cells and in biofilm formation, specifically demonstrating the direct role of the extracellular surface loops in this interaction. This work also hypothesises a role for the OmpH protein in chaperoning outer membrane proteins, with the identification of potential clients, such as OmpA and the gingipains. Finally, this work has developed an improved mutagenesis technique for the creation of *P. gingivalis* mutants based on a modified natural competence method.

Acknowledgments

First and foremost, I would like to thank The University of Sheffield for both providing me with this opportunity as well as the funding to go with it. Also thanks are given to the external funding from the Oral and Dental Research Trust, and the Microbiology Society.

Special thanks and appreciation go to my supervisor, Dr Graham Stafford for his continuous support, encouragement and motivation. I have greatly benefited from his advice, guidance and unfaltering confidence in me, without which this work would not have been possible. I would also like to thank my supporting supervisors, Professor Ian Douglas and Dr Craig Murdoch, for the academic help and support. I would like to also give thanks to the kind donations of antibodies from Dr Keiji Nagano and Professor Ashu Sharma.

Thanks go to the technical support staff, Jason Heath and Brenka McCabe, who work tirelessly behind the scenes and without whom the lab would be absolute chaos. Thank you to you both for providing a friendly environment that has been a pleasure to work in. Also thanks to David Thompson for your technical expertise in electron microscopy.

I would like to thank particularly the current and previous folk of the Dental School and MBB for all the good times and friendship throughout my time here. Special thanks to Genevieve, Ellie, Caroline, Viki, Sarah, Andy, Mark, Laura and Serina who have provided me with all the encouragement and support, multiple delicious dinners with copious amounts of wine and chocolate to get me through the tough times. I'm sure together, we have managed to keep many Prosecco vineyards afloat throughout the years. You guys are the best!

I am so grateful for my amazing family during this time, to listen to me babble on about science things that go above their heads, providing excellent words of encouragement when I whinge about insoluble proteins and failed Western blots even if they don't understand what these are. And I can't forget to say thanks to the Bank of Mum and Dad for the financial support when my PhD funding finished but my experiments hadn't!

Finally and most importantly, I would like to mention my favourites, Liz, Charlotte and Aidan. There aren't words adequate enough to describe how much you guys have meant to me during this PhD and thesis writing (and all the years before!), for all the love and support you guys have given me through all of the good times and the bad. As much as I hate using the word, I *literally* could not have done this without you guys. Much love.

List of Abbreviations

A-LPS – A-antigen lipopolysaccharide

Amp – ampicillin

APS – ammonium persulphate

ATCC – American Type Culture Collection

BA – blood agar plates

BHI – brain heart infusion

BSA – bovine serum albumin

CFU – colony forming units

CIP – calf alkaline phosphatase

c-JNK – c-Jun N-terminal kinase

CPS - capsular polysaccharide

CR3 – complement receptor 3

CTD – C-terminal domain

CY – cytoplasm

DKSFM – defined keratinocyte serum free media

DMEM – Dulbecco's modified Eagle's medium

DTT - dithiothreitol

EC - extracellular

ECM – extracellular matrix

eDNA – extracellular DNA

EDTA – ethlenediaminetetraacetic acid

EPEC – enteropathogenic *E. coli*

EPS – extracellular polysaccharide

Ery – Erythromycin

FA – fastidious anaerobic agar

FAK – focal adhesion kinase

FBS – foetal bovine serum

GST – Glutathione-S-transferase

HAART – highly active antiretroviral therapy

HagA – Haemagglutinin A

IL – interleukin

IM – inner membrane

IMAC – immobilised metal-ion affinity chromatography

IPTG – isopropyl β-D-1-thiogalactopyranoside

Kgp – Lysine-specific gingipain

LB – Luria broth

LPS – lipopolysaccharide

MBP – maltose binding protein

MOI – multiplicity of infection

Msp – major outer sheath protein

mTOR – mammalian target of rapamycin

MTP – microtitre plate

MUNANAC – 2'-(4-Methylumbelliferyl)-α-D-*N*-acetylneuraminic acid

NAM – N-acetylmuramic acid

NC - nitrocellulose

NETs – neutrophil extracellular traps

NUG – necrotising ulcerative gingivitis

NUP – necrotising ulcerative periodontitis

OD – optical density

O-LPS – O-antigen lipopolysaccharide

OMP – outer membrane protein

OmpA – outer membrane protein A

OmpH – outer membrane protein H

OMVs – outer membrane vesicles

OppA – oligopeptide transporter

P - pellet

PADs –peptidyl-arginine deaminase

PAMPs – pathogen-associated molecular patterns

PBS – phosphate buffered saline

PCR – polymerase chain reaction

PG - peptidoglycan

PorSS – Por secretion system

PP - periplasm

PPADs – *P. gingivalis* peptidyl-arginine deaminase

PRR – pattern recognition receptor

Rgp – Arginine-specific gingipain

S - Secreted (gingipains)

S - Soluble (dialysis)

S-layer – surface layer

SD – standard deviation

SDS-PAGE – Sodium dodecyl sulphate polyacrylamide gel electrophoresis

SEM – standard error of the mean

Skp – Seventeen kilodalton protein

T9SS – Type 9 secretion system (PorSS)

TAE – tris-acetate EDTA

TEM – transmission electron microscopy

Tet – tetracycline

Tir – translocated intimin receptor

TLCK – *N*-α-tosyl-L-phenylalanine chloromethyl ketone

TLRs – Toll-like Receptors

TNF – Tumour necrosis factor

TO – thiazole orange

TPCK – *N*-α-p-tosyl-L-lysine chloromethyl ketone

TRPS – tuneable Resistance Pulse Sensing

TRX – thioredoxin

TTSS – Type 3 secretion system

Ub - ubiquitin

WC – whole cell

WGA – wheat germ agglutinin

WHO – World Health Organisation

WT – wild-type

Table of contents

Summary 1
Acknowledgments 2
List of Abbreviations 3
Table of contents 7
List of Figures 12
List of Tables 15
Chapter 1 16
Introduction and Literature Review 16
1.1 Overview of Periodontal Disease 17
1.2 Periodontitis: The clinical setting 18
1.3 Links to other diseases 21
1.3.1 Diabetes 21
1.3.2 Heart Disease 22
1.3.3 Pre-term Birth 24
1.3.4 HIV/AIDS 24
1.3.5 Periodontal disease and arthritis 25
1.3.6 Periodontal disease and cancer 26
1.4 Factors Affecting Periodontitis 27
1.4.1 Periodontitis and ageing 27
1.4.2 Influence of host-genetics 27
1.4.3 Modifiable risk factors 28
1.4.4 The role of innate immunity at the host-pathogen interface 29
1.4.5 Genetic considerations in periodontal disease 30
1.5 Aetiology of Periodontitis 31
1.6 Microbiology of periodontitis 32
1.6.1 Subgingival Plaque and Biofilm formation 33
1.6.2 Microbial Complexes Involved in Periodontitis 37
1.6.2.1 The Red Complex 39
1.6.3 *Treponema denticola* 40
1.6.4 *Tannerella forsythia* 41
1.6.5 *Porphyromonas gingivalis* 42
1.6.6 Virulence Factors of *P. gingivalis* 43
1.6.6.1 Capsular Polysaccharide 43
1.6.6.2 Lipopolysaccharide 44
1.6.6.3 Attachment & Invasion 45
1.6.6.4 Adherence and Invasion of *P. gingivalis* 46
1.6.6.4.1 Fimbriae 46
1.6.6.4.2 Gingipains 48
1.6.6.4.3 Haemagglutinins 51
1.6.6.4.4 Sialidases 51
1.6.7 Effects on the immune system: the oral context. 52
1.6.8 Intracellular spreading of *P. gingivalis* 54
1.6.9 The Gram-negative outer membrane 57

1.6.10 Outer membrane of *P. gingivalis* 58
1.6.11 The OmpA protein in Gram-negative bacteria 59
1.6.12 OmpA in *P. gingivalis* 61
1.6.13 The OmpH protein 63
1.6.14 OmpH in *P. gingivalis* 65
1.7 Aims 66
1.7.1 Specific Aims of the project 66
Chapter 2 68
Materials and Methods 68
2.1 Manufacturers and Suppliers 69
2.2 Main Buffers and Reagents 70
2.2.1 Phosphate Buffered Saline 70
2.2.2 Crystal Violet Stain 70
2.2.3 Protein Purification Elution Buffer 70
2.3 Bacterial Strains, plasmids and primers used in this study 70
2.4 Bacterial Cell Culture 77
2.4.1 Antibiotics 77
2.4.2 Bacterial culture 78
2.4.3 Long term storage of Bacteria 78
2.5 Epithelial Cell Lines and Growth 78
2.5.1 Epithelial cell line 78
2.5.2 Epithelial Cell Culture 79
2.5.3 Growth Media 79
2.5.4 Defrosting Mammalian Cells 79
2.5.6 Cell Passaging 79
2.6 Molecular biology methods 80
2.6.1 Bacterial chromosomal DNA Isolation 80
2.6.2 DNA analysis 80
2.6.2.1 Tris-Acetate-EDTA Buffer 80
2.6.2.2 Agarose gel analysis 80
2.6.2.3 Polymerase Chain Reaction 81
2.6.2.4 Overlap PCR for ompA1 and A2 gene knockout cassette amplification 83
2.6.2.5 DNA Extraction from Agarose Gel 83
2.6.2.6 Restriction Enzyme Digest & Ligation 84
2.6.3 Preparation of *E. coli* for Electroporation and Cloning 85
2.6.4 Preparation of *P. gingivalis* for Electroporation and Cloning 86
2.6.5 *P. gingivalis* Transformation Using Natural Competency 87
2.6.5.1 Plate-based *P. gingivalis* transformation 87
2.6.5.2 Liquid-based *P. gingivalis* transformation 88
2.6.6 Complementation of Δ*ompA2* 88
2.7 Protein Methods 89
2.7.1 Protein Purification 89
2.7.1.1 Overexpression of Protein & Cell Free Extract Preparation 89
2.7.1.2 His-tagged protein purification using affinity column 89
2.7.1.3 GST-tagged protein purification using affinity column 90

2.7.2 Purified protein analysis 90
2.7.3 Sodium Dodecyl Sulphate Polyacrylamide Gel Electrophoresis 91
2.7.3.1 SDS-PAGE buffers 91
2.7.3.1.1 SDS-PAGE Upper and Lower Tris 91
2.7.3.1.2 SDS-PAGE Running Buffer 91
2.7.3.1.3 2X SDS Loading Buffer 91
2.7.3.1.4 SDS-PAGE Destain Buffer 91
2.7.3.2 SDS-PAGE gel analysis 91
2.7.3.3 Silver staining of proteins in polyacrylamide gels 93
2.7.4 Western Blot 93
2.7.4.1 Western blot general buffers 93
2.7.4.1.1 Semi-Dry Transfer Buffer 93
2.7.4.1.2 blocking buffer 93
2.7.4.2 Antibodies 93
2.7.4.3 Protein analysis using Western blot 94
2.7.5 Outer Membrane Protein fraction preparation 95
2.8 Phenotypic Characterisation methods 95
2.8.1 Antibiotic Protection Assay 95
2.8.2 Antibiotic Protection Assay in the Presence of Peptides 96
2.8.3 Fluorescence binding assay of extracellular peptide loops to OK-F6 monolayers 96
2.8.4 Biofilm Formation Assay 97
2.8.5 Electron Microscopy 98
2.8.5.1 Sample Processing for Sectioning 98
2.8.5.2 Staining of electron microscope grids 99
2.8.9 Proteinase Activity Assays 99
2.8.9.1 Colorimetric Assays 100
2.8.9.2 Fluorometric Proteinase Assay 100
2.8.9.3 Sialidase Assay 101
2.8.9.4 Membrane Permeability Assay 101
2.8.9.10 Outer Membrane Vesicle Quantification 102
2.9 Statistical Analysis 102
Chapter 3 103
Role of the *ompA* Gene Cluster in Host-Cell Interactions and Biofilm Formation 103
3.1 Introduction 104
3.2 Aims 105
3.3 Results 105
3.3.1 Basic bioinformatic analysis of the *ompA* genes 105
3.3.2 Generation of Δ*ompA1* and Δ*ompA2* mutants 106
3.3.2.1 Characterisation of the OM profile of Δ*ompA* mutants 113
3.3.3 Phenotypic analysis of *P. gingivalis* wild-type and Δ*ompA* mutants 114
3.3.3.1 Visualisation of bacterial cells through transmission electron microscopy. 114
3.3.3.2 Assessment of outer membrane vesicle formation 117
3.3.3.3 Assessment of gingipain activity 119
3.3.3.4 Assessment of sialidase activity 121
3.3.3.5 Biofilm assay of *P. gingivalis* wild-type and Δ*ompA* mutants 122

3.3.4 Generation of an Δ*ompA2* + pT-COW-*A2* complement mutant 124
3.3.5 Biofilm assay of Δ*ompA2* complemented strain 127
3.3.6 Detection of major fimbriae (FimA) on outer membrane fractions of *P. gingivalis* wild-type and Δ*ompA* mutants. 128
3.3.7 OmpA-host cell interaction 131
3.3.7.1 Antibiotic protection assay of *P. gingivalis* wild-type and Δ*ompA* mutants 131
3.3.7.2 Viability of mutants during standard antibiotic protection assay 135
3.4 Discussion 136
3.4.1 Phenotypic characterisation of *P. gingivalis* and Δ*ompA* mutants 137
3.4.2 Enzymatic activity profiling of mutant strains indicate *ompA2* specific phenotypes 140
3.4.3 Biofilm formation by *P. gingivalis* and Δ*ompA* mutants 141
3.4.4 *P. gingivalis* invasion and adhesion of oral epithelial cells 142
3.5 Summary 144
Chapter 4 145
Molecular mechanism of OmpA interaction with host epithelial cells 145
4.1 Introduction 146
4.2 Aims 146
4.3 Results 147
4.3.1 OmpA1 and OmpA2 Protein Overexpression 147
4.3.1.1 His-tag Protein Purification 147
4.3.1.2 GST-tagged Protein Purification 150
4.3.2 GST-tagged OmpA2 interaction with oral epithelial cells 155
4.3.3 Investigation into increasing protein solubility 157
4.3.4 Investigation of OmpA dialysis 158
4.3.5 OmpA Protein Structure Prediction 161
4.3.6 Barrel overexpression 162
4.3.7 Identification of Extracellular Protein Loops of OmpA2 168
4.3.8 Analysis of the extracellular loops of *P. gingivalis* OmpA2 interactions with oral epithelial cells 171
4.3.9 Peptide-Coating of Microspheres Directs Interaction with Oral Epithelial Cells 177
4.3.10 Immunofluorescence of OmpA2 Extracellular Loops Interaction with Oral Epithelial cells 178
4.4 Discussion 180
4.5 Summary 188
Chapter 5 189
Preliminary characterisation of the putative OmpH/Skp locus of *P. gingivalis* 189
5.1 Introduction 190
5.2 Aims 194
5.3 Results 195
5.3.1 Bioinformatic Analysis of OmpH 195
5.3.2 Generation of *ompH1H2* mutant 197
5.3.3 Morphological analysis of Δ*ompH1H2* 201
5.3.4 Protein profiling of the Δ*ompH1H2* mutant 204

5.3.5 Assessment of the integrity of the outer membrane in the Δ*ompH1H2* mutant: Imaging and Vesicle Counts 206
5.3.6 Assessment of the integrity of the outer membrane in the Δ*ompH1H2* mutant: assessment of permeability using a fluorescent dye. 209
5.3.7 Assessment of virulence factor production in the Δ*ompH1H2* mutant 211
5.3.8 Assessment of general virulence of the Δ*ompH1H2* mutant 213
5.4 Discussion 215
5.5 Summary 222
Chapter 6 223
Discussion & Future Prospects 223
6.1 Summary of major findings 224
6.1.1 Chapter 3: Role of the *ompA* gene cluster in host-cell interactions and biofilm formation 224
6.1.2 Chapter 4: Molecular mechanism of OmpA interaction with host epithelial cells. 226
6.1.3 Chapter 5: Preliminary characterisation of the putative OmpH/Skp locus of *P. gingivalis.* 227
6.2 Host cell interaction of *P. gingivalis* with human cells: OmpA surface loops at the host-interface 229
6.3 Periodontal disease: A targeted approach? 230
6.4 The role of OmpH chaperone: implications for surface proteome involvement in *P. gingivalis* biology 232
6.5 Conclusion 234
References 237
Appendix 286
Appendix I 286

List of Figures

Figure 1.1 Schematic demonstrating the healthy and diseased periodontium.....18
Figure 1.2 The six major stages of periodontal disease progression.....19
Figure 1.3 The critical pathway model.....20
Figure 1.4 Oral biofilm formation.....35
Figure 1.5 The major complexes of bacteria found in the periodontal cavity.....38
Figure 1.6 Electron microscopy of *P. gingivalis* indicating the presence of Fimbriae.....47
Figure 1.7 Summary of the secretion of the gingipains via PorSS.....50
Figure 1.8 Schematic of the invasive population of *P. gingivalis.*.....55
Figure 1.9 Schematic of the typical cell membrane of a Gram-negative cell.....57
Figure 1.10 The predicted structure of OmpA.....58
Figure 1.11 The *ompA* operon of *P. gingivalis.*.....62
Figure 3.1 Schematic representation of the *ompA* operon in the *P. gingivalis* chromosome.....105
Figure 3.2 Protein sequence alignments between *E. coli* OmpA and *P. gingivalis* OmpA1 and OmpA2.....106
Figure 3.3 Overlap Extension PCR and Allelic Exchange for *P. gingivalis ompA* mutant production.....107
Figure 3.4 PCR Amplification of *ompA1* and *ompA2* flanking regions and *ery*^{R} cassette for gene knock out (A) and combined constructs for transformation (B).....108
Figure 3.5 Schematic demonstrating primer pair locations for knock out mutagenesis PCR confirmation.....110
Figure 3.6 Confirmation of Δ*ompA1* and Δ*ompA2* mutant generation through colony PCR.....111
Figure 3.7 Silver staining assessment of the outer membrane of wild-type *P. gingivalis* and respective Δ*ompA* mutants.....113
Figure 3.8 Western blotting detection of OmpA protein in outer membrane preparations.....114
Figure 3.9 TEM Imaging of wild-type and Δ*ompA* mutant strains of *P. gingivalis*.....116
Figure 3.10 Vesicle formation by wild-type *P. gingivalis* and Δ*ompA* mutants.....118
Figure 3.11 Whole cell and secreted gingipain activity of wild-type *P. gingivalis* and Δ*ompA* mutants.....120
Figure 3.12 Sialidase Activity of wild-type *P. gingivalis* and Δ*ompA* mutants.....121
Figure 3.13 Biofilm formation *in vitro* of *P. gingivalis* and mutant Δ*ompA* strains.....123
Figure 3.14 Quantification of biofilm formation of Δ*ompA* mutants.....123
Figure 3.15 pT-COW plasmid map.....125
Figure 3.16 Agarose analysis of the construction of the *ompA2* complementation construct.....126
Figure 3.17 Confirmation of the *ompA2* complementation insert in pT-COW.....127
Figure 3.18 Quantification of biofilm formation in the Δ*ompA2* complement strain.....128
Figure 3.19 Cell membrane fractionation and detection of FimA subunits in *P. gingivalis* wild-type and *ompA* mutants.....130

Figure 3.20 Bacterial adhesion and invasion of oral epithelial cells by *P. gingivalis* wild-type and Δ*ompA* mutants.....133
Figure 3.21 Bacterial adhesion and invasion of oral epithelial cells by wild-type *P. gingivalis*, Δ*ompA2* mutant and Δ*ompA2* mutant complement.....135
Figure 3.22 Viability of *P. gingivalis* wild-type and mutant strains throughout the standard antibiotic protection assay.....136
Figure 4.1 SDS-PAGE showing the overexpression of the OmpA1 (A) and OmpA2 (B) protein subunits.....148
Figure 4.2 SDS-PAGE Analysis of the Purification Profile of His-OmpA1 (A) and His-OmpA2 (B) After Urea Solubilisation.....149
Figure 4.3 SDS-PAGE Analysis of the Dialysis of His-OmpA1 and His-OmpA2.....150
Figure 4.4 Cloning of *ompA1* and *ompA2* for GST-tagged protein overexpression.....151
Figure 4.5 SDS-PAGE Analysis of GST-OmpA1 and GST-OmpA2 protein expression at 37°C (A) and ~24°C (B).....152
Figure 4.6 SDS-PAGE Analysis of GST-OmpA1 and –A2 Overexpression (A) and Insoluble and Soluble Cell Lysis Fractions (B).....153
Figure 4.7 GST-tagged purification of OmpA1 (A) and OmpA2 (B).....154
Figure 4.8 Dialysis of purified GST-OmpA1 (A) and GST-OmpA2 (B).....155
Figure 4.9 GST-Tagged OmpA2 protein applied to OK-F6 cells, epithelial cell membranes stained with CellMask™ Plasma Membrane Stain (A) or Wheat Germ Agglutinin-Texas Red® (B).....156
Figure 4.10 Purification Profile of His-OmpA2.....159
Figure 4.11 Dialysis Trials of His-OmpA1 (A) and His-OmpA2 (B) protein after purification.....160
Figure 4.12 *In silico* Analysis of OmpA1 and OmpA2 Protein Structure.....161
Figure 4.13 Schematic of full OmpA1 /A2 protein and truncated versions for recombinant protein overexpression of the β-barrel.....163
Figure 4.14 Cloning of truncated $OmpA1_{21-245}$ and $OmpA2_{22-236}$ into pET15 plasmid for His-tagged Expression.....164
Figure 4.15 Overexpression of His-$OmpA1_{21-245}$ (A) and His-$OmpA2_{22-236}$ (B) in different expression strains.....165
Figure 4.16 Overexpression of His-$OmpA1_{21-245}$ (A) and His-$OmpA2_{22-236}$ (B) at different induction temperatures.....166
Figure 4.17 Purification of His-$OmpA1_{21-245}$ (A) and His-$OmpA2_{22-236}$ (B) protein.....167
Figure 4.18 Dialysed His-$OmpA1_{21-245}$ and His-$OmpA2_{22-236}$ after purification.....168
Figure 4.19 *In silico* analysis of the OmpA2 protein and identification of extracellular loops.....169
Figure 4.20 Bioinformatic analysis of *P. gingivalis* OmpA structure.....170
Figure 4.21 Effect of a pre-incubation of OmpA2 extracellular loops on adherence and invasion of wild type *P. gingivalis*.....172
Figure 4.22 Effect of the presence of extracellular loops throughout the standard antibiotic protection assay.....173
Figure 4.23 Standard antibiotic protection assay in the presence of combined peptides.....174

Figure 4.24 Comparison of peptide 4 and scrambled peptide on adherence and invasion of oral epithelial cells.....175
Figure 4.25 Viability of OK-F6 and *P. gingivalis* in the presence of the peptides.....176
Figure 4.26 Fluorescence determination of peptide-coated Microspheres bound to OK-F6 cells.....177
Figure 4.27 Immunofluorescence imaging of peptide-bound microspheres interaction with oral epithelial cells.....179
Figure 4.28 Enumerated peptide-coated microspheres interaction with OK-F6 cells.....180
Figure 5.1 Schematic representation of the OmpH chaperone delivery of protein to the Bam complex.....191
Figure 5.2 Location of the *ompH1* and *ompH2* genes in the *P. gingivalis* genome.....195
Figure 5.3 Alignment of *E. coli* Skp with *P. gingivalis* OmpH1 and H2 proteins.....195
Figure 5.4 Protein structure prediction of *P. gingivalis* OmpH1, OmpH2 and *E. coli* Skp...196
Figure 5.5 Schematic representation of the optimisation of *P. gingivalis* transformation methods.....199
Figure 5.6 PCR analysis of the generation of a Δ*ompH1H2* mutant.....201
Figure 5.7 Δ*ompH1H2* mutant morphology.....202
Figure 5.8 Time lapse of growth of *P. gingivalis* wild-type and Δ*ompH1H2* mutant.....203
Figure 5.9 SDS-PAGE analysis of purified outer membranes of wild-type and Δ*ompH1H2 P. gingivalis*.....204
Figure 5.10 SDS-PAGE (A) and anti-OmpA Western blot (B) of outer membrane preparations from wild-type *P. gingivalis* and Δ*ompA* and Δ*ompH* mutants.....206
Figure 5.11 *P. gingivalis* wild-type and Δ*ompH1H2* membrane morphology assessed via TEM imaging.....207
Figure 5.12 Assessment of OMVs of *P. gingivalis* wild-type and Δ*ompH1H2* mutant.....208
Figure 5.13 Membrane integrity assay using Thiazole Orange.....210
Figure 5.14 Sialidase activity of wild-type and Δ*ompH1H2 P. gingivalis*.....211
Figure 5.15 Whole cell Rgp and Kgp gingipain activity of wild-type and Δ*ompH1H2 P. gingivalis*.....212
Figure 5.16 Standard antibiotic protection assay of wild-type *P. gingivalis* and Δ*ompH1H2* mutant.....213
Figure 5.17 Biofilm formation of wild-type *P. gingivalis* and the Δ*ompH1H2* mutant.....215
Figure 6.1 Schematic diagram representing the surface proteins of *P. gingivalis* and their interactions with the host epithelial cell.....235

List of Tables

Table 1.1 Regulated genes in the signature gene set.....56
Table 2.1 Main Manufacturers and Suppliers.....70
Table 2.2 *P. gingivalis* strains.....71
Table 2.3 *E. coli* strains used in this study.....71
Table 2.4 Plasmids used in this study.....72
Table 2.5 Primers for *ompA1* gene knock out.....74
Table 2.6 Primers for *ompA2* gene knock out.....74
Table 2.7 Primers for *ompA2* gene complementation.....75
Table 2.8 Primers for *ompH1H2* gene knock out confirmation.....75
Table 2.9 Primers for GST-tagged OmpA1 protein overexpression.....76
Table 2.10 Primers for GST-tagged OmpA2 protein overexpression.....76
Table 2.11 Primers for His-tagged OmpA1 barrel only protein overexpression.....76
Table 2.12 Primers for His-tagged OmpA2 barrel only protein overexpression.....76
Table 2.13 Plasmid primers for template insertion confirmation.....77
Table 2.14 Antibiotics used in this study.....77
Table 2.15 Reagents and their volumes for PCRs needed for cloning and expression.....81
Table 2.16 Reagents and their volumes for PCRs needed for routine screening.....82
Table 2.17 Reaction conditions for PCR with different polymerase enzymes.....83
Table 2.18 Reagents and volume required for a restriction enzyme digest.....84
Table 2.19 Reagents and volumes needed for a ligation reaction.....85
Table 2.20 Parameters for electroporation.....86
Table 2.21 Reagents and volumes needed for the resolving gel.....92
Table 2.22 Reagents and volumes needed for the stacking gel.....92
Table 2.23 Antibodies used in this study.....94
Table 2.24 Agar 100 Resin reagents for medium blocks.....99
Table 2.25 Lead citrate buffer.....99
Table 2.26 TNCT buffer.....100
Table 3.1 Number of *ompA* mutant colonies generated through different methods of *P. gingivalis* transformation.....112
Table 4.1 OmpA sequence homology between *P. gingivalis* and *E. coli* in the N- and C-terminal domains.....162
Table 4.2 Sequence of extracellular loops of the OmpA2 protein.....171
Table 4.3 Collation of the most widely used additives for protein purification enhancement.....185
Table 5.1 Common chaperone and related proteins found in *E. coli* and *P. gingivalis* for comparison.....192
Table 5.2 Transformation efficiency of each method of transformation for *P. gingivalis*.....200

Chapter 1

Introduction and Literature Review

1.1 Overview of Periodontal Disease

Periodontal disease is a group of inflammatory infections initiated by oral pathogens which exist as complex populations in biofilms on the tooth structure and cause tissue destruction, loss of alveolar bone and eventually can lead to loss of teeth. The World Health Organisation (WHO) classes periodontal disease as a "global burden" and incidence is ever increasing. The treatment of periodontal disease is thought to be at a great cost to health care systems worldwide, with over £1.6 billion per annum spent by the NHS (Marsh, 2003) and estimated $14 billion in the U.S. (Brown *et al.*, 2002).

The incidence for periodontal disease is difficult to accurately analyse as a significant proportion of sufferers avoid professional treatment until a problem arises, as shown in the 2009 Adult Dental Health Survey (http://www.hscic.gov.uk/pubs/dentalsurveyfullreport09). On a global scale, it has been reported that gingivitis affects up to 90% of the entire world's population (Pihlstrom *et al.*, 2005), with periodontal disease affecting up to 15% of the adult population worldwide (Petersen and Ogawa, 2012), meaning dental caries and chronic periodontitis occupy the top two spots on the list for Global Burden of Disease in terms of sheer population numbers (Borgnakke *et al.,* 2013), demonstrating that periodontal disease is a major health issue.

Periodontitis is a complicated multifactorial disease; however it is agreed by the majority that the cause is due to a build-up of dental plaque which is made up of oral pathogens, extracellular matrix proteins from bacterial and salivary origins (Marsh, 2006), coupled with the host immune response to these bacteria. A specific subset of bacteria known as the "red complex" is highly associated with periodontitis with raised numbers in sub-gingival plaque (Socransky *et al.*, 1998; Griffen *et al.*, 2011). This red complex is made up of *Porphyromonas gingivalis*, *Tannerella forsythia* and *Treponema denticola*, a group that possess many virulence factors that are thought to contribute to the disease, such as the lipopolysaccharide (LPS) layer, capsule, fimbriae, glycosidases, sialidases and surface proteins and which are capable of causing periodontal symptoms in animal models (Sharma *et al.*, 2001; Singh *et al.*, 2011). In addition, several oral bacteria such as *P. gingivalis* have been shown to invade human cells as part of the disease process (Lamont *et al.*, 1995). Notably, bacteria from the red complex have been shown to reside within the buccal epithelial cells of the oral cavity (Rudney *et al.*, 2001; Rudney *et al.*, 2005; Rudney and Chen, 2006) and can persist even after treatment, such as root planing, antibiotic and anti-

microbial rinses (Johnson *et al.*, 2008), which may lead to a rapid repopulation of disease-related bacteria and the progression into aggressive periodontitis.

The understanding of the molecular mechanisms behind host cell interaction is therefore critical in the prevention of periodontal disease, and the aim of this project will be to further understand the molecular mechanisms that the oral pathogen *P. gingivalis* used in the adherence to and invasion of oral epithelial cells.

1.2 Periodontitis: The Clinical Setting

The periodontium is made up the major components as seen in Figure 1.1. These structures are inflamed or destroyed during periodontal disease, resulting in loss of periodontal attachment, dissolving of the alveolar bone and eventual loss of teeth if left untreated.

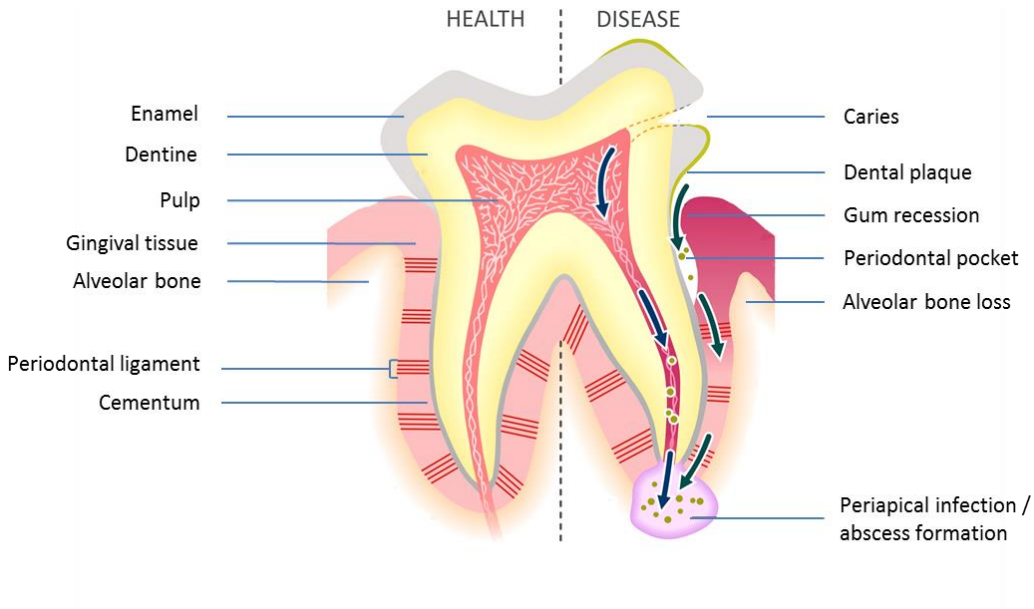

Figure 1.1 Schematic demonstrating the healthy and diseased periodontium. The left shows the healthy gingiva, whereas the right shows the inflamed gums and loss of bone typical of periodontitis. Tooth image obtained from Dr Graham Stafford and used with permission.

It is thought that there are 6 major steps in the progression of periodontal diseases, as shown in Figure 1.2. The severity of periodontal disease can range from reversible and mild (category 1) to an irreversible chronic destruction of the supportive tissues, formation of the periodontal pocket and loss of teeth (category 2 onwards). Category one is what is commonly known as gingivitis, the acute inflammation of gingival tissues and is present in a

large proportion of the population, up to 90% (Pihlstrom *et al.*, 2005). Gingivitis usually presents with mild bleeding from the gums during tooth brushing. If left untreated, gingivitis can progress into chronic periodontitis, which initially appears as mostly asymptomatic except for inflammation, but progresses further to be diagnosed by a loss of bone structure and tooth loss, known as aggressive periodontitis. The diagnosis of chronic periodontitis clinically is usually through visual checking and radiographic methods such as X-rays to detect any underlying alveolar bone loss (Kim *et al.*, 2008). Visual methods include the probing of periodontal pocket depth, which in a healthy individual are between 1-3 mm in depth, but increase as bone and connective tissue are lost. Visual examinations also include the observation of supragingival plaque, gingival bleeding and exudate recording (Loesche and Grossman, 2001). Chronic and aggressive periodontitis are classed as irreversible, visualised by the junctional epithelium migrating away from the tooth surface, creating a periodontal pocket as shown in Figure 1.1. Necrotising periodontitis and abscess formation (category 5 and 6) clinically present with large necrotic regions of the gingival tissues coupled to severe pain and include a weakening of the immune system, such as a defective lymphocyte reaction and a reduction in immunoglobulin expression (Bermejo-Fenoll and Sánchez-Pérez, 2004).

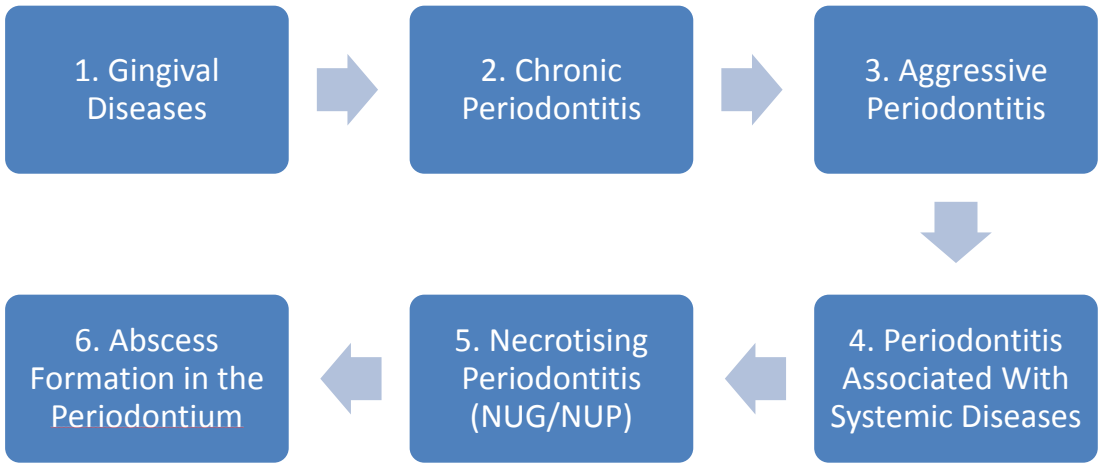

Figure 1.2 The six major stages of periodontal disease progression. Adapted from (Soskolne and Klinger, 2001)

As periodontitis is classed as a multifactorial and complex disease, the initial gingivitis steps do not always progress into a chronic disease. Salvi (1997) described a "critical path model" which details the major steps in progression of periodontal disease. This progression can be seen in Figure 1.3, and details not only the microbial components but also the host components, which make critical contributions to allow the progression from gingivitis to chronic periodontitis (Salvi *et al.*, 1997). Initial steps include the progression into gingivitis and then the host-produced response brings the disease under control. Progression through the cycle leads to periodontitis, but it is not always the outcome. This model demonstrates only the essential elements for the progression, not inclusive of the risk factors which are discussed later.

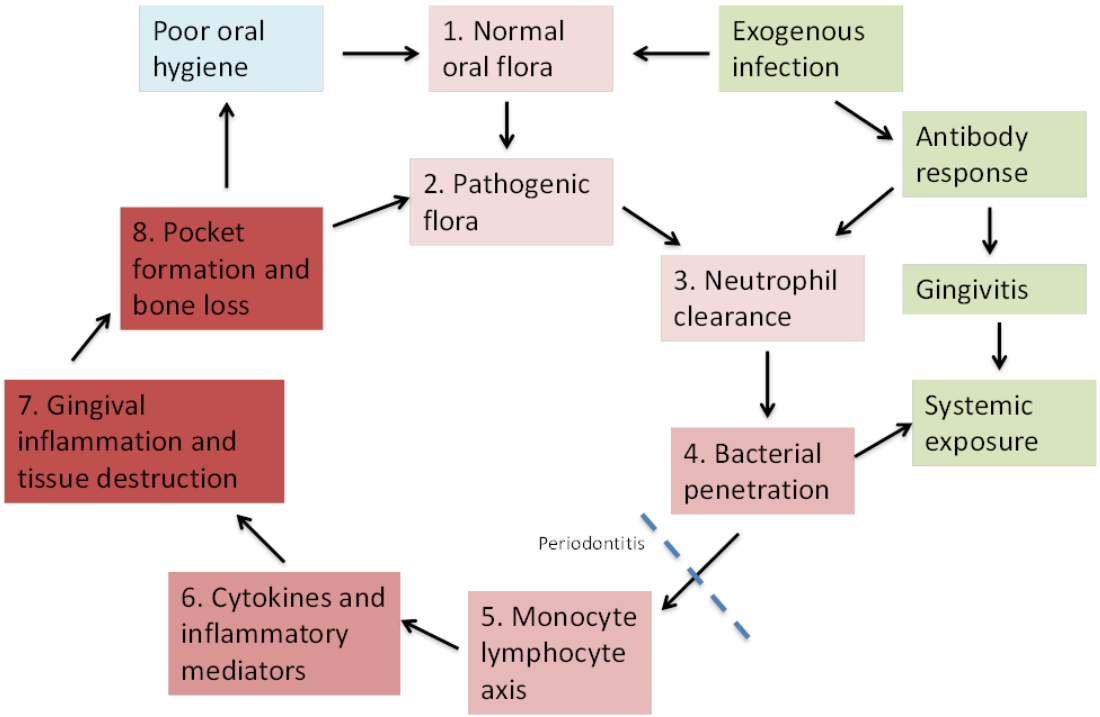

Figure 1.3 The critical pathway model. Steps 1-8 represent the major steps in progression of disease, including both the bacterial aetiology and the components of the host response. Adapted from (Salvi *et al.*, 1997).

Periodontal diseases can be treated in a number of ways. Because gingivitis and periodontitis begin with the build-up of dental plaque, the first method of prevention or treatment is the removal of this plaque biofilm. This can be removed with tooth brushing, flossing (Sambunjak *et al.*, 2011; Poklepovic *et al.*, 2013) or the use of mouthwash which contains some antimicrobial agents, such as chlorohexidine and salifluor (Eley, 1999).

Previous studies have shown after all oral hygiene procedures stop, the biofilm build up begins within 24 h and results in gingivitis within as little as 10 days, and when followed by thorough tooth cleaning, the gingiva return to health within 7 days (Theilade *et al.*, 1966), demonstrating the clear importance of biofilm control in the prevention and treatment of gingivitis. Non-surgical techniques may also be employed professionally to remove biofilms from periodontal pockets, including scaling and root planing, which if coupled to better oral hygiene at home, can reverse gingivitis effects and improve periodontal attachment. With aggressive periodontitis, treatment may involve the need for the prescription of systemic antibiotics, such as azithromycin which also contributes as an anti-inflammatory (Hirsch *et al.*, 2012) alongside the usual non-surgical subgingival debridement (Pihlstrom *et al.*, 2005).

1.3 Links to Other Diseases

1.3.1 Diabetes

The association between periodontal diseases and diabetes has been a long standing discussion and of all the links to systemic diseases, provides the most consistent evidence. There appears to be a bidirectional association between diabetic patients and prevalence of periodontitis (Grossi and Genco, 1998; Taylor, 2001). It is thought that poorly controlled diabetes can increase the risk of periodontal diseases, especially due to the healing of wounds being adversely affected by diabetes (Emrich *et al.*, 1991). In the periodontium, the fibroblast cells act as the reparative cells when tissue destruction occurs. These cells are incapable of functioning properly in high-glucose environments (Moore *et al.*, 1999), such as those found in poorly-controlled diabetic patients. Coupled to this, the collagen produced in the healing process by fibroblasts is broken down by matrix metalloproteinases, the levels of which are increased in in diabetic patients (Sbordone *et al.*, 1998), thus exacerbating the disease and propelling the evidence between the association.

Studies of the literature by Taylor *et al*., have shown significant associations between the severity of periodontal disease and the diabetes, and concluded not only that there appears to be a greater prevalence of the symptoms of periodontal disease in diabetic patients, but also that the progression of the periodontal disease symptoms are a lot more aggressive in these patients also (Taylor, 2001; Taylor and Borgnakke, 2008; Preshaw *et al.*, 2012). A cohort study by Soskolne and Klinger (2001) demonstrated that 12.5% of patients that had periodontitis also had diabetes, or that 17.3% patients with diabetes also presented with

periodontitis. In comparison, diabetic non-periodontitis patients (6.3%) and non-diabetic, periodontitis patients (9%), suggesting that periodontitis is more prevalent amongst patients with diabetes (Soskolne and Klinger, 2001). More recently, the idea that the periodontal pathogen can adversely affect glycaemic control in diabetes has been studied and evidence shown that nonsurgical treatment of periodontal disease can improve the blood glucose levels (Telgi *et al.*, 2013). However the link between diabetes and periodontal disease still remains under question as a large study of all the recent literature by Borgnakke *et al* (2013) demonstrated that there is limited current evidence to suggest that periodontal disease has an adversely affect or promote diabetes (Borgnakke *et al.*, 2013). The link between diabetes and periodontal disease may just rely on the synergistic influences the two have on each other, both exacerbating the effects of the other on the immunoinflammatory response whereby inflammation is a central feature of both periodontal disease and diabetes, and therefore appear to be interlinked. This is supported by the evidence from the bacterial load or species being relatively unchanged between diabetic and non-diabetic patients with periodontitis (Emrich *et al.*, 1991).

1.3.2 Heart Disease

An association between periodontal disease and coronary heart disease has been speculated since the 1960's (Mackenzie *et al.*, 1963), where a study examined the links between diabetes, arteriosclerotic, non-diabetic patients and a group suffering from neither condition. The arteriosclerotic individuals were the only group to demonstrate more alveolar bone loss than the control group, suggesting a link between the two. This study also coincidentally showed no association between diabetes and periodontal disease (Beck *et al.*, 1996). Periodontal pathogens have also been implicated in cardiovascular disease with studies showing an association with myocardial infarction (Marcus and Hajjar, 1993), with some studies even showing poor periodontal health preceding a cardiovascular event , although various follow up studies have shown no such association (Howell *et al.*, 2001); (Hujoel *et al.*, 2000). This inconsistency between studies has left a shadow of doubt over the true association between cardiovascular disease and periodontitis. More recent studies have implicated the periodontium as the source of the bacteria and inflammatory mediators which are then disseminated into the blood stream, leading to cardiovascular events (Li *et al.*, 2000), and the inflammatory burden of periodontitis appears significant in atherosclerosis (Schenkein and Loos, 2013), however the direct role in stimulating the inflammatory response in the vessel wall is still unclear. Some studies have even gone as far

as to detect the DNA of *T. forsythia* and *P. gingivalis* in atherosclerotic plaques using microarrays (Kozarov, *et al.*, 2006; Gaetti-Jardim, *et al.,* 2009), and simple PCRs using primers against *P. gingivalis*, *A. actinomycetemcomitans* and *T. forsythia* detected high levels of these pathogens in atheromatous plaque in patients that had periodontal disease, whereas *P. intermedia* was found in all plaque samples but not in atheromatous samples (Rath *et al.*, 2014).

It is thought that oral pathogens are capable of entering the bloodstream, causing inflammation and increasing plaque build-up which subsequently leads to a contribution in the dilation of the arteries (Bartold and Narayanan, 2006). The cariogenic bacteria, *Streptococcus mutans*, has been identified in heart valve tissues and atheromatous plaque at a higher frequency than any other species (Nakano *et al.*, 2006), and when coupled with *P. gingivalis,* the two species have been shown to accelerate atherogenic plaque formation in a mouse model (Kuramitsu *et al.*, 2001), whilst follow up studies have shown a polymicrobial infection of oral bacteria are capable of accelerating the plaque formation (Chukkapalli *et al.*, 2015). There is evidence demonstrating the ability of *P. gingivalis* to invade cardiovascular endothelial cells (Deshpande *et al.*, 1998; Kozarov *et al.*, 2005), and cultivable *P. gingivalis* has been isolated from atheromatous tissue (Rafferty *et al.*, 2011). These various studies demonstrate there are severe implications on the systemic health of a patient with periodontitis. More recently, as *P. gingivalis* is often found associated with atherosclerotic plaque and atheromatous tissue, a study investigated the causal link between *P. gingivalis* and plaque development (Velsko *et al.*, 2014). Velsko *et al* demonstrated that in an ApoE-knock out mouse (used as a model as it develops extensive atherosclerotic lesions), long term periodontal disease allowed a constant exposure of periodontal bacteria systemically, increasing the interactions of *P. gingivalis* with endothelial cells and the arterial wall, responding with an increase in inflammatory cells and leading to the formation of atherosclerotic plaque (Velsko *et al.*, 2014). This study so far has been the most convincing link between periodontal disease and heart disease. It has been relatively well established that there is a direct link between periodontal disease and heart disease (Pizzo *et al.*, 2010) but conversely, the American Heart Association has recently noted that neither the treatment of periodontal disease has been proven to treat cardiovascular disease, nor that periodontal disease has been proven to cause atherosclerotic disease (Lockhart *et al.*, 2012; Hayashi *et al.*, 2015), demonstrating that it may just be a correlation of shared risk factors (obesity, aging, tobacco use etc.) that indicates a causality between the two diseases (Genco and Borgnakke, 2013).

1.3.3 Pre-Term Birth

Several cohort studies have also attempted to understand the links between poor maternal periodontal health and the association with low birth weight and pre-term birth. The role of bacterial infections influencing premature births is well understood, such as bacterial vaginosis (BV) causing chorioamnionitis (Reviewed by Romero *et al.*, 2004). BV, like periodontal disease, is caused by an imbalance of the bacteria which leads to an over population of disease-causing bacteria (Gilbert *et al.*, 2013). The putative link between pre-term birth and periodontal disease is thought to be due to inflammatory mediators entering the blood stream and triggering an inflammatory cascade in the uterine lining, or the bacteria themselves entering the systemic circulation causing a repeat exposure in the same tissues (Gibbs, 2001). To further support this hypothesis, various animal studies have shown than injection of mice with periodontal pathogens can lead to preterm or still births (Han *et al.*, 2004), and various oral microorganisms have been detected in the amniotic fluid, such as *F. nucleatum* and *Capnocytophaga sputigena* (Bearfield *et al.*, 2002). The use of 16S sequencing rather than culture-dependant methods has indicated a far greater microbial diversity in amniotic fluid than previously expected. A study by Wang *et al* demonstrated the presence of *F. nucleatum, Bergeyella lachnospiraceae, S. sanguinegens* and *S. mitis* amongst other non-periodontal species, in the amniotic fluid and cord blood, which leads to the heightened inflammatory state found within many preterm newborns, and hypothesised *F. nucleatum* especially, is as important at *E. coli* in causing early-onset neonatal sepsis (Wang *et al.*, 2013). Wang *et al* hypothesised that as *F. nucleatum* has previously been shown to invade epithelial and endothelial cells (Han *et al.*, 2000; Han *et al.*, 2004) and is capable of colonising the placenta (Han *et al.*, 2004; Liu *et al.*, 2007) which leads to a high level of inflammation and foetal loss, that the presence of other oral species in the amniotic fluid is due to a co-migration with *F. nucleatum* from the oral cavity (Wang *et al.*, 2013).

1.3.4 HIV/AIDS

HIV/AIDS has a difficult connection with periodontal disease to dissect as the geographical location of high prevalence of HIV/AIDS is usually coupled to areas of little access to oral health care, such as in Sub-Saharan Africa (Petersen and Ogawa, 2012). The prevalence of patients being HIV positive and suffering from chronic periodontitis is relatively low compared to other pathogenic associations with HIV positive patients, although these patients often suffer from distinct types of necrotising ulcerating periodontitis (Robinson,

1992). Studies have shown that when periodontitis presents in this way, it is a strong indication of a $CD4^+$ cell count being under 200 cells / µl (Glick *et al.*, 1994), as observed in HIV positive patients. This has links to the geographical influence on a disease, as the is a higher prevalence of people who are HIV^+ in sub-Saharan Africa, who also have a higher number of cases of necrotising periodontitis (Arendorf *et al.*, 1998) as the access to highly active antiretroviral therapy (HAART) used for managing HIV, is limited (Pihlstrom *et al.*, 2005).

1.3.5 Periodontal Disease and Arthritis

Periodontal disease and rheumatoid arthritis are two very common chronic inflammatory diseases affecting the human population, and despite differing etiological mechanisms that initiate the two, evidence for an association between these diseases is appearing, with periodontal disease being two-fold more prevalent in patients with rheumatoid arthritis than the general population (Koziel *et al.*, 2014). Rheumatoid arthritis is generally accepted as being caused by an autoimmune response to an accumulation of citrullinated proteins. Citrullinated proteins are produced under normal physiological conditions but susceptible genetically individuals generate antibodies against these citrullinated proteins (Klareskog *et al.*, 2008; Wegner *et al.*, 2010), causing this autoimmune response. Citrullination of proteins is a necessary post translational modification in a variety of physiological processes, from the proteins involved in brain development to the chromatin remodelling to regulate gene expression (György *et al.*, 2006; Wang *et al.*, 2009). Protein citrullination also occurs in inflammatory conditions, for example, hypercitrullination of histones in the production of neutrophil extracellular traps (NETs) which are necessary in the host innate immune response (Wang *et al.*, 2009). The citrullination of these proteins is carried out by peptidyl-arginine deaminases (PADs), and recently *P. gingivalis* has been shown to express a homolog of this enzyme, which is found to be colocalised in the outer membrane with the arginine specific gingipains (Rgps) (Quirke *et al.*, 2014). The gingipains cleave the mammalian proteins to expose C-terminal arginines which are rapidly citrullinated by the *P. gingivalis* PAD (PPAD), which has been hypothesised to set in motion a chain of events that leads to a significant build-up of citrullinated proteins and therefore causes an intolerance and leads to the development of rheumatoid arthritis (Dissick *et al.*, 2010). Recent Mass Spectrometry data has revealed that PPAD not only citrullinates other proteins, but itself is citrullinated and acts as a potent antigen to further increase the intolerance in the host (Quirke *et al.*, 2014). The PAD enzyme of *P. gingivalis* is therefore being investigated as a

potential target to develop a novel treatment for both periodontal disease as well as rheumatoid arthritis.

1.3.6 Periodontal Disease and Cancer

Both *F. nucleatum* and *P. gingivalis* are well characterised to establish chronic infections with immune disruptive properties, and similarly, the modulation of the tumour microenvironment and the development of tumours has been attributed to chronic and dysregulated inflammation (Whitmore and Lamont, 2014), suggesting a potential link. A study by McCoy *at al* has demonstrated a strong positive correlation between cytokines and *F. nucleatum* in colorectal cancer (McCoy *et al.*, 2013), and is thought to be responsible for producing a strongly proinflammatory response in colorectal cancer cases in mice by the recruitment of tumour-infiltrating immune cells (Kostic *et al.*, 2013) which leads to the progression of cancer. More direct evidence for the involvement of *F. nucleatum* and cancer progression has been demonstrated recently, where the adhesin FadA activates the β-catenin signalling pathway by binding to the E-cadherin receptor, which leads to an increase in the transcription of oncogenes, pro-inflammatory cytokines and stimulated cell proliferation (Rubinstein *et al.*, 2013), however at present there is no clear link to oral cancer.

As *P. gingivalis* is responsible to producing both pro- and anti-inflammatory responses, it is harder to tease out a link between *P. gingivalis* and cancer, however it is widely observed that *P. gingivalis* causes a severely disruptive effect on the host immune response, which may lead to the progression of cancer (Whitmore and Lamont, 2014). The link between *P. gingivalis* and oral cancer is more observational, as *P. gingivalis* is highly antiapoptotic through suppression of apoptotic pathways such as Jak1/Akt/Stat3 pathway (Mao *et al.*, 2007), whilst causing accelerated progression through the cell cycle by reducing the level of p53 tumour suppressor (Kuboniwa *et al.*, 2008), and therefore increases the dysfunctionality of cell death pathways, which by definition is what causes cancer. The fimbrial protein subunit, FimA, is thought to induce this cell cycle progression, as it has been noted that a *fimA*-deficient mutant is not capable of elevating cell cycle progression (Kuboniwa *et al.*, 2008).

The implications of the involvement of oral bacteria in cancer still remain unknown, but in future could potentially lead to the appearance of the bacteria in cancer cases as prognosis indicators or an improvement in oral hygiene could lead to the limitations of cancer

progression and spreading if the link with oral bacterial proves to be more convincing in future studies.

1.4 Factors Affecting Periodontitis

1.4.1 Periodontitis and Ageing

Originally, periodontal disease was thought of as an inevitability of ageing, but more recently the molecular factors behind this association have been examined. Several studies have shown that in older populations who still retain their teeth, periodontal diseases are one of the most prevalent chronic conditions and is often coupled to an increase in severity with age (Beck *et al.*, 1990; Hugoson *et al.*, 1992; Locker and Leake, 1993), with a particular study showing the rate of bone loss was significantly higher in 70-year-old individuals compared to 25-year-olds, demonstrating an increased severity (Papapanou and Wennström, 1989). This is a potential reflection of the individual's cumulative oral history, whereby the severity of the disease reflects the length of time the periodontal tissues have been exposed to plaque (Löe *et al.*, 1986). At a biological level, the tissues are subject to progressive and irreversible deterioration with age, especially in the gingival recession, and this change to structure and function may affect the host response to pathogens in the oral cavity, and ultimately influence the rate of periodontal destruction (Razak *et al.*, 2014). Again, this demonstrates that periodontal disease is not only due to the presence of certain microorganisms, but is a complicated balance of host response and microbial interactions.

The age composition of the human population has changed drastically in the later decades of the 20th century, with a huge increase in the number of people living to older ages (Razak *et al.*, 2014). With the connections of increased age to heightened risk of periodontal disease, and the aged population ever increasing, it is imperative to increase our understanding of periodontal disease to reduce this burden on our healthcare systems

1.4.2 Influence of Host-Genetics

Strong links with certain genetic disorders have been identified that result in severe periodontal manifestations. For example, rare autosomal recessive disorders such as Haim-Munk and Papillon-Lefèvre syndromes are associated with the onset of periodontitis at childhood, with the loss of both deciduous and adult teeth (Hart *et al.*, 2000). Several studies involving twins indicate that around 50% of the population variance in periodontitis is affected by genetic factors (Michalowicz *et al.*, 1991; Corey *et al.*, 1993), however despite

several genetic polymorphisms being identified to contribute to periodontal disease (Greenstein *et al.*, 2002; Kinane and Hart, 2003), currently there is not enough evidence to provide an effective genetic test to assess the risk of developing periodontal disease or to determine the response to periodontal treatment.

1.4.3 Modifiable Risk Factors

It is widely accepted that periodontal disease is due mainly to the pathogenic microflora found in the dental subgingival biofilm. However, several "modifiable" causes have also been identified which effect disease progression, for example, the use of tobacco, individuals suffering from high levels of stress, and those with poor diets. It has been shown that the development of periodontitis is much more likely in smokers than non-smokers, including the use of smokeless tobacco products (Bergström, 2004). A study by Preber and Bergstrom (1990) showed that even periodontal treatment, such as surgical intervention, is much less effective in smokers, which highlights the detrimental effects of smoking on periodontitis (Preber and Bergström, 1990). In contrast, a significant but very small association can be found between development of periodontitis and alcohol consumption (Tezal *et al*, 2004). Nutrition has historically been associated with periodontal disease, especially a lack of Vitamin C. A deficiency in Vitamin C intake is well known for leading to scurvy, but this also leads to a decrease in the maintenance of collagen, which leads to loss of supporting structures and an increase in inflammation, leading to tooth loss (Pihlstrom *et al.*, 2005).

Associations between trauma and stress and periodontal disease have been observed where previously it was thought to be most likely due to a lack of motivation (Genco *et al.*, 2002; Bakri *et al.*, 2013), however more recently it is being increasingly understood with a growing body of evidence. Several groups have demonstrated a potential link between the psychological status of a patient and alterations in their immune activity, known as "Psychoneuroimmunology", which connects the psychological and physiological sides of a disease (Ader *et al* 1995). Stress and anxiety have been shown by a number of studies to influence the onset of periodontal disease, by altering the periodontal environment such as the temperature and gingival circulation, and also by suppressing the host immune response (Peruzzo *et al.*, 2007; Pöllänen *et al.*, 2013), leading to an exacerbation of the disease, although why this occurs is still unclear. Studies have theorised this phenomenon could be due to an increase in pro-inflammatory cytokines by the hypothalamic-pituitary-adrenal axis, whereas immunosuppressive effects may occur from adrenaline, cortisol and

noradrenaline released by the sympathetic nervous system, and interestingly, cortisol has been suggested to promote the growth of *P. gingivalis*, the keystone pathogen of periodontal disease (Akcalı *et al.*, 2014). The lack of motivation when stressed or anxious coupled to physical immune responses pose an interesting challenge and added complication in the treatment of periodontal disease.

1.4.4 The Role of Innate Immunity at the Host-Pathogen Interface

The innate immune system is a critical subsection of the overall immune system of the host which comprises of complex mechanisms that recognise non-specific pathogen associated molecular patterns (PAMPs), which are molecular motifs found conserved across the class of microbes and are necessary for bacterial survival, and allow a rapid response to the impending infection (Medzhitov, 2007). The major functions of the host innate immune system include 1) the recruitment of neutrophils and macrophages to the site of infection through the production of cytokines (which include the interleukins); 2) the activation of the complement cascade to initiate the identification of the invading pathogens, recruitment of phagocytes and initiate direct killing of the pathogen, and 3) to activate the adaptive immune system to allow a more heightened response to the infection (Roitt *et al.*, 2011). It is comprised mainly of mechanical (the epithelial cell barrier), cellular (epithelial cells, macrophages, dendritic cells, etc.) and chemical elements (pattern recognition receptors, cytokines, chemokines, etc.) (Basset *et al.*, 2003).

The gingival epithelium first provides a physical barrier against infection, with tight junctions between cells to prevent entry by pathogens (Sammartino *et al.*, 2010), although as discussed later, many bacteria overcome this by invasion of the cells. Part of the innate response is the fact the oral epithelium is also coated with saliva and mucins which physically prevent adherence by the pathogens, whilst also containing antimicrobial peptides like defensins and cathelicidins, which kill the invading pathogens (Roitt *et al.*, 2011). The epithelial cells also contain pattern recognition receptors (PRRs) which recognise PAMPs, such as LPS or flagella. The best characterised family of PRRs are the Toll-like receptors (TLRs), which are transmembrane receptors capable of recognising several bacterial products, such as TLR-4 recognises LPS, whereas TLR-9 recognises bacterial DNA (Medzhitov, 2007). These TLRs are known to elicit an inflammatory response, by activating macrophages and dendritic cells resident in the tissues to produce pro-inflammatory cytokines such as tumour necrosis factor (TNF), and interleukins (IL), such as IL-1β and IL-6,

which increase the vasodilation of the local blood vessels, whilst recruiting neutrophils to trigger other sections of the immune response (Basset *et al.*, 2003).

The complement system is also crucial in the innate immune response. It consists of ~20 soluble interacting proteins that circulate in the blood, and are inactive until triggered by an infection. These complement proteins are also PRRs that can be activated by PAMPs, which leads to the activation of the early complement components from either of the three complement pathways (classical, lectin and alternative) which all activate the C3 complement protein (Medzhitov, 2007; Roitt *et al.*, 2011), a pivotal component as previous studies have shown individuals the contain a deficiency of C3 are repeatedly subject to bacterial infections (Pickering *et al.*, 2000; Botto *et al.*, 2009). The activation of each complement protein sequentially activates the next protein, causing a cascade, liberating a membrane binding large fragment which binds to the surface of the pathogen and leads to the phagocytosis of the pathogen (Cekici *et al.*, 2014). This liberation also releases a small biologically active fragment that can lead to the promotion of the inflammatory response through the recruitment of phagocytes and lymphocytes (Hajishengallis, 2015).

The action of many of these components of the innate immune response is to induce a pro-inflammatory response, which is a protective response against microbial invasion on a local scale (Tracey, 2002). The response is usually short-lived as it can be damaging for the tissues involved, and a long-term inflammatory response becomes a chronic inflammatory disease (Lawrence and Gilroy, 2007). The periodontal pathogens hijack this pro-inflammatory response to promote inflammation to cause periodontitis, which by definition, is a chronic inflammatory disease (Hajishengallis, 2015).

1.4.5 Genetic Considerations in Periodontal Disease

Various studies have shown a genetic component to the risk factor associated with periodontitis. Direct evidence for the genetic contribution to the heritable susceptibility of periodontitis is unclear, however rapid progression of chronic gingivitis to destructive periodontitis affects around 10-15% of the population, consistent with a high-risk group for an inheritance of susceptibility (Johnson *et al.*, 1988). Reports in the literature indicate a familial aggregation of periodontal disease, however due to lack of standard classifications and inconsistent methods of clinical examination it is difficult to determine a familial link (Hassell and Harris, 1995).

One theory that appears to have credence in the severity of periodontal disease linked to genetic factors is the particular genotype of the IL-1 proinflammatory cytokine. The IL-1 cytokine is a key regulator of the response by the host to the microbial infection, and it has been reported that variations in the gene cluster of IL-1 could be influential on the severity of periodontitis (Gore *et al.*, 1998), and one of the alleles is associated with a four-fold increase in the production of IL-1 (Pociot *et al.*, 1992). High levels of IL-1 are detected in gingival crevicular fluid from patients with severe inflammation and tissue destruction (Feldner *et al.*, 1994; Ebersole *et al.*, 2000). Patient cohort studies by McDevitt *et al* demonstrated that the IL-1 positive genotypes showed a strong correlation with severe adult periodontitis, at higher levels than IL-1 negative patients who were smokers (Mcdevitt *et al.*, 2000), indicating the genotype of IL-1 is a significant risk factor of severe adult periodontitis. These studies are interesting as they provide a potential biomarker for the development of severe periodontal disease, and therefore can be used to apply appropriate treatment before the disease becomes chronic.

1.5 Aetiology of Periodontitis

As previously mentioned, the cause of periodontal disease is thought to be mainly down to the presence of bacteria in a biofilm known as subgingival plaque. The presence of harmful oral pathogens in periodontal plaque is not necessarily enough to cause disease, as for example, *P. gingivalis* is found in the periodontium of healthy patients (Ximenez-Fyvie *et al.*, 2000). It is the disruption of the balance between health and disease due to an ecological pressure, such as one species of disease-causing bacteria out-competing a bacterial species associated with health, coupled with the introduction of environmental changes, such as a sugar-rich diet (Marsh, 2006). There are several hypotheses developed to understand the role of plaque bacteria and the causation of disease, but two major ideas are the most recognised. These being the specific plaque hypothesis developed by Loesche in the 1970's which theorises that out of a large collection of bacteria involved in the resident microflora, only a select few species are involved in causing the disease (Loesche, 1976), which explains why there are many patients whose oral cavities contain considerable levels of plaque deposits, but only a minority of these patients suffer from severe destructive periodontitis (Hasan and Palmer, 2014). This hypothesis leads to the idea that targeting only those bacteria can produce preventative treatments for periodontal disease. However, to date there has only been identification of "keystone" pathogens (Hajishengallis *et al.*, 2012) and the idea of a dysbiotic population as opposed to a single species

responsible for the disease. The theory of microbial dysbiosis indicates a "shift" in the membership of the local microbiota of the mouth, where a decrease in the number of beneficial bacteria occurs coupled to an increase in pathogens, especially those found in the keystone population (Nath and Raveendran, 2013), leading to the deterioration of the oral health of the host until periodontal disease occurs. The other major idea is the non-specific plaque hypothesis developed by Theilade over a decade later from Loesche. This theorises that it is the overall action of the entire plaque microflora which produces the disease (Theilade, 1986). This theory implies that no one specific bacterium has the ability to cause disease; rather it is due to the bacterial accumulation irrespective of the bacterial composition. Both hypotheses, although seemingly opposing, complement each other well as plaque is a polymicrobial infection where only a limited number of species can be dominant. In response to these hypotheses, Marsh developed another theory known as the "ecological plaque hypothesis" that describes the key elements in both. It theorises that plaque-mediated diseases are due to an enrichment of oral pathogens, causing an imbalance in the resident microflora (Marsh, 2006). This theory proposes a shift from predominantly Gram-positive aerobic bacteria to the more disease-associated Gram-negative anaerobic bacteria. Thus, the production of a mainly alkaline environment suitable for asaccharolytic bacteria due to the production of novel nutrients that allows the enrichment of these anaerobic Gram-negative bacteria such as *P. gingivalis* (Zilm *et al.*, 2007). These theories all demonstrate the complex relationship between bacteria and the host which results in periodontal disease.

1.6 Microbiology of Periodontitis

Periodontitis is thought to be one of the major polymicrobial infections in the human body (Saito *et al.*, 2009). A polymicrobial disease consists of a number of complex interactions between multiple causative agents acting in a synergistic manner to elicit a range of host responses. The oral microbiome is thought to harbour over six billion bacteria, making up over 700 bacterial species (Kuramitsu *et al.*, 2007), as well as other microorganisms such as protozoa, mycoplasma and fungi, and possibly even viruses (Pennisi, 2005). Despite this complex community, only relatively few bacteria, around 10-20 species, are thought to participate significantly in the disease process (Socransky *et al.*, 1998). The primary contributing factors to periodontitis can be split into two groups; an immunological factor and a microbial factor. The immunological contributor is the host's destructive inflammatory response to the infection, which will be discussed later in reference to *P.*

gingivalis specifically, whereas microbial factors of disease is the shift in the content of the oral microbiota from a health-associated population to a disease-associated one (Berezow and Darveau, 2012), causing a dysbiosis of the oral microbial population (Hajishengallis, 2014). The shift in oral microbiota involves various complex reactions between several different species but originally comes due to a build-up in the number of bacteria as a whole in what is known as subgingival plaque.

1.6.1 Subgingival Plaque and Biofilm Formation

Biofilms are clinically relevant as over 65-80% of human bacterial infections involve biofilms (Rasamiravaka *et al.*, 2015), the understanding of the interactions is important to be able to eradicate the issue. Biofilms form on a variety of surfaces, from living tissue such as heart valves, to medical devices such as prosthetic devices and implants, often causing rejection (Prieto-langarica, 2013). It is thought that bacteria growing within a biofilm express differing phenotypes to their planktonic counterparts, exhibiting a greater tolerance to environmental conditions such as pH and oxygen levels, encouraging growth (Hojo *et al.*, 2009).

The first steps in biofilm formation depends on the bacterium, for example the opportunistic pathogen *Pseudomonas aeruginosa* uses flagella to swim along surfaces to find potential sites, and then type IV pili are employed to pull themselves towards other early colonisers to begin to form microcolonies (O'Toole and Kolter, 1998; Barken *et al.*, 2008). Other bacteria rely mainly on cell division to form the sheer numbers needed for biofilm formation (Chicurel, 2000). Once established, various genes are expressed to begin producing the components of the surrounding biofilm matrix, whereas others are activated to adapt the bacterial phenotype to the biofilm community environment. Studies have shown that up to 38% of the genes are altered in *E. coli* (Prigent-Combaret *et al.*, 1999), whereas *P. aeruginosa* appears to be much more modest at ~200 of the 5750 genes being altered (Chicurel, 2000). These genetic changes are thought to be coordinated by quorum sensing, whereby small diffusible signalling molecules are constantly secreted by the bacteria, and only when the population becomes large enough the critical threshold is reached and changes within the bacterial gene expression occur leading to behavioural changes. This has been extensively studied in the biofilm of *P. aeruginosa* which uses two main quorum sensing systems (*las* and *rhl*) which coupled to two-component regulatory systems (Rasamiravaka *et al.*, 2015), interact with the formation and production of the biofilm matrix, known as the extracellular polysaccharides (EPS). The EPS constitutes

around 85% of the mature biofilm biomass (Flemming *et al.*, 2007), and is comprised of biomolecules, extracellular DNA (eDNA), cellular components, exopolysaccharides and polypeptides, which form a scaffolding architecture to the biofilm by forming a highly hydrated polar structure (Sutherland, 2001; Branda *et al.*, 2005), providing both protection and nutrition for the bacterial component.

Biofilms are of great interest to medical research due to the ability of the bacteria to become less susceptible to antimicrobial agents and can show an enhancement of pathogenicity, known as pathogenic synergism (Steenbergen *et al.*, 1984). For example, one study demonstrated that *F. nucleatum* will support the growth of *P. gingivalis* and *P. nigrescens* in an oxygenated and CO_2-depleted environment by providing a capnophilic environment (Bradshaw *et al.*, 1998). The most significant gain to a bacterium in a biofilm is that of greater tolerance to antimicrobial agents, with certain studies (Sedlacek and Walker, 2007) showing the inhibitory concentration for growth of bacteria in a biofilm was increased 250 times compared to the same culture grown planktonically. Primarily, it is thought that the EPS prevents the diffusion of antimicrobial agents, so the drugs cannot physically reach the bacteria. Secondly, if the drugs can diffuse in to the EPS, the bacteria are shown to grow markedly slower in a biofilm, and therefore the biofilm formation causes a decrease in sensitivity to these drugs. The third major mechanism is thought to be that if the drugs can enter the EPS and effect targets not to do with growth, the sheer number of species involved in a biofilm will make it more likely that at least one species will possess a drug-inactivating enzyme, which allows any neighbouring species that do not produce the enzyme to benefit from a drug-free area (Hojo *et al.*, 2009). A more recently observed mechanism of survival through antibiotic application is the presence of “persister” cells, which are dormant, non-dividing cells making up less than 1% of the biofilm population. These are present in late-stage biofilms and their tolerance to antibiotics isn’t thought to be due to a genetic modification but merely a phenotypic state in which they do not divide in the presence of antibiotics. Once these bacteria resume growth, they return to a normal antibiotic susceptible phenotype (Lebeaux *et al.*, 2014; Conlon *et al.*, 2015). As the name suggests, these bacteria persist through antibiotic treatments and can then resume normal growth when there is no longer a presence of antibiotics, reforming the biofilm. These persister cells play a major role in the resistance of chronic infections to antibiotics.

Of the 700 bacterial species found in the oral microbiome, approximately 400 species are found in the subgingival plaque (Al-Jehani, 2014). Dental plaque has been defined as a community of microorganisms that form as a biofilm on the surface of the tooth (Marsh,

2006). Dental plaque is a dynamic and very complex structure, with initial colonisers of the sub- and supra-gingival surfaces being predominantly commensals which are Gram-positive, including *Streptococcus* species such as *Streptococcus gordonii* as well as *Actinomyces* species (Park *et al.*, 2005). The biofilm that forms in the oral cavity can be seen as a schematic in Figure 1.4 and begins with the formation of a pellicle, a thin glycoprotein rich film, which attaches to the tooth surface.

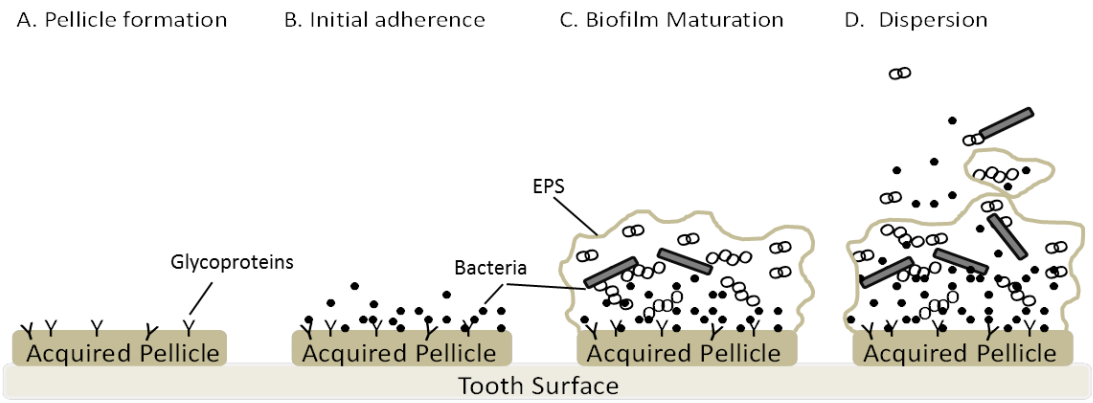

Figure 1.4 Oral biofilm formation. A) represents the formation of the pellicle, derived from salivary glycoproteins attached to the tooth surface. B) Shows the initial adhesion of the early bacterial colonizers, which bind to the glycoproteins. C) Shows the maturation, and the change from a reversible to irreversible form of bacterial adherence. D) Demonstrates the dispersal of bacteria from the biofilm surface and spread so as to colonise a new site.

The oral biofilm is unique in its requirement of a host-derived protein surface to attach to (Huang *et al.*, 2011). Once the pellicle has been formed, planktonic bacteria can recognise binding sites, such as α-amylase, and bind (reversibly) to the pellicle. The initial binding of the bacteria is mainly due to a physical attachment, usually via protein appendages such as fimbriae and adhesins, therefore the bacteria can detach easily (Filoche *et al.*, 2010). It isn't until the biofilm matures that the attachment becomes more permanent. Once the foundation of bacterial cells are laid down, the bacteria are able to grow and synthesise outer membrane components to allow adherence of bacteria that are incapable of binding to the pellicle directly (Hasan and Palmer, 2014). Later colonising bacteria recognise binding sites on the early pioneering bacteria, such as cell surface receptors or polysaccharides, which leads to bacterial aggregation and a maturation of the biofilm. Mature biofilms contain water channels and porous layers to allow essential nutrients to enter the biofilm, however oxygen gradients begin to form as the superficial bacterial layers rapidly utilise the

oxygen, leading to more anaerobic conditions developing within the biofilm (Hasan and Palmer, 2014). Bacteria are capable of leaving the biofilm via sloughing, erosion or seeding when the bacteria are dispersed due to the sheer force of the salvia movement, which is a passive host defence to remove biofilms, or the bacteria can actively be dispersed when limiting factors arise, such as a lack of nutrients (Huang *et al.*, 2011).

Despite a study by Kolenbrander in the early 1990's showing that over 90% of oral bacteria are capable of co-aggregating in paired tests, very specific cell-to-cell interactions need to take place for this to occur in biofilms, for example *S. mutans* is capable of aggregating with *F. nucleatum*, but *P. gingivalis* cannot (Bradshaw *et al.*, 1998). The mechanism behind bacterial aggregation is recognition of polysaccharides between bacteria. One bacterium has a specific recognition site to a specific adhesion molecule on another bacterium, leading to a timeline of events in biofilm formation depending on the presence of certain bacteria (Hojo *et al.*, 2009). Early pioneering colonisers consist mainly of *Streptococci*, which contribute up to 80% of the bacteria found in dental plaque. Other early colonisers include *Actinomyces* complexes which are thought to attach via its Type I fimbriae, and using its Type II fimbriae to allow inter-bacterial binding (Rosan and Lamont, 2000).

Early colonising bacteria may help facilitate the attachment of *P. gingivalis* through providing attachment sites or changing conditions to be more favourable for the attachment, such as the anaerobic facultative bacteria, *S. gordonii* which it thought to encourage colonisation through reduction of oxygen tension to levels that would allow growth of an obligate anaerobe such as *P. gingivalis* (Gaffen and Hajishengallis, 2009). The presence of *S. gordonii* is also thought to be the major binding point for *P. gingivalis* via the interaction of the long and short fimbriae of both species (Lamont *et al.*, 2002). The long fimbriae of *P. gingivalis* have been shown to bind to the surface protein, glyceraldehyde-3-phosphate dehydrogenase of *S. gordonii*, and rapidly then progressing to a biofilm (Cook, 1998). This bridging of early and late colonising species of the oral cavity in biofilm formations is also observed between *F. nucleatum* and *T. forsythia*, whereby the former (an early coloniser) synergises with the latter during biofilm formation and pathogenesis (Sharma *et al.*, 2005). Coinfections with these two species induces a much more potent infection than either alone, inducing a severe pro-inflammatory response for monocytes and macrophages, and a greater increase in bone loss compared to the single species infections of a murine model (Settem *et al.*, 2012). The interactions between these pathogens during biofilm formation and infection of the host are especially important in the pathogenesis and severity of periodontal disease.

1.6.2 Microbial Complexes Involved in Periodontitis

Understanding the complex relationship and their interactions between different bacterial species is important to understand how to control the infection. It is believed that there is no one species that causes the tissue changes and periodontal destruction that is associated with disease, but instead a mixture of species and complexes is likely required for the progression of disease (Marsh, 2006). The defining study of microbial complexes in subgingival plaque was performed by Socransky and his group in 1998. Using both cluster analysis and community ordination techniques on over 13,000 samples, the work set out to understand the relationship between closely related species within a community of bacteria in subgingival plaque and to then relate that to other communities in periodontal disease as a whole (Socransky *et al.*, 1998). Socransky highlighted several bacteria observed in association with either the healthy state in the mouth or with periodontal disease, grouping them into various complexes. Figure 1.5 details these complexes. The green, blue yellow and purple complexes are associated with a "disease-free" state, including mainly Gram positive bacteria such as *Streptococcus* species. The other two complexes are highly associated with a periodontal disease state, detailing an increased pocket depth and bleeding on probing. The orange complex contains *P. intermedia, Peptostreptococcus* and *Fusobacterium nucleatum*. The latter of which is accredited with bridging the gap between early colonisers such as *Streptococcus gordonii* and red complex members in biofilm formation (Socransky *et al.,* 1998). It is thought that these species act as bridging species due to their expression of specific cell surface structures for binding both early colonisers and red complex bacteria, and also the ability to utilise and release nutrients from the dental plaque biofilm, encouraging growth of other bacteria (Socransky *et al.*, 1998).

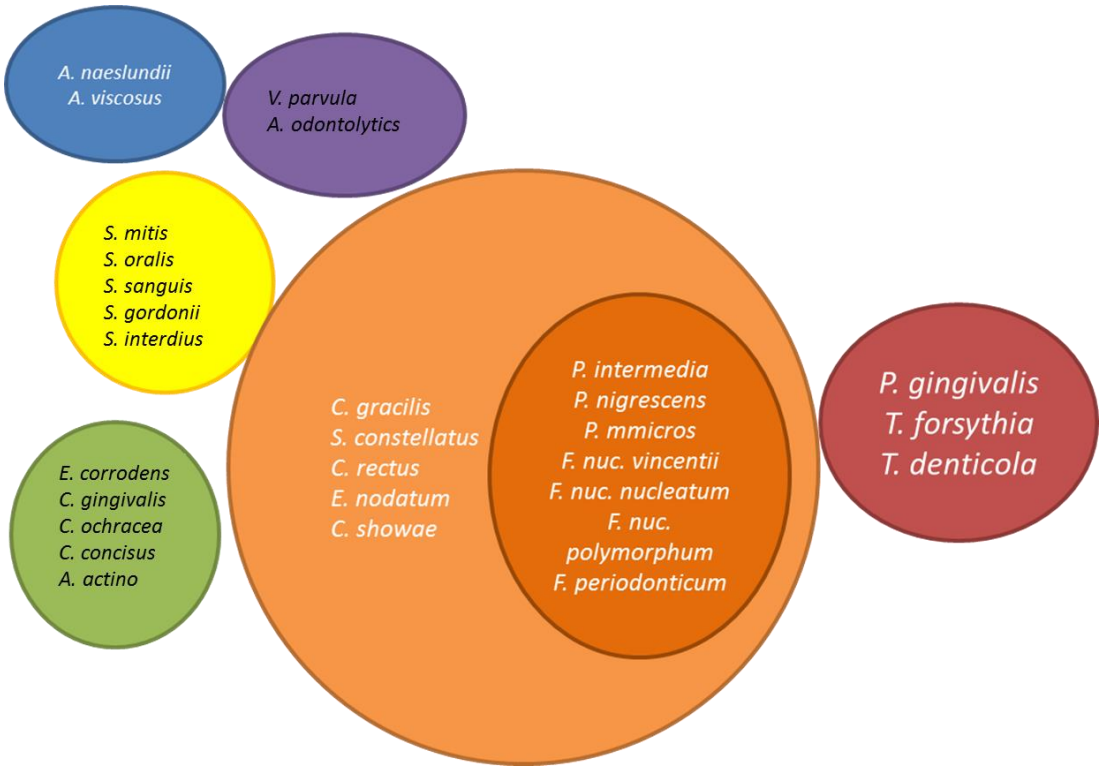

Figure 1.5 The major complexes of bacteria found in the periodontal cavity. Complexes yellow, blue, green and purple are associated with oral health, whereas the orange and red complexes are associated with periodontal diseases. Subgingival plaque complexes adapted from (Socransky *et al.*, 1998).

The study identified that members of the red complex of bacteria are rarely observed in the absence of members of the orange complex. It was surmised that the orange species preceded the colonisation of the red complex members. Socransky demonstrated the relationship between bacterial complexes and the clinical parameters of the disease via studies of pocket depth on the gingival tissue. A strong correlation between the presence of orange complex members and greater pocket depth was observed, and a further increasing pocket depth when red complex bacteria were present. This study exemplified the idea that periodontal disease was a polymicrobial infection whereby no one bacterial species is the causative agent, with data showing pocket depth and bleeding on probing increasing with an increasing number of pathogens of a diverse range of species. It did however demonstrate that most of the disease-causing bacteria are Gram-negative anaerobes (Socransky *et al.*, 1998). More recently, a study has confirmed these complexes through 16S pyrosequencing technology, which involves the extraction of DNA and circumvents the need for culturing the bacteria whilst allowing the collection of thousands of sequences per sample collected, giving high level of information on the composition of the oral community

at the species level. This study confirms the presence of the Gram negatives dominating the disease-related microbiome, however it showed the additional species to the disease-related microbiome, specifically with the novel addition of a Gram-positive *Spirochetes*, *Filifactor alocis* which is appears to be at least as common as *P. gingivalis* and *T. denticola* and strongly associated with disease (Griffen *et al.*, 2011), and still remains relatively under investigated to date.

A noted relationship within the red complex is that of *P. gingivalis* and *T. forsythia* where both are detected in higher numbers and more frequently in deeper periodontal pockets. *P. gingivalis* is never detected without *T. forsythia,* whilst *P. gingivalis* was always present in the sites with the deepest mean pocket depth (Socransky *et al.*, 1998) which has led to the "keystone pathogen hypothesis" which is defined as "the species whose effects on their communities are disproportionately large relative to their abundance" (Hajishengallis *et al.*, 2012). If the keystone pathogen of a disease can be identified, the structure of the microbial community can be further understood and therefore the mechanisms that maintain the healthy relationship with the host, or indeed, the mechanisms that cause dysbiosis can also be investigated. *P. gingivalis* is considered to be the keystone pathogen of periodontal disease due to its ability to instigate inflammation despite being present at relatively low numbers, at the same time causing a significant alteration to the community organisation and the number or oral commensals (Curtis *et al.*, 2011). A recent mouse model supports the keystone qualities of *P. gingivalis* as periodontitis was induced at very low colonization levels (0.01%), coupled to significant alterations to the organization of the oral microbiota (Hajishengallis *et al.*, 2011). Because *P. gingivalis* is considered the keystone pathogen, this facilitates the possibility of novel treatments for polymicrobial diseases that target the limited number of species that cause the dysbiosis, stabilising the homeostatic balance and leaving the "health-associated" bacteria unharmed (Hajishengallis *et al.*, 2012).

1.6.2.1 The Red Complex

The red complex bacteria are considered to be the major contributors to the progression of periodontal disease, with an increase in numbers and prevalence in these members are coupled to an increase in the clinical parameters of periodontitis (Steenbergen *et al.*, 1984). A study by Rôças *et al.,* (2001) detailed this consortium of bacteria as being heavily associated with endodontic infection , with clinical isolates from root canals, identifying the presence of at least one member of the complex in 33 out of 50 cases, with the detection of *T. denticola, T. forsythia* and *P. gingivalis* at 44%, 30% and 26% respectively in the number

of cases (Rôças, *et al*, 2001). These bacteria are thought to be the major contributors to the later stages of periodontal disease as they are found deep inside the periodontal pocket (Suzuki *et al.*, 2013). The appearance of these bacterial in many cases of periodontal disease suggests the presence of virulence factors which contribute to disease progression, including lipopolysaccharide, the capsule, secreted proteins for tissue destruction or fimbriae for attachment (Hajishengallis and Lamont, 2012).

1.6.3 *Treponema denticola*

The periodontal pathogen, *T. denticola* is a Gram-negative aerotolerant anaerobic spirochete (Syed *et al.*, 1993) that is a member of the red complex responsible for furthering the progression of periodontal disease. *T. denticola* is one of at least ten species of the *Treponema* genus found in the oral cavity (Visser and Ellen, 2011) and displays a wide variety of virulence factors that allow host tissue penetration, immune evasion and ultimately survival and replication within the oral environment.

The colonisation of the oral cavity by *T. denticola* has been well studied, and the bacterium is capable of forming a multispecies biofilm via adherence to other bacteria as well as various host proteins. *T. denticola* is capable of co-aggregating with various periodontal pathogens, such as *P. gingivalis*, *F. nucleatum* and *T. forsythia* through various surface proteins to form subgingival plaque (Hashimoto *et al.*, 2003; Ikegami *et al.*, 2004; Rosen *et al.*, 2008). More recently, it has been shown that the haemagglutinins of these bacteria are essential in this interaction, such as the Hgp44 domain of the *P. gingivalis* gingipains and haemagglutinin A (Ito *et al.*, 2010).

The adherence and colonisation of the host is crucial in the virulence of this pathogen, *T. denticola* has been demonstrated to interact with various extracellular matrix (ECM) proteins, such as collagen, fibronectin and laminin (Haapasalo *et al.*, 1991) to initiate the process of cell adherence and tissue penetration. *T. denticola* is also able to adhere to epithelial cells (Cells *et al.*, 1819) as well as endothelial cells (Peters *et al.*, 1999). This adherence is facilitated by the outer membrane proteins such as the major outer sheath protein (Msp) and the oligopeptide transporter unit (OppA). The Msp proteins are classic β-barrel outer membrane proteins with surface-exposed loops, and demonstrate a plethora of roles in pathogenesis, from the adherence to ECM molecules and co-aggregation with other pathogens as mentioned above, as well immune activation and evasion, to the formation of pores in cell membranes of epithelial cells (Egli *et al.*, 1993; Mathers *et al.*, 1996), which may contribute to nutrient acquisition via cell lysis or delivery of toxins into

the host cell (Mathers *et al.*, 1996). The innate immune response is induced by *T. denticola* Msp proteins, such as MspA and MspTL, which initiate the production of pro-inflammatory cytokines IL-6, IL-8, TNF-α and IL-1β by macrophages and epithelial cells (Lee *et al.*, 2009; Gaibani *et al.*, 2010), which lead to the destruction of host tissues through an inflammatory response.

One of the other major virulence factors of *T. denticola* is the protease, dentilisin. This protease complex, made up of three lipoproteins encoded by *prcB-prcA-prtP* gene locus (Fenno, 2012), displays a wide range of cytopathic effects on the host tissue, namely due to this proteolytic activity. In particular, this protease complex induces the permeability of intercellular junctions and the shrinkage of cells, which vastly increases the penetration ability of this bacterium (Chi *et al.*, 2003), contributing to the pathogenesis of the chronic infection.

Synergistic infections with this bacterium and other members of the red complex have demonstrated a significantly enhanced virulence and rapid progression of periodontal disease (Nath and Raveendran, 2013), and therefore it is important to have awareness of more than a single pathogen in the study of molecular determinant of periodontal disease.

1.6.4 *Tannerella forsythia*

Studies of the Gram-negative anaerobe, *T. forsythia* were relatively slow to come about due to its difficulty to culture *in vitro* and mechanisms for genetic manipulation were unavailable until around 2001 (Honma *et al.*, 2001). *T. forsythia* has an essential requirement of the sugar N-acetylmuramic acid (NAM), which is a component of the cell wall; however this bacterium cannot synthesise NAM alone, so *T. forsythia* is often found growing synergistically with the other members of the red complex (Sharma, 2010). This synergy also is thought to contribute to an enhancement of the virulence of *T. forsythia,* as abscess formation in rabbits and alveolar bone loss in rats was greatly enhanced when coinfected with *F. nucleatum* or *P. gingivalis* (Takemoto *et al.*, 1997; Kesavalu *et al.*, 2007).

T. forsythia is found associated with various form of periodontal disease, from early gingivitis to aggressive periodontitis (Tanner and Izard, 2006), and numerous studies have found *T. forsythia* to be implicated in the clinical attachment loss of the periodontal support structures in aggressive periodontal disease (Dzink *et al.*, 1988; Listgarten *et al.*, 1993). To date, only a relatively low number of putative virulence factors have been identified in *T. forsythia*, largely due to difficultly in genetic manipulation. *T. forsythia* possesses a surface-

layer (S-layer) composed of at least two glycoproteins, encoded by *tfsA* and *tsfB* (Lee *et al.*, 2006). This S-layer provides a protective layer, whilst trapping metabolites from the environment and contributes to epithelial cell adherence and invasion (Sabet *et al.*, 2003; Sakakibara *et al.*, 2007). *T. forsythia* also encodes several homologs of a protein known as BspA, which has been shown to bind to the extracellular matrix components (Sharma *et al.*, 1998) as well as the other red complex pathogen, *T. denticola* (Hirt *et al.*, 2002), indicating important interaction roles in the virulence of this pathogen. BspA also induces the release of various pro-inflammatory cytokines, such as IL-1β, IL-8 and TNF-α, contributing to the to the inflammatory destruction of periodontal disease (Bryzek *et al.*, 2014). Sialidases, such as NanH, are also a critical virulence factor as they allow the cleavage of the terminal sialic acid residues from sialoglycoconjuates which are ubiquitously present in the oral cavity, in mucin and on epithelial cells for example (Roy *et al.*, 2011). The sialic acid residues can be then used as a nutrient source, or to coat ligands on the cell surface for immune evasion and mediate cell-to-cell interactions (Honma *et al.*, 2011). The bacterial sialidases themselves are involved in the induction of chemokines from epithelial cells (Kuroiwa *et al.*, 2009), revealing of cryptitopes for cell adhesion and invasion (Honma *et al.*, 2011), degradation of host glycoproteins for nutrients (Bradshaw *et al.*, 1994) and promoting the formation of biofilm (Soong *et al.*, 2006).

The combination of these virulence factors coupled to the synergistic growth of this bacterium with other members of the red complex make *T. forsythia* a formidable pathogen in periodontal disease.

1.6.5 *Porphyromonas gingivalis*

The bacterium *P. gingivalis* is a black-pigmented, Gram-negative obligate anaerobe belonging to the *Bacteroidetes* genus. *P. gingivalis* belongs to the red complex of bacteria, and is recognised as a major aetiological agent of chronic and severe cases of adult periodontal disease (Lamont & Jenkinson, 1998), and in fact, *P. gingivalis* was found in 85.75% of subgingival plaque samples obtained from patients suffering from chronic periodontitis (Lenz *et al.*, 2016). It grows on horse-blood supplemented agar, changing colour from beige to black after 4 – 5 days of growth (Holt *et al.*, 1999) due to the essential acquisition of hemin from host cells. The acquirement of hemin is also coupled to pathogenesis as the host tissue is damaged due to haemolytic activity, releasing the hemin to support bacterial growth (Bramanti and Holt, 1991). The haemolytic activity of *P. gingivalis* is one of many virulence factors which contribute to the progression of

periodontal disease. Working either on its own or in an agonistic manner with other members of the orange and red complex, *P. gingivalis* can attach and invade host cells and apply a variety of virulence factors to cause disease, such as the lipopolysaccharide (LPS), capsule polysaccharide (CPS), gingipains, fimbriae and outer membrane proteins. More recently, strains of *P. gingivalis* have been classed as either non-invasive or invasive regarding their ability to form abscesses in murine models, and further demonstration has shown the invasive strains contain more pathogenic activities than their non-invasive counterparts, which will be discussed further in the next few sections (Dorn *et al.*, 2000; Baek *et al.*, 2015).

1.6.6 Virulence Factors of *P. gingivalis*

The virulence factors of *P. gingivalis* allow the bacteria to not only attach to cells and acquire nutrients for growth, but also to invade cells to multiply and evade the host immune system and cause tissue destruction leading to the progression of disease in a hostile host environment. The following section will deal with various structural and secreted virulence factors, and in particular how they relate to attachment and invasion of host cells, and the avoidance and subversion of the host immune system.

1.6.6.1 Capsular Polysaccharide

For a bacterium to colonise the oral cavity, it must be capable of adhering to oral structures such as teeth or mucosal surfaces, or to other bacteria to be able to resist the removal by the force of the saliva flow (Yoshimura *et al.*, 2009). Not all strains of *P. gingivalis* contain a capsule, and the chemical composition varies between different strains, producing at least six serotypes of capsule antigens (K1-K6) (Laine *et al.*, 1997). The capsule of *P. gingivalis* has been shown to influence the ability of *P. gingivalis* to adhere to epithelial cells found in the periodontal pocket (Dierickx *et al.*, 2003), whilst other studies have demonstrated the adherence and aggregation with the “bridging” pathogen, *F. nucleatum* from the orange complex, is capsular dependant (Rosen and Sela, 2006).

Capsulation of bacteria was originally seen to only protect bacteria from the host immune system by reducing the ability of immune effectors to reach the bacteria, however more recently, the capsule is seen to induce an immune response and promoting virulence. This leads to a long-term survival and a long-term, low level of inflammation leading to a chronic infection. Two complementary studies showed encapsulated strains of *P. gingivalis* trigger different immune responses from the host in comparison to mutant strains absent in

capsules (Glaros, *et al.,* 2009; Vernal *et al.,* 2009). However, these studies used mutants with differing genotypic backgrounds to the capsule-possessing strains so the data couldn't ultimately confirm the role of the capsule. A recent study from Brunner *et al.,* (2010) demonstrated that the presence of a capsule can cover the short fimbriae, hiding them from the host immune system, and suppressing a pro-inflammatory response. The capsulated strain also was shown to down-regulate the cytokine response, another pro-inflammatory response, in addition to an increased induction of various interleukins (IL-6, IL-8) in the absence of a capsule (Brunner *et al.*, 2010). This study was supported by Singh *et al.,* (2011) who show an increase in the level of cytokine suppressors, inhibiting an inflammatory response which keeps the bacteria hidden from the immune system for longer, in comparison to the non-capsulated strain (Singh *et al.*, 2011). In addition to this survival method, the capsule has been shown to also reduce the effects of defensins, the bactericidal small antimicrobial peptides (Igboin, 2011), leading to increased survival and prolonged infection.

1.6.6.2 Lipopolysaccharide

The LPS of Gram-negative bacteria is the major outer membrane component, which provides structural integrity, protection from chemical attack and causes a strong immune response from the host due to its endotoxin properties (Caroff and Karibian, 2003). The pure LPS of *P. gingivalis* reduces the expression of E-selectin, a cell adhesion molecule expressed on the surface of endothelial cells, which reduces the ability of neutrophils to attach to endothelial cells, and thereby decreasing migration to the site of infection (Darveau *et al*., 1995). The LPS of *P. gingivalis* has also been shown to play a vital role in facilitating inflammation by inducing cells to secrete pro-inflammatory cytokines, such as IL-1β and TNF-α, causing tissue destruction (Kadono *et al.*, 1999), whilst disrupting the bone remodelling process (Kato *et al.*, 2014). The LPS has been shown to bind TLRs, activating intracellular inflammatory signalling pathways of the host cell, such as the c-Jun N-terminal kinase (c-JNK) pathway and upregulating cytokine gene expression (Okahashi *et al.*, 2004). The LPS of *P. gingivalis* has also been shown to cause "chemokine paralysis" whereby it contributes to the prevention of gingival epithelial cells to secrete IL-8 which would usually activate neutrophils and basophils (Darveau *et al.*, 1998). This results in an absence of an effective innate response allowing a sharp increase in bacterial load in the gingival area, consistently seen in the aetiology of periodontal disease.

The LPS is made up of three components, the core oligosaccharide, the O-antigen and the Lipid A molecules (the endotoxin portion of LPS) (Ogawa and Yagi, 2010). *P. gingivalis* is capable of expressing a heterogeneous mixture of structures of the latter which interact with TLRs of the innate immune system. Different lipid A structures interact with TLRs in very different ways, from triggering TLR2, to antagonising TLR4 activation, which is the reverse of most Gram-negative bacteria (Darveau *et al*., 2004). The Lipid A produced by *P. gingivalis* can be a mixture of two glycan repeating units, O-antigen tetrasaccharide repeating units or anionic (A-antigen) polysaccharide repeating units (Rangarajan *et al.*, 2008), and the structure relies upon the influence of microenvironmental hemin concentrations, which itself is reliant upon inflammation (Gaffen and Hajishengallis, 2009). This differentially regulated structure production indicates an ability to manipulate the host innate immune response and eventually suppress the TLR-mediated immunity. Recent studies have shown the differences in the LPS profile contributes to a resistance to polymyxin B (Díaz *et al.*, 2015), however the role of the different structures and components of LPS is still poorly understood.

1.6.6.3 Attachment and Invasion

Host cell invasion by an infecting bacterium is hugely advantageous in a number of ways. An intracellular location provides protection from the host immune system, facilitate replication in a nutrient-rich environment, whilst also affording cell-to-cell spreading of the bacteria or allow tissue destruction. The mechanism of invasion, in general terms, begins with the attachment of bacteria to the cell membrane thereby inducing a collection of biochemical and structural changes, resulting in the entry of the host cell (Beachy, 1981). In many cases after attachment, the subsequent signalling cascade in the host cell causes protein phosphorylation, ion fluxes and protein synthesis leading to cytoskeleton rearrangement, facilitating entry of the bacterium (Bliska *et al.*, 1993).

A well-studied mechanism of invasion through actin rearrangement is by the pathogenic *Salmonella* strains. These bacteria are not only highly adherent to the host cell but have particularly efficient invasive machinery through secretion of effectors by the Type Three Secretion System (TTSS) into the host cell (Pizarro-Cerdá and Cossart, 2006). The bacteria are especially effective in invasion as they use both “trigger” and “zipper” mechanisms of invasion, the former involving the injection of effectors triggers a large-scale cytoskeleton rearrangement from the inside of the host and formation of membrane ruffles, allowing internalisation of the bacterium. Specifically, the SpiC protein of the TTSS drives actin

polymerisation and bundling of the actin filaments, whilst SopE activates GTPases for actin polymerisation and the formation of the membrane ruffles (Agbor and McCormick, 2011; Ribet and Cossart, 2015). The latter "zipper" mechanism causes only minor cytoskeletal rearrangements relying on specific contact to a host cell receptor, and has only been recently recognised for certain strains of *Salmonella* (Rosselin *et al.*, 2010).

Rather than using a host cell receptor for invasion, the Enteropathogenic *E. coli* (EPEC) generates its own receptor for adhesion by injecting the translocated intimin receptor (Tir) into the host via the TTSS, which inserts itself into the host cell membrane for the bacterial adhesins to interact with (Kenny *et al.*, 1997)

There is a huge diversity amongst bacteria in the adherence and invasion for colonisation of the host. The identification of host cell receptors used by pathogenic invading bacteria is a valuable tool in the combating of disease, as it can be used to design therapeutic agents to interrupt the host-pathogen interaction and prevent the disease occurring.

1.6.6.4 Adherence and Invasion of *P. gingivalis*

The invasive capabilities of *P. gingivalis* were first demonstrated by Lamont and his group in the early 1990's, where primary cultures of gingival epithelial cells were subject to *P. gingivalis* through an antibiotic protection assay which counts the number of bacteria that can invade a host cell, and the total number of bacteria that associate with the host cells to determine attachment and invasive capabilities (Lamont *et al.*, 1992). Further work has shown invasion of a multi-layered pocket epithelium (Papapanou, *et al.*, 1994) and even invasion of aortic and heart endothelium (Deshpande *et al.*, 1998). It has been proposed that one of the major factors contributing to the pathogenesis of *P. gingivalis* is in its ability to invade host cells, and facilitating the invasion of other Gram-negative species to further the progression of periodontitis (Hajishengallis *et al.*, 2012).

Various molecular mechanisms of invasion by *P. gingivalis* have been well characterised and will be discussed below. Invasion is a very complex process there appears to be no one definitive method of invasion. Whilst some mechanisms are deemed "major" there are multiple routes available to the bacteria to use in a complementative manner.

1.6.6.4.1 Fimbriae

There is a great deal of evidence indicating the involvement of *P. gingivalis* fimbriae for attachment and invasion purposes and a large number of studies have been carried out

since its first identification by Yoshimura *et al.* in 1984. Fimbriae are non-flagellar protein filaments which project out from the bacterial cell surface (see Fig 1.6). Yoshimura purified and characterised a 43 kDa protein subunit, fimbrillin, using SDS-PAGE techniques, and detailed the morphological and immunological features (Yoshimura *et al.*, 1984). This protein subunit was later discovered to be encoded by the *fimA* gene and was identified as the major type of fimbriae that *P. gingivalis* possesses. The minor type known as Mfa1 is comprised of a 74 kDa protein but is less well characterised due to its shortened length making it more difficult to purify (Hasegawa *et al.*, 2009).

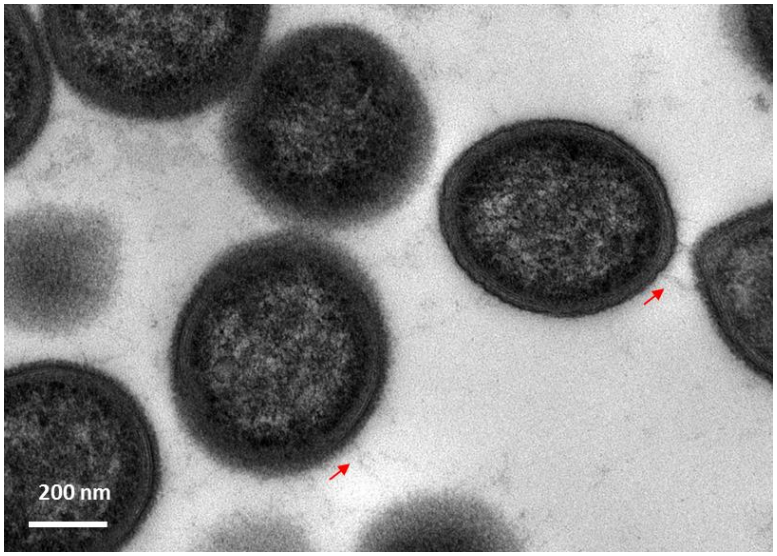

Figure 1.6 Electron microscopy of *P. gingivalis* indicating the presence of Fimbriae. Red arrows indicate the fimbrial structures. Images taken from this study.

Recently, it was demonstrated that the fimbriae of *P. gingivalis* may be involved in adherence to the cell through their specific binding to fucose moieties, which indicates a potential fucose-specific interaction with the fimbriae of *P. gingivalis* with the host cell for adherence (Sojar and Smith, 2012). Whereas the major fimbriae have been shown to be involved in adhesion to epithelial cells and the subsequent downstream signalling events involved in invasion in many studies, and indeed the mutation of the *fimA* gene causes a great reduction in the invasive capability (Weinberg *et al.*, 1997; Njoroge *et al.*, 1997). Fimbrial-deficient strains of *P. gingivalis* have been shown to display poor invasive capabilities, poor binding to tooth surfaces and salivary components, and cannot produce periodontitis in rats, suggesting their clear role in invasion and the disease process (Malek

et al., 1994). Yilmaz *et al.* demonstrated a direct physical association between fimbriae and β1 integrins, and using anti-ß1 antibodies to inhibit binding, elucidated the target of epithelial cells as the α5β1 integrins (Yilmaz, 2003). Integrin activation is thought to be linked to phosphorylation of paxicillin, a focal adhesion protein, and focal adhesion kinase (FAK), which activate signalling molecules, leading to the assembly of focal adhesion complexes (Yamada and Geiger, 1997). The construction of these complexes is thought to contribute to the generation of forces which regulate cytoskeleton dynamics through affecting actin and microtubule activity (Yilmaz, 2003). A *fimA* mutant created in this study showed only a 10-fold decrease in internalisation by epithelial cells, so therefore showing that fimbriae are not the only method for invasion. Indeed, not all variants of invasive *P. gingivalis* contain the *fimA* gene (Andrian *et al.*, 2006). The FimA protein is noted to not only be involved with the interaction of human epithelial cells, but also to other bacterial species during colonisation of the subgingival surfaces. Studies have shown that FimA is capable of interacting with the prokaryotic protein, glyceraldehyde-3-phosphate dehydrogenase on many *Streptococcus* species (Maeda *et al.*, 2004). The subsequent build-up of *P. gingivalis* into a mixed-species biofilm is thought to be due to an additional interaction of Ssp proteins on the surface of *Streptococcus* species with the minor fimbriae, Mfa1 (Park *et al.*, 2005). Mfa1 has also been shown to facilitate autoaggregation of *P. gingivalis*, thereby permitting the bacteria to accumulate to prevent elimination from the subgingival regions due to shearing forces or salivary flow allowing efficient infection (Lin *et al.*, 2006). The minor fimbriae are also attributed to the stimulation of IL-1α, IL-1β, IL-6 and TNF-α, by macrophages, and is thought to be the causative agent of alveolar bone in murine models (Amano *et al.*, 2004).

1.6.6.4.2 Gingipains

Gingipains are cell-surface anchored proteolytic enzymes that are used by the bacterium in a multitude of ways, including the cleavage of receptors found on the host-cell surface, inactivation of components of the complement system such as cytokines, to obtain nutrients and also to stimulate certain protease-activated expression by host-cell receptors (Andrian *et al.*, 2006). As well as cell-associated, gingipains can also be secreted or membrane bound on vesicles, called “blebs” (Grenier *et al.*, 1989) and can be up to 85% of the extracellular proteolytic activity displayed by *P. gingivalis* at the site of infection (de Diego *et al.*, 2014). These targets and functions of gingipains activity contribute to the maintenance of the chronic inflammatory state at the infection site, which can lead to cell

lysis and the expelling of nutrients from host cells. Coupled to this, gingipains can activate plasma kallikrein (human serine proteases), degrade fibrinogen and increase the levels of thrombin, all to increase the vascular permeability and increase bleeding to increase the availability of heme, a requirement for *P. gingivalis* growth (de Diego *et al.*, 2013). Stafford *et al*., (2013) demonstrated how secreted gingipains also manipulate the host cell responses by the degradation of the mammalian target of rapamycin (mTOR). This study created mutants in the gingipains genes, including a triple *ragABkgp* mutant which couldn't invade cells, and showed that secreted gingipains, especially the Lys gingipain, degrades the mTOR which may contribute to the change in certain cellular process such as proliferation, cell survival and autophagy which are all observed during a *P. gingivalis* infection (Stafford *et al.*, 2013). The gingipains have also been shown to be important in the growth of *T. forsythia* and *A. actinomycetemcomitans* in multi-species biofilms (Bao *et al.*, 2014; Haraguchi *et al.*, 2014)

There are two types of gingipains, the arginine-specific gingipains, of which there are two, encoded by the *rgpA* and *rgpB* genes, and the lysine-specific gingipains, encoded by the *kgp* gene (Travis *et al.*, 1997). All three genes are conserved amongst both laboratory strains and clinical isolates, demonstrating the essentiality of gingipains for bacterial survival and proliferation. The arg-specific gingipains cleave the Arg-X dipeptide bond, and the lys-specific gingipains cleaves the carboxy-terminal (COOH) side of the lysine residue. RgpA and Kgp have been shown to contain a heamagglutinin-adhesin domain which has also been implicated in the coaggregation of *P. gingivalis* with other oral pathogens involved in periodontal disease, such as *T. denticola* and *S. gordonii* (Guo *et al.*, 2010). Gingipains are also required in the processing of other virulence factors, such as FimA, which is secreted in a precursor form onto the cell surface and needs the proteolysis from Rgps to be able to assemble into the filamentous form (Shoji *et al.*, 2004).

Gingipain proteolytic activity is thought to be modulated by a number of mechanisms. The putative outer membrane protein, VimA is thought to influence the proteolytic activity of the gingipains via post-translational modification of the protein with an uncharacterised glycan group. For example, a Δ*vimA* mutant shows significant reductions in haemolytic and proteolytic activities, resulting in a non-black pigmented phenotype, despite no alterations in the gingipain expression levels but does display altered reaction with a glycan specific antibody (Abaibou *et al.*, 2001; Vanterpool *et al.,* 2006). Gingipain maturation is also thought to be modulated by the Por secretion system (PorSS), which is thought to be

involved in translocation of proteins across the outer membrane (Sato *et al.*, 2010) and anchoring of the gingipains to the surface (Chen *et al.*, 2011). The PorSS gene locus is encoded by several *por* genes, which make up a unique secretion system that bears no homology to the type I-VIII secretion systems seen in many bacteria. *P. gingivalis* is known to produce upwards of 30 putative CTD motif-containing proteins (Veith *et al.*, 2013; Taguchi *et al.*, 2016), including the gingipains which are recognized by the *porT* gene product in the periplasm to be secreted (Sato *et al.*, 2010). Whilst in the periplasm, the gingipains are processed into the final form by the cleavage of the prodomains (Glew *et al.*, 2012), and glycosylated. The Sov protein then is involved in the translocation of the processed gingipain across the outer membrane (Saiki and Konishi, 2012), before PorU cleaves the CTD from the protein (Glew *et al.*, 2012) and conjugation to the A-LPS occurs of membrane-anchored gingipains. This process can be seen diagrammatically in Figure 1.7. Mutations in the *porR* gene of the PorSS gene locus showed production of Rgp and Kgp, but they were not retained on the bacterial cell surface (Shoji *et al.*, 2002), indicating a role in anchoring the gingipains to the A-LPS, and a deletion in the terminal 2 residues of the CTD results in the proteins being trapped in the periplasmic space (Chen *et al.*, 2011), detailing their critical need in the targeting of these proteins to the PorSS system.

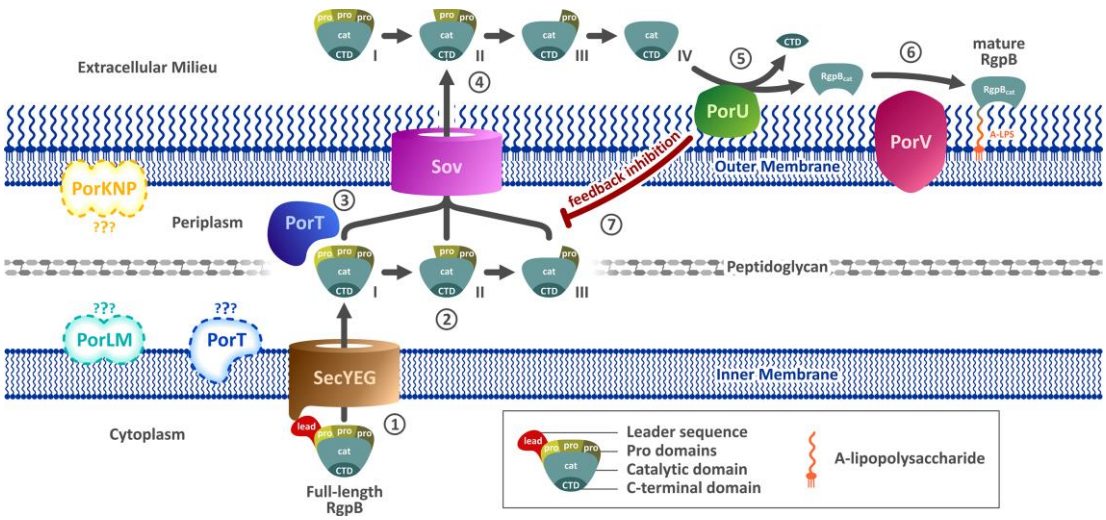

Figure 1.7 Summary of the secretion of the gingipains via PorSS. After secretion across the inner membrane via the Sec system (1), the Sec-signal is removed with the prodomains via PorT (2-3), whose location within the periplasm is still under investigation. This is followed by translocation across the outer membrane via the Sov protein (4), with further processing of the protein occurring to remove the CTD (5) via the action of PorU. The gingipains are then attached to the A-LPS via the PorV protein for membrane anchoring. Diagram created by Kathryn Naylor and Chatchawal Phansopa for a review (Douglas *et al.*, 2014), and used with permission.

Gingipains have been positively implicated in the attachment (Chen and Duncan, 2004) and negatively in the invasion (Suwannakul *et al.*, 2010) of host cells, i.e. the presence of gingipains increases the ability of attachment to epithelial cells, yet the deletion of gingipains by Suwannakul showed an increase in invasion (Suwannakul *et al.*, 2010). These demonstrate the ubiquitous nature of the gingipains and their involvement in many virulence processes of pathogenicity of *P. gingivalis.*

1.6.6.4.3 Haemagglutinins

The haemagglutinins are a large class of virulence factors of *P. gingivalis* with a variety of roles in the infection process, but with a particular importance in the acquisition of iron. As *P. gingivalis* lacks siderophore scavenging systems, the Hag proteins are involved in the acquisition of heme for growth from erythrocytes (Lépine *et al.*, 1996). Haemagglutinins are expressed on the cell surface of the bacteria, either in association with filamentous structures (fimbrial adhesins) or associated with nonfimbrial components (nonfimbrial adhesins) (Han *et al.*, 1996)

P. gingivalis possesses at least 8 haemagglutinins (Lamont and Jenkinson, 2000), however only a few of them have been well characterised in a role for host-cell interaction. The gingipains RgpA and Kgp both contain haemagglutinin domains (Hgp44, -15, -17 and -27) (Potempa *et al.*, 2003), where Hgp44 is also known as HagA and has been demonstrated to be important in the coaggregation of *P. gingivalis* with *T. denticola* as previously discussed (Ito *et al.*, 2010). Song *et al* (2005) demonstrated that HagB facilitates adherence to endothelial cells, but it alone is not sufficient for the internalisation of the bacterium (Song, Bélanger, Whitlock, Kozarov, Progulske-fox, *et al.*, 2005), suggesting other molecules are responsible for the invasive step. More recently, HagB and also HagC have been implicated in mediating the bacterium's adherence to oral epithelial cells, with an additional implication of the HagB involvement in invasion of the host cell (Connolly *et al.*, 2015).

1.6.6.4.4 Sialidases

P. gingivalis like many pathogenic bacteria, synthesise sialidase enzymes which utilize and cleave host sugars known as sialic acids for use as nutrients or as "camouflage" from the immune system, by decorating their own surface exposed molecules such as the LPS with the host-derived sialic acid (Li *et al.*, 2012). Sialidases are regarded as virulence factors in many bacteria, such as *Vibrio cholerae*, which uses sialidases to increase the activity of the

exotoxin (Galen *et al.*, 1992), whilst *P. aeruginosa* uses the sialidase enzymes to enhance the binding to the host cell (Cacalano *et al.*, 1992). *P. gingivalis* is also thought to use sialidases, neuraminidases in particular, for a multitude of virulence processes. A study by Aruni *et al.,* (2011) analysed the activities of several sialidases of *P. gingivalis* and hypothesised the use of neuraminidases PG0778 and/or PG1724 to hydrolyse the mucin on the epithelial cells, which exposes the terminal sialic acids for PG0352 to cleave and enhance the adherence to host cells. When the gene sequences for these neuraminidases are deleted, the adhesion and invasion of *P. gingivalis* is greatly affected. These mutants also showed no change in gene expression of the gingipains, but their activities were reduced by up to 90%, suggesting a role for sialidases in the post translational regulation of gingipains (Aruni *et al.*, 2011). An extensive study by Li *et al.,* (2011) demonstrated the importance of PG0352 in biofilm formation (reduced 2.5-fold in the mutant), and in capsular production, as an intact capsule was not observed using cryo-ET (Li *et al.*, 2012).

1.6.7 Effects on the Immune System: The Oral Context

The periodontal breakdown occurring in periodontal disease relies on very complex interactions between the bacterial components and the host defence mechanisms, which influence the balance between host protection and bacterial aggression, and ultimately can lead to chronic disease (Hajishengallis *et al.*, 2012). For *P. gingivalis* to be a successful pathogen it relies on more than just the capacity for virulence factors to secure a niche and persist within it, the bacterium must also evade or subvert the host immune system to be able to establish a chronic infection. Initially an infecting pathogen will encounter the innate immune system, which is thought to be preferentially targeted by many microbes (Rosenberger and Finlay, 2003); however by subverting the innate host mechanisms, this may also undermine the adaptive immune response, debilitating the overall host response mechanisms (Medzhitov, 2007).

At the start of infection, the bacteria are subject to detection and killing by the host immune system. As part of the innate immune system, neutrophils migrate to the site of infection via chemotaxis signalling, and indeed, the huge accumulation of neutrophils in the junctional epithelium, the gingival epithelial tissue and the periodontal pocket is a classic hallmark of chronic periodontitis (Murray and Patters, 1980). Gingival epithelial cells produce interleukin 8 (IL-8) to attract neutrophils and to activate them for intra- and extra-cellular killing. However, *P. gingivalis* is capable of causing “local chemokine paralysis” whereby they inhibit the production of IL-8 via several mechanisms to suppress the influx of

neutrophils to the crevicular niche. The serine phosphatase protein, SerB, inhibits synthesis of IL-8 by epithelial cells, thereby delaying the recruitment of neutrophils and allowing further time for the bacterium to colonise the host (Hajishengallis, 2012). The gingipains of *P. gingivalis* have also been shown to degrade the IL-8 cytokine using soluble and vesicle-associated gingipains, mainly Arg-specific gingipains. In the study by Mikolajczyk-Pawlinska (1998), the degradation of IL-8 appears to be in a concentration dependant manner, where the concentration of vesicle-associated gingipains is high in close proximity to the dental plaque biofilm on the tooth pellicle, providing a safe niche from neutrophil killing (Mikolajczyk-Pawlinska *et al.*, 1998). Soluble gingipains have the ability to diffuse away further and reach the gingival epithelial tissues to prevent release of IL-8, providing extra protection. *P. gingivalis* is also implicated in stimulating T helper cells, such as Th17, which causes the production of IL-17. This cytokine is thought to be involved in the destruction of alveolar bone that is often observed in severe cases of periodontitis (Gaffen and Hajishengallis, 2009).

Once reaching the host cells unharmed by neutrophils, *P. gingivalis* is known to invade epithelial cells, providing protection from the humoral immune system (i.e. recognition by antibodies). However, once inside the host cell, the bacteria are not completely protected as cell-mediated killing, such as the targeting of *P. gingivalis*-infected epithelial cells by cytotoxic T cells, macrophages and natural killer cells, which will encourage destruction of the host cell. These host-mediated killing cells are activated by IL-12 produced by macrophages. *P. gingivalis* can again inhibit this interleukin by the use of fimbriae to interact with the complement receptor-3 (CR-3), activating a kinase to selectively inhibit the production of IL-12.

If the infecting bacteria manages to subvert all other attacks from the host immune system, the cell has a last resort to prevent replication and spreading of the infection, to cause apoptotic cell death (Yilmaz, 2008). *P. gingivalis* can prevent the apoptosis process of host cells by the secretion of an ATP-hydrolysing enzyme, inhibiting ATP-induced apoptosis. Apoptosis may also be inhibited by the down-regulation of Bax expression, an apoptotic molecule, or the up-regulation of Bcl-2 expression, an anti-apoptotic molecule (Nakhjiri *et al.*, 2001). However, in certain circumstances, *P. gingivalis* may use the apoptosis event as a "safe exit" from the cell, to allow spreading of the infection (Gaffen and Hajishengallis, 2009).

1.6.8 Intracellular Spreading of *P. gingivalis*

The invasion of *P. gingivalis* is completed in around 15 minutes and once inside the cell, *P. gingivalis* is thought to localise at the perinuclear region where it has been observed to persist for up to 8 days without causing cell death (Belton *et al.*, 1999). Recently, a study by Yilmaz *et al.,* showed that *P. gingivalis* is capable of using the same actin-dependant mechanism used to invade the cell initially, to allow cell-to-cell spread. The results of the study demonstrated intercellular spreading utilises cytochalasin D for polymerisation of actin filaments to form projections for *P. gingivalis* to be transmitted to adjacent cells (Yilmaz *et al.,* 2002). This is been further supported by a study demonstrating the presence of *P. gingivalis* in the connective tissue between adjoining cells (Katz *et al.*, 2000).

The internal environment of a mammalian cell is vastly different for the *P. gingivalis* to enter compared to the extracellular space. There will be many environmental pressures the bacteria needs to adapt to via genetic and protein regulation. Hosogi & Duncan demonstrated using transcriptional profiling that during attachment to HeLa cells, there was an up-regulation in genes encoding heat-shock proteins and oxidative stress response genes, indicating an exposure to oxidative stress upon attachment to host cells (Hosogi and Duncan, 2005). A protein profiling study using whole-cell proteomic analysis was carried out between internal and external *P. gingivalis* showed interesting results. Virulence factors such as FimA, RgpAB and Kgp all show a decrease in expression when *P. gingivalis* is internalized (Xia *et al.*, 2007). It is evident that from this study, virulence factors that help the bacteria gain entry into the host cell soon become superfluous and are down regulated to prevent an excessive expenditure of energy.

A recent study from The University of Sheffield has shown a “signature” set of genes that are shown to be differentially regulated in the invading populations of *P. gingivalis.* Using a modified standard antibiotic protection assay, Suwannakul *et al.,* initially identified a sub-population of bacteria that were more adapted at invading host epithelial cells, before identifying the genes that appear to be involved (Suwannakul *et al.,* 2010). This involved exposing oral keratinocytes to two strains of *P. gingivalis* (NCTC 11834 and W50), isolating the invading bacteria and immediately allowed them to invade a fresh monolayer of keratinocytes as shown in Figure 1.8. The invaded bacteria form the second round were isolated and analysed through viable plating and microarrays. Bacteria found in the supernatant of the first round of invasion (non-invaded bacteria) were shown to be less invasive in the second round of invasion, compared to the bacteria isolated from inside the

host cell in the first round, indicating that different subpopulations exist within an entire population of *P. gingivalis*, including invasive and non-invasive subpopulations (Suwannakul *et al.,* 2010).

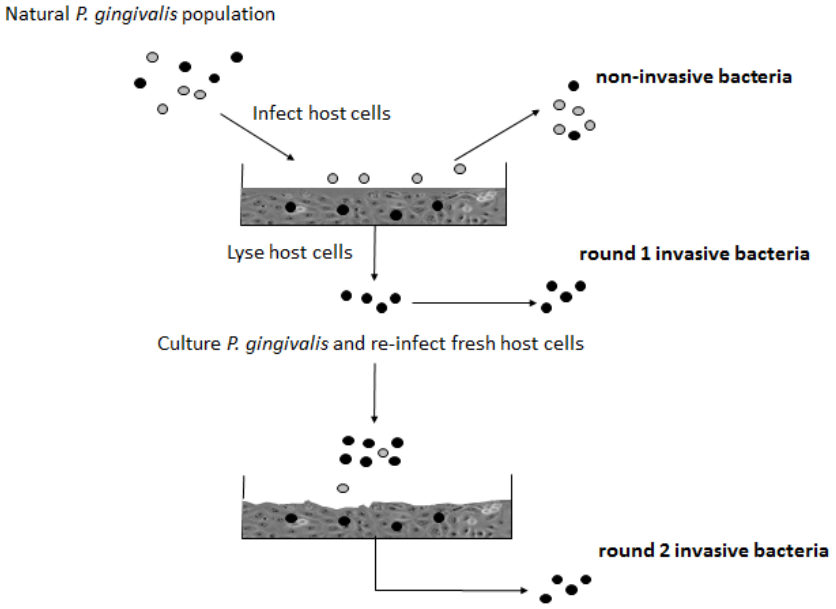

Figure 1.8 Schematic of the invasive population of *P. gingivalis.* A natural *P. gingivalis* population is thought to contain subpopulations of invasive and non-invasive bacteria. Invasive subpopulations invade host cells (round 1), and after culturing on blood agar plates, are capable of re-invading host cells before being isolated and cultured for a second round (round 2). Invasive populations retain their invasive capabilities when subcultured on blood agar for 12-18 generations before mixed invasive populations redeveloped. Figure adapted from (Suwannakul *et al.,* 2010).

The microarray experiments were carried out to assess global gene expression changes between the invasive and non-invasive subtypes, which identified 139 and 136 genes differentially regulated (>3.5 fold) in *P. gingivalis* ATCC 33277 (wild-type) and W50 (non-fimbriated strain) respectively. Because it was shown that a lower gingipain activity correlated with a higher invasive capability, the group tested the gene expression in two sets of microarray experiments; high versus low proteinase activity and invasive versus non-invasive sub-populations. This identified 19 genes which are differentially regulated in all four datasets, which can be seen in Table 1.1. Of note, it is interesting to see the down-regulation of cell-associated *rgpB,* which explains the reduced gingipain activity in the invasive subtype of the population. It is a necessity for the gingipain proteins to be down regulated as a potential overexpression intracellularly could result in excessive damage to the inside of the host cell. Also to note, the putative periplasmic chaperone protein, OmpH,

was upregulated in all four datasets. This protein is a periplasmic chaperone protein that assists in the assembly of many of the outer membrane proteins, some of which are thought to be involved in invasion, such as the OmpA protein. Various stress-related genes were upregulated in their expression, such as *oxyR* and *sodB*, which may be needed in response to the change to an intracellular environment, such as the exposure to reactive oxygen species. A common occurrence amongst the upregulated genes also included the heme-acquisition genes such as *feoB-1* and *hmuR*, suggesting that the intracellular environment may be hemin-limiting. Analysing the effects these genes have on invasion when a mutant is created with the gene deleted may hold further information on how the *P. gingivalis* bacteria is so adept at invading, and may yield potential pathways to target for disruption in an anti-microbial therapy.

Table 1.1 Regulated genes in the signature gene set

Gene No.	Name	Location	Function	Reg.[A]	SD[B]
PG0063	PG0063	OM	putative outer membrane efflux pump	6.30	2.9
PG0104	topB	CY	DNA topoisomerase III	3.64	0.2
PG0193	ompH	PP	cationic outer membrane protein OmpH	4.16	0.5
PG0205	prfC	CY	peptide chain release factor 3	4.33	0.7
PG0270	oxyR	CY	redox-sensitive transcriptional activator OxyR	6.61	1.4
PG0328	hutI	CY	imidazolonepropionase	7.58	4.7
PG1043	feoB-1	CY	ferrous iron transport protein B	4.81	1.9
PG1058	PG1058	OM	putative Outer membrane protein	4.65	1.9
PG1106	murF	CY	murein sacculus synthesis	9.86	8.1
PG1481	TraG	CY	conjugative transposon protein TraG	4.14	0.5
PG1545	sodB	CY	superoxide dismutase, Fe-Mn	8.01	0.6
PG1552	hmuR	OM	TonB-dependent receptor HmuR	5.78	3.5
PG1560	rfbB	CY	dTDP-glucose 4,6-dehydratase	10.29	6.6
PG1638	trx	PP	thioredoxin family protein	7.92	4.6
PG1807	atpK	IM	v-type ATPase, subunit K	10.09	4.1
PG2190	ftsE	IM	cell-division ATP-binding protein	6.70	0.8
PG0506	rgpB	EC	arginine-specific cysteine proteinase	-3.57	0.1
PG0910	PG0910	CY	FHA domain protein	-4.10	0.5
PG1824	eno	CY	enolase	-3.49	0.2

Abbreviations: Reg[A], Regulation; SD, Standard Deviation; OM, outer membrane; CY, cytoplasmic; PP, periplasmic; IM, inner membrane; EC, extracellular.

1.6.9 The Gram-negative Outer Membrane

The cell envelope of Gram-negative proteins consists of two membranes, the inner and the outer membrane, which display differing compositions. These membranes are separated by the periplasmic space, containing a peptidoglycan layer. The outer membrane is an asymmetric bilayer, made up of an inner phospholipid layer and a lipopolysaccharide layer (LPS) layer and usually several major proteins, known as outer membrane proteins (OMPs). The outer membrane provides a protective barrier against environment stresses, such as biophysical, chemical and biological attacks (Nikaido, 2003), whilst also allowing the selective uptake of nutrients essential for growth and the secretion of toxins, effectors and metabolic waste products (Masi and Pagès, 2013). A schematic of the cell envelope can be seen Figure 1.9. The outer membrane proteins also often serve as antigen-recognition sites to the host immune system, as studies have shown outer membrane proteins are capable of inducing pro-inflammatory cytokines (IL-1β and IL-6) from T-helper cells activated with proteins found in the outer membrane of *P. gingivalis* (Gonzales *et al.*, 2014).

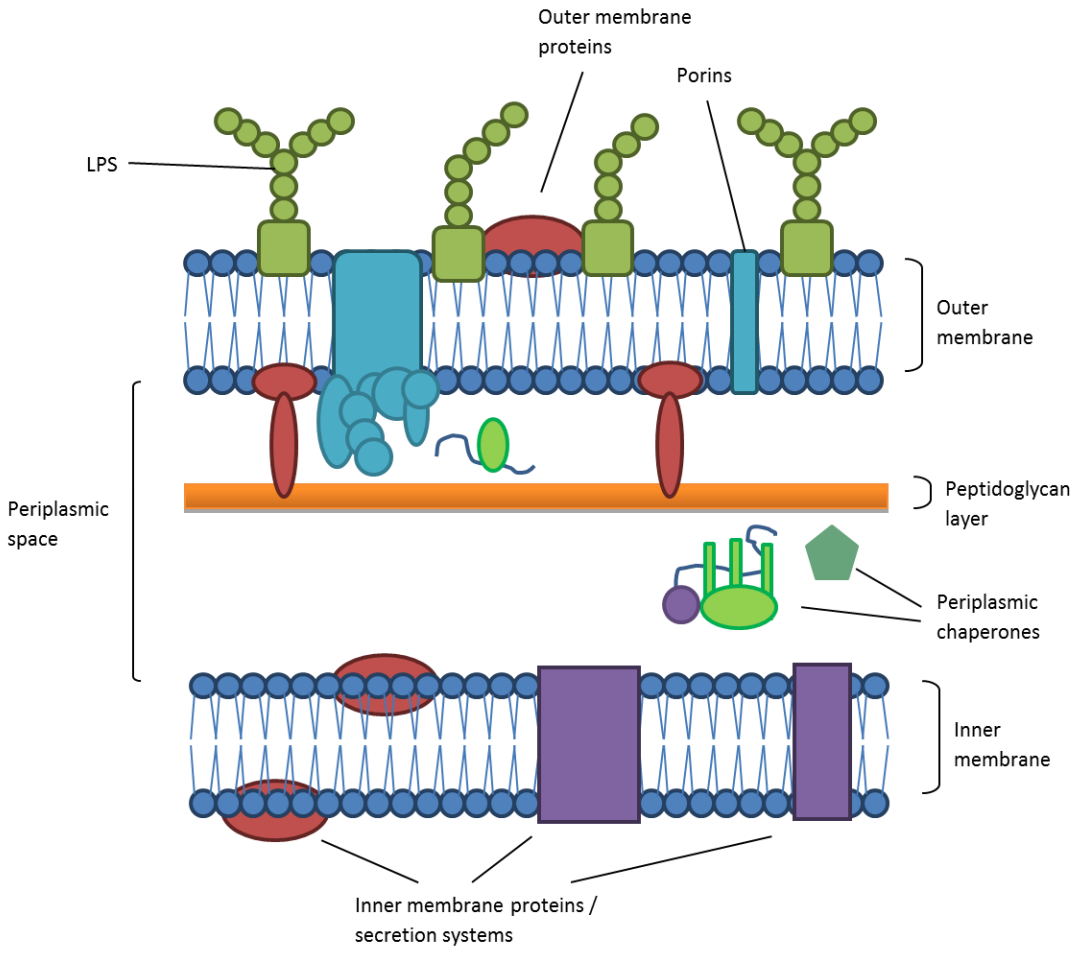

Figure 1.9 Schematic of the typical cell membrane of a Gram-negative cell.

Outer membrane proteins are usually classed as either outer membrane lipoproteins, which are anchored via an N-terminal lipid tail, or classed as integral outer membrane proteins, which contain membrane spanning regions, often β-barrels (Bos and Tommassen, 2004). Almost all of these types of proteins show an even number of β-sheets running in an antiparallel fashion (Fairman *et al.*, 2011), which is evolutionally conserved due the high stability they provide in the membrane. The outer membrane proteins are an integral part of the bacterium, with as much as 3% of the overall Gram-negative genome encoding them (Wimley, 2003), and therefore it is expected they demonstrate a wide variety of roles, ranging from virulence, transporters and channels for nutrient uptake, enzymatic roles such as proteases, etc. (Rollauer *et al.*, 2015) Due to the exposed location on the extracellular face of the bacterium, outer membrane proteins are often found associated with pathogenesis, such as the porin OprF in *Pseudomonas aeruginosa*, which is responsible for the virulence of the bacterium, with knock-out mutants causing significantly less necrosis in eukaryotic models and a reduction in the toxins secreted (Fito-Boncompte *et al.*, 2011). The OprF protein has been shown to be involved in adherence to epithelial cells (Azghani *et al.*, 2002; Fito-Boncompte *et al.*, 2011) and in the formation of a biofilm (Hassett *et al.*, 2002).

The outer membrane and its protein components are involved in a plethora of roles within pathogenesis, including the interaction with the host cell and the host defence mechanisms so it is important to understand the composition.

1.6.10 Outer Membrane of *P. gingivalis*

Analysis of the outer membrane proteins of *P. gingivalis* has been limited due to the hydrophobic nature of these proteins. One of the earliest studies of the outer membrane proteins was performed by Yoshimura *et al* (1989) which identified a 75 kDa protein involved in the activation of B-cells to produce IL-1 in murine macrophages (Yoshimura *et al.*, 1989; Watanabe *et al.*, 1992). This was followed by the identification of a 40 kDa protein by Saito *et al* (1997), which was shown to be involved in the aggregation of *P. gingivalis* with *A. viscous*, an early coloniser of tooth structures, and it therefore important in the ability of *P. gingivalis* to form a biofilm (Saito *et al.*, 1997; Maeba *et al.*, 2005). This protein since has been isolated and shown to provide protection against alveolar bone loss in animal models when used as a vaccine (Zhang *et al.*, 2009; Liu *et al.*, 2010), and proved especially effective when introduced nasally in conjunction with the cholera toxin (Cai *et al.*, 2013) demonstrating the importance of the understanding of the outer membrane of *P. gingivalis* against fighting periodontal disease.

A defining study by Murakami *et al* (2002) identified seven major outer membrane proteins, Pgm 1 – 7. Pgm 1 was identified using the then recently obtained genomic sequence of *P. gingivalis* as RagA. RagA (alongside RagB) is a TonB-linked receptor complex, with extensive homology to *susC* of *Bacteroides thetaiotaomicron* which is known to be involved in the uptake of maltose (Murakami *et al.*, 2002). Further studies have shown the deletion of the RagAB proteins result in a bacterium severely reduced in virulence, suggesting the need for the Rag proteins for the transport of large degradation products of proteins across the cell membrane as part of the virulence of *P. gingivalis* (Nagano *et al.*, 2007). The RagB protein has been associated with the invasion of epithelial cells (Nagano *et al.*, 2007; Dolgilevich *et al.*, 2011) and is involved in the induction of pro-inflammatory mediators (Hutcherson *et al.*, 2015), but one of its major functions inferred from the structural determination is that of a sugar transporter across the *P. gingivalis* membrane (Goulas *et al.*, 2015). Pgm 3 and 5 are noted to be the Lys- and Arg-gingipain proteins respectively, and are important in virulence as described previously. Pgm 6 / 7 were identified as the immunoreactive antigens PG32 and 33 respectively, also known as Omp40 and Omp41 (Veith *et al.*, 2001), or OmpA1 and OmpA2, and discussed further in a later section.

1.6.11 The OmpA Protein in Gram-negative Bacteria

The OmpA family of proteins are surface-exposed, temperature-affected porin proteins that are expressed in relatively high numbers in the outer membrane of all Gram-negative bacteria (Beher *et al.*, 1980). The structure is characterised by a C-terminal domain which forms a globular shape that associates with the peptidoglycan layer, and an N-terminal domain that forms an eight-stranded, ß-barrel structure embedded in the outer membrane with exposed extracellular loops (Wang, 2002), as shown in Figure 1.10.

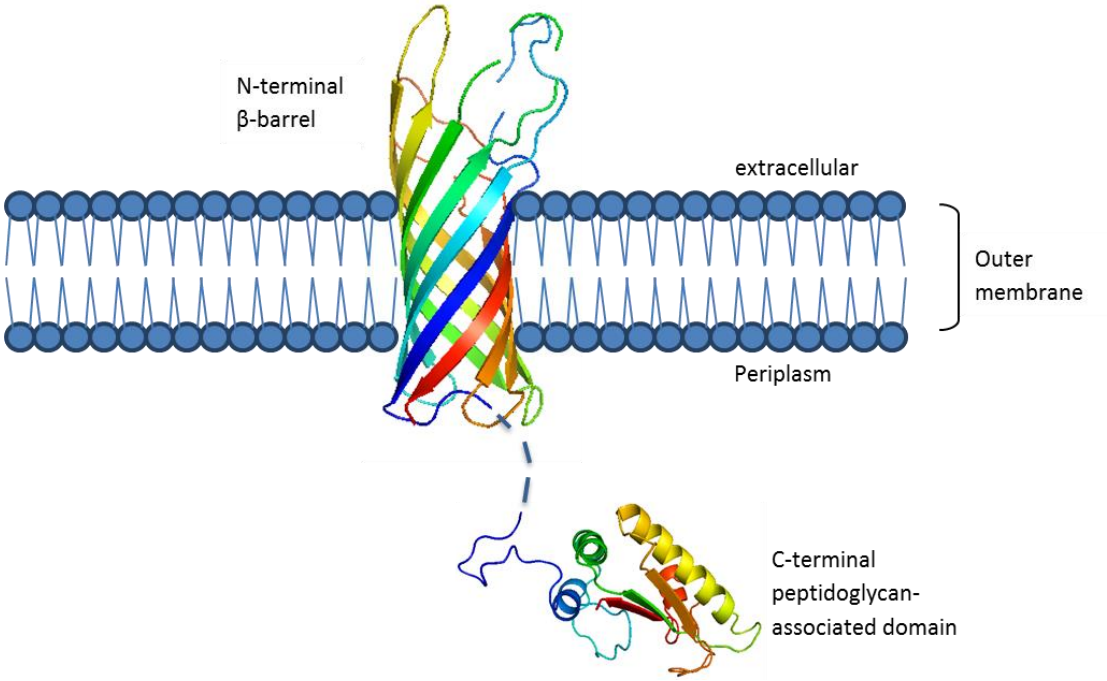

Figure 1.10 The predicted structure of *E. coli* OmpA. The structure is predicted to form a β-barrel structure in the outer membrane with a peptidoglycan-associated globular domain. Dotted line represents the expected chain between the two domains as each structure was submitted separately into Uniprot, and therefore doesn't model as one entity.

The overall structural homology remains largely conserved between species; however significant variations are observed in the extracellular loops (Pautsch and Schulz, 1998), implying a species-specific role dependant on the environmental niche. It has been shown that the external environment can influence the expression of OmpA-like proteins, such as nitrogen shortage or anaerobic culturing which increases the expression, or antimicrobial peptide exposure and challenging with acid causes the decrease in expression (Smith *et al.*, 2007), and later a study by Zhang *et al* (2011) showed that a phenol exposure causes upregulation of OmpA, suggesting a role for OmpA in stress resistance (Zhang *et al.*, 2011). The OmpA surface protein found in *Klebsiella pneumoniae* interacts with TLR2, which leads to activation of dendritic cells and natural killer cells (Chalifour *et al.*, 2004). In addition, OmpA is shown to be upregulated in biofilm formation in *E. coli*, as well as OmpA expression being closely linked to fimbrial expression, as shown by Teng *et al*., (2006) where a Δ*ompA* mutant showed suppressed expression of the type I fimbriae (Teng *et al.*, 2006). All of these examples found show an increasingly evident role in pathogenesis.

OmpA of *E. coli* is a relatively inefficient porin, compared to the classical OmpF and OmpC, and is thought to be involved in host cell attachment and invasion in certain strains as shown by Shin *et al.,* (2005), who applied purified samples of *E. coli* K1 OmpA to brain microvascular endothelial cells and demonstrated adherence (Shin *et al.*, 2005). Meningitis-causing strains of *E. coli* demonstrate the association between OmpA and invasion by the creation of an *ompA*-deficient strain which was 25-50 times less invasive than comparable parent strains (Meier *et al.*, 1996), or indeed the same reduction was achieved when incubating with an anti-OmpA antibody. Aside from *E. coli*, the OmpA protein has been found to be important in many Gram-negative bacteria, with a role attributing to the interaction with the host cell. The OmpA protein found in *Neisseria gonorrhoeae* has been shown to be involved in adhesion and invasion to human endometrial cells and cervical carcinoma cells, with a decrease in bacterial association by 3.5-fold in an Δ*ompA* mutant (Serino *et al.*, 2007). This work by Serino *et al*., also showed the involvement of OmpA in phagocytosis by macrophages and subsequent survival within the cell (Serino *et al.*, 2007). The OmpA found in *Coxiella burnetii*, the known pathogen for causing Q fever, has been shown to be involved in the interaction with the host, and more specifically the extracellular loops of the OmpA protein show specificity to increasing the ability of the bacterium to invade lung epithelial cells (Martinez *et al.*, 2014).

The OmpA protein isn't only important in the interaction with human cells, as elegant work by Weiss *et al.,* (2008) has shown that the OmpA of *Sodalis glossinidius*, a symbiotic bacterium, is important in the interaction with its host, the tsetse fly (*Glossina morsitans*). This work involved the introduction of recombinant OmpA from *E. coli* K12 to *Sodalis*, resulting in the transformation of the symbiotic bacterium into displaying a pathogenic phenotype (Weiss *et al.*, 2008). This work also demonstrated a comparison of alignments of the two OmpA proteins, resulting in significant insertions in one of the extracellular loops of the *Sodalis* OmpA, not found in the pathogenic-form of OmpA, indicating the specific role for OmpA in the bacterium's pathogenic phenotype.

1.6.12 OmpA in *P. gingivalis*

The study by Murakami *et* al., (2002) mentioned previously, identified a trimeric structure of the OmpA proteins of *P. gingivalis*, which is typical of porins, and showed extensive structural homology with the OmpA porin of *E. coli* along the entire length (Murakami *et al.*, 2002). The OmpA-like protein of *P. gingivalis* (from here on known simply as OmpA), is predicted to show a similar structure to those seen in other OmpA-like porins, as

demonstrated by Nagano, *et al* (2005). The *ompA* operon can be seen in Figure 1.11, and is made up of two genes (*pgm6/7* or *ompA1/A2*). Protein analysis by SDS-PAGE demonstrated a single band at ~40kDa and at ~120kDa when prepared with and without 2-mercaptoethanol respectively, suggesting the formation of a heterotrimer in native conditions. Immunoreactive studies demonstrated a greater concentration of Pgm6 produced compared to Pgm7, suggesting a 2:1 ratio in the heterotrimer. Deletion of the entire structure by Nagano *et al.,* produced mutants that had higher membrane permeability suggesting a structural role for OmpA, with a role for the anchoring of the protein to the peptidoglycan layer. This study also demonstrated a role for OmpA in the survival of *P. gingivalis* in the inflamed periodontal pockets during infection. An inability of Δ*ompA1A2* to grow in the presence of 0.2 M NaCl suggests a reduced survival rate in an environment with high osmotic pressure, such as that found in an infection (Nagano *et al.,* 2005). In the microarray analysis of the hyperinvasive subpopulations of *P. gingivalis* by Suwannakul, the OmpA protein was upregulated 4-fold in three of the four datasets, but as it wasn't upregulated in all four, it did not make the table of signature genes (Table 1.1); however it indicates a highly likely role in the adherence and invasion of the host cell.

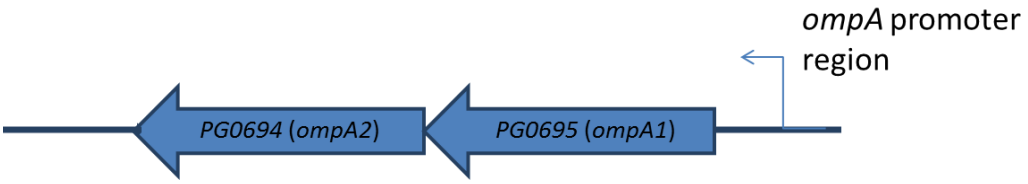

Figure 1.11 The *ompA* operon of *P. gingivalis.*

Studies describing the importance of *P. gingivalis* adherence and invasion of the host have been detailed by multiple investigators (Njoroge *et al.*, 1997; Chen *et al.*, 2001), with some studies demonstrating the intracellular location in buccal cells *in vivo* (Rudney *et al.*, 2005; Rudney and Chen, 2006). However, few studies have detailed the role of OmpA in these interactions. More recently, a study by Murakami *et al* (2014) has indicated the potential glycosylation of the OmpA1 protein subunit through identification of glycoprotein-attachment sites in mass spectrometry. This study also showed purified OmpA1A2 protein bound to extracellular matrix (ECM) proteins, such as fibronectin and laminin, whereas purified OmpA2 bound significantly less, indicating a potential role for the predicted glycosylation of the OmpA1 subunit in the adherence to the host cell (Murakami *et al.*,

2014). However, purified OmpA1 protein was not examined for its role in binding ECM molecules, and therefore the reduction in binding may be due to the loss of the heterotrimer.

In the context of TNF-α –stimulated endothelial cells, an increase in adherence of wild-type *P. gingivalis* was observed that was not seen in a Δ*ompA1A2* mutant (Komatsu *et al.*, 2012). This study also purified OmpA and demonstrated an inhibition of *P. gingivalis* binding endothelial cells in the presence of the recombinant protein, in concentrations as low as 0.25 ng ml^{-1}.

Currently, there is no evidence demonstrating the importance of OmpA in the interaction of oral epithelial cells, the cell type *P. gingivalis* is most likely to contact during the infection process.

1.6.13 The OmpH Protein

As demonstrated in the schematic of the cell envelope of Gram-negative bacteria (Fig. 1.9), once proteins bound for the outer membrane have been translocated across the inner membrane, they must be transported across the periplasm to be assembled and inserted in to the outer membrane. Chaperone proteins exist to transport these outer membrane proteins through their intermediate periplasmic stage, to prevent inappropriate folding and aggregation in the periplasm and guide them to the outer membrane. In *E. coli*, three major chaperone proteins are thought to exist, SurA, the protease, DegP, which also displays chaperone-like properties (Spiess *et al.*, 1999), and the Seventeen Kilodalton Protein (Skp, or OmpH). Individually, these proteins are not essential but merely result in a reduction of proteins in the outer membrane; however double mutants display often lethal phenotypes suggesting two parallel chaperone pathways are at work (Chen and Henning, 1996). It is thought the SurA-dependant pathway is the major chaperone pathway, and an alternative Skp- and DegP-dependant pathway is present as a minor route (Rizzitello *et al.*, 2001; Sklar *et al.*, 2007). SurA has been shown to have specificity for chaperoning the LptD, whereas the major role for DegP is to prevent the toxic accumulation of aggregated and misfolded proteins in the periplasm (Bos *et al.*, 2007; Walther *et al.*, 2009). *P. gingivalis* encodes proteins homologous to these systems and further chaperone-related proteins, which is discussed later in the bioinformatics analysis in Chapter 5.3.1.

The Skp/OmpH protein of *E. coli* is thought to form a homotrimer, composed of a β-barrel central domain with three α-helical extensions forming a pronged structure around an

internal cavity (Korndörfer *et al.*, 2004), which has been described as "jellyfish-like" (Walton and Sousa, 2004), with the outer membrane protein to be chaperoned binding in this cavity (Walton *et al.*, 2009). The Skp/OmpH chaperone is required for the efficient release of unfolded proteins that emerge from the Sec system on the inner membrane (Chen and Henning, 1996; Harms *et al.*, 2001), and was thought to be required in the correct folding of several outer membrane proteins before delivering them to the Bam complex on the outer membrane (De Cock *et al.*, 1999). However, more recently, the Skp/OmpH chaperone has been noted more as a holdase, preventing aggregation, rather than having an active role in folding of the outer membrane proteins (Walton and Sousa, 2004; Walton *et al.*, 2009), especially as *in vitro* experimental evidence demonstrates a prevention of aggregation of protein but no effect was observed on the folding rates of the proteins (Entzminger *et al.*, 2012). The substrates of the Skp/OmpH chaperone appear to be of a broad spectrum, with a bias towards proteins of an acidic nature (Jarchow *et al.*, 2008), and vary from outer membrane proteins such as OmpA, OmpC, OmpF and LamB (Chen and Henning, 1996) to periplasmic proteins such as MalE and OppA (Jarchow *et al.*, 2008), demonstrating a broad substrate spectrum. Multiple studies have shown evidence for the OmpA protein being a client of this chaperone system (De Cock *et al.*, 1999; Bulieris *et al.*, 2003; Patel *et al.*, 2009), from being identified as a binding partner in Skp-related pull down assays (Jarchow *et al.*, 2008), to the Skp/OmpH chaperone binding OmpA in solution (Qu *et al.*, 2007) and completely preventing the aggregation of OmpA in solution when the denaturing buffer is removed (Walton *et al.*, 2009).

Homologs of the Skp/OmpH protein have been described in various Gram-negative bacteria, suggesting a high level of importance to the protein. The *ompH* gene has been identified in many species of the Enterobacterial family, including *E. coli* as mentioned above, *Salmonella typhimurium* (Koski *et al.*, 1989) and *Yersinia enterocolitica* (Hirvas *et al.*, 1991) which all display remarkable homology within their OmpH proteins (up to 91% and 65% amino acid sequence homology respectively to *E. coli*) (Hirvas *et al.*, 1990), suggesting most species within this family will contain highly homologous versions of this protein. In all cases, the OmpH protein shows a similar chaperone-type role, often coupled to an interaction with LPS and the two genes (*skp* and lipid synthesis genes) are usually found coupled in a cistron or operon, and is also observed outside of this family, for example in *Pasteurella multocida* (Delemarche *et al.*, 1995), however this is not the case in *P. gingivalis.*

1.6.14 OmpH in *P. gingivalis*

Very few studies have been performed on the OmpH protein of *P. gingivalis.* The OmpH protein is encoded by two genes, PGN0300 and PGN0301, also known as PG0192/3 and *ompH1* and *ompH2*, however, currently there is no evidence if these genes encode a trimeric structure similar to the *E. coli* OmpH protein. Both genes have been shown to be upregulated in a multispecies community of *P. gingivalis*, *F. nucleatum* and *S. gordonii* (Kuboniwa *et al.*, 2009), indicating a potential involvement in delivering proteins to the outer membrane involved in multispecies interaction. These two genes were also upregulated in the signature gene set of genes differentially regulated in the hyperinvasive subset of the *P. gingivalis* population, described by Suwannakul *et al* (2010), indicating the OmpH protein may be involved in the chaperoning of proteins involved in interaction with the host cell (Suwannakul *et al.*, 2010). These two studies demonstrate the potentially broad spectrum of proteins that act as clients to the OmpH protein, involved in interacting with both host for infection and other bacteria for biofilm formation. As both of these processes are involved in the virulence of *P. gingivalis,* further investigation into the OmpH protein and its clients could reveal crucial information on the proteins involved in these processes and provide new antimicrobial therapeutic targets. Very recently, a study by Taguchi *et al* (2016) described the OmpH chaperone protein as being encoded by an operon containing PGN0299 (which encodes Omp85, or BamA), and the two *ompH1* and *ompH2* genes. The study created an *ompH1* mutant, detailing its location to be associated with the outer membrane due an N-terminal α-helix, whereas a knockout of *ompH2* couldn't be created and thus was determined to be an essential gene (Taguchi *et al.*, 2016), which is contradictory to all previous studies of the OmpH protein mentioned above. This study investigated the role of OmpH on gingipain production, showing with a loss of OmpH, the level of gingipain activity was severely reduced and a higher level of unprocessed gingipains were present. As the gingipain proteins contain a CTD for PorSS secretion (discussed in earlier in 1.6.6.4.2), the group connected the OmpH protein to potentially being the chaperone of the PorSS system. This was supported by MALDI-TOF analysis of the supernatant, which contained two other CTD-containing proteins, suggesting a potential role for OmpH in the PorSS secretion system (Taguchi *et al.*, 2016). This paper will be discussed in further detail in Chapter 5.4.

As the OmpH protein has been shown to be involved in the chaperoning of OmpA in *E. coli* (Chen and Henning, 1996; De Cock *et al.*, 1999; Jarchow *et al.*, 2008; Walton *et al.*, 2009), it

potentially shows a similar role in the *P. gingivalis* chaperone system. Coupled to the upregulation of OmpH in the hyperinvasive subset of the *P. gingivalis* population (Suwannakul *et al.*, 2010), and the postulated role for OmpA in the interaction with host, this protein may be an essential protein contributing to the virulence abilities of *P. gingivalis* and would therefore be an interesting target of study in this project.

1.7 Aims

An extensive review of the literature and the lab data on the signature gene set determined a gap in the research surrounding the interaction with the host oral epithelial cells via the *P. gingivalis* OmpA protein. This protein is indicated as important for host cell adherence and invasion largely due to the mutagenesis studies of Komatsu *et al* (2012) showing a reduction in invasion of endothelial cells with the loss of OmpA, coupled to data presented by Suwannakul *et al* (2010), demonstrating a four-fold increase in *ompA* expression in a hyperinvasive subset of the *P. gingivalis* population. This data also revealed the upregulation of *ompH* expression in the hyperinvasive subset, indicative of an importance of the clients of this chaperone being important in host cell interaction. Therefore, the specific research questions addressed in this thesis will be to determine the role of OmpA in adherence and invasion of the host, both through deletion of the genes and overexpression of the protein, as discussed below, whilst performing a preliminary characterisation of the OmpH protein of *P. gingivalis* through the creation of an Δ*ompH1H2* mutant.

1.7.1 Specific Aims of the Project

- To create individual *ompA1* and *ompA2 P. gingivalis* mutants
- To assess and compare the adhesion and invasion of an appropriate cell line between *ompA* mutant strains, and determine a role, if any, for the individual subunits of OmpA
- To assess and compare general phenotypic attributes of *P. gingivalis* and the *ompA* mutant strains, including several virulence factors and biofilm formation
- To express and purify the OmpA subunits, and assess their interaction with the host cell
- To model and analyse the OmpA protein bioinformatically, and determine structural aspects of the protein

- To utilize this structural information to determine host-cell interaction of the OmpA protein, and analyse through interaction studies and fluorescent labelling
- To perform general phenotypic characterization of the OmpH protein chaperone of *P. gingivalis* through deletion of the *ompH* operon
- To determine any potential substrates of the OmpH chaperone
- To develop and optimize a mutagenesis technique for *P. gingivalis*

Chapter 2

Materials and Methods

2.1 Manufacturers and Suppliers

All reagents used in this study were of analytical grade and were obtained from the following manufacturers and suppliers (Table 2.1). Reagents were purchased from Sigma-Aldrich or ThermoFisher Scientific unless otherwise stated.

Table 2.1 Main manufacturers and suppliers

Supplier	**Location**	
Agar Scientific	Essex	UK
BDH Laboratory Suppliers	Poole	UK
Bioline	London	UK
BioRad Laboratories	Hertfordshire	UK
BMG Labtech	Aylesbury	UK
Corning	Fisher Scientific Distributor, Loughborough	UK
Don Whitely Scientific	Shipley, West Yorkshire	UK
FlowGen Biosciences (SLS Life Sciences)	Hassle, East Riding of Yorkshire	UK
GE Healthcare Life Science (Amersham Biosciences)	Buckinghamshire	UK
Gibco (Thermo Fisher Scientific)	Leicestershire	UK
iNtRON Biotechnology	Kyungki-Do	Korea
Invitrogen	Paisley	UK
LabM	Bury	UK
Life Technologies (Thermo Fisher Scientific)	Leicestershire	UK
New England Biolabs (NEB)	Hitchin, Hertfordshire	UK
Novagen (Merck Millipore)	Darmstadt	Germany
NunC	Fisher Scientific Distributor, Loughborough	UK
Oxoid	Hampshire	UK
Progen Scientific	London	UK
Promega	Southampton	UK
QIAGEN	West Sussex	UK
Sigma-Aldrich	Poole	UK

Syngene	Cambridge	UK
ThermoFisher Scientific	Leicestershire	UK
Xograph	Gloucestershire	UK

2.2 Main Buffers and Reagents

2.2.1 Phosphate Buffered Saline

Phosphate buffered saline (PBS) was made by adding 8.18 g Sodium Chloride (NaCl), 0.2 g Potassium Chloride (KCl) (BDH Laboratory Suppliers), 1.41 g Sodium Phosphate Dibasic Anhydrous (Na_2HPO_4) and 0.244 g Potassium Dihydrous Orthophosphate (KH_2PO_4) (BDH Laboratory Suppliers). The pH was adjusted to 7.3 and the total was made up to 1000 ml with H_2O.

2.2.2 Crystal Violet Stain

The stain is a 0.1 % Crystal Violet stain made up of 20 ml Solution A (5 g crystal violet (BDH Laboratory supplies) in 95 ml Ethanol) and 80 ml Solution B (1% Aqueous Ammonium oxalate in H_2O).

2.2.3 Protein Purification Elution Buffer

Protein elution of His-tagged proteins was performed using increasing concentrations of imidazole in an elution buffer. The elution buffer comprised of 120 mM NaCl, 150 mM PBS and imidazole in varying concentrations (20 mM, 150 mM and 200 mM).

Glutathione-S-transferase (GST)-tagged proteins were eluted from glutathione resin using reduced glutathione (GSH) elution buffer. The elution buffer was made up of 20 mM GSH, 120 mM NaCl in a 50 mM Tris solution. The GSH was then aliquoted into 1 ml fractions and stored at -20°C.

2.3 Bacterial Strains, Plasmids and Primers Used In This Study

Table 2.2 shows the strains of *P. gingivalis* used in this study. Strains were either obtained from Dr. Graham Stafford or generated in this study.

Table 2.2 *P. gingivalis* strains

***P. gingivalis* strain**	**Relevant Characteristic(s)**	**Source**
ATCC 33277	Wild-type, type strain	ATCC
Δ*ompA1*	*ompA1* (PGN0729) deletion mutant of ATCC 33277 (ery^R)	This study
Δ*ompA2*	*ompA2* (PGN0728) deletion mutant of ATCC 33277 (ery^R)	This study
Δ*ompA1A2*	*ompA1* (PGN0729) and *ompA2* (PGN0728) deletion mutant of ATCC 33277 (ery^R)	Dr. Graham Stafford
Δ*ompA2* + pT-COW-A2	Δ*ompA2* complemented mutant with *ompA* operon promoter and *ompA2* gene (from ATCC 33277) on pT-COW plasmid (Tc^R)	This study
Δ*ompH1H2*	*ompH1* (PGN0300) and *ompH2* (PGN0301) deletion mutant of ATCC 33277 (ery^R)	This study

Ery^R – erythromycin resistance; Tc^R – Tetracycline resistance

The strains of *E. coli* used throughout this study can be seen below in Table 2.3.

Table 2.3 *E. coli* strains

Strain	**Genotype**	**Supplier**
E. coli C41 (DE3)	*F⁻ ompT hsdS*$_B$ (r_B^- m_B^-) *gal dcm* (DE3). Derived from BL21 (DE3) as described in (Miroux and Walker, 1996).	Strain collection
E. coli C41 Rosetta	F⁻ *ompT hsdS*$_B$(r_B^- m_B^-) *gal dcm* (DE3) pRARE (Cam^R)	Strain collection

E. coli BL21 (DE3)	*F⁻ompT gal dcm lon hsdS$_B$(r$_B^-$ m$_B^-$) λ(DE3 [lacI lacUV5-T7 gene 1 ind1 sam7 nin5])*	Strain collection
E. coli BL21 Rosetta	*F⁻ompT gal dcm hsdS$_B$ (r$_B^-$ m$_B^-$) λ (DE3) pRARE (Cam^R)*	Strain collection
E. coli BL21 Star	*F⁻ompT hsdS$_B$ (r$_B^-$,m$_B^-$) galdcmrne131 (DE3)*	Strain collection
E. coli DH5α	*E. coli fhuA2 lac(del)U169 phoA glnV44 Φ80' lacZ(del)M15 gyrA96 recA1 relA1 endA1 thi^{-1} hsdR17*	New England Biolabs (NEB)

Plasmids used and created in this study can be seen below in Table 2.4

Table 2.4 Plasmids

Plasmid	**Insert**	**Antibiotic Resistance**	**Supplier**
pGEX-4-T-3	Empty vector for GST-tagged protein overexpression	Ampicillin	GE Healthcare
pGEX-*ompA1*	*ompA1* for GST-tagged protein overexpression, inserted between *Bam*HI and *Eco*RI restriction sites.	Ampicillin	This study
pGEX-*ompA2*	*ompA2* for GST-tagged protein overexpression, inserted between *Bam*HI and *Eco*RI restriction sites.	Ampicillin	This study
pJET (Clone Jet)	Blunt end cloning storage vector	Ampicillin	Thermo Fisher Scientific

pJET-*ompA2::em*	Storage vector containing Insert of *P. gingivalis ompA2* gene interrupted with erythromycin gene for *ompA2* knock out, flanked with 1000 bp upstream and downstream of native *ompA2.* Inserted between *Hinc*II restriction sites.	Ampicillin	This study
pET-15b	Empty vector for His-tagged protein overexpression	Ampicillin	Novagen
pET-*ompA1*	*ompA1* for His-tagged protein overexpression, inserted between *Bam*HI and *Nde*I restriction sites.	Ampicillin	Dr Graham Stafford
pET-*ompA2*	*ompA2* for His-tagged protein overexpression, inserted between *Bam*HI and *Nde*I restriction sites.	Ampicillin	Dr Graham Stafford
pET-*ompA1b* (pJET-OmpA1$_{21-245}$)	*ompA1* (β-barrel only) for His-tagged protein overexpression, inserted between *Bam*HI and *Nde*I restriction sites.	Ampicillin	This study
pET-*ompA2b* (pJET-OmpA2$_{22-236}$)	*ompA2* (β-barrel only) for His-tagged protein overexpression, inserted between *Bam*HI and *Nde*I restriction sites.	Ampicillin	This study
pT-COW	Modified *Bacteroides-Prevotella* shuttle vector	Tetracycline	(Gardner *et al.*, 1996)
pT-COW + *A2*	Shuttle vector as above, containing *P. gingivalis omp*	Tetracycline	This study

	operon promoter joined to *ompA2* gene for mutant complementation inserted between *Bam*HI and *Sal*I restriction enzyme sites.		

The primers used in this study can be seen below in Tables 2.5-2.13.

Table 2.5 Primers for *ompA1* gene knock out

Primer	**Sequence**
ompA1-f1 for	TGGAAGTTAGCATCGCCAAC
ompA1-f1 rev	CGGGCAATTTCTTTTTTGTCATGCCTATTCGCTACACAAATG
ompA1-f2 for	GTCCCTGAAAAATTTCATCCTTCGTATTATTAGCACTTGCGGG
ompA1-f2 rev	GATCAAGGTAGTAGGTTAC
ompA1-em for	CATTTGTGTAGCGAATAGGCATGACAAAAAAGAAATTGCCCG
ompA1-em rev	CCCGCAAGTGCTAATAATACGAAGGATGAAATTTTTCAGGGAC

Table 2.6 Primers for *ompA2* gene knock out

Primer	**Sequence**
ompA2-f1 for	ATAGGTTCTCTTTCTGTCGG
ompA2-f1 rev	CGGGCAATTTCTTTTTTGTCATCTGTATGTCATTTTATATTATCC
ompA2-f2 for	CTCGTCATGAGACAGCCTCAGCCGAAGGATGAAATTTTTCAGGGAC
ompA2-f2 rev	TTCACTTTGTCTTTCAGATCCTCT

ompA2-em for	GGATAATATAAAATGACATACAGATGACAAAAAAGAAATTGCCCG
ompA2-em rev	GTCCCTGAAAAATTTCATCCTTCGGCTGAGGCTGTCTCATGACGAG

Table 2.7 Primers for *ompA2* gene complementation

Primer	**Sequence**
ompA promoter for	CAGGGATCCCCGGAGAATCTTCTTTGCAGC
ompA promoter rev – *ompA2* for tail	GCTAATAATAAAGATTTAGCTTTCATAGTTTTACTTTTCTAAGTGTATTT
ompA2 for – *ompA* promoter tail	AAATACACTTAGAAAAGTAAAACTATGAAAGCTAAATCTTTATTATTAGC
ompA2 rev	CAGGTCGACTTATTCCGCTGCAGTCATTACTAC

Table 2.8 Primers for *ompH1H2* gene knock out confirmation

Primer	**Sequence**
ompH1H2 for	ATGCGGATCCCAAGAAGCTACTACACAGAACAAAGC
ompH1H2 rev	TACGGAATTCTTATTCCGCTGCAGTCATTACTAC
Flank for	CCGGCGACCTCTATACTCAGGC
ery^{R} for	ATGACAAAAAAGAATTGCCCG
ery^{R} rev	GTCCCTGAAAAATTTCATCCTTCG
Flank 2 rev	GTCATCGACAAAGAGCCGG

Table 2.9 Primers for GST-tagged OmpA1 protein overexpression

Primer	**Sequence**

OmpA1 for	ATCGGGATTCCAGGAGAATACTGTACCGGCAACGGG
OmpA1 rev	ATCGGAATTCTTACTTGGAGCGAACGATTACAACACG

Table 2.10 Primers for GST-tagged OmpA2 protein overexpression

Primer	**Sequence**
OmpA2 for	ATATATCATATGCAGAACAAAGCAGGGATGC
OmpA2 rev	GGATACCTGATACGAAACATTCCTAGGTATATA

Table 2.11 Primers for His-tagged OmpA1 barrel only protein overexpression

Primer	**Sequence**
OmpA1b for	ATCGGGATTCCAGGAGAATACTGTACCGGCAACGGG
OmpA1b rev	ATCGGAATTCTTACTTGGAGCGAACGATTACAACACG

Table 2.12 Primers for His-tagged OmpA2 barrel only protein overexpression

Primer	**Sequence**
OmpA2b for	ATATATCATATGCAGAACAAAGCAGGGATGC
OmpA2b rev	ATATATGGATCCTTACAAAGCATAGTCCATAGG

Table 2.13 Plasmid primers for template insertion confirmation

Plasmid	Primer	Sequence
pET15b	**T7 promoter (for)**	TAATACGACTCACTATAGGG
	T7 Terminator (rev)	GCTAGTTATTGCTCAGCGG
pGEX-4T3	**pGEX 3' (for)**	CCGGGAGCTGCATGTGTCAGAGG
	M13 pUC (rev)	TCACACAGGAAACAGCTATGAC
pJET/1.2	**pJET (for)**	CGACTCACTATAGGGAGAGCGGC
	pJET (rev)	AAGAACATCGATTTTCCATGGCAG
pT-COW	***E. coli* TetC (for)**	TCAGGCACCGTGTATGAAATCTAAC
	***E. coli* TetC (rev)**	CCGGCTTCCATTCAGGTCGAGG

2.4 Bacterial Cell Culture

2.4.1 Antibiotics

Antibiotics were used to prevent contaminating infections and for selecting for an introduced mutation and are listed in the Table below at their appropriate concentrations for use.

Table 2.14 Antibiotics used in this study

Antibiotic	Concentration
Ampicillin Sodium Salt	100 µg/ml
Gentamycin	50 µg/ml
Erythromycin	10 µg/ml
Tetracycline	3 µg/ml

2.4.2 Bacterial Culture

The cultures for *E. coli* were grown either in day (starter) or overnight cultures. A single colony of *E. coli* was inoculated into a 5 ml Luria Broth (LB) and grown aerobically at 37°C with agitation (250 r.p.m) for the required amount of time. For strains harbouring plasmids encoding genes for protein overexpression, LB was supplemented with antibiotics (100 µg/ml ampicillin sodium salt) for selection.

P. gingivalis was cultured on fastidious anaerobic agar (Lab M Limited) supplemented with 7.5% horse blood (Oxoid) for 72 hours in an anaerobic incubation cabinet (Don Whitley Scientific miniMAC Anaerobic Workstation) at 37^{o}C and containing 10% CO_2, 10% H_2 and 80% N_2. A liquid culture of *P. gingivalis* was grown under the same anaerobic conditions, except liquid cultures were cultured for 16 hours and in Brain Heart Infusion (BHI) broth containing 0.5% yeast extract and supplemented with 250 µg/ml cysteine, 1 mg/ml vitamin K and 1 mg/ml hemin. Antibiotics were included in the media where appropriate, including gentamycin and erythromycin. Antibiotics were filter sterilised and added to media once autoclaved for sterilisation (20 minutes at 121^{o}C high pressure steam).

2.4.3 Long Term Storage of Bacteria

Bacterial cultures were stored at -80°C or in liquid nitrogen for long term purposes. A 5 ml culture of the bacterial strain was grown for 16 h under the specified conditions in 2.4.2 before harvesting through centrifugation (4,500 x *g*, 5 min) and resuspension in 1 ml of fresh growth media and 0.5 ml 50 % glycerol and immediately stored.

2.5 Epithelial Cell Lines and Growth

2.5.1 Epithelial Cell Line

The oral epithelial cell line, OK-F6, was originally obtained from James G. Rheinwald (Harvard Institute of Medicine, Boston, MA) (Mark a Dickson *et al.*, 2000), and for this study was obtained from freezer stocks at passage 3-5 from The Department of Oral Pathology, School of Clinical Dentistry, The University of Sheffield. The OK-F6 cell line was stored in 1 ml aliquots of 1 x 10^6 cells in liquid nitrogen.

2.5.2 Epithelial Cell Culture

All mammalian cell culture was undertaken in a Class II microbiology safety cabinet that had been sterilised using 70% industrial methylated spirits (IMS). Any items introduced to the cabinet throughout the cell seeding process were also thoroughly cleaned using 70% IMS. Any media and trypsin solutions were pre-heated to 37°C before use.

2.5.3 Growth Media

Defined keratinocyte serum-free media (DKSFM) (Gibco) was used for both weekly maintenance of cells and for the antibiotic protection assays and fluorescence studies. The 500 ml bottles of DKSFM were supplemented with the 1 ml aliquot of defined keratinocyte SFM growth supplement and stored at 4°C. Neutralising media (used in passaging OK-F6 cells) consisted of Dulbecco's Modified Eagle Media (DMEM) supplemented with 10 % Foetal Bovine Serum (FBS) and also stored at 4°C.

2.5.4 Defrosting Mammalian Cells

Cell aliquots were retrieved from liquid nitrogen and placed into a 37°C water bath to defrost and immediately resuspended in 2 ml DKSFM and centrifuged for 5 minutes at 1250 x *g* (room temperature). After centrifugation, the supernatant was decanted and the pellet gently resuspended in 8 ml DKSFM before being transferred to a T75 cm^2 cell culture flask (Nunc) and incubated at 37°C, 5% CO_2 with humidity.

2.5.6 Cell Passaging

The OK-F6 cells were grown until confluency levels reached 70 – 80% and then passaged. The DKSFM media was discarded and the cell monolayer washed twice with 8 ml sterile Dulbecco's PBS. To detach the cells from the flask, 2 ml trypsin-EDTA buffer 1X was applied to the cells and incubated at 37°C, 5% CO_2 with humidity for 10 minutes. Cell detachment from the flask was confirmed using light microscopy under x20 magnification. After complete cell detachment, 4 ml of neutralising media was added to neutralise the enzymatic activity of the trypsin. The cell suspension was centrifuged at 1250 x *g*. for 5 minutes at (room temperature) before the supernatant was discarded and the cell pellet resuspended in 2 ml DKSFM. The cell density was calculated using a Neubauer Improved

haemocytometer whereby 10 µl Trypan Blue stain 0.4% (Life Technologies) was added to 10 µl of the cell suspension and applied to the haemocytometer and four quadrants of 16 squares were counted for viable cells. The total cell density was calculated using the following equation:

Cells / ml = 2(n / 4) x 10000

Cells were then either seeded into a new T75 cm^2 flask at 2 x 10^7 cells / ml or into a microtitre plate (MTP) at the desired cell density. Due to unpredictable genetic changes during cell replication, when cells reached passage 20 they were discarded and a new aliquot of cells retrieved.

2.6 Molecular Biology Methods

2.6.1 Bacterial Chromosomal DNA Isolation

Genomic DNA isolation was carried out using the Wizard® Genomic DNA Purification Kit (Promega) as described by the manufacturer's instructions. Plasmid DNA was isolated using a QIAGEN miniprep kit as according to the manufacturer's instructions.

2.6.2 DNA Analysis

2.6.2.1 Tris-Acetate-EDTA Buffer

Tris-acetate-EDTA (TAE) buffer was used to make agarose gels for DNA analysis, and as a running buffer in the gel tank. A 50X stock solution was made and diluted to a 1X buffer when used. The 50X TAE buffer was made by adding 57.1 ml of glacial acetic acid, 242 g Tris(hydroxymethyl)aminomethane (Tris Base), 100 ml of 0.5 M ethlenediaminetetraacetic acid (EDTA) (pH 8), and made up to 1000 ml by adding 842.9 ml dH_2O and adjusted to pH 8.

2.6.2.2 Agarose Gel Analysis

Any DNA analysis was carried out using a 1% agarose gel. Agarose powder was added to a 1X TAE buffer to make a 1 % solution. 0.5 µl of ethidium bromide was added and the gel poured into the prepared mould. Gels were run at 90-120 v until the desired level of DNA separation had occurred.

2.6.2.3 Polymerase Chain Reaction

The polymerase chain reaction (PCR) was used to amplify specific sequences of DNA or to perform overlap PCRs for specific gene knock outs for the creation of mutants. The PCR reaction consists of a denaturing step to separate DNA strands, an annealing step for primers to anneal to the DNA and an extension step for the nucleotides to be added to create the complementary strand, which is catalysed by a DNA polymerase enzyme. These steps are repeated for several cycles to amplify the DNA.

Table 2.15 Reagents and their volumes for PCRs needed for cloning and expression

Reagent	**Volume (µl)**
dH_2O	31.8
DMSO	1
dNTPs (40 mM)	0.2
5 x Buffer	10
Phusion™ Polymerase Enzyme	1
DNA	1
Primer 1 (10 µM)	2.5
Primer 2 (10 µM)	2.5

Table 2.16 Reagents and their volumes for PCRs needed for routine screening

Reagent	**Volume (µl)**
dH_2O	4
GreenTaq 2X Master Mix	10
DNA	1
Primer 1 (10 µM)	2.5
Primer 2 (10 µM)	2.5

The components of the PCR reaction carried out can be seen in Table 2.15 and Table 2.16. DNA concentrations ranged between 50–250 ng (genomic) and 10-50 ng (plasmid). Two different enzymes were used depending on the reaction. Phusion™ (New England Biolabs) was used to amplify sequences needed for cloning and expression, whereas GreenTaq™ (Thermo Scientific) was used for routine screening, such as confirmation of successful transformation. The reaction conditions for both of these enzymes can be seen in Table 2.17.

Table 2.17 Reaction conditions for PCR with different polymerase enzymes

	Polymerase Enzyme			
	Phusion™		**GreenTaq™**	
PCR Step	**Temperature (°C)**	**Time (mins:secs)**	**Temperature (°C)**	**Time (mins:secs)**
Initial Denaturation	98	0:30	95	3:00
Denaturation	98	0:10	95	0:30
Annealing	55-65	0:30	50-55	0:30
Extension	72	0:30 / kb	72	1:00 / kb
Final Extension	72	5:00	72	5:00
Hold	4	∞	4	∞

PCR samples were then analysed using 1% agarose gel electrophoresis as described in Materials and Methods 2.6.2.2 DNA samples in the gel were detected using UV radiation and images taken were using a G:Box (Syngene).

2.6.2.4 Overlap PCR for *ompA1* and *A2* Gene Knockout Cassette Amplification

Overlap PCR was carried out under the same conditions as those reactions described in Table 2.17, using the primers described in Table 2.5 and 2.6.

2.6.2.5 DNA Extraction from Agarose Gel

DNA samples were extracted from the agarose gel using a Gel Extraction Kit (QIAGEN) as described in the manufacturer's instructions. DNA samples could also be purified from the PCR mixture using the Bioline ISOLATE PCR and Gel kit.

2.6.2.6 Restriction Enzyme Digest & Ligation

After the PCR product was analysed and purified, the product and plasmid were both digested using restriction enzymes. Table 2.18 denotes the various components and their quantities for a 30 µl reaction. The reaction was carried out at 37°C for 2 hours. After two hours of digestion using the restriction enzymes, 1 µl of calf intestinal alkaline phosphatase (CIP) (Promega) or Antarctic phosphatase (New England Biolabs) was added to the reaction containing the plasmid vector, and incubated at 37°C for one further hour. The enzymatic activity of the restriction enzymes was halted by heat inactivation or removed by using a PCR clean up kit (Bioline). The digested plasmid vector and PCR product were ligated together in a 20 µl reaction seen in Table 2.19. The reaction mixture was incubated at room temperature for 16 – 20 h. The plasmid containing the ligated insert was stored at -20°C.

Table 2.18 Reagents and volume required for a restriction enzyme digest

Reagent	**Volume (µl)**
DNA	15
10X Buffer	3
Restriction Enzyme 1	1
Restriction Enzyme 2	1
dH_2O	10

For digestion of the *ompA1* or *ompA2* gene for protein overexpression, *Bam*HI and *Eco*RI were used as the enzymes, and the buffer was buffer 4, all supplied from New England Biolabs.

Table 2.19 Reagents and volumes needed for a ligation reaction

Reagent	Volume (µl)
10X Buffer	2
T4 Ligase	1
Vector (plasmid)	3
Insert	14

T4 Ligase was purchased from New England Biolabs.

For OmpA1 or OmpA2 (insert) ligation for overexpression with a GST-tag, the vector was the pGEX-4T3 plasmid, or pET-15b for His-tag expression, from Table 2.4

Alternatively, PCR products or DNA strings purchased from GeneArt® (Life Technologies) were cloned into the pJET plasmid using the CloneJET PCR Cloning Kit (Thermo Scientific) according the manufacturer's instructions.

2.6.3 Preparation of *E. coli* for Electroporation and Cloning

The appropriate expression strain of *E. coli* was grown from a single colony in 10 ml of LB broth until OD_{600} reached 0.6. The culture was pelleted by centrifugation at 11200 x *g.* for 15 minutes at 4°C. The pellet was resuspended in 1 ml of sterile ice-cold 10% glycerol and transferred to a 1 ml Eppendorf before centrifugation for 1 minute at 11200 x *g*. The pellet was washed three times in 1 ml sterile ice-cold 10% glycerol. On the final centrifugation, the pellet was resuspended in 100 µl sterile ice-cold 10% glycerol. Then, 1 µl of the ligated plasmid with insert of interest was added to the *E. coli* suspension and the mixture incubated on ice for 5 minutes. The suspension was transferred to a 1 mm path length electroporation cuvette (Flowgen Biosciences). The cells were then electroporated using a BIO-RAD MicroPulser™ series 411BR (BioRad Laboratories), with the parameters set according to Table 2.20. The electroporated *E. coli* was then incubated on ice for a further 5 minutes before being added to 1 ml LB broth and incubated at 37°C for 1 h. The cells were then centrifuged at max speed for 1 minute and resuspended in 100 µl LB broth before

being spread onto LB agar with the appropriate antibiotics for selection. The cells were incubated for 16 h at 37°C to allow for colony growth.

Table 2.20 Parameters for electroporation

Potential Difference	2.5 kV
Resistance	200 Ω
Capacitance	25 µF

This provides a time constant between 2.9 – 4.3 milliseconds.

Alternatively, *E. coli* was transformed using DH5α competent cells (New England Biolabs) and heat-shock. Heat shock transformation was carried out according to the manufacturer's instructions. Cells were spread onto LB agar with the appropriate antibiotics for selection.

2.6.4 Preparation of *P. gingivalis* for Electroporation and Cloning

A 5 ml liquid culture of *P. gingivalis* ATCC 33277 was set up as described in Materials and Methods section 2.4.2 and grown for 16 h, whereby the OD_{600nm} was observed between 1.0-1.2. A 20 ml day culture was set up using 1:10 dilution from the overnight culture into fresh liquid broth and grown statically for 6 h at 37°C under anaerobic conditions.

The next steps were carried out in less than 40 minutes to minimise the amount of aerobic exposure for the *P. gingivalis* cells. The cell suspension was removed from anaerobic conditions and centrifuged for 10 minutes at 10000 x *g* at 4°C. The supernatant was discarded and the pellet was resuspended in 10 ml ice-cold 10% glycerol supplemented with 1 mM Magnesium Chloride ($MgCl_2$). The cells were then pelleted by centrifugation at 10000 x *g* for 10 minutes (4°C), the supernatant discarded and the pellet resuspended in 200 µl ice-cold sterile 10% glycerol. The cell suspension was then added to a 2 mm path length cuvette (Flowgen Biosciences) with 5 µl DNA and incubated on ice for 5 minutes. Electroporation was carried out as in Table 2.20 and the contents were added to 500 µl liquid broth before being spread on a blood agar plate supplemented with gentamycin and grown at 37°C under anaerobic conditions. After 24 h growth, the cells were removed from

the plate and suspended in 1 ml fresh liquid broth and centrifuged for 1 minute at 11200 x *g*. The cells were resuspended in 100 µl fresh liquid broth and spread onto blood agar plates supplemented with gentamycin and erythromycin as previously described. The plates were incubated at 37°C under anaerobic conditions and left undisturbed for 2 weeks before recovery of successful colonies.

2.6.5 *P. gingivalis* Transformation Using Natural Competency

Multiple variations in methods for transformation via natural competency were used to assess transformation efficiency. Wild-type *P. gingivalis* for transformation was harvested from either a blood agar plate grown for 72 hours (plate-to-plate or plate-to-liquid methods), or from a liquid culture (liquid-to-liquid or liquid-to-plate methods), prepared as previously described in Materials and Methods 2.4.2. In all cases DNA concentration was at least 200 ng/µl.

2.6.5.1 Plate-based *P. gingivalis* Transformation

For the plate-to-plate method, an inoculum loop of bacteria was removed and resuspended in 1 ml BHI broth with supplements described in Materials and Methods 2.4.2, to create OD_{600} ~1.0-1.2. Then, the bacterial suspension was centrifuged at 11200 x *g* for 1 min, resuspended in 100 µl, and 5 µl DNA (≥200 ng/µl) was added to the cell suspension. This was then incubated at room temperature for 15 minutes before plating on blood agar plates supplemented with gentamicin and incubated anaerobically for 24 h. After 24 h, cells were harvested and plated onto erythromycin-containing blood agar plates.

For the plate-to-liquid method, an inoculum loop of bacteria was removed and resuspended in 1 ml BHI broth with supplements described in Materials and Methods 2.4.2, to create OD_{600} ~1.0-1.2. Then DNA (5 µl at ≥200 ng/µl) was added to the *P. gingivalis* cell suspension and incubated anaerobically for 24 hours without agitation. After 24 hours, the 1ml cell suspension was centrifuged at 11200 x *g*. for 1 minute before plating onto erythromycin-containing blood agar plates.

2.6.5.2 Liquid-based *P. gingivalis* Transformation

For the liquid-to-liquid method, a 5 ml liquid culture of *P. gingivalis* ATCC 33277 was set up as described in Materials and Methods section 2.4.2 and grown for 16 h. Then, 1 ml from the overnight culture in to a fresh 9 ml liquid broth and grown for 6 h until OD_{600} reached between 1.0-1.2. Then, 1 ml of the cell suspension was centrifuged at 11200 x *g*. for 1 minute and the supernatant discarded. The pellet was resuspended in 1 ml of fresh liquid broth with supplements, and 5 µl DNA (≥200 ng/µl) was added, before the cell suspension was incubated under anaerobic conditions for 24 hours. The cells were then centrifuged (11200 x *g*, 1 min) before plating onto erythromycin-containing blood agar plates.

For the liquid-to-plate method, a 5 ml liquid culture of *P. gingivalis* ATCC 33277 was set up as described in Materials and Methods 2.4.2 and grown for 16 h. Then, 1 ml from the overnight culture in to a fresh 9 ml liquid broth and grown for 6 h until OD_{600} reached between 1.0-1.2. Then, 1 ml of the cell suspension was centrifuged at 11200 x *g*. for 1 minute and the supernatant discarded. The pellet was resuspended in 100 µl of fresh liquid broth with supplements, and 5 µl DNA (≥200 ng/µl) was added, before the cell suspension was incubated at room temperature for 15 min before being plated on blood agar plates supplemented with gentamycin and incubated under anaerobic conditions for 24 hours. The cells were then harvested from the plate and centrifuged (11200 x *g*, 1 min) before plating onto erythromycin-containing blood agar plates.

All erythromycin-containing plates with potential transformants were incubated at 37°C under anaerobic conditions and left undisturbed for 2 weeks before recovery of successful colonies.

2.6.6 Complementation of Δ*ompA2*

A complementation construct for the *ompA2* gene was created by overlap extension PCR fusing the *ompA2* gene to the 300 base pair upstream region of the *ompA1* gene which contains the *ompA* operon promoter region, using primers found in Table 2.7. Primers contained restriction enzyme sites of *Bam*HI and *Sal*I for cloning into pT-COW plasmid (Gardner *et al.*, 1996), and transformed into *E. coli* and plated onto LB plus ampicillin plates. Positive colonies were grown by selecting for colonies that would grow on ampicillin

containing plates, but not on tetracycline containing plates, due to the *ompA2* insert interrupting the *E. coli* tet^R gene, and confirmed by sequencing. Plasmids positive for the promoter and insert (pT-COW-*ompA2*) were transformed into *P. gingivalis* Δ*ompA2* mutants, alongside an empty pT-COW vector via natural competency as described in 2.6.5. An empty pT-COW vector was also transformed into wild-type ATCC 33277 *P. gingivalis* as a positive control. All *P. gingivalis* colonies were selected for positive inclusion of the plasmid by selection on tetracycline containing BA plates.

2.7 Protein Methods

2.7.1 Protein Purification

2.7.1.1 Overexpression of Protein & Cell Free Extract Preparation

A single colony of transformed *E. coli* c41 cells containing the plasmid positive for the insert for OmpA1 or OmpA2 protein overexpression was used to inoculate 5 ml LB broth and grown at 37°C with agitation for 16 h. The 5 ml culture was then used to inoculate a 500 ml LB broth in a 2 L flask. The 500 ml culture was grown at 37°C with agitation until the OD_{600nm} reached 0.6. The flask of *E. coli* was induced with 0.1 mM isopropyl β-D-1-thiogalactopyranoside (IPTG) (Calbiochem) and grown for another 4 hours with agitation at 37°C, or cooled to 20°C and grown for 16 h. The cells were then pelleted by centrifugation at 6000 x *g*. for 25 minutes at 4°C. The cell pellet was resuspended in 10 ml sterile PBS with 1 proteinase inhibitor tablet (cOmplete ULTRA Tablets, EDTA-free EASYpack, Roche) and the cells disrupted using a French Pressure Cell (Thermo Electron Corporation) at 1000 psi twice before a further centrifugation at 15000 x *g*. for 30 minutes at 4°C to separate the cell lysate from the insoluble material.

2.7.1.2 His-Tagged Protein Purification Using Affinity Column

Ni^{2+}-NTA resin (QIAGEN) was prepared by washing a washing a 0.5 ml (50%) slurry 3 times in PBS by centrifugation at 1000 x *g*. for 2 minutes. The final pellet was resuspended in 0.5 ml PBS and added to the cell lysate before incubation at 4°C with agitation for 1 hour.

After allowing the protein to bind to resin, it was applied to a 10 ml Polyprep® chromatography column (BioRad). For His-tag purification, the Ni^{2+}-NTA-resin containing cell lysate was added to the column and the flow through obtained. The column was

washed twice with two column volumes of 20 mM imidazole in PBS (pH 7.4) to remove any non-specifically bound proteins. The cap was then placed on the column and the resin was incubated with 2 ml 150 mM imidazole in PBS for 30 minutes at 4°C with agitation. The cap was then removed and the elution fractions were caught in 1 ml fractions by gravity flow. Then, 2 ml 200 mM imidazole in PBS was added and the incubation repeated twice more. Finally, 4 ml of the 200 mM imidazole in PBS was added and the elution was caught immediately in 1 ml fractions.

2.7.1.3 GST-Tagged Protein Purification Using Affinity Column

Glutathione resin (QIAGEN) for GST-tag purification was prepared by washing a 0.5 ml (50%) slurry 3 times in PBS by centrifugation at 1000 x *g* for 2 minutes. The final pellet was resuspended in 0.5 ml PBS and added to the cell lysate before incubation at 4°C with agitation for 1 hour.

After allowing the protein to bind to resin, it was applied to a 10 ml Polyprep® chromatography column (BioRad). For GST-tag purification, the glutathione-resin containing cell lysate was added to the column and the flow through obtained. The column was washed twice with two column volumes of 50 mM Tris (pH 7.4) to remove any non-specifically bound proteins. The cap was then placed on the column and the resin was incubated with 2 ml GST-elution buffer (see Materials and Methods, 2.2.3) for 30 minutes at 4°C with agitation. The cap was then removed and the elution fractions were caught in 1 ml fractions by gravity flow. Another 2 ml of elution buffer was added and the incubation repeated twice more. Finally, 4 ml of the elution buffer was added and the elution was caught immediately in 1 ml fractions.

2.7.2 Purified Protein Analysis

The fractions were visualised by sodium dodecyl sulphate polyacrylamide gel electrophoresis (SDS-PAGE) and stained with Coomassie Blue. The samples were then dialysed in 200 times volume of 50 mM Tris (GST-tagged protein) or 140 mM PBS (His-tagged protein) at 4°C for 16 h and the samples kept at -20°C.

2.7.3 Sodium Dodecyl Sulphate Polyacrylamide Gel Electrophoresis

2.7.3.1 SDS-PAGE buffers

2.7.3.1.1 SDS-PAGE Upper and Lower Tris

SDS-PAGE upper Tris buffer was made from 6.06 g Tris Base and 0.4 g Sodium dodecyl sulphate (SDS) and made up to 100 ml using dH_2O before adjusting the pH to 6.8.

SDS-PAGE lower Tris buffer was made from 18.17 g Tris Base and 0.4 g Sodium dodecyl sulphate (SDS) and made up to 100 ml using dH_2O before adjusting the pH to 8.8.

2.7.3.1.2 SDS-PAGE Running Buffer

SDS-PAGE running buffer was made by adding 12 g Tris Base, 4 g sodium dodecyl sulphate (SDS) and 57.5 g glycine and made up to 1000 ml using dH_2O. Before use, 160 ml of the solution was diluted in 840 ml H_2O

2.7.3.1.3 2X SDS Loading Buffer

The loading buffer is added to the protein samples before running them on an SDS-PAGE gel. A 50 ml solution was made by adding 40 ml of a 100 mM Tris-HCl solution, 10 ml of 20 % glycerol, 1 g of SDS and 0.1 g Bromophenol Blue. Just before use, 200 mM DTT was added.

2.7.3.1.4 SDS-PAGE Destain Buffer

Destain buffer was used to remove the InstantBlue™ stain from the SDS-PAGE gels. This buffer was a mixture of 40% methanol, 10% acetic acid and 50% H_2O.

2.7.3.2 SDS-PAGE gel analysis

Tables 2.21 and 2.22 show the reagents and their quantities needed for a 10% and 12% tris-glycine SDS-polyacrylamide gel.

Table 2.21 Reagents and volumes needed for the resolving gel

	Volume	
Reagent	**10 % Gel**	**12 % Gel**
dH_2O	4.825 ml	4.3 ml
Lower Tris	2.5 ml	2.5 ml
Acrylamide	2.475 ml	3 ml
TEMED	5 µl	5 µl
APS	350 µl	350 µl

Upper and Lower Tris compositions can be seen in section 2.7.3.1.1.

Table 2.22 Reagents and volumes needed for the stacking gel

Reagent	**Volume**
dH_2O	4.725 ml
Upper Tris	2.1 ml
Acrylamide	0.975 ml
TEMED	17 µl
APS	100 µl

Stacking gel reagents and volumes remained the same for all percentage gels.

The reagents for the resolving gel were added in the order of listing in the Table with the ammonium persulphate (APS) (0.25 g in 5 ml dH_2O) added last. Immediately after APS addition, the solution was mixed and the gel poured into BioRad glass plates to ~1 cm from the top of the lower plate. As soon as the resolving gel was poured, 100 µl of isopropanol was added on top to remove any air bubbles and to prevent the top of the gel drying out. After the resolving gel was set, the isopropanol was removed and washed away with distilled water. The stacking gel reagents were added, again with the APS added last,

poured on top of the resolving gel and the comb was placed to form separate wells. Once set, the gel was positioned into a BioRad protein gel tank (mini PROTEAN Tetra System) and the tank filled with SDS running buffer. Protein samples were prepared by addition of SDS-loading buffer and heated at 100°C for 5 minutes. The comb was removed from the gel and the 10 µl of each sample was added to the lanes, with one lane reserved for 5 µl EZ-Run™ Pre-stained protein ladder. The gel was run at 220 mA (constant milliamps) until the loading dye reached the bottom of the gel. The gel was removed from the glass plates and stained using InstantBlue™ (Expedeon) for 2 h at room temperature with agitation.

2.7.3.3 Silver Staining Of Proteins In Polyacrylamide Gels

If protein concentration was too low for visualisation by EZ-Blue™, silver staining with silver nitrite is used as a highly sensitive method for visualisation of protein bands. The stained SDS-PAGE gel is completely destained using destain buffer (section 2.7.3.1.4), and washed thoroughly in dH_2O before silver staining using Silver Stain Plus Kit (BioRad) according to the manufacturer's instructions.

2.7.4 Western Blot

2.7.4.1 Western Blot General Buffers

2.7.4.1.1 Semi-Dry Transfer Buffer

Semi-dry transfer buffer was made with 2.9 g Tris Base, 1.45 g glycine, 1.85 ml 10% SDS and 100 ml methanol. The reagents were mixed and the total made up to 500 ml with H_2O.

2.7.4.1.2 Blocking Buffer

The blocking buffer was made up of 5% semi-skimmed milk, 3% BSA and 0.1% Tween-20 in PBS

2.7.4.2 Antibodies

Antibodies used in this study are listed in the Table below including the dilution they were used at.

Table 2.23 Antibodies used in this study

Antibody	Type	Dilution	Supplier
Anti-OmpA	Primary, rabbit raised	1:1000	Professor Keiji Nagano (Aichi Gaukin University, Nagoya, Japan)
Anti-FimA	Primary, rabbit raised	1:1000	Professor Ashu Sharma (University at Buffalo, NY, USA)
Anti-rabbit IgG-HRP conjugated	Secondary, goat raised	1:3000	Cell Signalling

All antibodies were dilution to their correct concentrations in 0.1% Tween-20 in PBS.

2.7.4.3 Protein Analysis Using Western Blot

An SDS-PAGE gel is run as above, but prior to staining with Coomassie Blue, the proteins are transferred to a re-enforced nitrocellulose (NC) sheet (GE Healthcare). Six sheets of chromatography paper (GE Healthcare) and one sheet of NC paper were cut to 8.5 cm x 6 cm and soaked alongside the gel in semi-dry transfer buffer for 5 minutes. The gel and papers were transferred to a BioRad Trans-Blot Semi Dry Transfer Cell in the following order; three sheets of chromatography paper, the NC sheet, the gel and the final three sheets of chromatography paper. Transfer was achieved by running at 10 A for 60 minutes, or until the protein had fully transferred to the NC sheet (detected by the transfer of the coloured EZ-run™ protein ladder). The NC sheet was then transferred to a falcon tube containing 50 ml blocking buffer and incubated with agitation for either 2 hours at room temperature or 4°C overnight. The blocking solution was then poured off and the NC sheet washed three times with PBS supplemented 0.1% Tween-20. The NC sheet was then incubated for 1 h with the primary antibody, subject to the protein of interest. The NC was washed 3 times with PBS + 0.1% Tween-20 to remove excess antibody, and then the NC sheet was incubated with a secondary antibody before being washed 3 times and then exposed to the developing solution, Pierce® ECL Western Blotting Substrate (Thermo Scientific). Equal volumes of each of the solutions were mixed and added to the NC sheet and left for 1 minute. Excess liquid was removed and the NC sheet placed in cling film and placed into an X-Ray cassette folder (Kodak). Sheets of CL-Xposure™ X-ray films (Thermo

Scientific) were placed in the cassette in contact with the NC sheet for varying lengths of time, ranging from 1 second to 5 minutes, and the sheets developed using a Compact X4 X-ray Film Processor (Xograph).

2.7.5 Outer Membrane Protein Fraction Preparation

10 ml cultures of *P. gingivalis* were grown according to 2.4.2 to an OD_{600} 1.0 and pelleted at 5000 x *g* for 10 min at 4°C in a Beckman Coulter™ J-26 XP centrifuge. The supernatant was discarded before each pellet was resuspended in 2 ml resuspension buffer (0.01 M HEPES, pH 7.4, 2 µl deoxyribonuclease and 2 µl ribonuclease (both Promega)). The cell suspension was lysed by passage through a French Pressure Cell (2250 psi using a 800 medium ratio piston) before the addition of 2 µl 1 mM $MgCl_2$ and centrifugation at 5000 x *g* for 5 min (4°C). The supernatant was then transferred to a new Eppendorf and centrifuged at 75600 x *g* for 45 min at 4°C. The supernatant, containing the cytoplasmic and periplasmic fraction, was then removed and stored, whilst the pellet was resuspended in 500 µl 0.01 M HEPES (pH 7.4) containing 2 % Triton X-100 and incubated for 10 min at room temperature, before being centrifuged at 75600 x *g* for 45 min at 4°C. The supernatant containing the inner membrane fraction was removed and stored, before the pellet was resuspended in 500 µl 0.01 M HEPES (pH7.4) and centrifuged at 75600 x *g* for 45 min at 4°C. The supernatant was discarded, and the remaining pellet (the outer membrane fraction) was resuspended in 50 µl 2 x SDS loading buffer (without DTT) and spun in a microcentrifuge (GenFuge, Progen Scientific) for 5 min at 16000 x *g* before being heated to 95°C and run on a NuPAGE® Bis-Tris 4-12% gradient gel (Thermo Fisher Scientific) for greater protein resolution.

2.8 Phenotypic Characterisation Methods

2.8.1 Antibiotic Protection Assay

The antibiotic protection assay was carried out in a Class II Safety Cabinet, thoroughly cleaned with 70% IMS. All media was pre-warmed to 37°C and sterilised before being placed into the cabinet. OK-F6 cells were seeded identically at 2 x 10^5 cells / ml at 1 ml per well into two 24-well MTPs and incubated at 37°C, 5% CO_2 with humidity for 24 hours until 70-80% confluency was reached. After the desired confluency was reached, the media from each well was removed and the monolayer of cells was gently washed with PBS. In one “sacrificial” well, 500 µl trypsin-EDTA was added and the plate incubated for 10 minutes

until the cells detached. Then, 500 µl neutralising media was added and the cells counted as previously described. The remaining wells were incubated with 1 ml DKSFM supplemented with 2% bovine serum albumin (BSA) for 60 minutes at 37°C 5% CO_2 with humidity. During this incubation, *P. gingivalis* strains (wild-type or mutants) were removed from a 72 hour blood agar plate and suspended in 1 ml of DKSFM. The bacteria were counted and adjusted to match a 1:100 ratio (OK-F6 cells: bacteria) to create a multiplicity of infection (MOI) of 100. After the 60 minute incubation with BSA-containing DKSFM, the OK-F6 cells were washed three times with PBS and incubated with 1 ml of DKSFM containing the bacterial suspension and incubated aerobically for 90 minutes at 37°C, 5% CO_2 with humidity. Alongside the OK-F6 containing wells, 3 wells per bacterial strain were seeded with the bacterial suspension to analyse the bacterial cell viability throughout the assay. After 90 minutes incubation with *P. gingivalis,* the wells containing OK-F6 cells and bacteria were washed three times with PBS. One of the MTPs containing wells with OK-F6 cells and bacteria was incubated for a further 60 minutes with 200 µM metronidazole per well to kill any extracellular *P. gingivalis* as to assess the number of invaded bacteria. Both MTPs were then washed three times with PBS and 100 µl sterile H_2O was added for 1 minute to each well with scraping to lyse the OK-F6 cells. The cell lysate with bacterial cells was then serially diluted 10-fold down to 10^{-4} and 3 x 10 µl of each spot was then plated onto blood agar plates and grown anaerobically for 5 days. Wells containing only *P. gingivalis* were serially diluted and plated onto blood agar plates in the same way, with the exception of the washing, addition of water and scraping.

2.8.2 Antibiotic Protection Assay in the Presence of Peptides

Standard antibiotic protection assays were carried out as detailed in 2.8.1, with the addition of an additional incubation step following BSA incubation, whereby 50 µg/ml of each peptide was added to each well containing epithelial cells followed by the 90 min incubation step with bacteria in the presence of peptide (50 µg/ml), before processing as previously detailed. Biotinylated peptides were purchased from IscaBiochemicals Ltd. (Exeter, UK) or CovalAb (Cambridge, UK).

2.8.3 Fluorescence Binding Assay of Extracellular Peptide Loops to OK-F6 Monolayers

Peptides were bound to a final working concentration of 50 µg/ml to yellow-green fluorescent FluoSpheres® (NeutrAvidin®-labelled Microspheres, Invitrogen) by the following

method. Firstly, the beads were washed three times in 0.01 M HEPES buffer (pH 7.4), with centrifugation of 14,000 x *g* (10 min) and then gently sonicated. Peptides were added and allowed to adhere to the FluoSphere® for 16 h at 4°C with gentle agitation. Then, the FluoSpheres® were washed in HEPES, before gentle sonication and further 1 h incubation with 0.1 % BSA at 4°C. Peptide-bound FluoSpheres® were then washed three times in HEPES buffer, sonicated gently, and either stored at 4°C for up to one month, or used immediately in binding to oral epithelial cells. FluoSpheres® were also incubated with 2 % BSA as a negative control.

For peptide binding assessment, OK-F6 cells were grown to 90% confluency in a 96-well MTP before being washed twice with PBS, then 2% BSA blocking buffer in DKSFM was added and incubated for 1 hour at 37°C, 5% CO_2. Cell monolayers were washed thoroughly with HEPES buffer before the addition of 100 µl peptide-bound FluoSpheres® at a ratio of 1:100 (cells: FluoSpheres®) as to mimic the MOI of an invasion assay, and incubated at 37°C with 5 % CO_2 for 4 h. After incubation, wells were gently washed three times in HEPES buffer and fluorescence read using a TECAN Infinite® PRO plate reader, with 488_{nm} / 510_{nm} (ex/em) filters.

Alternatively, OK-F6 cells were seeded onto coverslips in a 24-well MTP and grown to a confluency of 70 %, before being washed in PBS and 2 % BSA added as above. Cells were washed in HEPES and 350 µl peptide-bound FluoSpheres® at a ratio of 1:100 (cells: FluoSpheres®) were added and incubated for 4 hours as previously described. After incubation, cells were gently washed in HEPES buffer before being fixed using 4 % paraformaldehyde and incubated at room temperature for 15 min. Cells were then washed in PBS and cell membranes were stained using Wheat Germ Agglutinin, Texas Red®-X Conjugated antibody (Life Technologies) at a 1:1000 dilution, and incubated without light for 15 min at 37°C with 5 % CO_2, before being thoroughly washed in PBS and mounted onto glass microscope slides using ProLong® Gold Antifade Mounting Medium with DAPI and imaged using an Axiovert 200M Microscope (Zeiss) 24 h post-mounting.

2.8.4 Biofilm Formation Assay

P. gingivalis strains were seeded at an OD_{600nm} of 0.05 into a 96 well MTP (Corning) and grown under anaerobic conditions without shaking. After 72 hours, the total growth was measured by reading the absorbance (600 nm) using a FLUOstar (BMG Labtech). The

planktonic bacteria were removed and the biofilm layer washed 3 times in PBS. The biofilm layer was then stained using 100 µl 0.1% Crystal Violet stain and incubated at room temperature for 20 minutes. Excess stain was removed and the stained layer was washed until the PBS became clear. Images were taken under 400 X magnification using a Nikon Elipse TS100 light microscope and then the Crystal Violet stain was extracted using 200 µl of 20 % acetic acid. Then, 80 µl of the extracted Crystal Violet was centrifuged (11,000 x *g*, 1 min) to remove any precipitate and then transferred from each well to a new 96-well MTP and the absorbance read at 575nm.

2.8.5 Electron Microscopy

2.8.5.1 Sample Processing for Sectioning

Liquid cultures of *P. gingivalis* and mutant strains were grown to OD_{600} 1.0, before 1 ml was pelleted and supernatant discarded. The cell pellet was washed twice for 5 min in cacodylate buffer (0.1 M Cacodylate buffer, pH7.4), and the supernatant removed. The pellet was then fixed in 3% glutaraldehyde for 4 hours at 4°C, before being washed three times at 4°C in cacodylate buffer (20 min washes). The pellets were then soaked in osmium tetraoxide (OsO_4) for 1 hour at room temperature before a series of washes were carried out:

- 3 x 2 min dH_2O
- 2 x 3 min 70 % ethanol
- 2 x 5 min 95 % ethanol
- 2 x 10 min 100 % ethanol

The pellet was then "dried" in 100 % dried ethanol (dried over copper sulphate) for 15 min before being soaked in propylene oxide for 15 min at room temperature. The pellets were then soaked for 16 h in a 50/50 reagent mixture of propylene oxide/Agar 100 resin (see Table 2.24 for Agar 100 resin) in sealed containers. After 16 h, the 50/50 mixture was replaced with 100% Agar 100 resin for 8 h in open containers, before embedding the pellet in fresh Agar 100 resin and left to polymerise in a flat embedding silicon mould (Agar Scientific) at 60°C for 24-48 h. Embedded pellets were sectioned at 70-90 mm and placed onto formvar-coated grids.

Table 2.24 Agar 100 Resin reagents for medium blocks

Reagent	Volume (ml)
Agar 100 epoxy resin	20
Hardener DDSA	16
Hardener MNA	8
Accelerator BDMA	1.3

Reagents were thoroughly mixed and air bubbles removed via sonication before application.

2.8.5.2 Staining of Electron Microscope Grids

The grids were stained with assistance from David Thompson (The University of Sheffield) by the following procedures and stains as previously discussed by Reynolds (Reynolds, 1963). In brief, a single drop of uranyl acetate (7% saturated in 50% methanol) was placed onto a strip of Parafilm M®, and the grid with sections was floated on top to stain for 20 mins in the dark. The grid was then rinsed for 20 s in dH_2O before being stained in lead citrate (Table 2.25) for 5 min in the same way but in a light environment. Grids were then washed well before electron microscopy.

Table 2.25 Lead citrate buffer

Reagent	Amount
Lead nitrate	1.33 g
Sodium citrate	1.76 g
Distilled H_2O	30 ml
1 M Sodium Hydroxide (NaOH)	Make up to 50 ml

2.8.9 Proteinase Activity Assays

These assays were used to assess the level of gingipain activities of whole cell wild-type *P. gingivalis* and mutant strains, as well as the activity of gingipains secreted by these strains.

2.8.9.1 Colorimetric Assays

Colorimetric Assays were used to measure the gingipain activity of whole cell bacteria. Overnight liquid cultures of *P. gingivalis* and mutant strains were grown as described in 2.4.2 before being centrifuged at 16000 x *g* for 10 min. Pellets were washed twice in PBS and adjusted to OD_{600} 1.0. In a 96-well MTP, triplicate wells of each strain were set up, containing 1 µl 1 M L-cysteine, 100 µl TNCT buffer (detailed in Table 2.26) and 10 µl bacteria (for Arg-gingipain activity) or 20 µl bacteria (for Lys-gingipain activity). The reaction was left to incubate for 5-10 min at room temperature before 100 µl 0.4 mM substrate (*N*-α-Benzoyl-L-arginine *p*-nitroanilide for Arg-gingipains, or toluenesulfonyl-glycyl-L-prolyl-L-lysine p-nitroanilide for Lys-gingipains, both diluted in TNCT buffer) and read immediately at Abs_{405nm} on a TECAN Infinite® PRO plate reader. The absorbance was measured every minute for 30 minutes to determine gingipain activity rate.

Table 2.26 TNCT buffer

Reagent	**Concentration**
Tris-HCl (pH7.5)	50 mM
NaCl	150 mM
Calcium Chloride ($CaCl_2$)	5 mM
Tween-20	0.05%
dH_2O	Up to 50 ml

2.8.9.2 Fluorometric Proteinase Assay

Fluorescence based substrates were used to determine the Arg- and Lys-proteinase activity of secreted gingipains, due to the disruption of the coloured culture media on the colorimetric substrate. Fluorometric assays were adapted from the protocol outlined by Chen (Chen *et al.*, 2001), except samples were generated from liquid cultures. Briefly, cultures of *P. gingivalis* strains were grown as outlined in Materials and Methods 2.4.2, the OD_{600} adjusted to 1.0 and the cells were centrifuged (16000 x *g*, 5 mins) and the pellets discarded. To measure Arg-proteinase activity, a reaction mixture of 100 µl PBS containing 1 mM L-cysteine, 200 µM *αN*-benzoyl-L-arginine-7-amido-4-methylcourmarin substrate and 50 µl supernatant was added in triplicate to a 96-well MTP and incubated at room

temperature for 10 minutes before the reaction was terminated by the addition of *N*-α-tosyl-L-phenylalanine chloromethyl ketone (TPCK) at 200 µM. Lys-proteinase activity was assayed in 100 µl PBS containing 1 mM L-cysteine, 10 µM *t*-butyloxycarboyl-Val-Leu-Lys-7-amido-4-methylcourmain substrate and 50 µl supernatant and incubated at 40°C for 10 min before the reaction was terminated using 500 µM *N*-α-p-tosyl-L-lysine chloromethyl ketone (TLCK). Both Arg- and Lys-gingipain activities were determined by measuring released 7-amido-4-methylcourmarin using a TECAN Infinite® PRO plate reader, with excitation and emission wavelengths of 365 nm and 460 nm respectively.

2.8.9.3 Sialidase Assay

Overnight cultures of *P. gingivalis* and mutant strains were set up according to Materials and Methods 2.4.2. Cultures were centrifuged (1600 x *g* for 5 min) and the pellets resuspended in PBS and adjusted to OD_{600} 1.0 and 0.5, before 5 µl of each OD and strain in triplicate were added to a 96-well MTP, with 42.5 µl PBS and 2.5 µl MUNANAC (2'-(4-Methylumbelliferyl)-α-D-*N*-acetylneuraminic acid) from stock solution of 2 mM and anaerobically incubated for 60 or 120 min at 37°C. The reaction was then terminated by the addition of 75 µl 100 mM sodium carbonate buffer (pH 10.5) before reading fluorescence at 355 nm / 420 nm (ex/em) using a TECAN Infinite® PRO plate reader.

2.8.9.4 Membrane Permeability Assay

Thiazole Orange (TO) was used to determine the permeability of wild type and Δ*ompH1H2* membranes. Bacterial strains were grown in a liquid culture as described previously. Cells were adjusted to 1 x 10^6 CFU/ml in 20 mM Sodium Phosphate buffer. A 1 ml aliquot of cells was added to a Hellma Analytics Quartz Cuvette and agitated using a magnetic stirrer. Excitation and emission (510 nm_{ex} / 530 nm_{em}) were read using a Varian Cary Eclipse fluorescence spectrophotometer every 100 ms for 10 s, before the addition of 25 µl TO at a concentration of 17 µM (final concentration of 420 nM). The rate of uptake of TO was measured every 100 ms for 20 s at the same excitation and emission wavelengths as before (510 nm_{ex} / 530 nm_{em}). The data was analysed through the Varian Cary Eclipse Software and the rate was determined using the initial uptake within the first 5 s after TO addition.

2.8.9.10 Outer Membrane Vesicle Quantification

Bacterial cultures were grown according to section 2.4.2 and cells were precleared from the culture by differential centrifugation. Bacterial cells were pelleted (8000 x *g*, 10 min) and cell-free supernatants were centrifuged for a further 30 min at 10000 x *g* to remove any cell debris. The supernatant was then passed through a 0.44 µm filter before being diluted 10 – fold in sterile PBS. The OMVs were then analysed using a qNANO (iZON Science Ltd) with the application of Tunable Resistance Pule Sensing (TRPS). Then, 40 µl of the diluted sample was applied to the upper fluid cell of an NP100 nanopore stretched to 45.5 mm, whilst a voltage (42 V) and positive pressure (2 mbr) was applied to cause unidirectional flow of the OMVs through the nanopore. Calibration particles (CPC100B) of a known size (114 nm) and concentration ($1x10^{13}$ particles ml^{-1}) were also applied for comparison to the wild-type and Δ*ompA* samples. The size and concentration of OMVs were analysed using the iZON Control Suite Software (provided with the instrument) and normalised to the OD_{600} of the corresponding bacterial culture.

2.9 Statistical Analysis

Each experiment was carried out with triplicate biological repeats unless otherwise stated. Statistical analysis used either students' *t*-test, One-way ANOVA or 2way ANOVA once normal distribution was determined, and is detailed in the figure legend.

Chapter 3

Role of the *ompA* Gene Cluster in Host-Cell Interactions and Biofilm Formation

3.1 Introduction

Host cell interaction is a crucial aspect of a bacterium's virulence. In particular, the ability for a periodontal pathogen to invade the host cell provides a nutrient-rich environment to facilitate replication (Madianos *et al.*, 1996), which can lead to cell-to-cell spread and contributes to tissue destruction and disease progression (Tribble and Lamont, 2010). It also provides an immune-privileged niche whereby the periodontal pathogen is protected from the host immune system as well as protection from external antimicrobial challenges (Rudney and Chen, 2006), such as the application of antibiotics or removal by mechanical methods such as non-surgical debridement (Duncan *et al.*, 1993; Lamont *et al.*, 1995). Invasive bacteria have evolved numerous mechanisms for entry into the host cell, however first the bacteria must attach to the host cell and induce a number of biochemical and structural changes for host cell penetration, there is an extensive literature in this area that is summarised in section 1.6.6.3 of the introduction to this thesis.

As discussed in Section 1.6.6.3, due to the importance for host adherence and invasion, *P. gingivalis* possesses multiple mechanisms to facilitate this. Two of the major mechanisms include the fimbriae and gingipain proteases. Briefly, initial binding is predominantly facilitated by the major fimbriae, composed of major FimA subunits and minor FimC, D and E subunits (Nishiyama *et al.*, 2007), which engage host cell integrins ($\alpha_v\beta_3$ and $\alpha_5\beta_1$) and cause bacterial internalisation through cytoskeleton rearrangement (Weinberg *et al.*, 1997; Yilmaz *et al.*, 2002). The gingipain proteases are integral for successful adherence to the host by modulation of host matrix proteins to reveal hidden host receptors (or "cryptitopes") and increase invasive efficiency (Kontani *et al.*, 1996; Park and Lamont, 1998).

Due to their cellular surface location, various membrane proteins have been implicated in the interaction with the host. This chapter focusses on the major outer membrane protein, OmpA. The OmpA protein has been previously shown to be involved in the interaction with host in many different Gram-negative bacterial species. Meningitis-causing *E. coli* (K1-type strain) uses the OmpA protein in host cell interaction (Prasadarao *et al.*, 1996), and the recently identified OmpA protein of *Neisseria gonorrhoeae* has been shown to be involved in the binding to epithelial cells (Serino *et al.*, 2007). OmpA has also previously been shown to interact with a host glycoprotein to induce actin cytoskeleton rearrangement, facilitating the internalisation of *E. coli* (Prasadarao *et al.*, 2002; Prasadarao *et al.*, 2003). The OmpA protein found in *P. gingivalis* shows a high structural homology to the *E. coli* protein

(Nagano *et al.*, 2005) (see section 3.3.1); and has been shown to be involved in interaction with human endothelial cells (Komatsu, et al. 2012), however nothing was known regarding its role in epithelial cell interactions, which we hypothesised might have a similar role in host-interactions with arguably greater relevance to periodontal disease.

This chapter uses a knockout mutagenesis approach to characterise the role of the *ompA* genes in host-cell interactions by investigating the process of adherence and invasion of host oral epithelial cells mediated by the OmpA proteins of *P. gingivalis*.

3.2 Aims

The major aim of this chapter was to investigate the role for individual OmpA subunits in the interaction with the host cells, in this case a disease relevant monolayer model of infection, using the oral epithelial cell line, OKF6. This was achieved by performing knockout mutagenesis of *P. gingivalis* using allelic replacement and utilising the newly found natural competence based method of *P. gingivalis* transformation.

N.B. much of the work in this chapter is included in a paper that has been accepted in MicrobiologyOpen (see appendix I)

3.3 Results

3.3.1 Basic Bioinformatic Analysis of the *ompA* Genes.

The *ompA* genes of *P. gingivalis* are predicted to sit in the *ompA* operon, with the two genes, *ompA1* (PGN_0729) and *ompA2* (PGN_0728), arranged in tandem on the bacterial chromosome as shown in Figure 3.1, and predicted to transcribed from a single promoter 5' of *ompA1*.

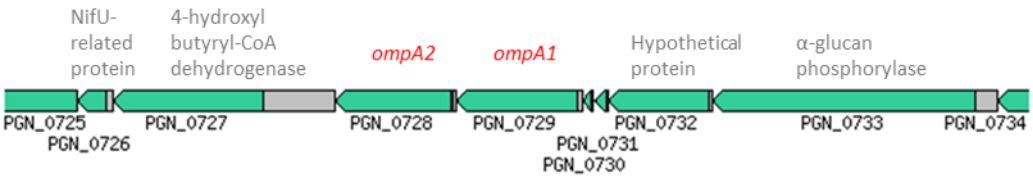

Figure 3.1 Schematic representation of the *ompA* operon in the *P. gingivalis* chromosome. The *ompA1* and *ompA2* genes are indicated in red, adjacent genes in grey. Adapted screenshot from (http://www.oralgen.org/microbe.php?class=oral).

The sequence similarities between *P. gingivalis ompA* coding sequences at the primary amino acid level and *ompA* from *E. coli* was assessed *in silico* using online alignment tools, originally in BLASTP, and then in programmes such as MultAlin (Corpet, 1988) and Clustal Omega (Mcwilliam *et al.*, 2013). Based on BLAST searching for homologous matches of *E. coli* OmpA in the *P. gingivalis* genome, homology only exists in the C-terminal domain of the protein and demonstrated by MultAlin alignments seen in Figure 3.2, as evidenced by high levels of similarity and identity in the last 100 amino acids.

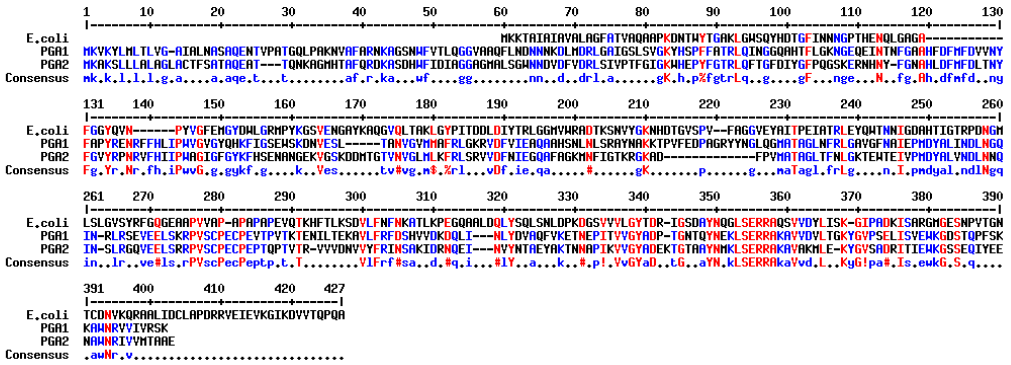

Figure 3.2 Protein sequence alignments between *E. coli* OmpA and *P. gingivalis* OmpA1 and OmpA2. Alignments performed with Multalin, showing *E. coli* OmpA (top sequence) compared to *P. gingivalis* OmpA1 (PGA1, middle sequence) and OmpA2 (PGA2, bottom sequence). Residues highlighted in Red indicate presence in all three sequences, whereas blue indicates alignment in only two sequences.

The similarity between protein sequences was limited, with only 23 and 24% homology observed for OmpA1 and OmpA2 respectively against *E. coli* OmpA, whereas the sequence homology between *P. gingivalis* OmpA1 and A2 is much higher, at 47% similarity. Structural homology is predicted to be much higher, as shown by Nagano *et al* (2005) and discussed in greater detail in Chapter 4.3.5, with all proteins having predicted eight-stranded β-barrel in the N-terminal region and a peptidoglycan-associated C-terminal domain.

3.3.2 Generation of Δ*ompA1* and Δ*ompA2* Mutants

Mutants of the single *ompA1* and *ompA2* genes were generated to understand their individual roles in host interaction. A double mutant (Δ*ompA1A2)*, whereby the entire *ompA* operon was deleted, was generated in a previous study by Mary Connolly at The University of Sheffield whilst part of Dr Stafford's research group and was provided for this research. Single Δ*ompA1* or *–A2* mutants were generated through the production of a gene

knock out construct through either overlap extension PCR or gene synthesis of similar constructs (GeneArt™, Thermo Fisher Scientific). The gene knock out constructs consisted of an erythromycin resistance cassette (*ery*^{R}) flanked on either side by DNA 5' and 3' of the gene of interest to allow homologous recombination and allelic exchange when introduced into the wild type *P. gingivalis*, thus replacing the gene of interest with an antibiotic resistance marker for selection. The technique of overlap extension PCR is detailed in Figure 3.3, and involves using methods of conventional PCR to assemble three double stranded DNA fragments into one large DNA construct. Primers for the single DNA fragments were designed with "tails" which complement the starting sequence of the next single fragment. Each single fragment is amplified through the first PCR reaction with the "tail" of the next fragment, and is then used as the template for the second PCR reaction which assembles the fragments into one large construct (Fig. 3.3).

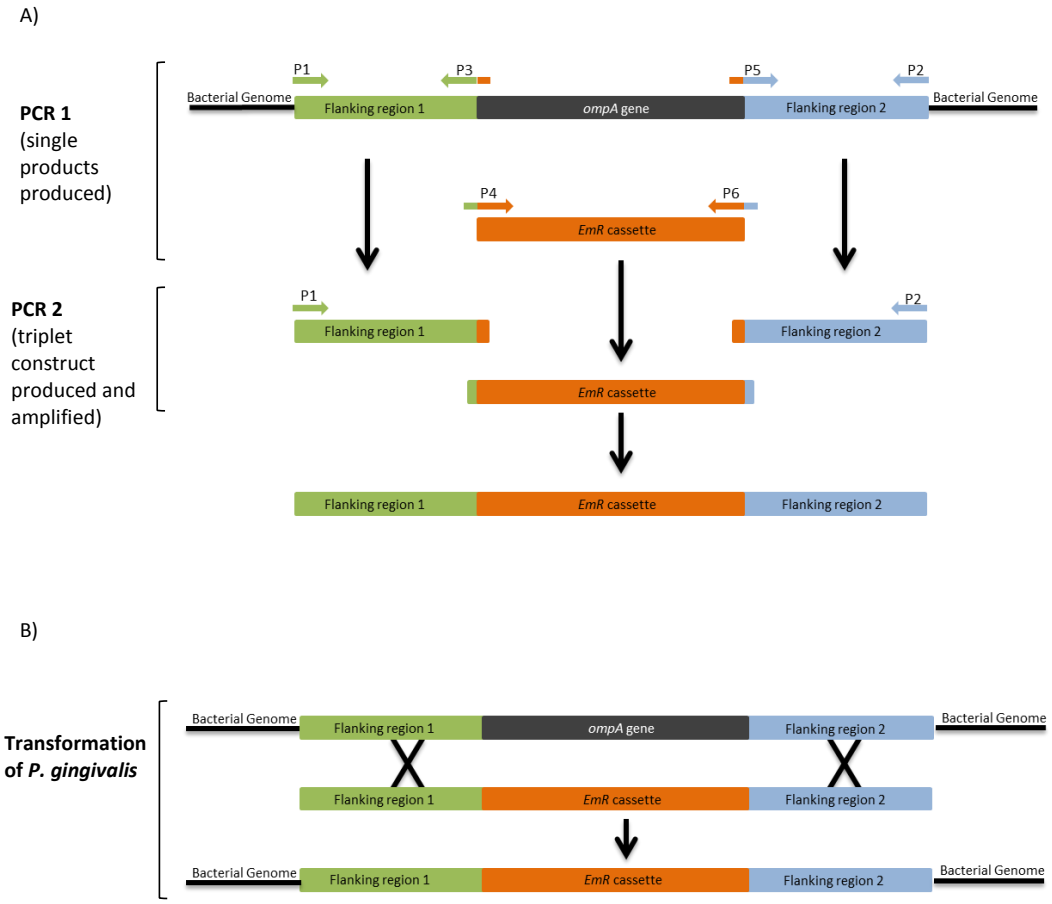

Figure 3.3 Overlap Extension PCR and Allelic Exchange for *P. gingivalis ompA* mutant production. (A) Two PCR reactions are carried out, first to amplify the flanking regions and the erythromycin cassette with tails complementary to the region they are to be linked to

then a second PCR is performed to combine the three separate regions and amplify the final construct. These constructs are then introduced to the wild-type bacterium as either linear fragments or incorporated into a plasmid for allelic exchange and production of the knock out mutation (B).

Genomic DNA from wild-type *P. gingivalis* ATCC 33277 was extracted using the Promega Wizard® Genomic DNA Extraction Kit and using primers detailed in Table2.5 and 2.6., flanking regions of ~1000 bp upstream (flank 1) and downstream (flank 2) of the *ompA1* or *–A2* gene were amplified, alongside an erythromycin resistance cassette gene, from genomic DNA of *P. gingivalis* ATCC 33277 from a previous study. A second PCR reaction was then performed using these single fragments as the DNA template, and primers *ompA1*-f1 for and *ompA1*-f2 rev (or the *ompA2* equivalent) (Table 2.5 and 2.6), to assemble these fragments into the gene knock out cassette (Flank 1- ery^R – Flank 2). After each PCR, products were analysed on a 1% TAE agarose gel, as shown in Figure 3.4, and cleaned up using a QIAGEN QIAquick PCR purification kit, or extracted from the gel before purification if multiple bands were present, which was often the case for the final 3-way PCR reaction products. All PCR reactions were carried out as detailed in Materials and Methods 2.6.2.4 using Phusion™ as the polymerase enzyme to ensure no errors in the erythromycin resistance gene or flanking regions.

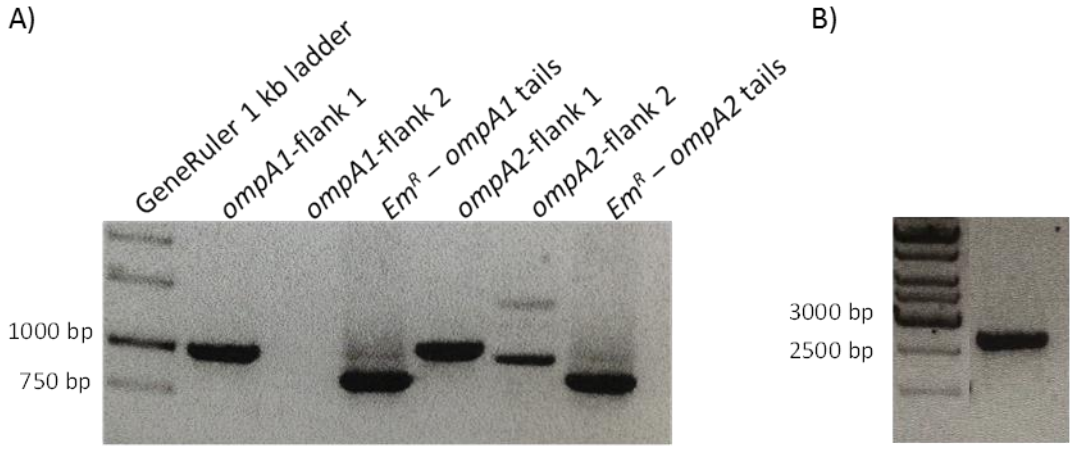

Figure 3.4 PCR Amplification of *ompA1* and *ompA2* flanking regions and ery^R cassette for gene knock out (A) and combined constructs for transformation (B). Regions were amplified using Phusion™ polymerase enzyme in conditions described in Table 2.17. Flanking regions appear as the prominent bands at ~1000 bp (except for *ompA1* flanking region 2), and erythromycin cassette appears at ~800 bp. A second PCR was carried out to combine single PCR products (B) into the full knock out construct (~2800 bp).

PCR constructs were sequenced using GATC sequencing (GATC-Biotech, Germany), and non-erroneous constructs were used in transformation of *P. gingivalis*. Only the *ompA2::em* construct was produced through the overlap PCR method, as the full flank 1-*ery*^{R}-flank 2 construct for *ompA1* gene knock out could not be assembled from singlet templates. Multiple annealing temperatures, DNA concentrations and extension times were used, as well as intermediate PCR reactions to assemble flank 1-*ery*^{R} and *ery*^{R}-flank 2 products before the final assembly; however no full construct could be created. Instead, the construct was generated by constructing the sequence *in silico*, replacing the *ompA1* gene with the sequence from the erythromycin cassette at the *ompA1* start codon. As with the *ompA2::em* construct, the erythromycin gene was flanked both side with 1000 bp from the original *ompA1* gene, and synthesised by GeneArt™ (Thermo Fisher Scientific). The construct was cloned into pJET1.2/blunt plasmid vector (a blunt-end cloning vector that cannot replicate in *P. gingivalis*) before transformation as circular plasmid DNA and stored in *E.coli* DH5-α.

Either the circularised plasmid DNA (~200-250 ng/µl) or linear PCR fragment (~200-250 ng/µl) was then used for transformation into *P. gingivalis* wild-type. Transformation for Δ*ompA1* and Δ*ompA2* was achieved through natural competency (as detailed by Tribble *et al.,* (2010)) as well as electrocompetency method, as detailed in Section 2.6.3 and 2.6.4. For both techniques, the transformed *P. gingivalis* were grown on plain BA plates for 24 hours to allow for the production of erythromycin resistance, before being transferred to BA plates supplemented with erythromycin for selection of successful mutants. After plating on erythromycin-containing BA-plates, the mutagenesis experiments were incubated at 37°C anaerobically for 14-21 days. Typically erythromycin-resistant colonies appeared after 9 days and were initially replated by streaking to fresh erythromycin-containing BA-plates before individual clones being assessed for correct recombination using PCR.

Colonies that grew on erythromycin supplemented plates were analysed to check for faithful insertion of the antibiotic cassette in place of the gene of interest using PCR, as illustrated in Figure 3.5, and in all cases wild-type DNA was used as a control. DNA was extracted from erythromycin-resistant colonies and used in PCR reactions using GreenTaq™ polymerase enzyme and primers *ompA1*-f1 for and *ompA1*-f2 rev (or the *ompA2* equivalent) for whole construct generation (flank 1 - *ery*^{R} - flank 2) to determine the gene had be successfully knocked out (Fig 3.6A, C) and primers *ompA1*-f1 for and *ompA1*-em rev (or the *ompA2* equivalent) for generation of a flank 1 – ery^{R} construct to ensure the

erythromycin gene is present (Fig 3.6B, D). Products from these confirmation PCRs were also sequenced to ensure the *ompA* gene had correctly been knocked out from the *P. gingivalis* genome.

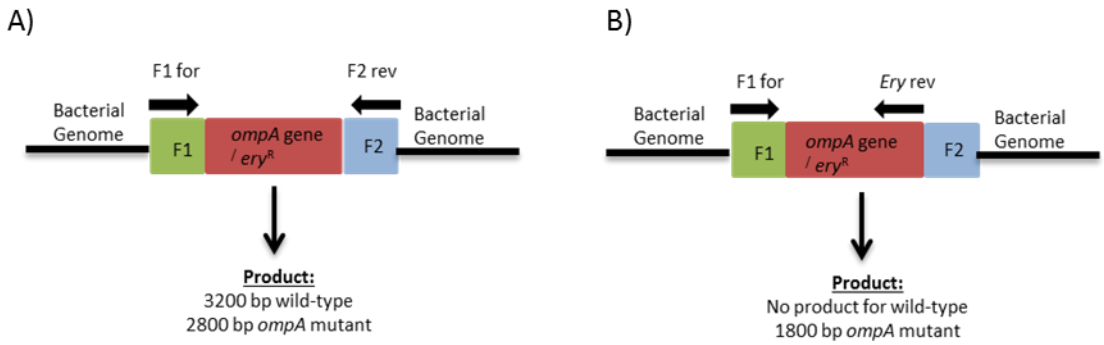

Figure 3.5 Schematic demonstrating primer pair locations for knock out mutagenesis PCR confirmation. (A) shows primers used to amplify the whole construct of (flank 1 – *ery*^{R} - flank 2) and the expected product sizes, whereas (B) shows the primer placements used to amplify the flank 1 - *ery*^{R} which would only appear if the erythromycin gene has been successfully incorporated.

These combinations of PCR reactions were also chosen as they would assess correct incorporation into the genome in the case of the plasmid transformation. In some cases, single crossovers may occur whereby the genome inherits the erythromycin resistance cassette by homologous recombination at one of the homologous regions, alongside the retention of the gene, whereas a double crossover of the knock out construct would nullify the gene by removal. Whole construct amplification would indicate a single crossover event as both the plasmid containing the gene knock out and the wild-type gene would be amplified, giving two bands upon agarose analysis.

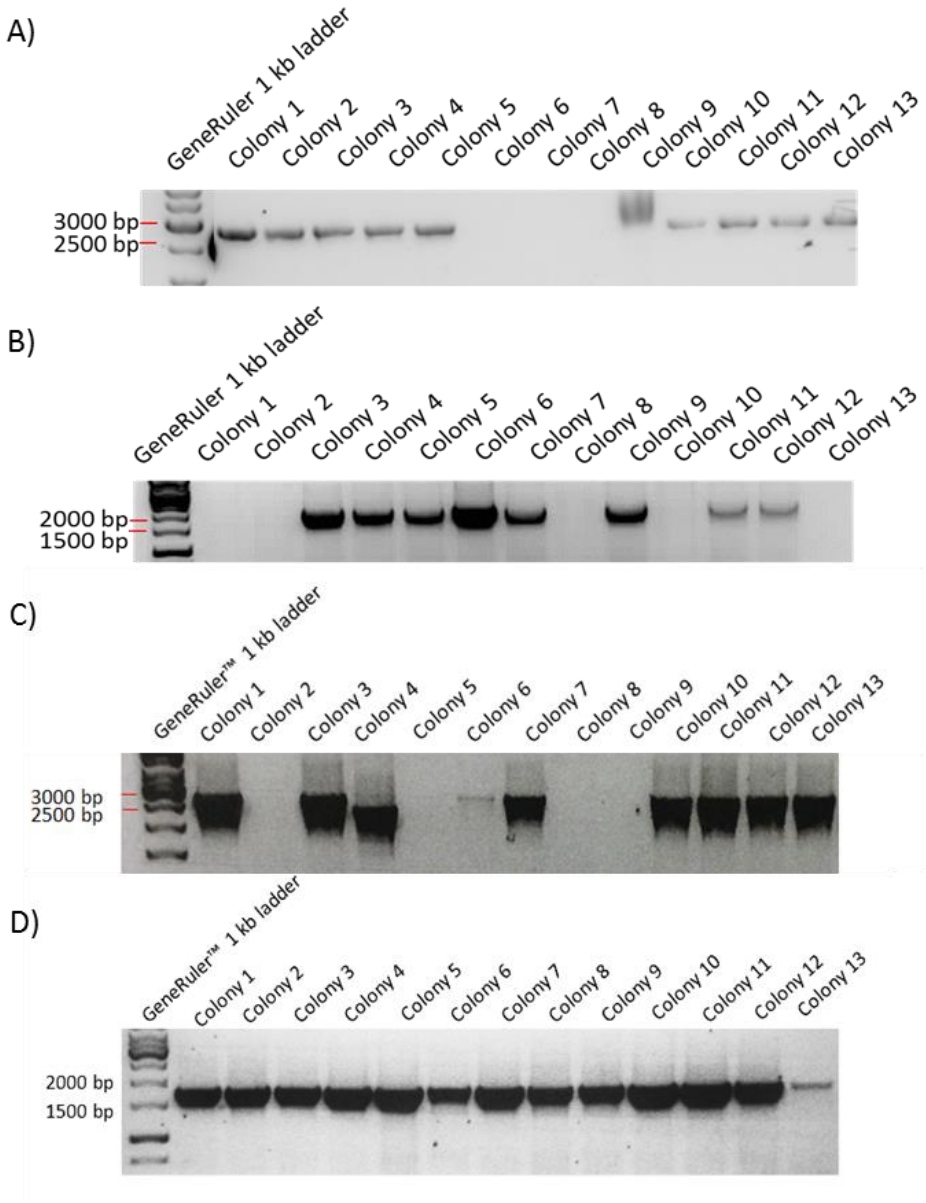

Figure 3.6 Confirmation of Δ*ompA1* and Δ*ompA2* mutant generation through colony PCR. DNA from 13 colonies that appeared on BA plates supplemented with erythromycin (10 µg/ml) was extracted and colony PCRs were carried out according to Chapter 2.6.2.3 using GreenTaq™ polymerase. Successful knockout of *ompA1* and *ompA2* displayed bands at ~2800 bp for full gene construct confirmation (A and C for Δ*ompA1* and Δ*ompA2* respectively) or ~1800 bp for flank – *ery*^{R} construct generation (B and D for Δ*ompA1* and Δ*ompA2* respectively). Wild-type controls were negative for the presence of the erythromycin resistance gene (not shown).

Only colonies that were positive for bands on both agarose gels were taken for sequencing and if they contained no errors in the sequence, these colonies were stored in -80°C for experimental use. It is of note that of all the antibiotic resistant colonies, none tested negative for the single recombination event, indicating double crossover events in all mutants and a successful knock out of the gene.

As mentioned above, in the generation of both Δ*ompA1* and *–A2* mutants, the natural competency method and electrocompetence methods were tested, in addition to comparison of linear PCR product and circular suicide plasmid DNA. As shown in Table 3.1 *P. gingivalis* transformation via the natural competency method generated more colonies compared (5-10-fold) to the traditional method of electrocompetency using identical amounts of DNA in the reactions (Table 3.1).

Table 3.1 Number of *ompA* mutant colonies generated through different methods of *P. gingivalis* transformation

	Method of Transformation			
	Electrocompetence		**Natural Competence**	
Mutant	**Linear (colonies µg^{-1})**	**Plasmid (colonies µg^{-1})**	**Linear (colonies µg^{-1})**	**Plasmid (colonies µg^{-1})**
Δ*ompA1*	1.6	0	14.4	12
Δ*ompA2*	4.8	3.2	>100	>100

The number denotes the number of colonies observed on the erythromycin plate in relation to the overall concentration of DNA input in the transformation, as the concentration of DNA varied between samples (between 200 ng/µl – 250 ng/µl) whilst the volume remained the same. Colony number observed for Δ*ompA2* was unquantifiable as a lawn of bacteria was observed (>100), which was later streaked to single colonies and these single colonies were confirmed using PCR for correct incorporation of the PCR construct.

The transformation efficiency for generating the Δ*ompA1* mutant was generally lower than Δ*ompA2* and overall fewer colonies were produced when introducing the externally generated construct of Δ*ompA1::em*. This data also demonstrated that the introduction of

DNA through natural competency is more effective for generation of mutants than the electrocompetency method.

3.3.2.1 Characterisation of the OM Profile of *ompA* Mutants

Aside from PCR confirmation, Δ*ompA1*, Δ*ompA2* and Δ*ompA1A2* mutants were confirmed by purifying the bacterial outer membrane and assessing the presence of the protein using SDS-PAGE analysis and silver-staining as detailed in Section 2.7.3.2 and 2.7.3.3., and probing for the presence of OmpA at ~41 kDa using an anti-OmpA antibody, obtained from Dr Keiji Nagano (Aichi Gaukin University, Nagoya, Japan). This was achieved using the method of differential detergent centrifugation with approximate normalisation of proteins by use of identical amounts of starting material and careful processing. Figure 3.7 indicates the presence of OmpA protein in wild-type *P. gingivalis,* Δ*ompA1* and Δ*ompA2* mutants, but demonstrates a lower density of protein in the 41 kDa region in these mutants, as expected due to the loss of the OmpA1 or OmpA2 subunit and suggesting successful generation of Δ*ompA1* and Δ*ompA2* mutants. No band is observed in the Δ*ompA1A2* mutant, suggesting a successful deletion of the entire *ompA* operon.

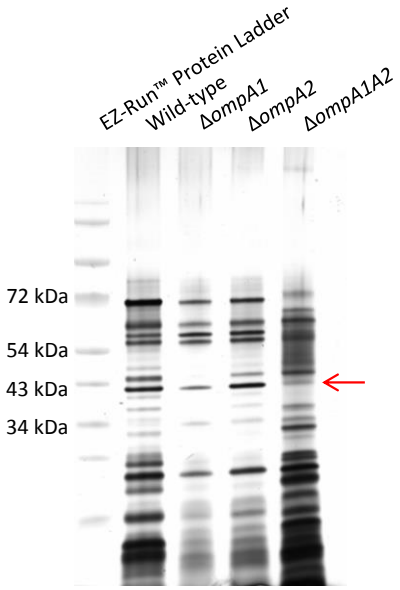

Figure 3.7 Silver staining assessment of the outer membrane of wild-type *P. gingivalis* and respective Δ*ompA* mutants. Outer membranes were purified and stained as described in Chapter 2.7.5 and 2.7.3.3. The OmpA proteins can be seen at ~41 kDa in wild-type, Δ*ompA1* and Δ*ompA2* preparations but is missing in Δ*ompA1A2* as indicated by the red arrow.

An anti-OmpA antibody was used at a 1:5000 dilution as the primary antibody against OmpA proteins in the outer membrane samples. A secondary anti-rabbit-HRP-conjugated

antibody was used at 1:3000 dilution to detect for anti-OmpA antibody binding to OmpA proteins, and processed as according to Section 2.7.4. The Western blot can be seen in Figure 3.8, which shows the presence of the OmpA bands in the wild-type strain, but only one of the bands in the Δ*ompA1* and Δ*ompA2* samples, whereas both are absent from the Δ*ompA1A2* sample, confirming the deletion of the *ompA* operon. Unfortunately the antibody reacts with a number of non-specific bands in the strain, but these are consistent between all three strains indicating the confirmation of mutants as expected.

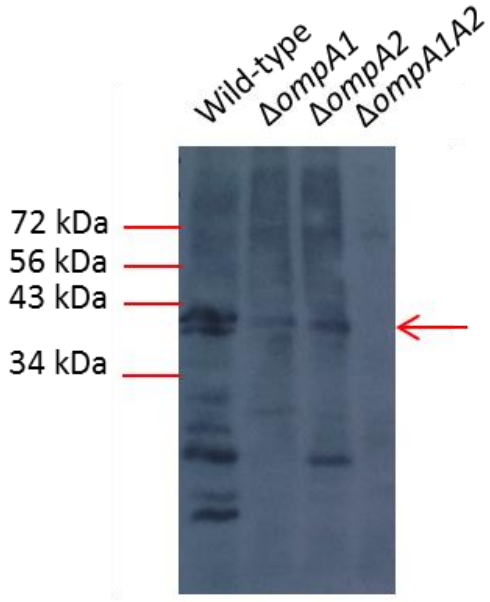

Figure 3.8 Western blotting detection of OmpA protein in outer membrane preparations. α-OmpA antibody (1:5000 dilution) was used to probe for the presence of OmpA in outer membranes of wild-type *P. gingivalis* and Δ*ompA* mutants. The OmpA1 and OmpA2 subunits can be seen as separate bands in the wild type preparation, whereas less OmpA can be seen in the single Δ*ompA* mutants. No OmpA is detected in the double mutant, as indicated by the red arrow.

3.3.3 Phenotypic Analysis of *P. gingivalis* Wild-Type and Δ*ompA* Mutants

3.3.3.1 Visualisation of Bacterial Cells through Transmission Electron Microscopy

The OmpA protein is a vastly abundant protein in the cell membrane, comprising of ~2-3 x 10^5 copies per cell in *E. coli* K12 (Smith *et al.*, 2007), and has been shown to have a multifunctional role, one of which is within membrane structural integrity (Sonntag *et al.*, 1978; Klose *et al.*, 1988). The role of OmpA in *P. gingivalis* in structural integrity has been relatively unreported, with only one study demonstrating a role for OmpA (Iwami et al.

2007). Transmission Electron Microscopy (TEM) was used to demonstrate any effect of losing OmpA on the outer membrane gross morphology.

Cultures were grown for 24 hours in broth culture, whereby the bacteria had reached stationary phase, and OD_{600} readings were similar in all strains (within 0.1). Cells were prepared for avaldite resin embedding and ultrathin sectioning (70-90 nm) as detailed in Section 2.8.5.1, before being stained with uranyl acetate and lead citrate as described by Reynolds *et al.,* (1963) and Section 2.8.5.2 (Reynolds, 1963). In these experiments, a disruption of the membrane was observed, as shown in Figure 3.9, whereby the membrane appears to have lost continuity and becomes wavy in some cells. This only appears in around 3 – 4 % of the population in the Δ*ompA1* and Δ*ompA2* mutants and around 4 – 6 % of the Δ*ompA1A2* population (Figure 3.9B), although the harsh preparation steps of the samples caused a lot of the Δ*ompA1A2* cells to lyse so the proportion of bacteria displaying the membrane disruptions is expected to be higher in the double mutant. This is in contrast to previous reports, which show a high level of membrane disruption, although the trend showing a more exaggerated phenotype in the double mutant remains the same.

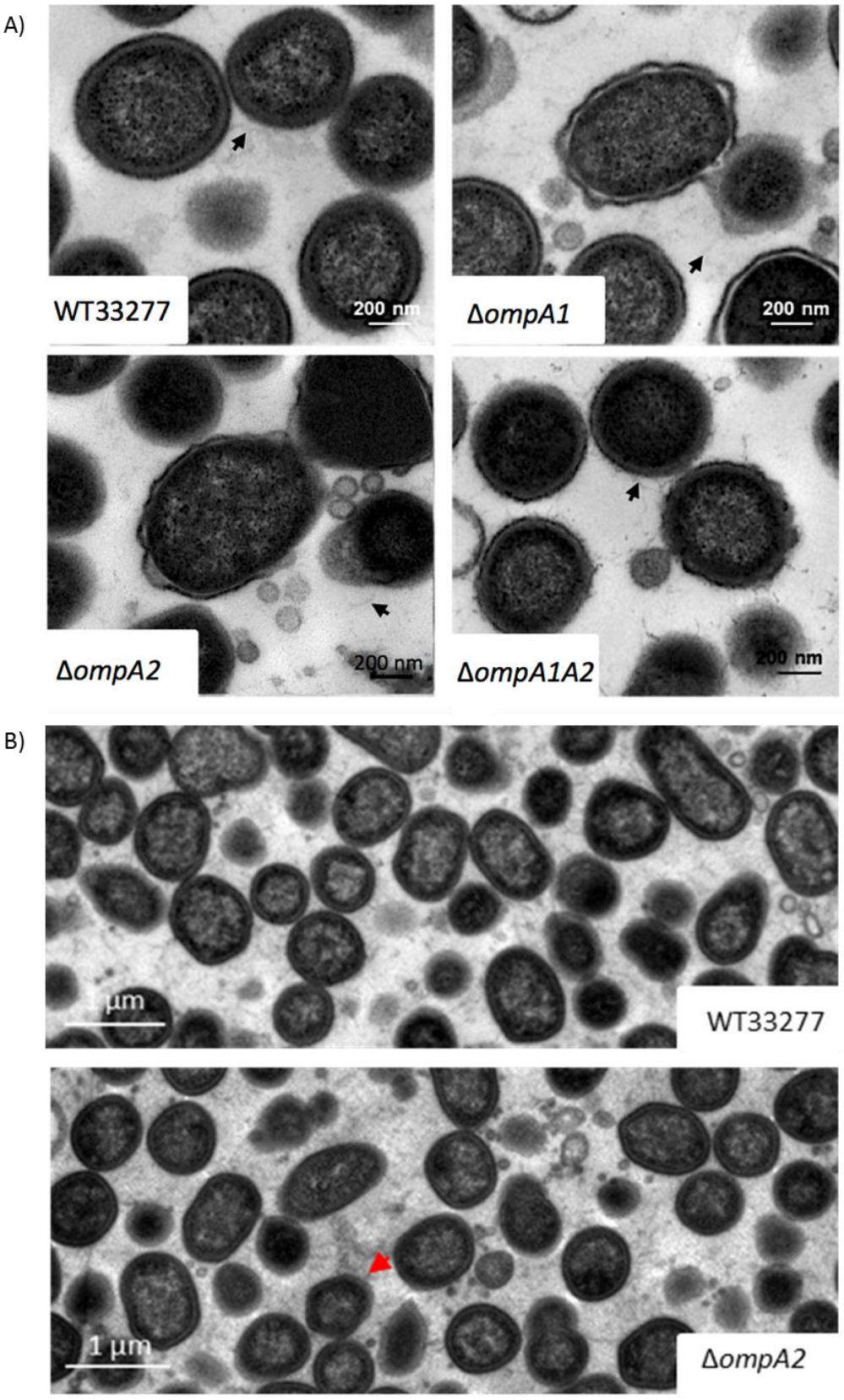
A)
WT33277
200 nm
ΔompA1
200 nm
ΔompA2
200 nm
ΔompA1A2
200 nm
B)
µm
WT33277
1 µm
ΔompA2

Figure 3.9 TEM Imaging of wild-type and Δ*ompA* mutant strains of *P. gingivalis.* Liquid cultures (OD_{600} 1.0) of *P. gingivalis* strains were fixed and dehydrated with ethanol before embedding in avaldite. Sections of embedded *P. gingivalis* were bound to formivar grids and stained using uranyl acetate and lead citrate before imaging using a Philips CM100 Transmission Electron Microscope. Figure (A) demonstrates the observation of the disrupted membranes in the Δ*ompA* mutants that is not observed in the wild-type; however Figure (B) demonstrates how infrequently this is observed in a population, using Δ*ompA2* as an example. Scale bars are represented on the bottom left or right of every image. Black arrows indicate the presence of fimbriae, whereas red arrows indicate the cells with observed membrane disruptions.

Due to the structure of the OmpA protein, which contains a β-barrel and a peptidoglycan-associated C-terminal domain, the loss of membrane integrity is an expected observation as the protein is no longer present to assist in anchoring the outer membrane to the peptidoglycan layer.

Interesting to note was the presence of the fimbriae in all of the mutants, as indicated by the black arrows in Figure 3.9A, implying the loss of the OmpA protein doesn't have an effect on the production of fimbriae, which has previously been noted for *E. coli* OmpA (Teng *et al.*, 2006). Also to note was the presence of outer membrane vesicle-like structures in the sections. These appeared to be present in higher levels in the mutants compared to the wild-type, and it is possible that these result in a loss of the membrane integrity with the loss of the major membrane protein OmpA, causing membrane blebbing. The number of vesicles present and their size distribution was investigated further in the next section.

3.3.3.2 Assessment of Outer Membrane Vesicle Formation

The formation of outer membrane vesicles is considered to be a mechanism of interaction with other species or the host, or for delivery of virulence factors (Kuehn and Kesty, 2005). Like other Gram-negative bacteria, *P. gingivalis* naturally produces outer membrane vesicles, likely through cell wall turnover and blebbing of the membrane (Ho *et al.*, 2015). Proteomic analysis of these vesicles have shown the presence of membrane-associated proteins, such as the gingipains (Rgp, Kgp), fimbriae (FimA) and Haemagglutinin A (HagA), demonstrating a role for these vesicles to deliver important virulence factors and proteolytic enzymes (Imai *et al.*, 2005; Nakao *et al.*, 2014).

Assessment of the vesicle number and size distribution was determined using a qNANO instrument, which quantified the number of vesicles produced by the bacteria. Vesicles were isolated from liquid cultures of *P. gingivalis* grown as described in Section 2.8.10,

before the culture precleared using differential centrifugation. Any resulting cellular debris was removed through further centrifugation and filtration, resulting in vesicle-containing preparations which were applied to the qNANO. The number and size of vesicles was determined by Tunable Resistance Pulse Sensing, whereby a voltage is applied to a pore stretched over the qNANO system and is filled with electrolyte, creating an ionic current. As the vesicle passes through the pore, a brief increase in electrical resistance occurs and a resistive pulse in created, which allows the particle volume to be precisely mapped. A rate of flow of the vesicles is also applied to allow detection of particle concentration. Due to the electron microscopy of Δ*ompA* mutants demonstrating a loss of membrane integrity with the loss of the OmpA protein, an increase in vesicle formation was expected, which was observed for the mutant strains, as shown in Figure 3.10.

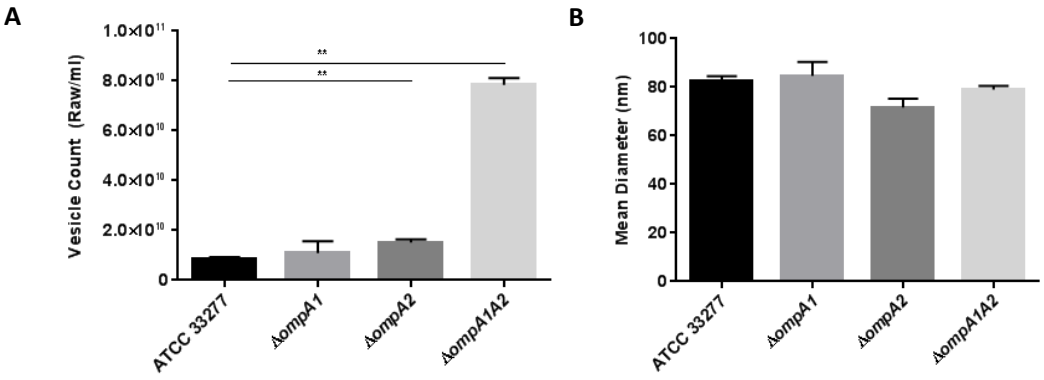

Figure 3.10 Vesicle formation by wild-type *P. gingivalis* and Δ*ompA* mutants. Vesicles were purified from liquid cultures (OD_{600} 1.0) precleared through differential centrifugation. Cell-free supernatants were passed through 0.44 µm filtration to remove any remaining cell debris to ensure a pure vesicle sample. Bacterial vesicles were analysed using a qNANO instrument (iZON Science Ltd) using tuneable resistive pulse sensing (TRPS), and compared to calibration particles of a known size and concentration. The concentration of vesicles was normalised to the OD_{600} of the corresponding culture. Error bars ± SEM. Statistical significance was ** $p < 0.01$, as determined by One-Way ANOVA (n = 3).

It can be seen in Figure 3.10 that there is a significant increase in the number of vesicles found in the Δ*ompA1A2* culture, with a 9.4-fold increase in the number of vesicles observed. A 1.3- and 1.8- fold increase was observed in Δ*ompA1* and Δ*ompA2* mutants respectively, with statistical significance only for the Δ*ompA2* mutant. All mutants produced vesicles around ~80 nm and no significant difference was observed in the size distribution

for any of the mutant strains (Fig. 3.10B), so only the number of vesicles produced was affected by the loss of the OmpA protein. Along with the TEM images, these data demonstrate that OmpA plays a role in the structural stability of the bacterial membrane and OMV production, most strikingly for double mutant.

3.3.3.3 Assessment of Gingipain Activity

The gingipain proteases have been implicated in the colonisation of host tissue through adhesion to the extracellular matrix proteins (Tokuda *et al.*, 1996) or through indirect methods, such as processing the subunits of the fimbriae (Nakayama *et al.*, 1996), the protein appendages also involved in host-cell adherence, as discussed previously in 1.6.6.3 *P. gingivalis* contains two major types of gingipains, the Arg- gingipains, which can be subdivided into RgpA and RgpB, and the Lys-gingipains, Kgp. The bacterium also encodes an additional gene encoding a surface protein, Haemagglutinin A (HagA), which alongside RgpA and Kgp, contains adhesion domains that are thought to be involved in the adherence to the host (Kozarov *et al.*, 1998). Studies have shown that an increase in gingipain activity causes a reduction in invasion of *P. gingivalis,* therefore it is important to understand the role of gingipains in the *ompA* mutants as the adhesion and invasion of the host may be affected by the loss of the gingipains, masking any effect of the OmpA protein loss. Both whole cell (cell-associated gingipains, WC) and supernatant (secreted gingipains, S) assays were carried out to determine gingipain activities in wild-type *P. gingivalis* and Δ*ompA* mutant strains, which can be seen in Figure 3.11.

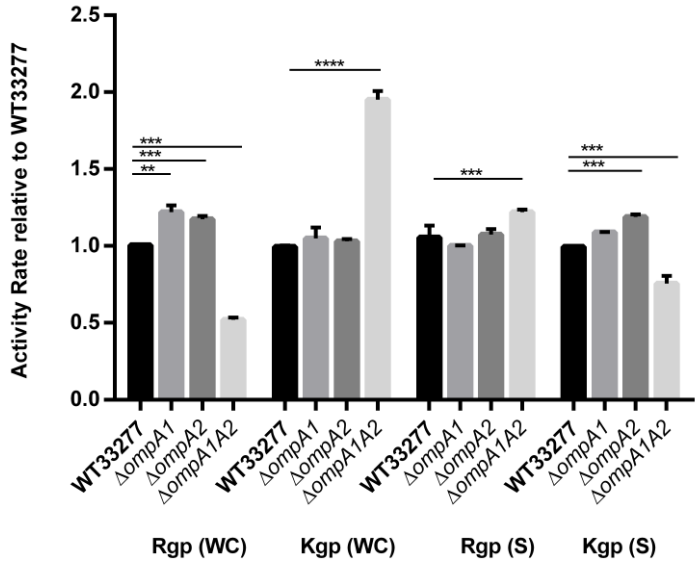

Figure 3.11 Whole cell and secreted gingipain activity of wild-type *P. gingivalis* and Δ*ompA* mutants. Both whole cells (WC) and secreted (S) gingipain activity was determined for Lysine (Kgp)- and Arginine (Rgp)-gingipains. The OD_{600} of overnight liquid cultures was corrected to 1.0 and whole cell activity was determined colorimetrically, whilst secreted gingipain activity was determined fluorescently through the release of methyl-coumarin. Activity was measured as the average of three biological repeats (of 3 technical repeats), with Error bars representing ± SEM. Statistical significance was defined by *** $p < 0.01$, *** $p < 0.005$, *** $p < 0.001$, determined by 2way-ANOVA

Figure 3.11 demonstrates a clear difference in whole cell gingipain activities for the Δ*ompA1A2* mutant, with a decrease of 50% and increase of 100% in Rgp and Lys gingipains activities respectively. A slight increase in whole-cell Rgp activity is observed for both Δ*ompA1* and Δ*ompA2* mutants, with increases of 20% and 15% respectively for each mutant, however, no change in whole cell Kgp activity was observed. Secreted gingipain activities were largely unaffected in all mutants, with only a marginal increase in Rgp-activity in the Δ*ompA1A2* mutant. Secreted Kgp levels again changed slightly, with a subtle increase for Δ*ompA2* (15 %) and larger decrease in Δ*ompA1A2* Kgp (20 %) activities.

Although differences in gingipain activities are observed, it is important to note that there appears to be little difference between Δ*ompA1* and Δ*ompA2* strains in gingipain activity, but large differences were observed between the single mutant phenotypes involved in host cell interaction observed later in this chapter.

3.3.3.4 Assessment of Sialidase Activity

The sialidase enzyme of *P. gingivalis* is a cell surface-associated virulence factor that is thought to facilitate interaction with other periodontal pathogens through breakdown of carbohydrates and glycoprotein conjugates to allow attachment and enhance commensalism, leading to the formation of the biofilm (Aruni *et al.*, 2011). Sialidases are glycosylhydrolase enzymes which cleave sialic acid for multiple purposes, such as nutrition or immune evasion (Li *et al.*, 2012). Sialidases have been considered a major virulence factor in many organisms, such as *Streptococcus pneumoniae, Vibrio cholerae* and *Corynebacterium diphtheriae* which all colonise mucosal surfaces (Corfield, 1992), and have also been shown to be present in the major periodontal pathogens found in the red complex, *Tanerella forsythia* (Roy *et al.*, 2011), which has been shown to be involved in the adherence to epithelial cell attachment (Honma *et al.*, 2011), and *Treponema denticola* (Wyss *et al.*, 2004), which is needed to scavenge sialic acids for growth and protects the bacteria from serum killing (Kurniyati *et al.*, 2013). *P. gingivalis* is known to have a sialidase enzyme and related genes, and its role in virulence has been recently studied (Aruni *et al.,* 2011), with an increase in invasion and a decrease in adherence in sialidase mutants, so as with the gingipain activity, it is important to understand the effect of Δ*ompA* mutation on this virulence factor. Sialidase assays were carried out according to Materials and Methods Section 2.8.9.3, with cultures of wild-type *P. gingivalis* and mutant strains at an OD_{600} of 0.5 and 1.0, and whole-cell sialidase activity read after 2 hours incubation, as shown in Figure 3.12.

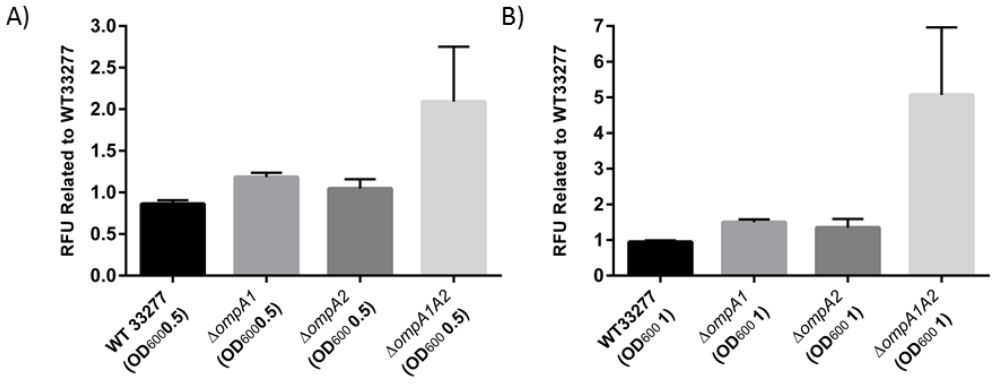

Figure 3.12 Sialidase activity of wild-type *P. gingivalis* and Δ*ompA* mutants. Sialidase activity was determined as described in chapter 2.8.9.3. Liquid cultures of *P. gingivalis* wild-type and mutant strains were prepared at two different OD_{600} concentrations and incubated with 0.1 mM MUNANAC for 2 h before the activity determined. Figure 12 demonstrates the sialidase activity plotted as a relative fold increase compared to wild-type

(=1). Activity was measured as the average of three biological repeats (of 3 technical repeats), with Error bars representing ± SEM.

Figure 12 demonstrates clear increase in sialidase activity in the double Δ*ompA1A2*, with a 2- and 5-fold increase in the OD 0.5 and OD 1.0 cultures respectively. However, due to the high inter-experimental variation, this was not a significant increase (p = 0.052 for wild-type – Δ*ompA1A2* increase). Coupled to the significant increase in the vesicle number observed in this double mutant, this data is expected as cell surface-associated proteins are often observed in vesicles expelled from the bacterium (Iwami *et al.*, 2007). No significant difference in sialidase activity was observed in either Δ*ompA1* or Δ*ompA2* mutants, similar to the gingipain activity, indicating neither is likely to be influencing any observed phenotypes of these mutants.

3.3.3.5 Biofilm Assay of *P. gingivalis* Wild-Type and Δ*ompA* Mutants

Biofilm formation is an important virulence factor for many microbes as it allows reduced susceptibility to antimicrobial agents, and can enhance pathogenicity in multispecies biofilms (pathogenic synergism) (Marsh, 2006). It is especially so for oral microbes as it forms the basis of plaque *in vivo*, and prevents removal by salivary fluid motion and protects from antimicrobial salivary proteins (Lamont and Jenkinson, 2000). Biofilm formation of *P. gingivalis* wild-type and Δ*ompA* mutant strains was examined using Crystal Violet staining of biofilm formed on polystyrene plates, as developed originally by Christensen *et al.,* (1985) for various *Staphylococcus* strains (Christensen *et al.*, 1985). Strains were grown statically for 72 h and initially the overall growth (planktonic and biofilm) of each strain was determined by observing the OD_{600} and the Crystal Violet staining applied as in Section 2.8.4 if all OD values were within 0.1 (10%). The biofilm was qualitatively assessed using light microscopy (x 400 magnification), which can be seen in Figure 3.13.

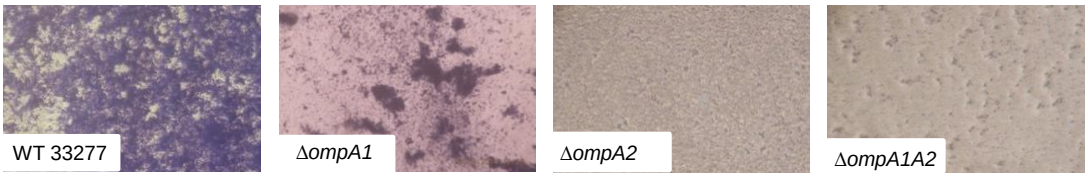

Figure 3.13 Biofilm formation *in vitro* of *P. gingivalis* and mutant Δ*ompA* strains. Cultures of *P. gingivalis* strains were seeded at OD_{600} 0.05 and grown anaerobically for 72 hours before staining with 1% Crystal Violet. Images were taken of the formed biofilm using Nikon Eclipse TS100 microscope with a digital camera attachment at x400 magnification.

It is important to note that in all mutant strains, the biofilm was more fragile and lifted easily from the plate bottom during washing, so extremely gentle washing was applied. Qualitative analysis of the Crystal Violet stain suggests that the formation of the biofilm by the Δ*ompA2* and Δ*ompA1A2* mutants has been abrogated with the loss of the protein. In the case of Δ*ompA1A2* it appeared that no biofilm was formed, and also the Δ*ompA2* mutant demonstrated little to no biofilm. The Δ*ompA1* mutant shows areas of biofilm formation, but not as coherent as the wild-type. The Crystal Violet was extracted using ethanol, and the biofilm formation assessed quantitatively by observing the absorbance (Abs_{575}), as shown in Figure 3.14.

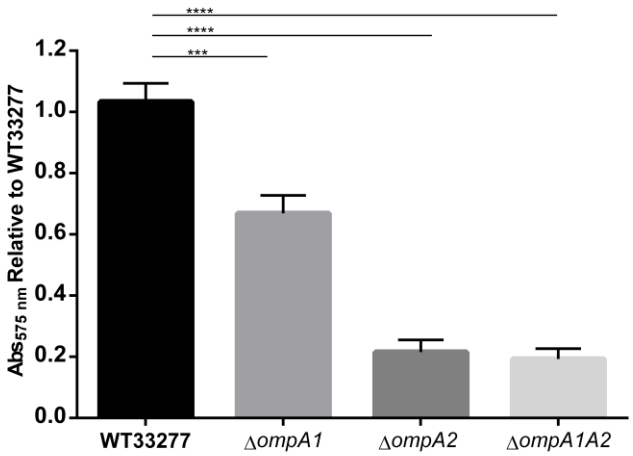

Figure 3.14 Quantification of biofilm formation of Δ*ompA* mutants. Crystal Violet was extracted from stained biofilms and OD_{575} absorbance was measured using a TECAN Infinite 200 Pro Plate reader (Tecan Group Ltd.). Figure 3.14 demonstrates the quantified biofilm of wild-type *P. gingivalis* and the Δ*ompA* mutants. Biofilm formation was determined relative to wild-type. Biofilms were quantified as the average of three biological repeats (of 5

technical repeats), with error bars representing ± SEM. Significance was applied using a students' *t*-test (***$p < 0.001$ and ****$p < 0.0001$).

The qualitative imaging of the biofilms is supported by the quantitative analysis using extracted Crystal Violet, which demonstrated a 4.5-fold and 8.8-fold reduction in the biofilm formed in the Δ*ompA2* and Δ*ompA1A2* mutant strains respectively, compared to only a 1.5-fold reduction in Δ*ompA1* mutant biofilm formation. Because the Δ*ompA2* mutant showed a greater phenotype with the loss of biofilm formation, the next section aims to examine the role of *ompA2* specifically by providing it on a plasmid to complement for the loss of *ompA2 in trans* to demonstrate the loss of biofilm formation was a result of the loss of the OmpA2 protein alone.

3.3.4 Generation of an Δ*ompA2* + pT-COW-*A2* Complement Mutant

In order to fully assess the role of the *ompA2* gene in biofilm formation, a complementation construct was made using the *ompA* operon natural promoter and the *ompA2* gene from wild-type *P. gingivalis* which was then cloned into the pT-COW plasmid (Fig. 3.15) before transformation into the Δ*ompA2* mutant.

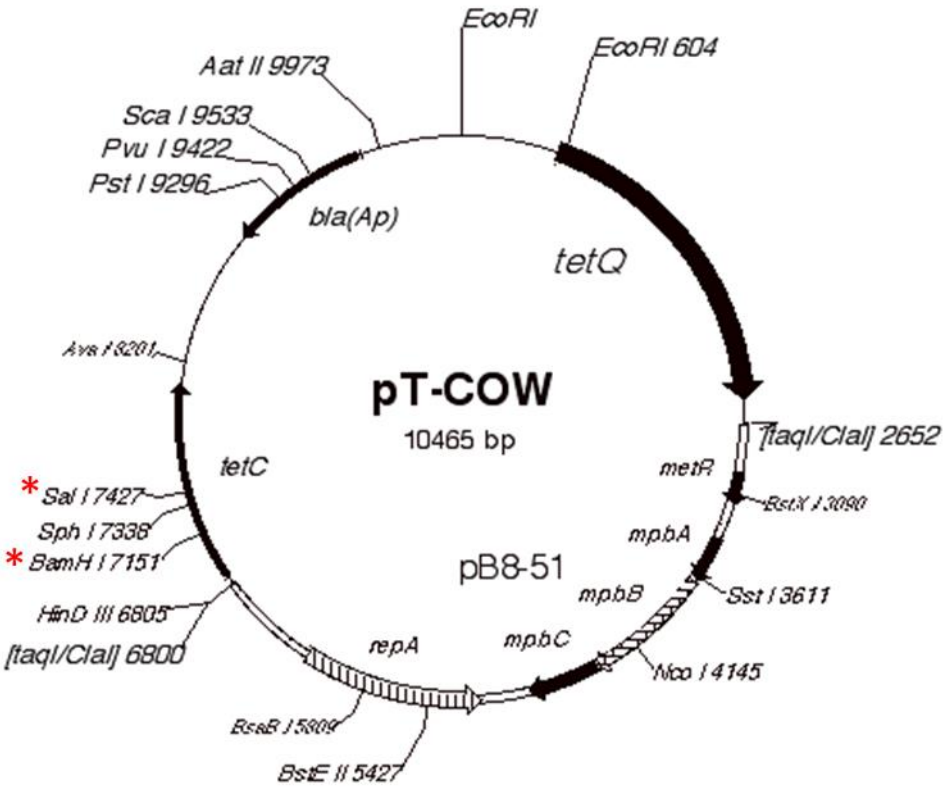

Figure 3.15 pT-COW plasmid map. The pT-COW plasmid (Gardner *et al.*, 1996) was used to carry the *ompA* promoter fused to the *ompA2* encoding gene for Δ*ompA2* mutant complementation. The *ompA2* complement construct was cloned into the *tetC* gene using *Bam*HI and *Sal*I restriction sites, indicated by the red *.

The two DNA fragments were amplified using PCR with primers described in Table 2.7 in materials and methods section 2.3. This generated a 300 bp DNA fragment containing the natural *ompA* promoter (Figure 3.16A) and a 1100 bp fragment encoding the *ompA2* gene (Figure 3.16B). The primers used to amplify these individual fragments contained "tails" of the other fragment to assembly the two fragments into a complement construct, which was generated through overlap extension PCR as detailed in Section 2.6.2.4. These primers also contained restriction enzyme sites (*Bam*HI and *Sal*I) so the construct could be cloned into the pT-COW vector. A successful construct was generated (Figure 3.16C), digested using *Bam*HI and *Sal*I (alongside restriction enzyme digest of the pT-COW plasmid) and cloned into pT-COW.

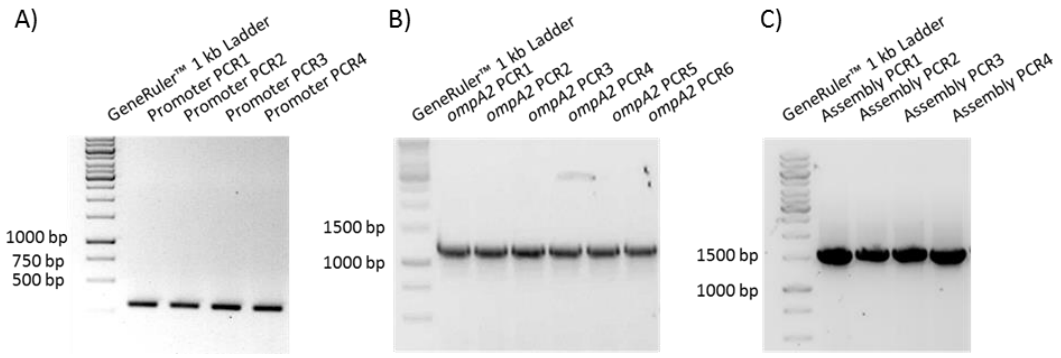

Figure 3.16 Agarose analysis of the construction of the *ompA2* complementation construct. (A) Demonstrates the amplification of the *ompA* promoter region (300 bp) with a 5' *Bam*HI restriction enzyme site and a 3' *ompA2* tail, (B) shows the amplification of the *ompA2* gene (~1100 bp) with a 5' reverse complement *ompA* promoter tail and a 3' *Sal*I restriction enzyme site and (C) demonstrates the two PCR fragments assembled into one construct with 5' *Bam*HI and 3' *Sal*I restriction enzyme sites (~1400 bp). PCRs were carried out using Phusion™ polymerase enzyme as detailed in Section 2.6.2.3.

Ligated plasmid was transformed into *E. coli* DH5α cells, and incorporation of the plasmid was determined through antibiotic selection on ampicillin-containing LB-agar plates. As the *ompA2* complement construct was cloned into the tetracycline-encoding gene for *E.coli* (*tetC*), colonies growing on Ampicillin-containing agar were also streaked onto tetracycline-containing LB-agar plates. If no growth occurred on the tetracycline plates, it was assumed that these colonies contained the pT-COW-*A2* vector as the *ompA2* complement gene construct would interrupt the tetracycline-encoding gene for *E. coli*. Plasmids from these colonies were extracted and confirmed for their correct incorporation of the complement construct by restriction digest *Bam*HI and *Sal*I (Figure 3.17A) and PCR using pT-COW designed primers (Figure 3.17B) as described in Materials and methods 2.6.2.6 and 2.6.2.3.

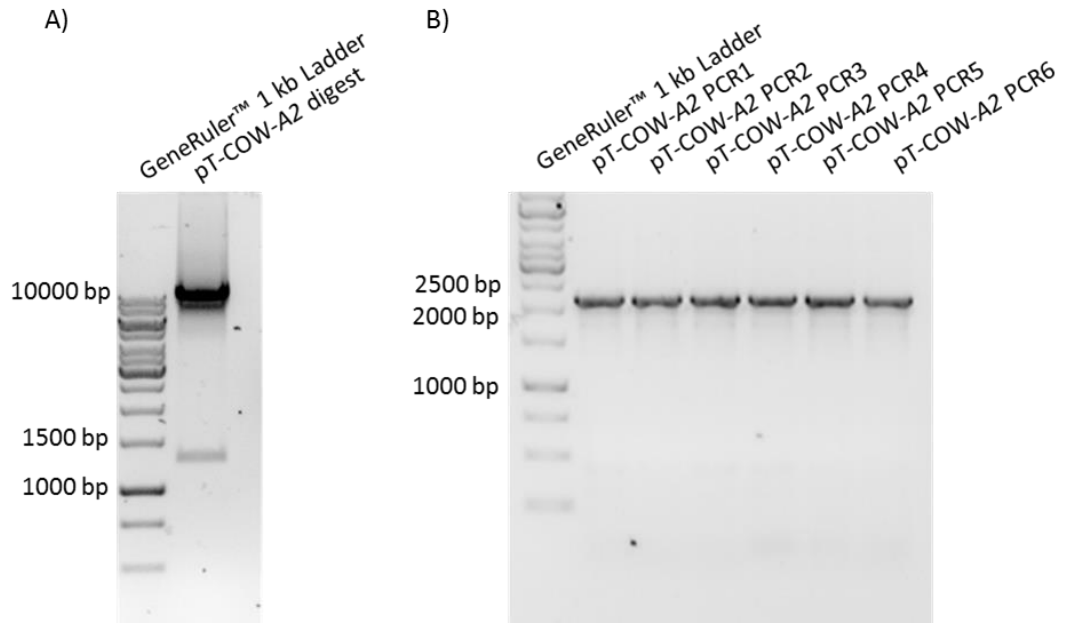

Figure 3.17 Confirmation of the *ompA2* complementation insert in pT-COW. (A) Demonstrates the *Bam*HI and *Sal*I digest, with the insert at ~1400 bp, and (B) shows PCR confirmation of purified plasmid using pT-COW primers which amplify the *tetC* region of the plasmid (~2200 bp including insert). PCR was carried out using GreenTaq™ polymerase enzyme as described in chapter 2.6.2.3.

The complementation construct was sequenced (Appendix I) to check for any mistakes, of which none were found, and the pT-COW-*A2* complement plasmid was transformed into the *P. gingivalis* Δ*ompA2* strain using the natural competency method described earlier in this chapter. Positive colonies containing the pT-COW-*A2* plasmid were selected from tetracycline-containing BA plates (3 µg/ml), alongside wild-type *P. gingivalis* + pT-COW (empty vector) and Δ*ompA2* + pT-COW (empty vector) colonies as positive and negative controls respectively.

3.3.5 Biofilm Assay of Δ*ompA2* Complemented Strain

Because the Δ*ompA2* mutant showed a similar phenotype to the Δ*ompA1A2* mutant in biofilm formation, the Δ*ompA2* +pT-COW-*A2* complement strain was also assessed quantitatively for the formation of biofilm, to determine if the phenotype observed was due to the loss of the protein. All strains were measured for total growth (planktonic and biofilm), and corrections in the original total growth were applied, before determining the

biofilm formation of *P. gingivalis* +pT-COW*,* Δ*ompA2* +pT-COW mutant and Δ*ompA2* + pT-COW-*A2* complemented strain, as shown in Figure 3.18.

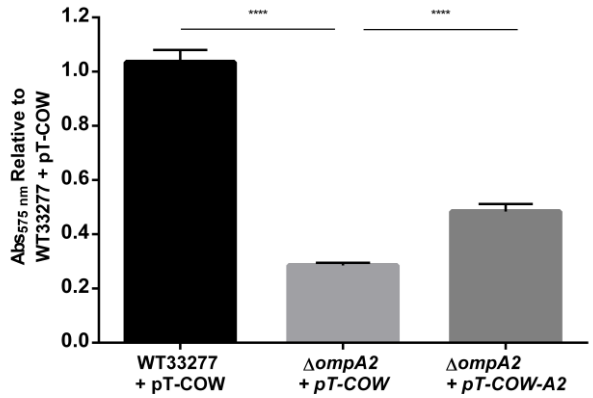

Figure 3.18 Quantification of biofilm formation in the Δ*ompA2* complement strain. Crystal Violet was extracted from stained biofilms and OD_{575} absorbance was measured using a TECAN Infinite 200 Pro plate reader, showing a partial restoration of the biofilm forming phenotype in the Δ*ompA* mutant complement. Biofilm formation was determined relative to wild-type. Biofilms were quantified as the average of three biological repeats (of 5 technical repeats), with Error bars representing ± SEM. Significance applied using a students' *t*-test (****$p < 0.001$).

The *in trans* reintroduction of the *ompA2* gene in the Δ*ompA2* + pT-COW-*A2* complement strain shows a partial, 2-fold, restoration of the ability of Δ*ompA2* for formation of a biofilm ($p < 0.001$), however it did not fully complement compared to wild-type *P. gingivalis* containing the empty pT-COW vector (Fig. 3.18). While there is no clear explanation for this, we performed experiments on separate clones of the *ompA2* mutant, indicating that it any observed phenotype are not due to extraneous mutations. These data indicate a role for *ompA2* in biofilm formation on an inert surface.

3.3.6 Detection of Major Fimbriae (FimA) on Outer Membrane Fractions of *P. gingivalis* Wild-Type and Δ*ompA* Mutants.

As previously described, the fimbriae are the filamentous protein appendages extruding from the cell surface, made up of fimbrillin (FimA) subunits. The fimbriae have been reported to mediate adhesion to the host cell to allow colonisation (Slots and Gibbons, 1978; Njoroge *et al.*, 1997; Nakagawa *et al.*, 2002; Enersen *et al.*, 2013) and are classed as a

major virulence factor of the bacterium. It has previously been shown in *E. coli* that the loss of OmpA influences the expression of the fimbriae (Teng *et al.*, 2006). It was therefore important to determine whether or not the reduction in bacterial interaction with the host cell is due to the OmpA protein or interference in the production of fimbriae. The TEM imaging in Figure 3.9 shows the presence of fimbrial structures on the wild-type and all of the mutant bacterial strains, however an anti-FimA antibody was obtained from Professor Ashu Sharma (SUNY, University at Buffalo, USA) to fully determine the presence or absence of the fimbriae in the Δ*ompA* mutant strains.

Outer membranes of wild-type and Δ*ompA* mutants were extracted using differential detergent centrifugation as previously described for the detection of OmpA in Western blotting (Section 3.3.2.1 and Materials and Methods 2.7.5), before cytoplasmic, inner membrane and outer membrane fractions were analysed through SDS-PAGE (Figure 3.19A). As observed in the SDS-PAGE gel, the protein concentration was relatively low so the bands were not well visible, and therefore the gels were silver stained (Fig. 3.19B) for higher clarity of protein bands. Corresponding gels were run with the same samples for Western blot analysis using an anti-FimA antibody (1:2000) to detect for the presence of fimbriae in the fractions, and the resulting Western blot can be seen in Figure 3.19C.

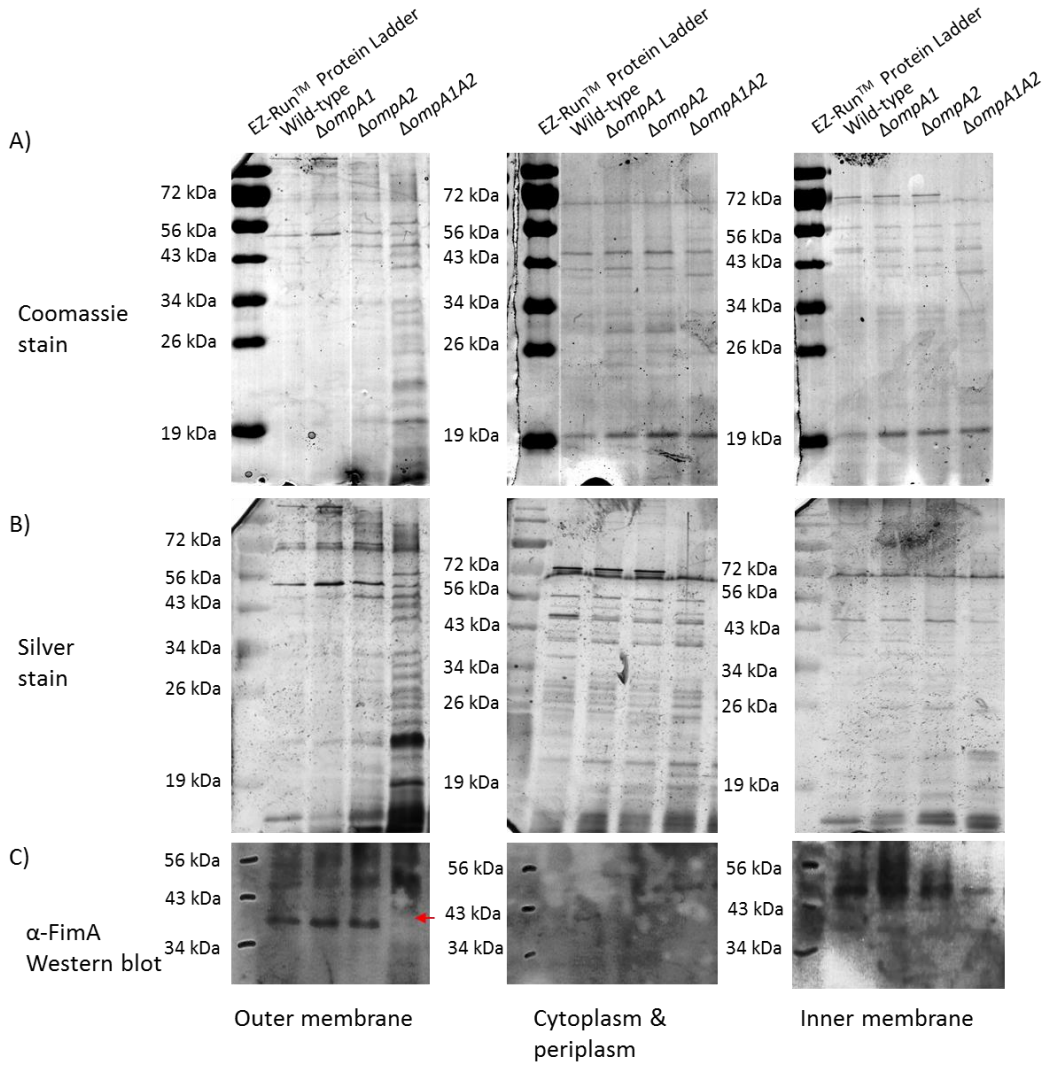

Figure 3.19 Cell membrane fractionation and detection of FimA subunits in *P. gingivalis* wild-type and *ompA* mutants. Cell fractions (outer membrane, cytoplasm and inner membrane) were run in parallel for Coomassie staining (A) and Western blot analysis (C). As the banding was weakly observable in the Coomassie stain, these gels were silver stained (B) for clearer observation. The red arrow indicates the expected presence of FimA subunits when probed for using anti-FimA antibody (1:2000) with an anti-rabbit-HRP conjugated secondary (1:3000).

Although the presence of the fimbriae was being determined by observing the outer membrane fraction, both the inner membrane and cytoplasmic fractions were included in the analysis to demonstrate the fractionation was successful, which is indicated by the difference in banding patterns between the three fractions. These data also indicate that

while the outer membrane profile of the WT, *ompA1* and *ompA2* mutants are largely similar, the double *ompA1A2* mutant is significantly altered.

The size of the FimA subunit varies between 39 – 49 kDa depending on the genotype expressed by the *P. gingivalis* (Nakagawa *et al.*, 2002), and in reference to the FimA detected on the Western blots in Figure 3.19C, the FimA subunits are on the smaller size of this scale. In the outer membrane, FimA is only detected in the wild-type, Δ*ompA1* and Δ*ompA2* mutants, as indicated by the red arrow, and not in the Δ*ompA1A2* mutant. Bands are detected in the inner membrane fraction at ~47 kDa, which may indicate the immature form of FimA, which has been observed at ~45-46 kDa previously (Sato *et al.*, 2005). There appears to be no difference in the presence of the FimA subunit in the outer membrane fraction between the Δ*ompA1* and Δ*ompA2* mutants.

3.3.7 OmpA-Host Cell Interaction

The ability of *P. gingivalis* to interact with the host cell is key to the virulence and survival of the bacterium, allowing the progression into a chronic periodontal infection. This interaction begins with an adherence to the cell, which prevents removal of the bacteria by the mechanical action of the saliva, whilst allowing the bacteria to colonise the host and lead to invasion. Invasion of the host cell provides an intracellular location, protecting the bacteria from the host immune system, provides a nutrient-rich environment and facilitated replication leading to cell spreading, tissue destruction and the progression of the disease (Lamont *et al.*, 1995). The adherence and invasion of *P. gingivalis* and the Δ*ompA* strains was assessed using standard antibiotic protection assays which were first detailed by Lamont *et al* (1995) to determine the number of bacteria located intracellularly, and developed further by Suwannakul *et al* (2010) to allow the adhered bacteria to be enumerated (Lamont *et al.*, 1995; Suwannakul *et al.*, 2010).

3.3.7.1 Antibiotic Protection Assay of *P. gingivalis* Wild-Type and Δ*ompA* Mutants

Antibiotic protection assays were carried out to examine the role of the OmpA protein in interactions with human cells, specifically, the adherence and invasion of a gingival keratinocyte cell line, OK-F6, which is a specialised cell found in the epithelial layer. Antibiotic protection assays involve the incubation of *P. gingivalis* with an epithelial cell monolayer for 90 min to allow adherence and invasion of the cells by the bacteria. After this incubation, any bacteria that have not adhered or invaded the cells are removed by PBS washing. These cells are either lysed to give the total number of bacteria associated with

the cells (adhered and invaded) or metronidazole is applied to kill any extracellular bacteria (i.e. adhered bacteria), so that the number of bacteria that have invaded can be calculated. The OK-F6 cell line was chosen for study as it is derived from human oral epithelial cells, cells which *P. gingivalis* encounters during the infection process. The OK-F6 cells are also immortalised by affecting the $p16^{INK4a}$ cell cycle pathway. This allows extended growth without reaching senescence (Dickson *et al.*, 2000), and in contrast to cells isolated from oral squamous cell carcinomas, targeted pathway deletions ensure the cells remain more similar to the native oral cell in terms of protein expression and are therefore more representative of the natural *P. gingivalis* infection.

Standard antibiotic protection assays were carried out as detailed in Section 2.8.1, and originally by Lamont *et al.,* (1995), but further developed by Suwannakul *et al* (2010) to include an analysis of intracellular levels of bacteria (Suwannakul *et al.*, 2010). Multiplicity of infection (MOI) was chosen to be 1:100 (epithelial cells: bacteria) as this was determined as the optimum infectious dose for invasion of epithelial cells by Lamont (Lamont *et al.*, 1995). As mentioned above, the standard antibiotic protection assay allows the calculation of the number of bacteria that have invaded the cells as well as the total number of bacteria associated with the cells (adhered and invaded). This allows the calculation of the number of bacteria adhered to the cells by the subtraction of the invaded count from the total association count. The number of bacteria isolated from all three conditions (invaded, adhered and total association) is determined as a percentage of the total viable counts of each strain to eliminate any errors in that strain's preparation (% Recovery), for example, if one strain has a lower number of bacteria in the sample applied to the host cells. Results from the standard antibiotic protection assays can be seen in Figure 3.20.

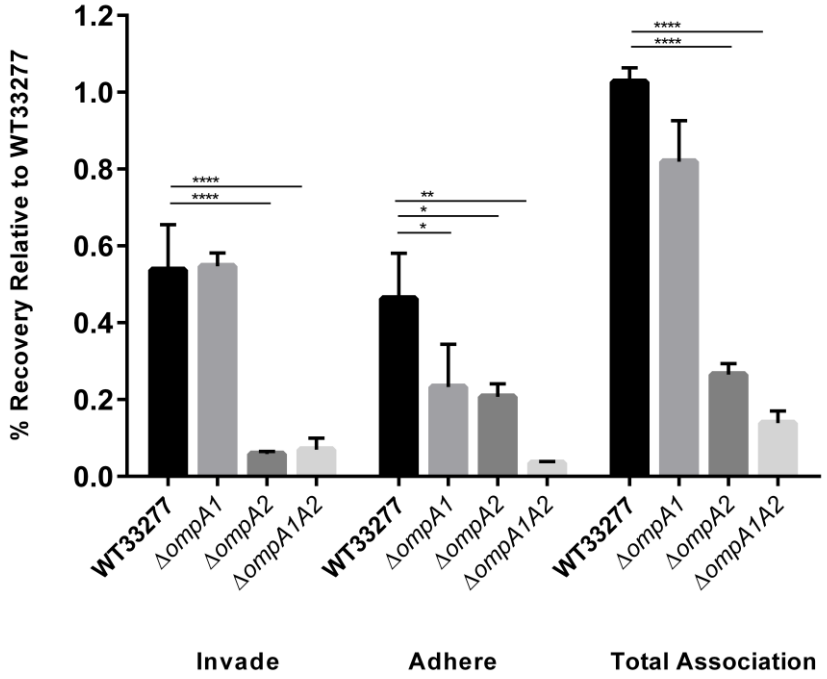

Figure 3.20 Bacterial adhesion and invasion of oral epithelial cells by *P. gingivalis* wild-type and Δ*ompA* mutants. Bacterial strains were incubated with OK-F6 cells at 1:100 MOI as detailed in Chapter 2.8.1. Viable counts were taken for each strain and the number of bacteria recovered was determined as a % of the viable count. Invasion was defined as the percentage of the bacterial inoculum protected from metronidazole killing, whereas total association denotes the number of bacteria that adhere to and invade the OK-F6 cells. Adherence was determined by subtracting invasion CFUs from the total associated. Each % Recovery was corrected to the wild-type *P. gingivalis* total association (=1). Error bars ± SEM. Statistical significance was defined by * $p < 0.05$, ** $p < 0.01$, *** $p < 0.001$ and **** $p < 0.0001$, determined by 2way ANOVA. Antibiotic protection assays were carried out in triplicate, with 3 counts per technical repeat observed (overall n = 27).

Figure 3.20 shows that all isogenic mutants of *P. gingivalis* display a differential adherence to OK-F6 cells compared to wild-type, with Δ*ompA1A2* displaying the least adherence. Adherence by Δ*ompA* mutants was reduced 2.1-fold, 2.45-fold and 13-fold for the Δ*ompA1,* Δ*ompA2* and Δ*ompA1A2* mutants respectively compared to wild-type *P. gingivalis* (*p < 0.05* single mutants, *p < 0.01* double mutant), demonstrating that the OmpA protein is implicated in the adhesion to the host cell. The ability for *P. gingivalis* to invade the host cell was also significantly affected by the deletion of the *ompA* operon (Δ*ompA1A2* mutant), which demonstrated an 8.3-fold reduction in invasion compared to wild-type. Interestingly, the Δ*ompA2* single mutant also demonstrated a significant reduction in the

invasive capability, showing a 10-fold reduction, as seen in Figure 3.20. No change to the number of Δ*ompA1* bacteria capable of invading the host cell compared to wild-type was observed. These data therefore suggest the OmpA2 protein subunit is key in the interaction with the host epithelial cell rather than OmpA1.

It is clear from the data that the entire OmpA1A2 protein is crucial in the interaction with the host due to the almost complete abrogation of adherence and invasion, but as the overall phenotype in this double mutant is vastly different from the wild-type (altered outer membrane profile, significant increases in vesicle formation and sialidase activity etc.), it would be difficult to determine if the effects seen by the loss of the OmpA protein is solely due to the mutation, or if it is due to its downstream effects. Therefore as the deletion of *ompA2* had a greater effect on invasion and adhesion of the OK-F6 cells but showed similar phenotype to the wild-type, this mutant was investigated further. In order to test a specific role for OmpA2 in these host-cell interactions the pTCOW-A2 complementation plasmid was again employed (Section 3.3.4) and used in a standard antibiotic protection assay against OK-F6 cells and the levels of invasion and adhesion assessed, as shown in Figure 3.21.

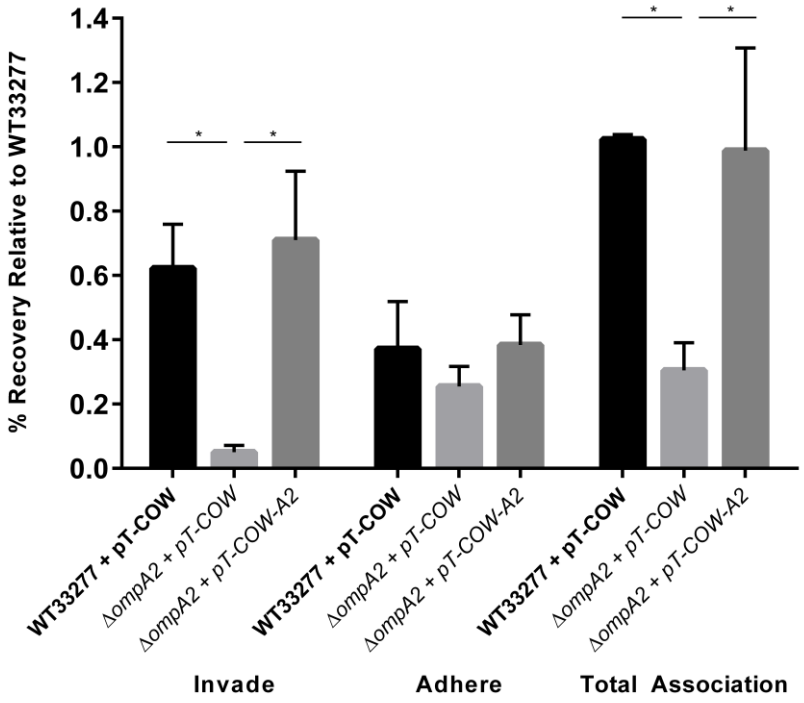

Figure 3.21 Bacterial adhesion and invasion of oral epithelial cells by wild-type *P. gingivalis*, Δ*ompA2* mutant and Δ*ompA2* mutant complement. Standard antibiotic protection assays were carried out as previously described in Chapter 2.8.1 with bacterial MOI 1:100. Wild-type and Δ*ompA2 P. gingivalis* strains carried empty pT-COW vectors as negative controls. All values were calculated as described in Figure 3.20, and % Recovery levels were corrected to wild-type *P. gingivalis* total association (=1). Error bars ± SEM. Statistical significance was defined by * $p < 0.05$, determined by students' *t*-test. Antibiotic protection assays were carried out in triplicate, with 3 counts per technical repeat observed (overall n = 27).

Figure 3.21 demonstrates that the complementation of the *ompA2* gene restores the levels of invasion and adhesion to wild-type levels. This was especially observed in the levels of invasion which was increased 14-fold in the complemented mutant compared to Δ*ompA2* invasion alone. This again supports the idea that the OmpA2 protein has a greater influence on the host cell interaction.

3.3.7.2 Viability Of Mutants During Standard Antibiotic Protection Assay

To confirm that the loss of adherence and invasive capabilities of the Δ*ompA* mutants was due to the loss of the OmpA protein (or singular subunits) from the cell membrane, not just due to a loss of membrane integrity causing the bacteria to be less viable in tissue culture media, the viability of the wild-type and mutant strains was determined through the time

course of the invasion assay. Figure 3.22 demonstrates that although there appeared to be high levels of variation between repeats, the viabilities of the mutant strains are not significantly different to the wild-type strain. This therefore indicated the loss of the protein does not have a particular effect on the viability of the bacterial cell. In addition, in each experiment, all invasion levels are compared to a viability control.

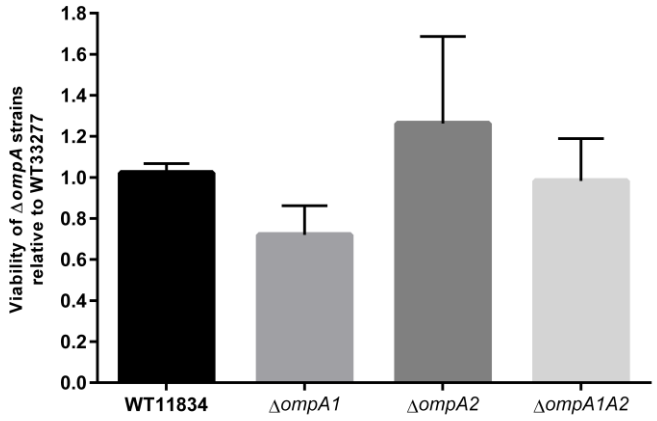

Figure 3.22 Viability of *P. gingivalis* wild-type and mutant strains throughout the standard antibiotic protection assay. CFUs of the plated viability wells of *P. gingivalis* were corrected to wild-type viability (=1) and compared. No statistical difference was observed between strains. Error bars ± SEM.

3.4 Discussion

The ability of *P. gingivalis* to interact with the host cell is a key virulence factor in the survival of the bacterium and the progression into a chronic periodontal infection. The OmpA protein of *P. gingivalis* has been implicated as important in this process by a number of previous studies. In a "hyperinvasive" subtype of the natural *P. gingivalis* population, gene expression of *ompA* was found to be upregulated in two strains of *P. gingivalis* tested (Suwannakul *et al.*, 2010), whilst purified native OmpA heterotrimer prevented the interaction of wild-type *P. gingivalis* with endothelial cells (Komatsu *et al.*, 2012). This chapter investigated the role for OmpA in host cell epithelial interaction, using both a Δ*ompA1A2* full heterotrimer mutation and single Δ*ompA1* and Δ*ompA2* mutants, alongside general phenotypic characterisation of these strains.

3.4.1 Phenotypic Characterisation of *P. gingivalis* and Δ*ompA* Mutants

Mutants of *ompA* were generated in this study to understand the effects of the OmpA protein on the cell membrane itself and its interaction with the host and surrounding environment. The traditional method for introducing recombinant DNA to *P. gingivalis* for the generation of mutants is via electroporation (Yoshimoto *et al.*, 1993; Smith, 1995) with many genetic studies of *P. gingivalis* creating isogenic mutants via this method (Salyers *et al.*, 2000). However, the included steps in generating electrocompetent bacteria are laborious and for practical reasons, are carried out in an aerobic environment which causes physiological stress to the bacteria, whilst the electrical pulse can cause cell lysis resulting in reduced electroporation efficiency. A recent study by Tribble *et al.,* (2012) observed the *P. gingivalis* ATCC 33277 strain was capable of horizontal DNA transformation, and therefore was "naturally competent". This method involved fewer steps and less exposure to aerobic conditions, whilst vastly increasing the transformation efficiency (Tribble *et al.*, 2012) and was therefore utilised in this study and compared with the traditional electroporation method to generate Δ*ompA1* and Δ*ompA2* mutants and a complemented Δ*ompA2* + pT-COW-*A2* strain, alongside the electrocompetency method to determine the efficiency.

Both linear and plasmid DNA was used in the transformation of *P. gingivalis,* and no significant difference was observed between the two. This was expected as *P. gingivalis* contains a ComF protein which translocates DNA across the membrane shows no bias between uptake of DNA from natural *P. gingivalis* sources and unmethylated DNA generated from PCR (Tribble *et al.,* 2012), so the use of PCR-generated constructs for *ompA* mutation would not interrupt the efficiency of this method, nor would the origin of DNA being plasmid or PCR-generated affect the transformation efficiency. Linear DNA was a preferred choice of DNA origin as it would reduce the occurrence of a single crossover event whereby the erythromycin gene would be incorporated, but the gene of interest still retained in the chromosome creating a false positive. This was inspected for using PCR confirmations and not observed in the plasmid-containing transformations; however, the linear DNA-based origin was preferred.

The transformation efficiency for generating the Δ*ompA1* mutant was generally lower than Δ*ompA2* and overall fewer colonies were produced when introducing the externally generated construct of Δ*ompA1::em*. This was attributed to the design of the construct being based on a different *P. gingivalis* strain genome (W50 instead of ATCC33277), reducing the homology in the flanking regions to 93% (flank 1) and 96% (flank 2) which

reduced recombination efficiency. Despite this, the number of mutant colonies generated was overall higher when transforming *P. gingivalis* using the natural competency method which is expected to be due to the preparation steps of *P. gingivalis* for each transformation method. The electrocompetency method preparation involved multiple centrifugation steps in an aerobic environment, which causes physiological stress to the bacteria and may lead to cell death. Natural competency involves minimal centrifugation and minimal exposure to the aerobic environment, reducing the loss of viability and increasing the number of bacteria capable of uptaking DNA for transformation, and increasing overall mutant colony generation. During both Δ*ompA1* and Δ*ompA2* mutant generation, the natural competency method greatly surpassed the electrocompetency method in efficiency, with a 9-fold and ≥16-fold increase in colonies observed on erythromycin-containing BA plates, respectively. Because of these observations, natural competency has been deduced as the preferred method of *P. gingivalis* transformation and will be recommended for implementation in the lab as the future method of generating *P. gingivalis* mutants.

The successful mutation of the *ompA1* and *ompA2* genes was confirmed through PCR and sequencing, however as the *ompA* genes are in an operon, there is the possibility of polar effects with the mutation, i.e. the loss of *ompA1* may cause read-through problems leading to *ompA2* not being expressed. The outer membranes of the wild-type and mutant strains were therefore purified and analysed using SDS-PAGE where if polar effects were observed, the *ompA1* mutant would show a similar outer membrane protein profile to the double mutant. The protein bands observed were at the correct size for the presence of OmpA, with a prominent band in the wild-type outer membrane, fainter bands in the single mutants and no band observed in the double mutant. To further confirm this, the presence of OmpA in the wild-type and mutants was investigated using an anti-OmpA antibody. Bands were observed at the correct sizes in the wild-type strain and fainter in the single mutants, whereas no banding was observed in the double mutant, confirming the successful mutation without causing polar effects.

The OmpA protein is a major outer membrane protein, contributing to a large proportion of the protein found on the surface of Gram-negative bacteria (Smith *et al.*, 2007). Previous studies of the OmpA protein of *P. gingivalis* have indicated that the protein is key in stabilisation of the outer membranes (Sonntag *et al.*, 1978; Klose *et al.*, 1988), so electron microscopy was used to further characterise the effects of the loss of OmpA on the

membrane of *P. gingivalis*. Thin-section microscopy revealed "wavy" membranes in all three mutants, but to a larger extent in the double mutant. This agrees with previous observations of the disruption of the cell membrane integrity seen in the study by Iwami *et al.*, however in contrast, this is only observed in a small percentage of the population, (Iwami *et al.*, 2007). As OmpA proteins are found to have a C-terminal domain that is predicted to associate with the peptidoglycan layer, the loss of membrane integrity and rigidity is a possibility with the loss of OmpA. Without the peptidoglycan-associated C-terminal domain, the outer membrane is predicted to be no longer associated with the peptidoglycan layer via the OmpA protein, and therefore the rigidity of the membrane is lost. This C-terminal domain is conserved amongst many species' OmpA protein, regardless of the similarity of the N-terminal domain (De Mot and Vanderleyden, 1994) implying that the OmpA protein is an important structural protein in the cell envelope.

As OmpA is implicated in the stability of the membrane, the number of vesicles produced in the mutant strains was investigated. Multiple groups have previously shown that a lack of OmpA in a variety of bacteria result in hypervesiculation, as observed in *E. coli, Vibrio cholerae* and *Salmonella* (Sonntag *et al.*, 1978; Song *et al.*, 2008; Deatherage *et al.*, 2010). The outer membrane vesicle production of *P. gingivalis* and *ompA* mutants was using a qNANO, which assesses the number and size of vesicles produced. A slight increase in vesicle formation was observed in both single Δ*ompA1* and Δ*ompA2* mutants, with a large increase was observed in the double Δ*ompA1A2* mutant. This complies with general OmpA studies, as previously referenced above, however fewer vesicles are observed in the single mutants compared to Iwami *et al* studies in *P. gingivalis ompA* mutants, which is likely due to the shortened length of time these samples were grown for (16 – 24 h) whereas the Iwami *et al.,* grew cultures for 48 h, and showed more vesicles were produced later in the growth stages (Iwami *et al.*, 2007). Again, because the Δ*ompA1* mutant doesn't display a vesicle-producing phenotype similar to that of the Δ*ompA1A2* mutant, it is likely that there is no polar effect in the protein expression in this mutant.

The TEM provided contradictory results when observing the presence of fimbriae on the mutants. It appears that the fimbriae are unaffected by the loss of the OmpA protein in all mutants, however when using an anti-FimA antibody, no FimA subunits were observed in the Δ*ompA1A2* mutant. Whilst this was not unexpected, due to previous data shown in *E. coli* which demonstrates the fimbrial expression is affected with the loss of OmpA, this proved contradictory here. It is more likely the fimbrial-like extrusions from the TEM images

are artefacts from the processing of the cells for electron microscopy. However, it is more important to note that no differences are seen in the fimbrial expression between the Δ*ompA1* and Δ*ompA2* mutants, which excludes the possibility that the loss of adherence and invasion in the Δ*ompA2* mutant compared to the Δ*ompA1* mutant is due to the loss of fimbriae.

3.4.2 Enzymatic Activity Profiling of Mutant Strains Indicate *ompA2* Specific Phenotypes

As the deletion of *ompA* has previously been shown to affect the expression of other virulence factors in *E. coli*, including a decrease in the expression of the fimbriae (Teng *et al.*, 2006), the effects of the deletion of *ompA1A2* and the single *ompA1* and *ompA2* genes on the expression of other major virulence factors of *P. gingivalis* was assessed.

The Arg- and Lys- gingipains are proteases that are heavily implicated in the colonisation of the host tissue (Nakayama *et al.*, 1996; Tokuda *et al.*, 1996). Previous studies have demonstrated that an increase in gingipain activity can lead to a reduction in the invasion of *P. gingivalis* (Suwannakul *et al.*, 2010), and therefore it was important for this study to determine if there are any effects on the gingipain activity due to the deletion of the *ompA* genes. As gingipains are both cell-associated and secreted, two different activity assays were used to investigate the activity of both the Arg- and Lys- gingipains. Significant changes to the gingipain activity were observed for all conditions (Arg- and Lys-, secreted and cell-associated) in the Δ*ompA1A2* double mutant, however no significant change between the single Δ*ompA1* and Δ*ompA2* mutants were observed. This was important to note as the differential abilities of the Δ*ompA1* and Δ*ompA2* mutants in the interaction with the host is therefore not attributed to a change in bacterial-associated proteins that are also implicated in host cell adhesion, and therefore the effects of the deletion of the OmpA protein and individual subunits is likely due to the loss of protein itself.

The sialidase activity of *P. gingivalis* and Δ*ompA* mutants was also investigated in this study as sialidases in other oral pathogens have been shown to be involved in the formation of biofilms (Roy *et al.*, 2011) as well as the adherence to epithelial cells (Honma *et al.*, 2011). It was important to determine again if the deletion of *ompA* had any further effects on other virulence factors which would mask the effects of OmpA on host cell interaction. Sialidase activity was increased in the double Δ*ompA1A2* mutant, however no change was observed in the single Δ*ompA1* and Δ*ompA2* mutants. Similarly to the gingipain activity, the disruption by the loss of the entire OmpA1A2 protein complex causes changes to the outer-

membrane associated sialidase proteins, but no difference is observed between the single Δ*ompA1* and Δ*ompA2* mutants.

The enzymatic assays were of importance in this study to determine if the effects seen by the loss of the OmpA protein were due to the protein itself or its downstream effects. As the loss of an integral outer membrane protein has major effects on the rest of the membrane, it was key to understand these effects on the hypothesis that OmpA is interacting with the host. As expected, the loss of the entire OmpA1A2 protein has multiple detrimental effects on the cell, showing a significant increase in vesicle formation, and therefore changes to gingipain and sialidase activity levels. It is impossible to segregate the changes in virulence factors of *P. gingivalis* with the loss of the entire OmpA1A2 protein as it is a major protein of the outer membrane, however as the Δ*ompA2* mutant demonstrates a strong phenotype in the adherence and invasion of the host (as discussed later) that is not observed in the Δ*ompA1* mutant, as well as little difference observed in the activities of sialidase and gingipains in both Δ*ompA1* and Δ*ompA2* single mutants, this suggests that the host-cell interaction phenotypes observed with Δ*ompA2* and Δ*ompA1A2* are due to the loss of protein, not downstream effects.

3.4.3 Biofilm Formation by *P. gingivalis* and Δ*ompA* Mutants

The formation of a biofilm by oral microbes is a central point in periodontal disease as the biofilm formed on tooth structures forms the basis of dental plaque (Cook, 1998). Orme *et al.,* (2006) identified an overexpression of OmpA in biofilm formation of *E. coli*, (Orme *et al.*, 2006), whilst the studies into the involvement of OmpA in biofilm showed a differential formation of biofilm on hydrophilic and hydrophobic surfaces, potentially mediated by the OmpA protein inducing the CpxRA two-component pathway, which regulates the expression of cellulose and influences biofilm formation (Barrios *et al.*, 2006; Ma and Wood, 2009).

The data presented in this chapter demonstrate a role for OmpA in *P. gingivalis* in the formation of the biofilm. A loss of the entire OmpA heterotrimeric complex, or the OmpA2 subunit alone results in a significant reduction in the formation of a biofilm on the inert surface of a 96-well MTP, suggesting a specific role for the OmpA2 subunit in the interaction of *P. gingivalis* with the surrounding environment. Important to note was the equivalent level of growth between all wild-type and mutant strains over the 72-hour period, suggesting that there were no growth deficiencies in the different mutant strains of

bacteria compared to the wild-type and therefore the lack of biofilm formed was likely due specifically to the loss of OmpA. The levels of biofilm formation were only partially restored using the Δ*ompA2* + pT-COW-*A2* complement strain, but a significant increase in biofilm formation was observed.

More biologically relevant studies using 96-well MTPs coated in salivary mucin or purified saliva would provide a more accurate representation of OmpA-influenced biofilm formation, or even the overexpression of *P. gingivalis* OmpA in wild-type *P. gingivalis* to determine an increase in biofilm formation, would contribute to confirming the role of OmpA in biofilm formation. Multi-species biofilm formation assays using confocal microscopy would also contribute to a more biologically relevant study, as *P. gingivalis* is well known for interacting with other bacterial species in the oral cavity, such as *Streptococcus gordonii* (Lamont *et al.*, 2002; Park *et al.*, 2005), *Treponema denticola* (Yamada *et al.*, 2005; Bao *et al.*, 2014), especially for initial adherence, such as the interaction with the bridging pathogen, *Fusobacterium nucleatum* (Kolenbrander *et al.*, 2002; Kolenbrander *et al.*, 2006), and provide a greater analysis of the role of OmpA in biofilm formation.

3.4.4 *P. gingivalis* Invasion and Adhesion of Oral Epithelial Cells

The ability of *P. gingivalis* to adhere to and invade host cells has been reported on numerous occasions (Njoroge *et al.*, 1997; Chen *et al.*, 2001; Chen and Duncan, 2004) and in both gingival epithelial cells (Lamont *et al.*, 1995) and aortic endothelial cells (Komatsu, *et al.*, 2012). Various studies have also shown the buccal epithelial cells contain a polymicrobial intracellular flora, including the presence of *P. gingivalis* whilst showing no inflammatory response (Rudney *et al.*, 2001; Rudney *et al.*, 2005), indicating that the bacteria communicate with one another to suppress the inflammatory response and remain undetected by the host immune system (Rudney and Chen, 2006).

The invasion and adherence data was obtained through a standard antibiotic protection assay as first described by Lamont *et al*., (1995) with the addition of a metronidazole incubation step to kill extracellular bacteria so the number of invaded bacteria can be determined from the number of bacteria associated with the cell (i.e. adhered and invaded). The cell line chosen for the standard antibiotic protection assays was an oral keratinocyte cell line as this is the principal cell type that *P. gingivalis* will directly come into contact with in the oral cavity. The invasion and adherence to these cells was greatly

abrogated with the loss of the OmpA heterotrimer, as shown in the Δ*ompA1A2* mutant resulting in very few cells being observed adhered to or invading the host cell. In contrast, very little difference in invasion of the Δ*ompA1* mutant was observed with a 2-fold reduction in the adherence of the bacteria. A similar 2-fold loss of adherence in the Δ*ompA2* strain was observed; however the intracellular number of this mutant was similar to that of the double Δ*ompA1A2* mutant, suggesting a potentially role for the OmpA2 protein subunit in the internalisation of the bacterium, through possible stronger engagement of the host cell receptors. Previous reports of the OmpA protein binding host cell molecules (namely extracellular matrix molecules) have suggested the entire OmpA protein is necessary (Murakami *et al.*, 2014), however the data presented here suggest a stronger role for the OmpA2 subunit in the interaction with epithelial cells. As the phenotypes of the two single mutants show very little differences in enzyme activity (sialidases and gingipains) and fimbrial possession, but show significant differences in the ability to invade the host, this further supports the hypothesis that OmpA (more specifically, OmpA2) is involved in the host cell interaction.

The role of OmpA2 in the adherence and invasion of the host was supported by the creation of an Δ*ompA2* + pT-COW-*A2* complement strain. Standard antibiotic protection assays were carried out with all three strains to determine if the loss of adherence and invasion observed in the Δ*ompA2* strain was truly due to the loss of the protein. The complemented strain restored the levels of adherence and invasion to wild-type, supporting the hypothesis that the loss of invasion and adherence is specifically due to the loss of the OmpA2 protein in the single mutant. This is the first time a role for individual OmpA subunits has been observed in *P. gingivalis.*

These data were obtained using only a single strain of *P. gingivalis*, whereas the oral cavity contains hundreds of species of bacteria, and it has been well documented that *P. gingivalis* interacts with other species such as *Fusobacterium nucleatum* in the colonisation of the host (Lamont and Jenkinson, 2000). Future work could include the analysis of multi-species standard antibiotic protection assays, with the inclusion of other oral pathogens such as *F. nucleatum* which would also help to determine if OmpA has a role in adherence and interaction with other bacteria as well as the host.

These data are only presented on one cell line, whereas the bacteria would come in contact with many more cell types during the infection process. *P. gingivalis* has been shown to interact with endothelial cells (Deshpande & Khan 1998; Komatsu, *et al.*, 2012), enhancing

the theory that *P. gingivalis* may be associated with cardiovascular disease (Marcus and Hajjar, 1993; Li *et al.*, 2000; Kozarov *et al.*, 2006). Future work would include the use of different cell lines in the investigation of *P. gingivalis* interaction with the host, for example, the use of primary epithelial cell lines as these would represent the infection process in the oral cavity more accurately.

3.5 Summary

In conclusion, this chapter has enforced the hypothesis that OmpA has a role in the integrity of the outer membrane, leading to an increase in vesicle production, and therefore an increase in the activity of membrane-associated enzymes with the loss of the entire OmpA1A2 protein. This chapter has also identified a novel role for OmpA2 in the interaction with the host, causing a significant decrease in the invasion and adhesion of the host when this subunit of the OmpA protein is lost, which is restored when a complemented strain of the mutant is employed. The ability of *P. gingivalis* to form a biofilm is also affected with the loss of OmpA2, highlighting a specific role for the OmpA2 subunit in *P. gingivalis* virulence. These data also indicate a direct interaction between OmpA2 and a cellular factor on the host cell, which will be investigated further in Chapter 4.

These findings are important as they have identified a specific protein that could be targeted therapeutically for the treatment of periodontal disease, by specifically targeting the keystone pathogen of periodontal disease, *P. gingivalis*.

Chapter 4

Molecular Mechanism of OmpA Interaction with Host Epithelial Cells

4.1 Introduction

Data from Chapter 3 indicated a strong possibility that the OmpA proteins of *P. gingivalis* are involved in the formation of biofilms and the adherence and invasion of the host, of which the data also identified a greater role for OmpA2 in these interactions. This chapter will aim to investigate the molecular determinants behind these interactions to further dissect the role of OmpA in the interaction with the host cell.

The classic structure of OmpA conforms to a two-domain structure, with an N-terminal transmembrane β-barrel adjoined to a C-terminal peptidoglycan-associated domain (Wang 2002). The OmpA of *P. gingivalis* was first discovered by Murakami *et al* (2002) as a heterologous trimer of OmpA1 and OmpA2 subunits (around 40 and 41 kDa respectively) and determined to exhibit the same structure, sharing a high structural homology to *E. coli* OmpA (Murakami *et al.*, 2002; Nagano *et al.*, 2005; Yoshimura *et al.*, 2009). The importance of *P. gingivalis* OmpA has been implicated in host cell interaction through limited studies, namely in the interaction with host endothelial cells (Komatsu *et al.,* 2012) but also by its upregulation of expression in hyperinvasive subpopulations of the bacteria (Suwannakul *et al.*, 2010) and more strongly through data presented in Chapter 3 of this study, and therefore forms the basis of the hypothesis in this chapter.

Data presented in the previous chapter demonstrates a role for OmpA in host-cell interaction through the loss of the protein leading to a loss of invasion and adherence of oral epithelial cells (Fig. 3.20). Again as presented in the previous chapter, the OmpA2 protein subunit appears to perform as the dominant subunit in the interaction with oral epithelial cells, this chapter will investigate further into the role for OmpA2 in this host-pathogen interaction.

In this chapter, the interaction of OmpA, specifically the OmpA2 subunit is explored through overexpression of the protein and structural modelling analysis of the OmpA protein. This is built upon by the identification of structural features of the OmpA2 protein that lead to direct interactions with the host cell.

4.2 Aims

The specific aims of this chapter are to investigate the interaction of OmpA, and specifically the OmpA2 subunit through overexpression of the protein and structural analysis of the

OmpA protein. This is built upon by the identification of structural features of the OmpA2 protein, and the investigation of direct interaction with the host cell.

4.3 Results

4.3.1 OmpA1 and OmpA2 Protein Overexpression

To determine the role of OmpA in interaction with the host, it was necessary to attempt to produce soluble recombinant versions of the protein that then be used in a number of assays aimed at probing whether OmpA proteins directly interact with host-cells. For example, in immunofluorescence assays to examine if OmpA binds to cell surfaces or in more direct assays by attempting immunoprecipitation or pull-down assays to detect binding and identify human protein interaction partners. As previously discussed, the OmpA protein of *P. gingivalis* is composed of two different subunits in a heterotrimer. These subunits were cloned and overexpressed individually and purification attempted to determine if there was a role for host cell interaction for each subunit.

4.3.1.1 His-tag Protein Purification

Initially, the OmpA1- and OmpA2-expressing *E. coli* (DE3 C41) were provided by Dr Graham Stafford, whereby the gene encoding the OmpA1 or OmpA2 protein was inserted into pET15b plasmid to be expressed with an N-terminal Hexa-His tag. The *E. coli* C41 strain was chosen for protein overexpression as it has been shown to be a stable strain, easily transformed and capable of expressing recombinant proteins that would otherwise prove toxic to the cell (Dumon-Seignovert *et al.*, 2004). The His-tag is comprised of a short 6-histidine residue extension to the protein which will allow binding to immobilised metal affinity chromatography media as the negatively charged hexa-his tag will interact with high affinity with a immobilised divalent cation, (in this case Ni^{2+}) to allow purification of the recombinant OmpA protein (Hochuli *et al.*, 1987).

Cultures of *E. coli* C41 for OmpA1 and –A2 overexpression were grown to OD_{600} 0.6 before induction with IPTG and grown for 4 h at 37°C as described in Materials and Methods Section 2.7.1. Cells were harvested and lysed, before centrifugation was carried out to separate soluble and insoluble fractions. Outer membrane proteins are often particularly insoluble due to the hydrophobic residues being exposed during overexpression without the presence of their usual chaperones, which leads to aggregation and insolubility in the aqueous environment of the cytoplasm (Seddon *et al.*, 2004). Several research groups have

successfully purified the OmpA protein in other bacterial species (Prasadarao *et al.*, 1996; Serino *et al.*, 2007; Martinez *et al.*, 2014), demonstrating that although it is not without its issues, it is still possible to purify outer membrane proteins. Figure 4.1 demonstrates both OmpA1 and OmpA2 subunits overexpress well in these conditions, however, most of the OmpA1 and OmpA2 protein was found in the insoluble fraction after lysis and fractionation (Figure 4.1B).

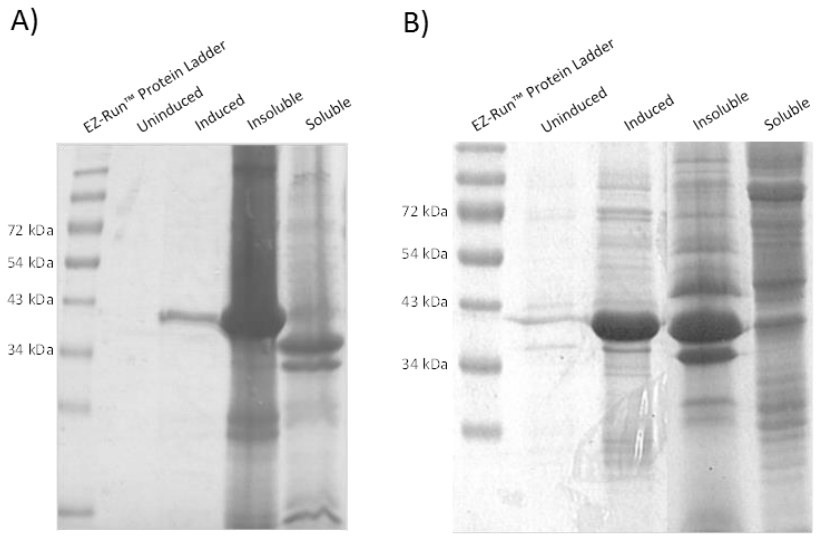

Figure 4.1 SDS-PAGE showing the overexpression of the OmpA1 (A) and OmpA2 (B) protein subunits. *E. coli* DE3 (C41) strains containing the pET15-*ompA1* or *–A2* plasmid for overexpression were grown in large batch cultures and induced using IPTG for protein expression as described in Chapter 2. Uninduced and induced lanes display 1 ml samples removed from the culture, pelleted and resuspended in SDS-loading dye, and denote the cells before IPTG induction and 4 h post induction when cells were harvested. Cells were lysed using a French Pressure Cell and centrifuged to determine the solubility of the protein, resulting in the insoluble and soluble fractions. The large protein band at ~41 kDa denotes the presence of the OmpA protein, and is shown here to be insoluble after overexpression.

Because the purification of the protein was using the His-tag on Nickel-coated resin, solubilising reagents were used to solubilise the OmpA1 and OmpA2 found in the cell lysate insoluble fractions. Urea (8 M) was used to solubilise the pellet after centrifugation of the cell lysate, and the protein was purified from the Ni^{2+}-NTA resin, as shown in Figure 4.2.

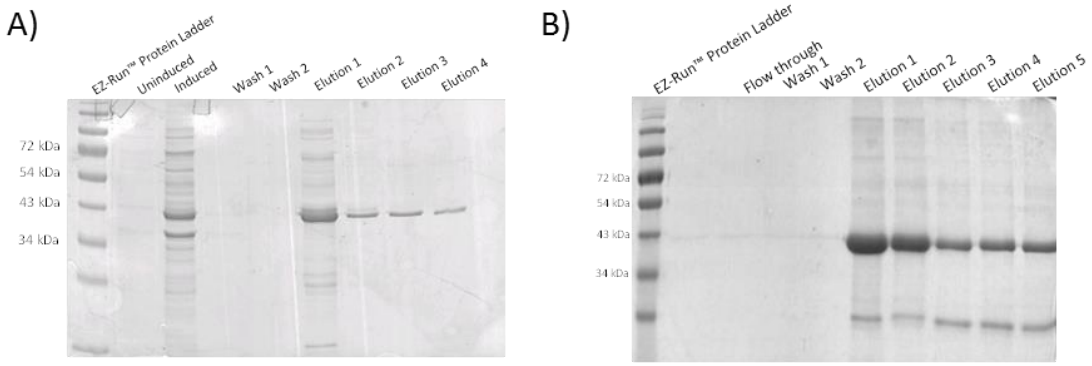

Figure 4.2 SDS-PAGE analysis of the purification profile of His-OmpA1 (A) and His-OmpA2 (B) after urea solubilisation. Insoluble fractions post cell lysis were solubilised in 8M urea for 4 h (4°C) before centrifugation and the supernatant applied to Ni^{2+}-NTA resin pre-loaded into a Poly-Prep Gravity Flow Column (BioRad). His-OmpA-bound resin was washed twice (PBS, 120 mM NaCl, 20 mM imidazole) followed by elution buffers of PBS, 120 mM NaCl, and either 150 mM imidazole (elution 1 and 2) or 200 mM imidazole (elution 3, 4 and 5). Uninduced and induced samples of the cells before lysis were included for OmpA1 as a reference for ensuring protein expression as the expression was lower than His-OmpA2 (Fig 4.1). The His-OmpA1 can be seen clearly as the strong bands at ~41 kDa in the induced sample and the elution fractions, whereas His-OmpA2 can be seen as the major band at ~41 kDa in Elution fractions 1-5.

High yields of protein could be purified after solubilisation in urea, especially seen in OmpA2 (Figure 4.2B), which demonstrates a high level of overexpression of the protein in the pET15b vector in *E. coli* DE3 C41. The SDS-PAGE gels also demonstrate mostly a high level of purity in the purifications. However, when the purified protein elution fractions were then dialysed into PBS to remove all imidazole and urea and to allow re-folding of the protein to a native state, all protein precipitated and became insoluble once again, as shown in Figure 4.3.

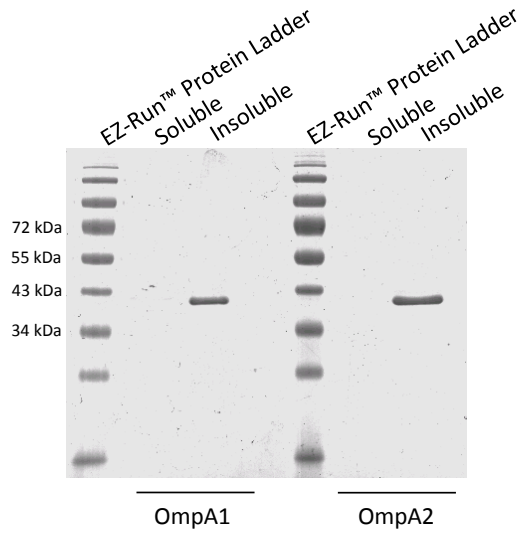

Figure 4.3 SDS-PAGE analysis of the dialysis of His-OmpA1 and His-OmpA2. Elution fractions were pooled and dialysed in PBS dialysis buffer (PBS, 120 mM NaCl) for 16 h at 4°C. The contents of the dialysis tubes were centrifuged and the supernatant (soluble fraction) and the pellet (insoluble fraction) were analysed. In both cases, protein aggregated during dialysis and become insoluble.

4.3.1.2 GST-tagged Protein Purification

The solubility of a proteins during overexpression can be assisted through the fusion to other proteins, such as Glutathione-S-Transferase (GST), or Maltose Binding Protein (MBP) which stabilise the folding of the recombinant protein and help to increase the solubility (Biosciences, 2001). As well as increasing the solubility, the addition of the GST-tag is also advantageous as it can be removed using Thrombin, so a pure version of the protein can be used in downstream experiments. To increase OmpA1 and A2 protein solubility, the genes expressing these proteins were amplified through PCR using Phusion HF™ polymerase enzyme (Figure 4.4A) using primers from Table 2.9 and 2.10 which contained *Bam*HI and *Eco*RI restriction enzyme tails, and ligated into pGEX-4T3 vector which encodes the 26 kDa GST fusion protein. Initially the pGEX-OmpA1 and pGEX-OmpA2 plasmids were transformed into DH5α and colonies that appeared on LB-Ampicillin plates had the plasmid extracted and then digested with *Bam*HI and *Eco*RI restriction enzymes. The specific banding pattern of plasmid and insert was analysed and successful insert incorporation was observed (Figure 4.4B).

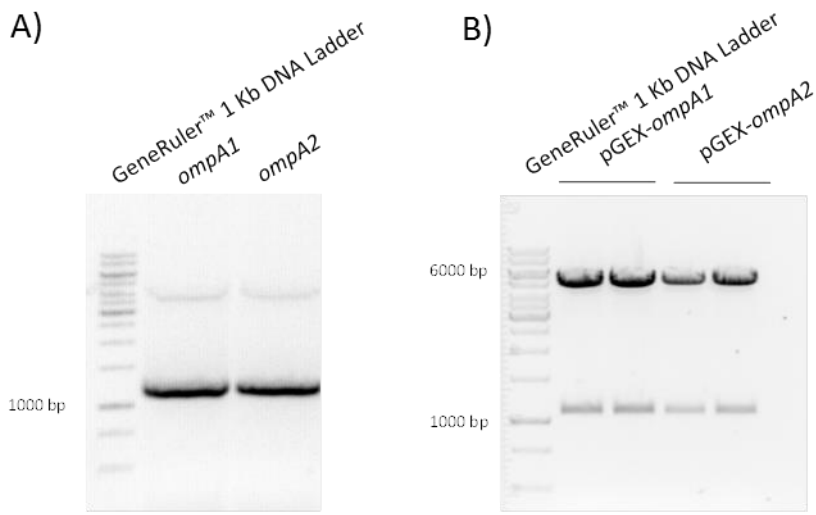

Figure 4.4 Cloning of *ompA1* and *ompA2* for GST-tagged protein overexpression. The *ompA1* and *ompA2* genes were amplified using Phusion HF™ enzyme in a PCR reaction detailed in Chapter 2.6.2.3. before being analysed on a 1 % agarose gel (A). After ligation, transformation, clone selection after colony PCR, plasmids were extracted from positive colonies for ampicillin resistance and digested using BamHI and EcoRI and analysed on a 1% agarose gel (B). All plasmids showed incorporation of the insert (~1200 bp) into the plasmid (~5000 bp), as demonstrated by the two bands present on the agarose gel.

Plasmids were sequenced to ensure no mistakes were found in the sequence transcript which would result in misfolded or truncated and inactive protein upon expression. All pGEX-*ompA1* and pGEX-*ompA2* plasmids demonstrated a correct sequence, so one plasmid for each protein subunit was chosen and transformed into *E. coli* DE3 C41 for protein overexpression. Small 5 ml overnight cultures of *E. coli* DE3 C41 + pGEX-*ompA1* or *–A2* were used to determine optimal expression conditions through different incubation temperatures (post IPTG induction), which were 37°C for 4 h, as previously used for His-tagged protein overexpression and ~24°C for 16 h (overnight). The protein expression was determined at these temperatures, as shown in Figure 4.5.

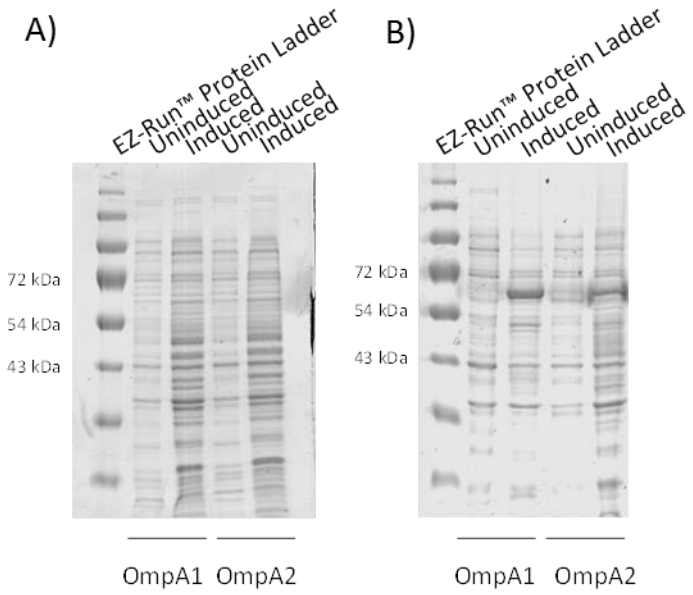

Figure 4.5 SDS-PAGE analysis of GST-OmpA1 and GST-OmpA2 protein expression at 37°C (A) and ~24°C (B). The overexpression of the protein was carried out as described in Materials and Methods 2.7.1.1, however in smaller (5 ml) cultures. A 1 ml sample was removed before induction with IPTG (uninduced) and 4 hours after induction with IPTG (0.1 mM) (induced), before being pelleted by centrifugation and resuspension in an appropriate volume of SDS-PAGE loading buffer. GST-tagged protein appears as a band ~67 kDa, and can be observed as the prominent bands in (B) in both OmpA1 and OmpA2 induced samples.

The concept behind using a lower temperature is to reduce the rate of protein expression to prevent aggregation and the formation of inclusion bodies, leading to insolubility of the protein (Sørensen and Mortensen, 2005). Figure 4.5A demonstrates a minimal overexpression of protein at 37°C, whereas induction and growth at ~24°C does display production of protein (Figure 4.5B), albeit less efficiently than previously observed with His-tagged OmpA. The solubility of the protein at these temperatures was then determined after cell lysis using a French Pressure Cell and centrifugation to separate soluble and insoluble fractions. The soluble and insoluble fractions are shown in Figure 4.6B.

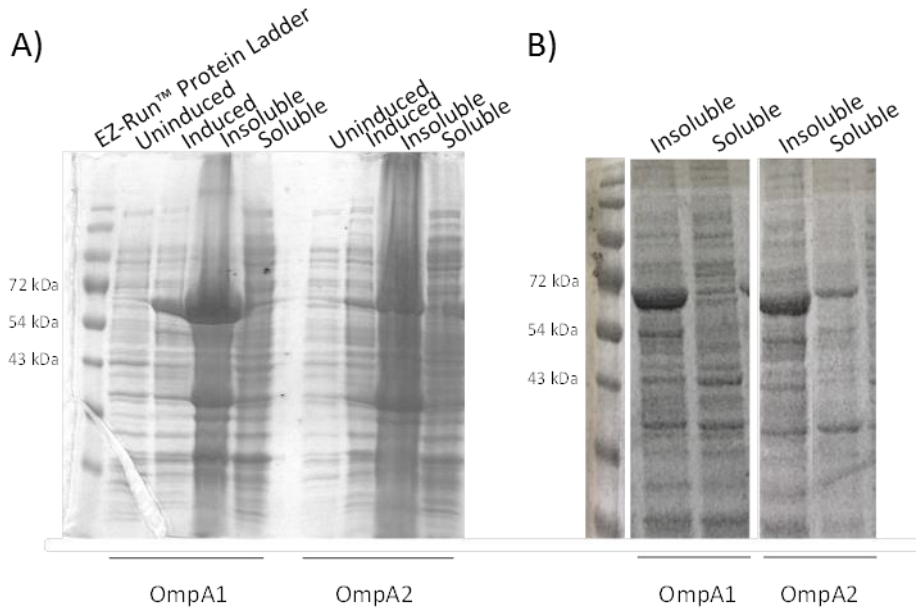

Figure 4.6 SDS-PAGE analysis of GST-OmpA1 and –A2 overexpression (A) and insoluble and soluble cell lysis fractions (B). *E. coli* DE3 C41 + pGEX-OmpA1 or –A2 was grown as detailed in Materials and Methods 2.7.1.1, and a samples taken before induction with IPTG (Uninduced), then the batch culture was induced with 0.1 mM IPTG and grown ~20°C for 16 h, before a sample was taken (induced). Cells were lysed using a French Pressure Cell and centrifuged to separate cell debris and insoluble proteins (insoluble) from soluble proteins in the cell (soluble). As before with His-tagged overexpression, the majority of the OmpA protein can be observed in the insoluble fraction, denoted by the large band ~67 kDa in both OmpA1 and OmpA2 induced and insoluble fractions (A). As the insoluble fractions contained a high concentration of protein and skewed the other fractions, the OmpA1 and OmpA2 insoluble fractions were diluted 10-fold and run alongside undiluted soluble fractions in (B). Samples in (B) were analysed on the same gel, but cropped here for clarity.

From Figure 4.6A, it is clear that the GST-tagged protein is being expressed, as seen as the band at ~67 kDa (26 kDa GST tag + 41 kDa OmpA protein) however as before with the His-tag, the majority of the protein is insoluble. Due to the high level of protein in the insoluble lane, the other lanes are distorted, so the insoluble fraction was diluted 1:10 before being re-analysed in Figure 4.6B. A minor amount of protein appears to be soluble (more so in GST-OmpA2) as indicated by the arrow, so the soluble fraction was applied to a glutathione-bound resin column to purify any GST-tagged OmpA1 and –A2 protein. The soluble fraction was incubated with the glutathione resin for 4 h to increase binding of the GST-tagged protein, before being passed through a column, washed and the protein eluted with 10 mM reduced glutathione. Figure 4.7 shows the SDS-PAGE analysis of the eluted OmpA1 and OmpA2 proteins.

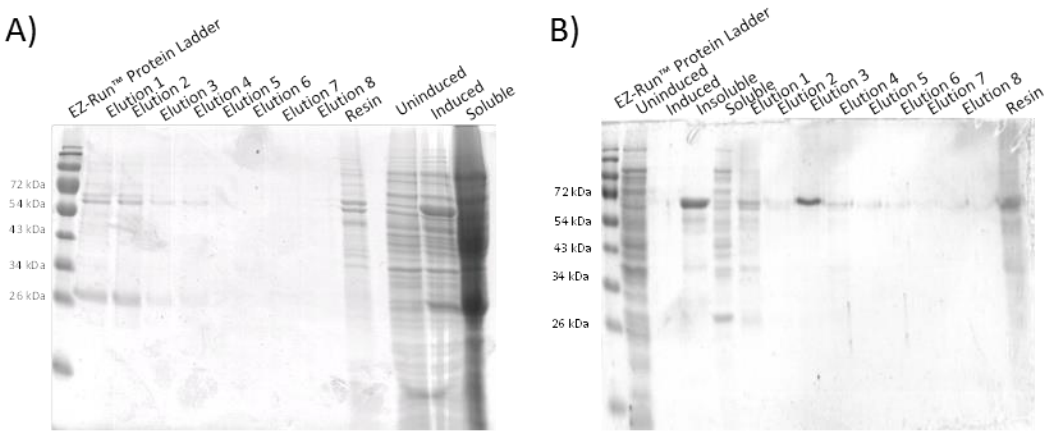

Figure 4.7 GST-tagged purification of OmpA1 (A) and OmpA2 (B). OmpA protein was overexpressed as described in Chapter 2.7.1.1. and cells lysed through a French Pressure cell before the soluble fraction was applied to glutathione (GSH) resin. After incubation for 4 hours at 4°C, GST-tagged protein was eluted using 20 mM reduced glutathione. After purification, the leftover resin was also applied to the SDS-PAGE gel to determine if all protein had been eluted. GST-OmpA1 and OmpA2 can be seen as the prominent band ~67 kDa. Smaller bands at ~26 kDa can be observed in both gels which equate to the GST tag being cleaved.

Figure 4.7 shows purification of a low concentration of OmpA1 and OmpA2 protein, as demonstrated by the bands at ~67 kDa; however dialysis again led to most of the protein precipitating. Elution fractions were pooled and dialysed, and some protein was observed in the soluble fraction post dialysis for OmpA2, as seen in Figure 4.8B, but the yield per elution fraction was determined to be too low for any experimental use.

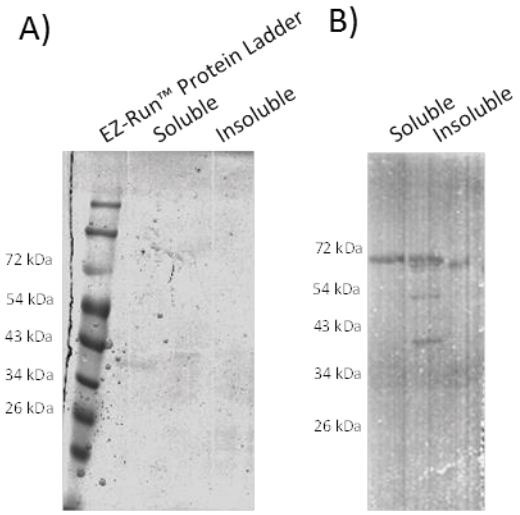

Figure 4.8 Dialysis of purified GST-OmpA1 (A) and GST-OmpA2 (B). Elution fractions for each protein were pooled and dialysed in one dialysis tube in dialysis buffer Tris-HCl (pH7.4), 120 mM NaCl. After 24 hours agitation at 4°C, the contents of the dialysis tube were centrifuged and the supernatant (soluble fraction) and the pellet (insoluble fraction) were analysed using SDS-PAGE, as shown here.

The dialysed GST-OmpA2 fractions showed a detectable amount of soluble protein but at a low concentration in a large volume, so the protein concentrated using a VivaSpin® 6 column (GE Healthcare) which decreased the volume from 10 ml to 500 µl. Using a BCA assay, the protein concentration was determined to be 301.6 µg / ml.

4.3.2 GST-tagged OmpA2 Interaction With Oral Epithelial Cells

The GST-OmpA2 protein was then used to determine if there is any direct interaction between OmpA and the host oral epithelial cells using immunofluorescence. A monolayer of OKF6 cells was seeded onto coverslips and grown to 70 % confluency. The cells were incubated with BSA to prevent any non-specific binding before being incubated with the GST-OmpA2 protein at 30 µg/ml or 30 µg/ ml GST for 4 h before the protein was removed and the cells were fixed using paraformaldehyde and anti-GST Tag antibody (Alexa Fluor® 488 conjugate) applied to detect the GST-tag. Cell membranes were stained using either CellMask™ Plasma Membrane Stain (ThermoFisher Scientific) (Figure 4.9A) or Wheat Germ Agglutinin-Texas Red® conjugate (ThermoFisher Scientific) (Figure 4.9B) and the coverslips were mounted using a DAPI mount to detect the cell nuclei. Immunofluorescence microscopy analysis of the OmpA2 protein interaction with the oral epithelial cells can be seen in Figure 4.9.

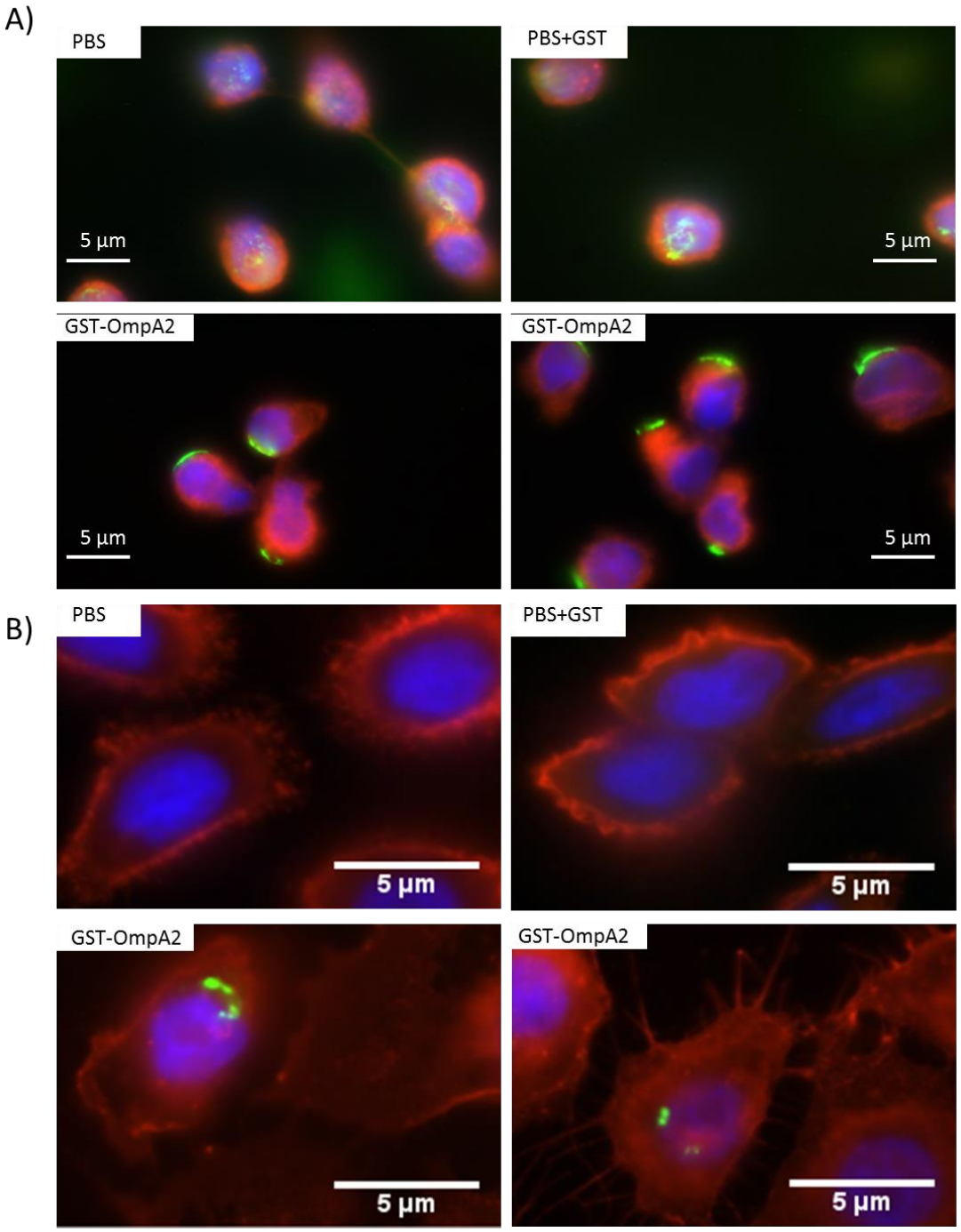

Figure 4.9 GST-Tagged OmpA2 protein applied to OK-F6 cells, epithelial cell membranes stained with CellMask™ Plasma Membrane Stain (A) or Wheat Germ Agglutinin-Texas Red® (B). PBS only and GST-only (30 µg / ml) are used as negative controls. OmpA2 (30 µg / ml) can be seen (green) to be interacting with the OK-F6 cell monolayers (cell membranes red, nuclei DAPI stained blue). Ant-GST antibody was used at 1:3000 concentration, CellMask™ at 1:1000 and Wheat Germ Agglutinin at 1:1000.

The immunofluorescence images clearly suggest an interaction between the purified OmpA2 protein and the host cell. The CellMask™ cell membrane stain only partially stains the cell membranes as the membranes only appear to be marginally larger than the nuclei themselves, whereas the Wheat Germ Agglutinin stain indicates the membranes more accurately. Despite the membrane stain, in both cases, the GST-OmpA2 protein can be clearly seen to directly interact with the host cell, with green fluorescently-labelled OmpA2 protein apparently binding in the peri-nuclear region. This would need to be further analysed through confocal microscopy to investigate this interaction further. A GST-only control was used to show the binding is specifically seen with the OmpA2 protein rather than occurring due to the presence of the GST protein.

These immunofluorescence images were generated from two separate experiments with three technical repeats per condition. The GST-OmpA2 protein was very unstable and precipitated between the CellMask™ and Wheat Germ Agglutinin experiment, even when stored at -20°C, and after the Wheat Germ Agglutinin staining experiment, the protein was no longer detectable via SDS-PAGE analysis. Further attempts to purify GST-OmpA1 or GST-OmpA2 proved unsuccessful, with little to no soluble protein produced so these interaction studies could not be repeated to statistically relevant levels (i.e. n = 3), and therefore further experimental analysis of the OmpA interaction with the host is needed, but was not possible given the insolubility and lability of the protein.

4.3.3 Investigation into Increasing Protein Solubility

Various conditions were applied during the protein purification process to attempt to increase solubility of the protein. Firstly, the addition of the detergent CHAPS to the cells from the start of the purification process (before cell lysis), which disrupt the lipid membrane increasing the solubilisation of the proteins (Radford, 1970), whilst increasing the purity of the purified proteins (Hong Lu *et al.*, 2001). CHAPS was chosen as it can be removed using dialysis due its small micellar molecular weight and high critical micellar concentration (Sigma Aldrich, 2008), so will not disrupt the membranes of the host cells during interaction studies (Pierce Thermo Scientific, 2010). Another method to increase solubility of the protein during the purification process was to determine the Isoelectric point (pI) of the proteins and use purification buffers at an opposing pH (GE Healthcare, 2010; Coutard *et al.*, 2012). Proteins are generally less soluble at the pH at which the protein has no net charge (the pI value), therefore using buffers at a different pH to the pI is thought to help increase solubility of the protein (Coutard *et al.*, 2012). The pI values for

OmpA1 and OmpA2 (without the signal sequence) were 8.61 and 7.69 respectively, so a purification buffer at pH 6 was used. However, neither of these methods appeared to increase the solubility and no soluble protein was recovered after purification (not shown).

4.3.4 Investigation of OmpA Dialysis

As the issues with solubility of the protein appear to be hindered by the loss of solubility during the dialysis of the protein, this part of the process was analysed to increase solubility. Studies in the literature provided various viable techniques to encourage solubility of the protein during the dialysis process and are explored in this section. The His-tagged protein was chosen for further analysis as it provided a greater yield of protein on overexpression compared to the GST-tagged OmpA.

Stepwise dialysis involves the slow decrease in concentration of the urea used to initially solubilise the protein (Bagby *et al.*, 2001). The concentration is gradually decreased from 8 M to 0 M urea in 2 M increments (i.e. 8 M > 6 M > 4 M > 2 M > 0 M) every 4 hours so that the protein can reach an equilibrium at each urea concentration. The intermediate concentrations of urea theoretically will allow sequential refolding of the protein with the prevention of aggregates forming (Maeda *et al.*, 1995; Tsumoto *et al.*, 2010).

The addition of the charged amino acids, L-arginine and L-glutamate to the dialysis buffer was shown to increase solubility of various proteins up to 9-fold whilst increasing their stability long-term (Golovanov *et al.*, 2004). These amino acids were added to the dialysis buffer (140 mM PBS, pH 6), each at 50 mM to determine if they increase the solubility of the OmpA proteins during dialysis.

As it appears that proteins are more likely to aggregate at higher concentrations (Kiefhaber *et al.*, 1991; Philo and Arakawa, 2009; Lebendiker and Danieli, 2014), it was hypothesised that if the proteins were diluted in their elution fractions before dialysis, they would be less likely to aggregate. This was hypothesised much the same as a slower production of protein is expected to produce more soluble protein due to less protein aggregating when the temperature during *E. coli* overexpression was lower (Schein, 1989; Vasina, 1997). The protein was diluted 5-fold before dialysis to determine if this would increase solubility.

Medium-scale protein purification was carried out, growing 500 ml of *E. coli* (DE3) C41 + pET15-OmpA1 or –A2 per dialysis condition (6 conditions total). Cultures were grown to OD_{600} 0.6 – 0.8 before being cooled to room temperature, induced with 0.1 mM IPTG and grown for a further 16 h at ~24°C as this was shown to be a more optimal growth

temperature (as shown in Figure 4.5 previously). Purification of the overexpressed protein was carried out as previously described, with the insoluble protein being solubilised in 8 M urea (pH 6, away from the pI of either protein) and purified on Ni^{2+}-NTA resin in 150 mM imidazole. An example of the purification demonstrating the typical yield for this trial can be seen in Figure 4.10.

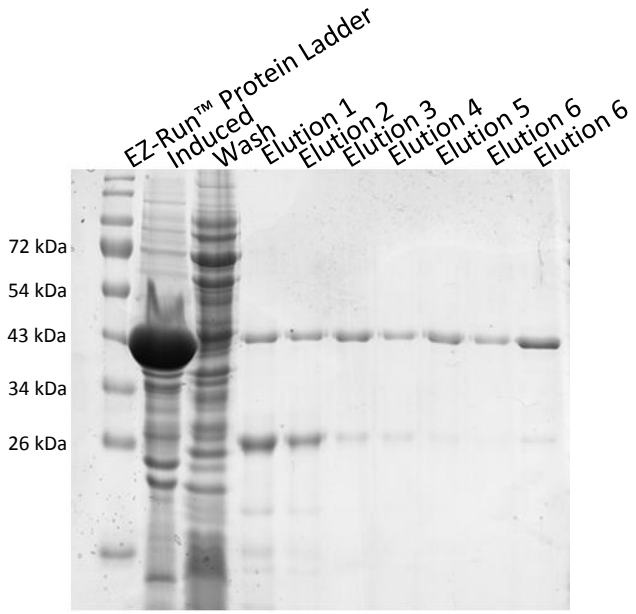

Figure 4.10 Purification profile of His-OmpA2. Protein was overexpressed and purified as described in Materials and Methods 2.7.1.1. Resin-bound protein was washed in 20 mM imidazole and protein then eluted in 200 mM imidazole. His-OmpA2 can be seen as the prominent bands at ~41 kDa. Bands are also observed ~26 kDa which are likely to be degraded protein.

Despite using protease inhibitors in the buffers used in the resuspension of the cell pellet and cell lysis, some protein degradation was observed, as seen in the band at ~26 kDa.

The elution fractions were pooled and dialysed using stepwise, addition of 50 mM L-arginine and L-glutamine and dilution of the elution fractions 5-fold, as described earlier in this section. Combinations of these were also trialled, i.e. the addition of L-arginine and L-glutamine coupled to stepwise dialysis and diluted elutions with stepwise dialysis. The gel images seen in Figure 4.11 demonstrate the success of the dialysis trial for both OmpA1 and OmpA2, as shown by the soluble (Supernatant or "S") and insoluble (Pellet or "P") fractions once the contents of the dialysis tubes have been centrifuged.

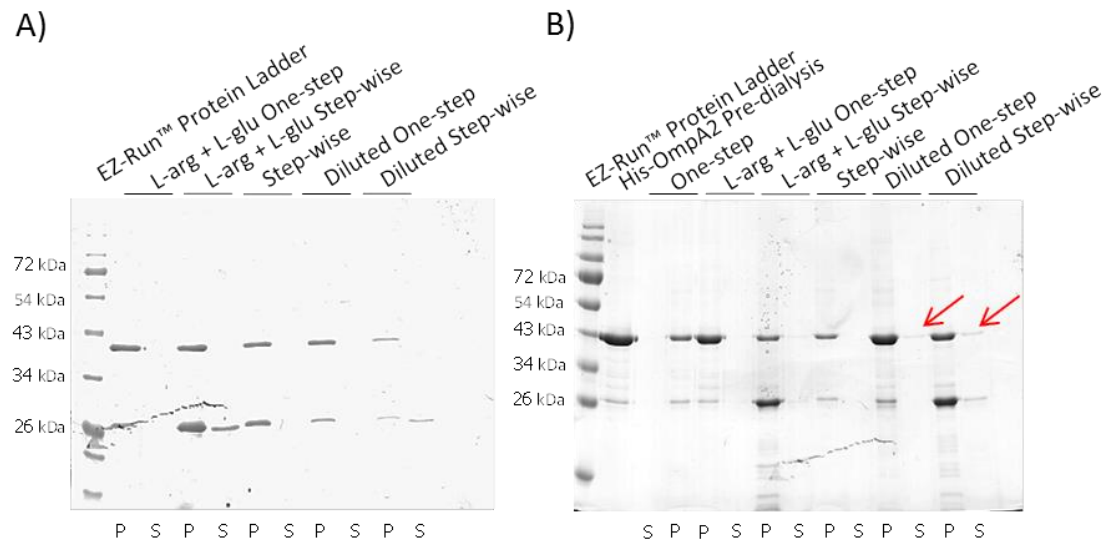

Figure 4.11 Dialysis trials of His-OmpA1 (A) and His-OmpA2 (B) protein after purification. Various dialysis conditions were used to increase protein solubility. After dialysis, the protein was removed from the dialysis tubing and centrifuged to separate soluble protein (S) from the precipitated protein (P). His-tagged protein appears as the band ~41 kDa, whereas degraded protein can be seen ~26 kDa. The SDS-PAGE image of OmpA2 dialysis (B) also includes a protein elution sample pre-dialysis for reference (His-OmpA2 Pre-dialysis). Red arrows indicate fractions containing soluble protein

The pellet (P) after centrifugation demonstrates the protein that has aggregated and precipitated during dialysis, becoming insoluble and therefore unusable for further experiments. In all conditions for OmpA1, no soluble protein was observed in the soluble fraction (S) in any of the five conditions after dialysis. In the case of OmpA2, extra lanes were used to show the soluble and insoluble fractions after dialysis when the samples from the original one-step dialysis were used (i.e. all urea was removed in one step), as well as the tested conditions. The addition of L-arginine and L-glutamine had no effect on increasing the solubility of the protein, with all the protein precipitating through dialysis, even when stepwise dialysis was employed. The only conditions that increased solubility during dialysis were the diluted protein coupled to stepwise and the diluted dialysis alone as seen in the soluble fractions in lanes “Diluted One-step” and “Diluted Step-wise” respectively, indicated by the red arrows. The concentrations of these two soluble fractions were analysed to determine if a viable amount of soluble protein could be produced for interaction studies, however in both cases a very low yield (< 50 µg / ml) of protein was measured, even after concentration using a Vivaspin® 6 column, thus making the overexpression and dialysis of OmpA1 and OmpA2 an impractical method for to study the

interaction of the OmpA protein with the host cell, and other methods were then researched.

4.3.5 OmpA Protein Structure Prediction

Due to the insoluble nature of the OmpA protein, a different approach to examining whether there exists an interaction with the host cell was undertaken using software protein structure modelling. Bioinformatic analysis using two different programmes, Phyre2 and RaptorX, both identified 8 N-terminal transmembrane β-sheets which were predicted to form a transmembrane β-barrel domain, alongside a C-terminal predicted peptidoglycan associated domain, as shown in Figure 4.12. Both programmes predicted similar structures, indicating the protein structure was correctly predicted.

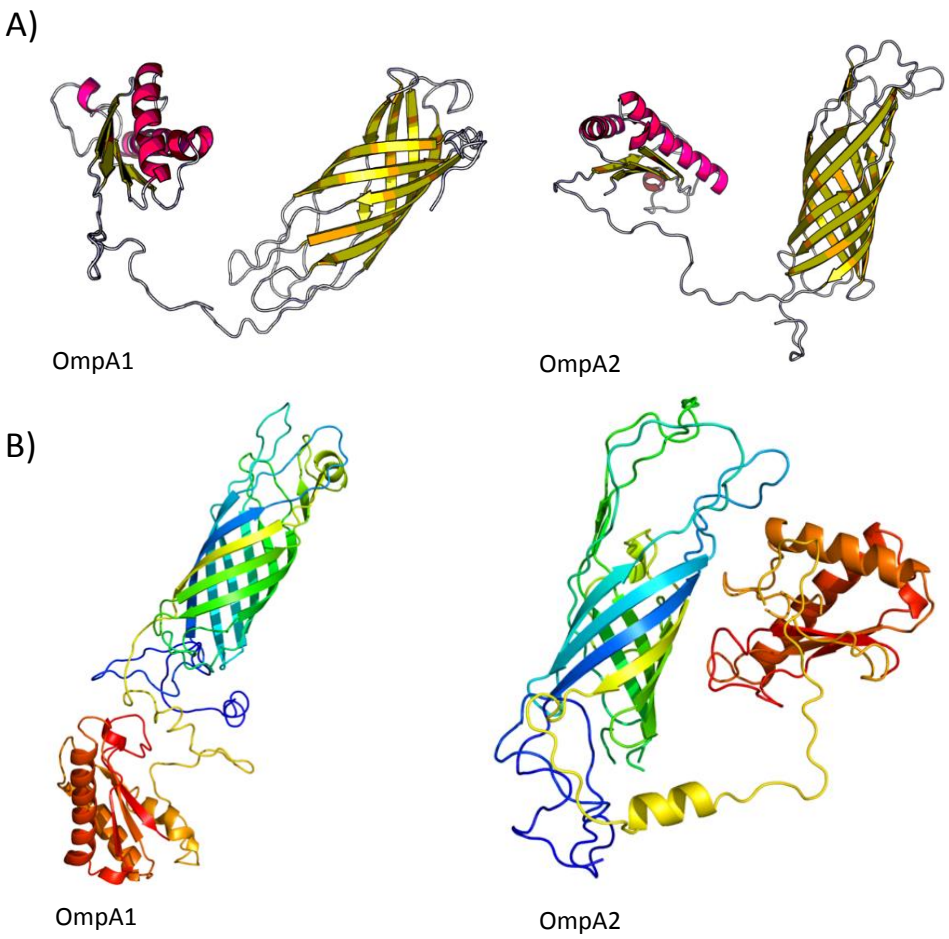

Figure 4.12 *In silico* analysis of OmpA1 and OmpA2 protein structure. The protein structure was predicted using RaptorX (A) and Phyre2 (B).

The predicted structure for *P. gingivalis* OmpA resembles high structural similarity to the OmpA protein of *E. coli* which also shows the classical two-domain structure of the N-terminal β-barrel and C-terminal peptidoglycan-associated globular domain (Bremer *et al.*, 1982; Koebnik *et al.*, 2000). The N-terminal sequence similarity of *P. gingivalis* and *E. coli* OmpA proteins is relatively low, when amino acid sequences are compared through Clustal Omega. However, a high homology is observed in the C-terminal peptidoglycan-associated domain, shown as the percentage identity matrix (% identity) in Table 4.1.

Table 4.1 OmpA sequence homology between *P. gingivalis* and *E. coli* in the N- and C-terminal domains

	OmpA1		OmpA2	
	N-terminal	C-terminal	N-terminal	C-terminal
Escherichia coli OmpA	26.95%	58.3%	29.7%	60.4%

% similarity generated through the Percentage Identity Matrix when comparing sequences through Clustal Omega.

4.3.6 Barrel Overexpression

A previous study by Martinez *et al.,* (2014) demonstrated increased solubility of the protein during overexpression if a truncated version using only the β-barrel domain was expressed for the OmpA of *Coxiella burnetii* (Martinez *et al.*, 2014). Due to the insolubility of the whole *P. gingivalis* OmpA protein, this hypothesis was employed in this study. A truncated version of OmpA1 and OmpA2 was produced, with primers to amplify the residues of $OmpA1_{21-245}$ and $OmpA2_{22-236}$ designed as shown in Table 2.11 and 2.12, and in Figure 4.13.

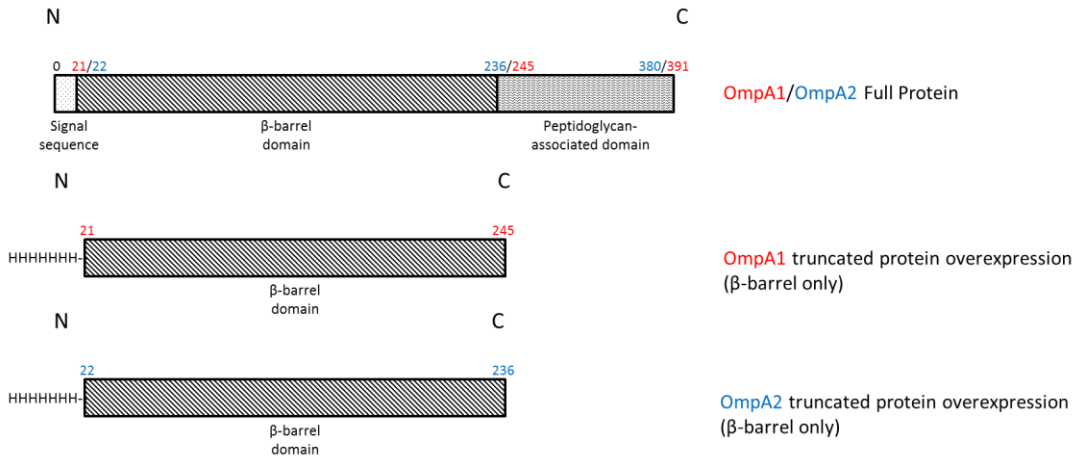

Figure 4.13 Schematic of full OmpA1 /A2 protein and truncated versions for recombinant protein overexpression of the β-barrel. Amino acid residue numbers indicate the location of each protein domain (signal sequence, β-barrel and PG-associated), with red indicated OmpA1 residue numbers and blue indicating OmpA2 residue numbers. Truncated β-barrel domains for recombinant protein overexpression are also shown with His-tag location for protein purification.

PCR reactions were carried out to amplify the truncated version of the *ompA1* and *ompA2* genes with *Bam*HI and *Nde*I restriction digest tails for cloning into pET15b for His-tagged expression. Successful PCRs were determined on a 1% Agarose gel, as shown in Figure 4.14A before the PCR constructs were digested using their respective enzymes, cleaned up and cloned into the pET15b plasmid according to Materials and Methods Section 2.6.2.6. Ligation reactions were transformed into *E. coli* DH5α strain and colonies incorporating the plasmid were selected using LB plates containing Ampicillin. Correct incorporation of the truncated gene insert into the plasmid was determined by using Bioline Plasmid Miniprep kits and enzyme digests (using the restriction enzymes used to cut the original PCR constructs), or using a PCR amplification with T7 primers that target the flanking regions around the cloning site and this amplify any inserts present. Agarose gel analysis was then used to determine the particular banding pattern of insert incorporation into the plasmid, as shown in Figure 4.14B and C

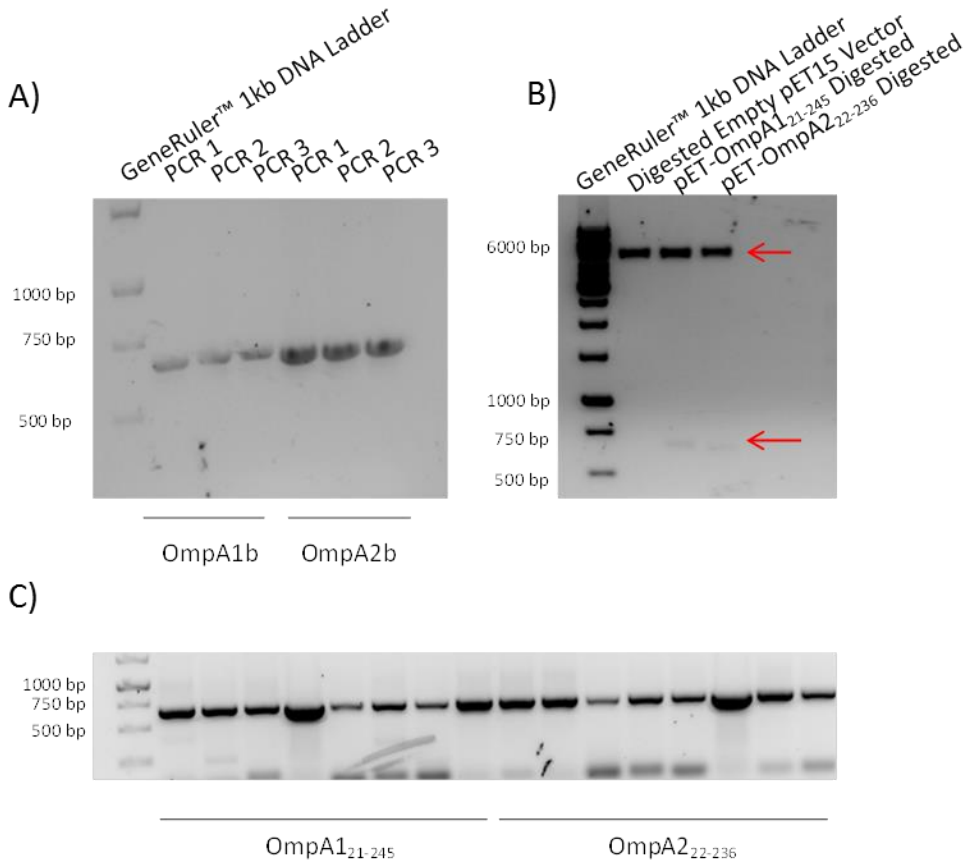

Figure 4.14 Cloning of truncated OmpA1$_{21-245}$ and OmpA2$_{22-236}$ into pET15 plasmid for His-tagged Expression. Three PCR reactions for the amplification of each protein insert were carried out (A), before ligation into *Bam*HI and *Nde*I-digested pET15b plasmid and transformed into *E. coli* DH5α. Colonies were examined for the incorporation of the pET-OmpA1$_{21-245}$ or –OmpA2$_{22-236}$ plasmid through isolation of the plasmid and restriction enzyme digestion (B) or PCR (C). Only two colonies had the plasmid extracted for restriction enzyme digest confirmation, and as indicated by the lower arrow both contained the insert. All colonies chosen for PCR were positive for the insert, as demonstrated by the band at ~650 bp, demonstrating successful incorporation of OmpA1 and OmpA2 into pET15b for overexpression.

Once a successful colony of *E. coli* DH5α was identified as containing the plasmid with the truncated *ompA1* or *ompA2* gene insert, the plasmid was isolated through a Bioline Plasmid Miniprep, sequenced and then transformed into DE3 C41, BL21 and BL21-Rosetta expression strains of *E. coli*. Overexpression of *E.coli* + pET15b was carried out under several conditions, initially different expression strains were tested to determine which strain would produce the highest yield of protein, as shown in Figure 4.15.

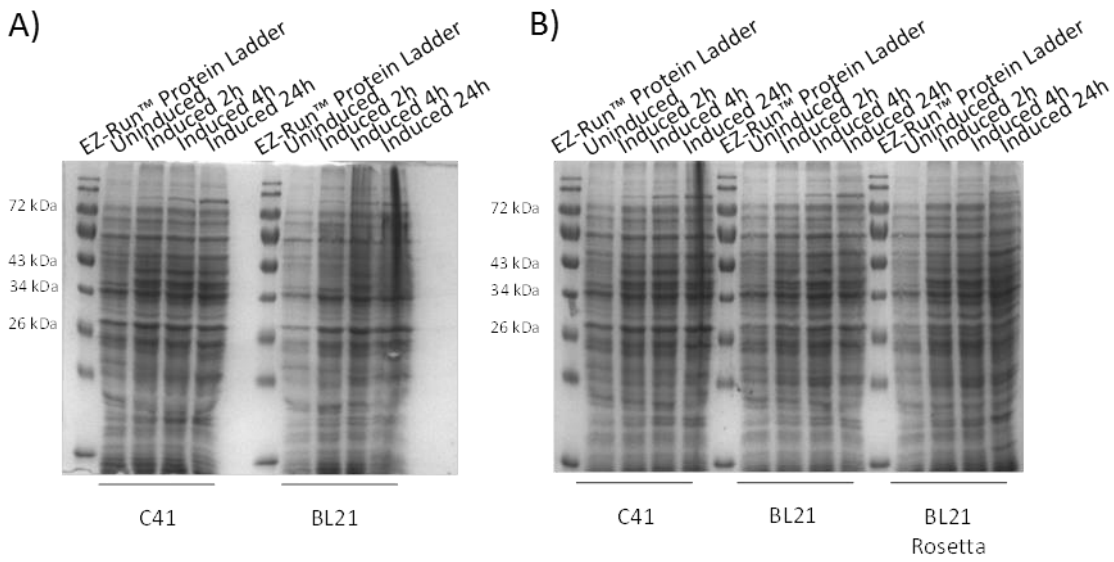

Figure 4.15 Overexpression of His-OmpA1$_{21\text{-}245}$ (A) and His-OmpA2$_{22\text{-}236}$ (B) in different expression strains. Expression of the truncated OmpA protein was carried out according to Chapter 2.7.1, and 1 ml aliquots were removed at 2 h, 4 h and 24 h post induction with 0.1 mM IPTG to determine expression levels of the protein. No expression of His-OmpA2$_{22\text{-}236}$ was observed in BL21 Rosetta strain (B) so this was not employed as an expression strain for His-OmpA1$_{21\text{-}245}$. Truncated OmpA1 and OmpA2 appear as the dominant band ~26 kDa.

Strain C41 was chosen as the expression strain as it produced a higher yield of protein. BL21 Rosetta was not used to determine OmpA1 overexpression as the growth was retarded in multiple attempts at overexpression; often taking up to 12 h to reach OD 0.6 (compared to 2-3 h for C41 and BL21) so was discarded as a strain option and not shown on the gel in Figure 4.15A. Once the expression strain was chosen, two different expression conditions were used to determine greatest yield, which were 37°C for 4 h post induction with 0.1 mM IPTG, and at 24°C for 16 h post induction with 0.1 mM IPTG, shown in Figure 4.16.

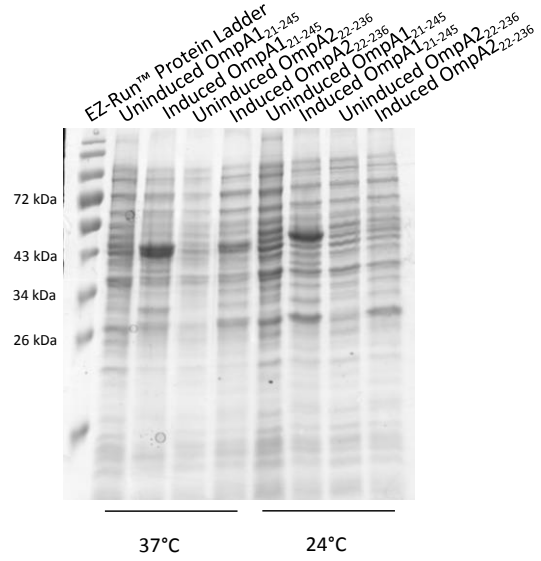

Figure 4.16 Overexpression of His-OmpA1$_{21-245}$ (A) and His-OmpA2$_{22-236}$ (B) at different induction temperatures. *E. coli* C41 expressing His-OmpA1$_{21-245}$ (A) and His-OmpA2$_{22-236}$ was grown to OD_{600} 0.6 before a sample was removed (Uninduced) and induced with 0.1 mM IPTG for 4 h at either 37°C or 24°C before a sample removed (Induced). Expression of the truncated OmpA proteins can be seen as the band at ~26 kDa.

Overexpression in strain DE3 C41 was trialled at both 24°C and 37°C, as shown in Figure 4.16, which shows only mild induction of the protein in both conditions, however for both OmpA1$_{21-245}$ and OmpA2$_{22-236}$, expression appeared to be increased at 24°C, so this temperature was chosen for overexpression of the β-barrel of both OmpA1 and OmpA2.

Expression of the OmpA1$_{21-245}$ and OmpA2$_{22-236}$ proteins was carried out at the conditions optimised, before the cells were lysed and purified via the His-tag as described in Materials and Methods, Section 2.7.1.2. The soluble fraction of the lysed cells was incubated with the Ni^{2+}-NTA resin for 4 h at 4°C and fractions of protein were eluted using imidazole, as demonstrated in Figure 4.17.

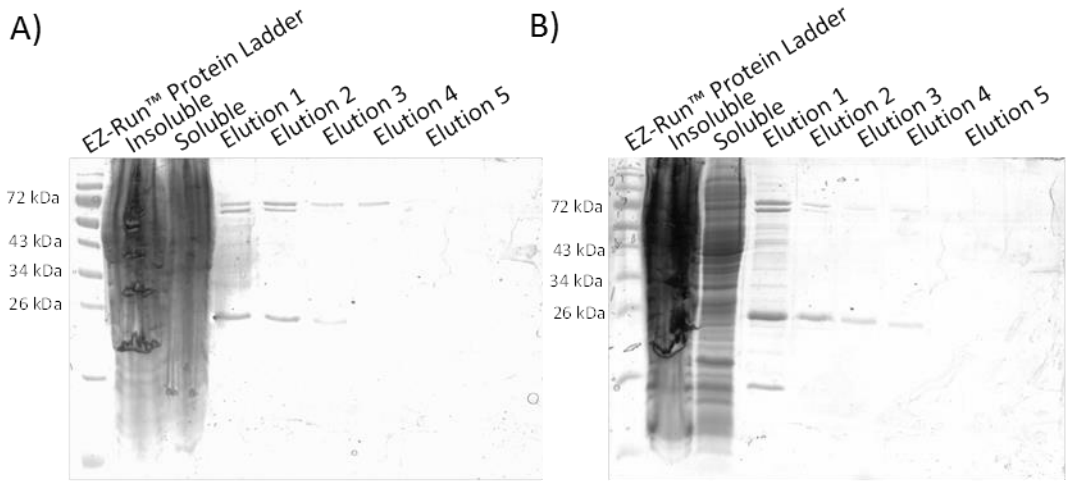

Figure 4.17 Purification of His-OmpA1$_{21-245}$ (A) and His-OmpA2$_{22-236}$ (B) protein. Truncated OmpA proteins were purified from Ni-NTA Resin as described in Chapter 2.7.1.2, using 200 mM imidazole in the elution buffer. His-OmpA1$_{21-245}$ and His-OmpA2$_{22-236}$ purified protein can be seen as the dominant bands at ~26 kDa. Bands of ~75 kDa also appear which is likely to be trimerised protein.

As previously seen with OmpA protein expression, multiple bands were observed in the elution fractions, despite using DTT to dissociate any protein dimers and trimers. As the protein size of the extra band was ~75 kDa, it was expected to be a trimer of the protein subunits. Dialysis of the protein again resulted in insolubility of the majority of the protein, as shown in Figure 4.18, including under step-down dialysis and after the protein had been diluted pre-dialysis. A small amount of protein remained soluble after step-wise dialysis, but when the concentration was determined using a BCA assay, the concentration was not high enough for any downstream assays (<30 µg / ml).

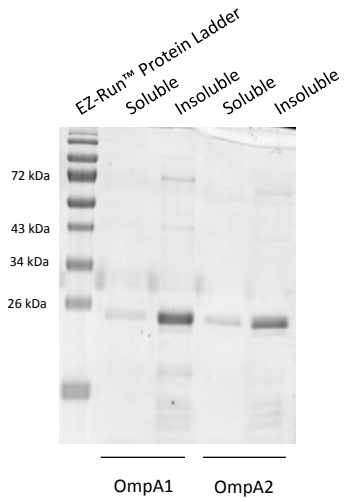

Figure 4.18 Dialysed His-OmpA1$_{21-245}$ and His-OmpA2$_{22-236}$ after purification. Truncated OmpA proteins were dialysed after purification using Step-down dialysis as described in Chapter 4.3.4. The contents of the dialysis tubing were centrifuged after dialysis to separate precipitated protein (insoluble) from the supernatant (soluble). Most of the truncated OmpA proteins precipitate, however some soluble protein remains, as seen at ~26 kDa.

4.3.7 Identification of Extracellular Protein Loops of OmpA2

Due to the insolubility of the protein in both full and truncated forms, more information was determined from the structure to allow the study of OmpA-host interactions. As the results from Chapter 3 indicated clearly that OmpA2 displayed the largest influence on cell interaction within the *P. gingivalis* OmpA protein (as shown by a reduction in adherence and a significant loss of invasion displayed by the Δ*ompA2* mutant but not seen in the Δ*ompA1* mutant) further interaction studies with the host were decided to only involve the OmpA2 protein subunit.

The predicted structure of OmpA2 identified loops exposed between β-sheet strands, as shown schematically in the truncated version of the OmpA2 in Figure 4.19. Due to the orientation of the protein predicted using TMPRED, these loops would appear extracellularly and exposed on the surface of the protein. Previous studies in various Gram-negative bacteria indicate these surface-exposed loops to be involved in a variety of functions, such as the extracellular loops of the OmpA-like proteins found in *Neisseria gonorrhoeae* and *Coxiella burnettii* have been shown to be involved in host cell interaction (Serino *et al.*, 2007; Martinez *et al.*, 2014), whereas the extracellular loops of *E. coli* OmpA act as a phage docking receptor (Koebnik, 1999). It was therefore hypothesised that these

protein loops might be involved or even sufficient for any interaction with human cells, as these loops would be the section of the protein that was exposed and potentially able to interact with the host.

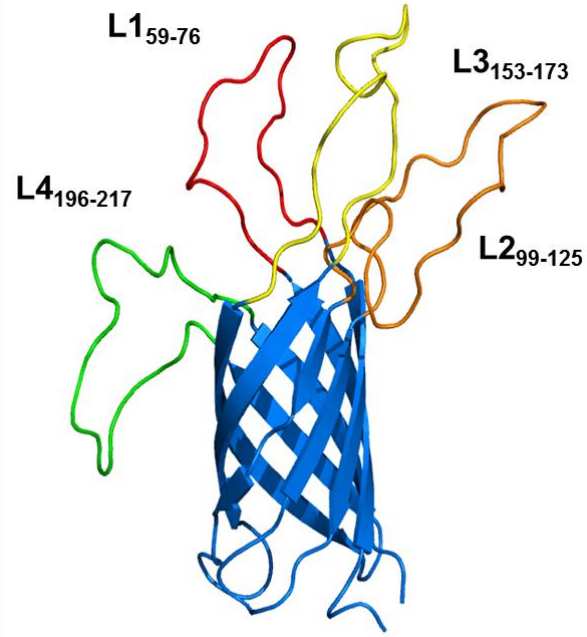

Figure 4.19 *In silico* analysis of the OmpA2 protein and identification of extracellular loops. Structural modelling of OmpA2 identified four extracellular loops between β-sheets, shown here as L1-L4 with the location in the protein sequence denoted by the subscript numbers. N-terminal α-helix and C-terminal peptidoglycan associated domain have been removed for display purposes here.

As the OmpA protein from *E. coli* is the most understood of the OmpA-family proteins, most OmpA proteins discovered are compared in their similarity to the *E. coli* OmpA, as has been done for *P. gingivalis* OmpA here. However, using an intensive search through Phyre2, the bioinformatic analysis of the structure of *P. gingivalis* OmpA demonstrates the OmpA-like protein with the highest homology comes from *Klebsiella pneumoniae*. The OmpA of *K. pneumoniae* confers resistance to antimicrobials (Llobet *et al.*, 2009), potentially after interaction with the extracellular loops, due to their external location, although this has not been shown experimentally. The structure of the β-barrel of OmpA is generally found to be highly conserved across many species, whereas the sequence and size of the extracellular loops are highly variable and more suited to the function of the protein (Pautsch and Schulz, 1998; Schulz, 2002). Sequence alignment of the two OmpA subunits of *P. gingivalis* and the OmpA protein of *K. pneumoniae* demonstrate this, with little sequence similarity

between the two but with the location of the β-sheets and extracellular regions matching well between the sequences of *K. pneumoniae* and OmpA2 but less so with OmpA1 as highlighted by the black arrows (β-sheets) and green bars (extracellular loop regions) (Figure 4.20).

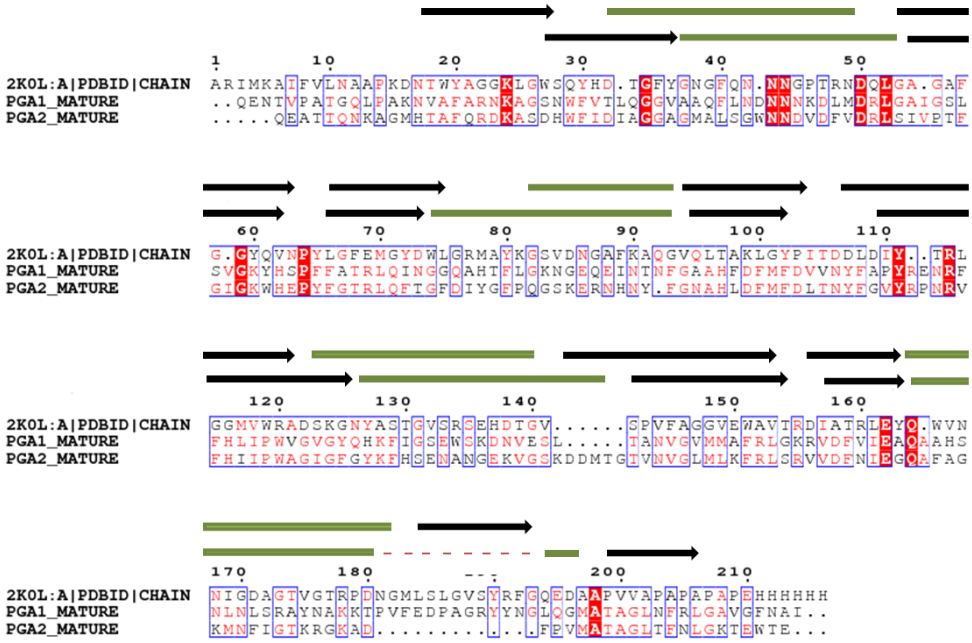

Figure 4.20 Bioinformatic analysis of *P. gingivalis* OmpA structure. The OmpA2 (PGA2_MATURE) subunit β-sheets and extracellular loops location in the sequence compared to the closest structural match, *K. pneumoniae* OmpA (2K0L:A). Black arrows indicate the β-sheet location, whilst green indicates the extracellular loops. The top line of arrows indicates *K. pneumoniae* OmpA features, whilst the lower line represents *P. gingivalis* OmpA2 features. OmpA1 (PGA1) features are not displayed, but the sequence is included to demonstrate the sequence similarities and differences between OmpA1 and OmpA2 subunits. The C-terminal domain (residues 215-391 (A1) or 214 – 380 (A2)) has been removed from these sequences for clarity.

The sequences of the predicted extracellular loops from *P. gingivalis* OmpA2 were extracted from the sequence and labelled L1, L2, L3 and L4 (Table 4.2), and then commercially purchased from CovalAb (Cambridge, UK), with a Biotin tag for downstream applications. The biotin moiety was chosen for the tag as it is a small molecule, which would reduce any significant interference in any peptide-cell interactions, and has a very high specificity for its avidin molecule. This would give the potential to immobilise these peptides via the biotin tag should any interaction occur. Only the extracellular loops from

the OmpA2 subunit were purchased alongside a scrambled peptide, which was designed to be a complete scramble of peptide 4, i.e. overall contained the same amino acids but none in the same position and the distribution of charged amino acids was changed to ensure a complete sequence alteration.

Table 4.2 Sequence of extracellular loops of the OmpA2 protein

	Sequence
Peptide 1 (L1)	GMALSGWNNDVDFVDRLS
Peptide 2 (L2)	GFDIYGFPQGSKERNHNYFGNAHLDFM
Peptide 3 (L3)	YKFHSENANGEKVGSKDDMTG
Peptide 4 (L4)	QAFAGKMNFIGTKRGKADFPVM
Scrambled	RINFMAGMPGFADTVGKAKQKF

A Biotin tag was added to the N-terminal end of the peptide. The names “peptide” and “loop (L)” are used interchangeably throughout.

4.3.8 Analysis of the Extracellular Loops of *P. gingivalis* OmpA2 Interactions with Oral Epithelial Cells

Due to the effect on invasion and adhesion shown by the deletion of the *ompA2* gene, and the difficulties determined in overexpressing the OmpA2 protein, the purchased peptides were used in place of overexpressed protein to investigate the molecular basis of interaction between OmpA2 and human oral epithelial cells. An initial modified standard antibiotic protection assay was established, which involved carrying out a normal standard antibiotic protection assay as described in 2.8.1, but with the addition a pre-incubation step of the OK-F6 cell monolayer with each peptide individually (at a concentration of 50 µg/ml) for 60 min (post 2% BSA incubation and washing), before peptides were washed off and the cell monolayer was incubated with wild type *P. gingivalis* for 90 min and then the cells processed as usual. Results can be seen in Figure 4.21.

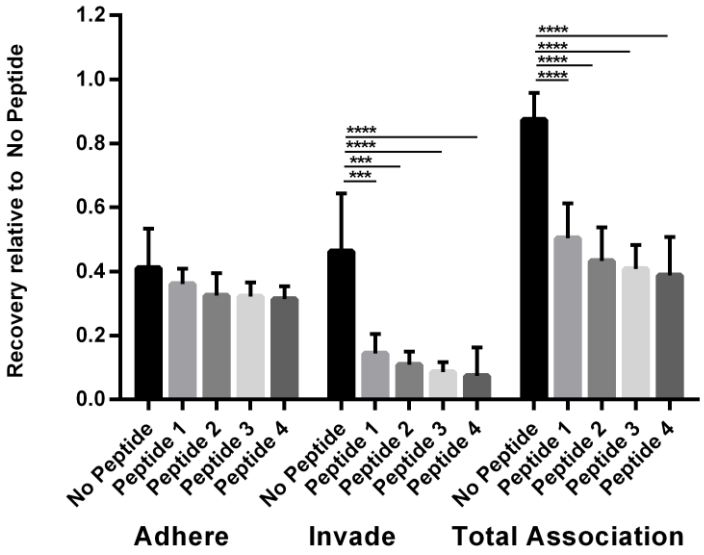

Figure 4.21 Effect of a pre-incubation of OmpA2 extracellular loops on adherence and invasion of wild type *P. gingivalis*. The OK-F6 cells were pre-incubated with 50 µg / ml individual peptides (1 h), before removal and application of wild-type *P. gingivalis* (MOI 1:100) and the standard antibiotic protection assay carried out as detailed in Chapter 2.8.2. Total association refers to all bacteria adhered to and invaded the OK-F6 cells, whereas invade refers to the number of internalised bacteria post incubation with 200 µg / ml metronidazole to kill external adhered bacteria. The effect of peptides on adherence and invasion was determined relative to no peptide, and statistical significance was accepted if $p < 0.05$. Antibiotic protection assays were carried out in triplicate, with 3 counts per technical repeat observed (overall n = 27). Error bars represent ± SEM. *** $p < 0.001$, **** $p < 0.0001$, determined by 2way-ANOVA.

The invasion of wild-type *P. gingivalis* into the host cell monolayer was significantly reduced (between 3.2- and 6.5-fold) in the presence of the peptides ($p < 0.005$ peptides 1 and 2, $p < 0.001$ peptides 3 and 4), indicating that the peptides of OmpA2 are interfering with the ability of *P. gingivalis* to invade the host. The adherence of the bacteria to the host was not significantly reduced for any of the peptides, potentially indicating that the peptides do not hinder the binding of the bacteria. This almost opposing result to what was expected could be due to two factors, the first being that the *P. gingivalis* are utilising two different pathways in adherence and invasion of the host, and the peptides are only interfering with the pathway involved in the invasion, or potentially more likely, because the peptides are only applied briefly and then removed before the bacteria were added, the host cell receptors could be processing the peptides causing protein turnover and removal of the peptide from the receptor allowing the bacteria to bind. As this process would take time,

the delay in access to the host cell receptor would cause a decrease in the number of bacteria that were internalised in the 90 min time frame. This hypothesis was tested by a second modification of the standard antibiotic protection assay, by the addition of individual peptides (50 µg/ml) to the 90 min bacterial incubation step as well as the pre-incubation step as used for Figure 4.21 to prevent peptide turnover once they had been removed. Incubation with OmpA2 extracellular loops throughout the standard antibiotic protection assay significantly decreased the ability of wild type *P. gingivalis* to adhere to and invade the oral epithelial cells, as shown in Figure 4.22.

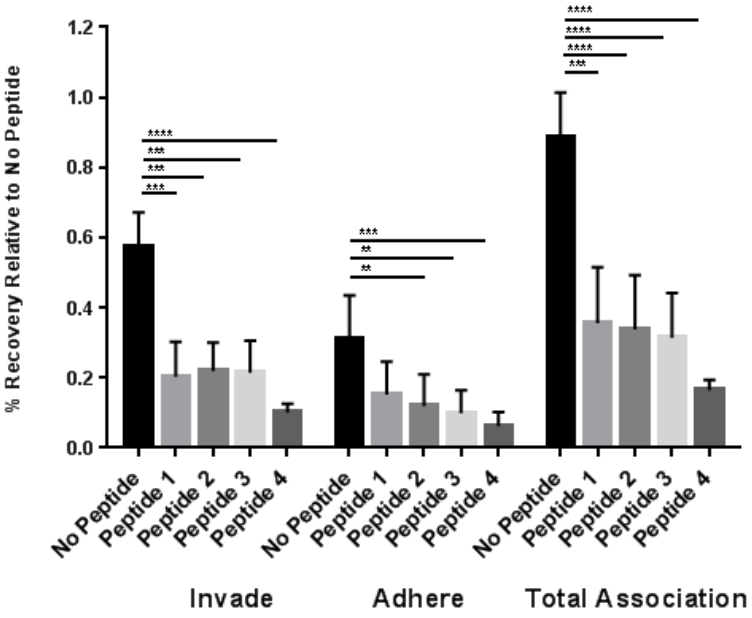

Figure 4.22 Effect of the presence of extracellular loops throughout the standard antibiotic protection assay. Individual peptides (50 µg/ml) were pre-incubated with the OK-F6 cells for 1 h, before cells washed and the peptides applied again individually (50 µg/ml) with the wild type *P. gingivalis* (MOI 1:100), and the standard antibiotic protection assay carried out as previously detailed in Chapter 2.8.2. The effect of peptides on adherence and invasion was determined relative to no peptide, and statistical significance was accepted if $p < 0.05$. Antibiotic protection assays were carried out in triplicate, with 3 counts per technical repeat observed (overall n = 27). Error bars represent ± SEM. ** $p < 0.01$ *** $p < 0.001$, **** $p < 0.0001$, determined by 2way-ANOVA

The presence of peptides 1-4 caused a significant reduction the wild-type *P. gingivalis* adherence (between 2.7 - 5.7-fold) and invasion (between 2 – 4.9-fold) of the host cell when applied individually. Peptide 4, with sequence QAFAGKMNFIGTKRGKADFPVM,

demonstrated the greatest effect in disrupting wild-type *P. gingivalis* adhesion and invasion, with a 5-fold reduction ($p < 0.001$).

Incubation with all four extracellular loops simultaneously was also examined, whereby the total concentration of peptides was 50 µg / ml (i.e. 12.5 µg/ml each peptide), which had no effect on the ability of wild-type *P. gingivalis* to adhere and invade the oral epithelial cells (Figure 4.23), suggesting the effect was dependant on a higher concentration of each individual peptide.

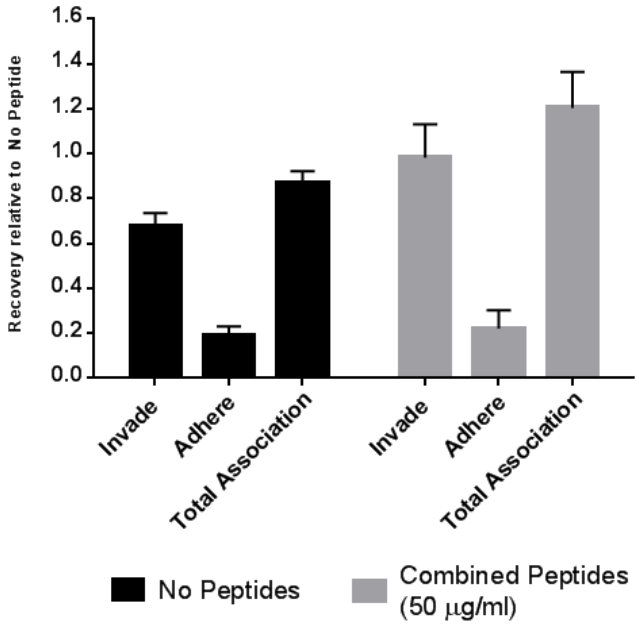

Figure 4.23 Standard antibiotic protection assay in the presence of combined peptides. Peptides were combined to 50 µg/ml total concentration, and were pre-incubated with the OK-F6 cells for 1 h, before cells washed and the peptides applied again (50 µg/ml total) with the wild type *P. gingivalis* (MOI 1:100), and the standard antibiotic protection assay carried out as previously detailed in Chapter 2.8.2. The effect of peptides on adherence and invasion was determined relative to no peptide. No statistical significance was observed in the levels of invasion, adherence or total association in the presence of the peptides. Antibiotic protection assays were carried out in triplicate, with 3 counts per technical repeat observed (overall n = 27). Error bars represent ±SEM.

As peptide 4 had the greatest effect on the adherence and invasion of the host, this peptide was used in comparison to the scrambled peptide to determine if the interaction with the host cell receptors was specific or just due to the presence of non-specific binding of the peptide or biotin moiety. The standard antibiotic protection assay was carried as out

previously described as used for the invasion in the presence of peptides and the results can be seen in Figure 4.24. No significant difference in adherence and invasion of the oral epithelial cells was observed between no peptide controls (with 2% BSA) and the scrambled peptide, whereas a significant decrease of at least 2-fold was observed in the ability of wild-type *P. gingivalis* to adhere and invade when peptide 4 was included, against both no peptide and the scrambled peptide. As the scrambled peptide was also designed with a Biotin-tag, this eliminates the idea that it is the Biotin moiety binding the host as no difference in adhesion or invasion in the presence of the scrambled peptide was observed. As no difference was seen in the scrambled peptide in comparison to the addition of no peptide, this also demonstrates that the binding and interruption of adhesion and invasion of wild-type *P. gingivalis* seen in the addition of peptide 4 is a specific and direct interaction of peptide 4 with the host.

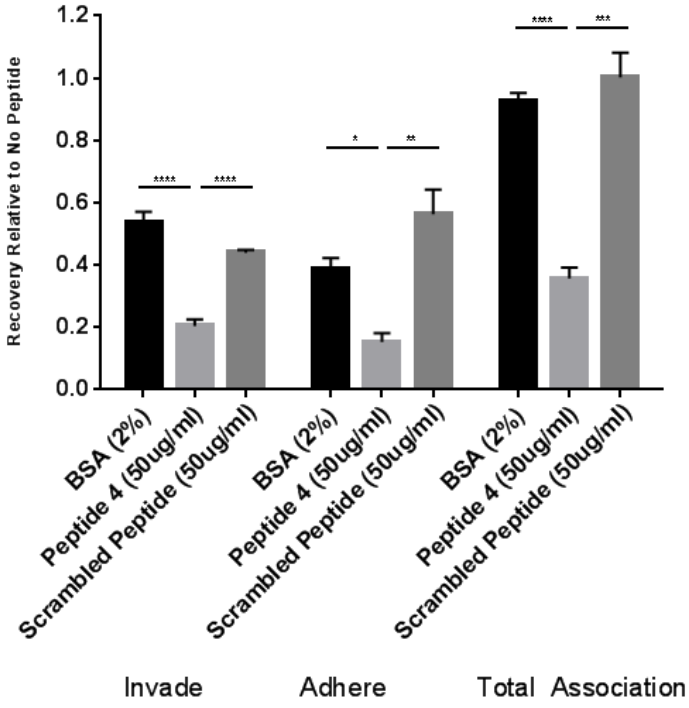

Figure 4.24 Comparison of peptide 4 and scrambled peptide on adherence and invasion of oral epithelial cells. Peptides were included in both the pre-incubation step and incubation with wild-type *P. gingivalis* as described in Figure 4.22. The effect of peptides on adherence and invasion was determined relative to a pre-incubation with 2% BSA and no peptide, and statistical significance was accepted if $p < 0.05$. No significant difference was observed between no peptide and the scrambled peptide, whereas a significant reduction in adherence and invasion was observed for peptide 4 against both no peptide and the scrambled peptide. Antibiotic protection assays were carried out in triplicate, with 3 counts

per technical repeat observed (overall n = 27). Error bars represent ± SEM. * $p < 0.05$ ** $p < 0.01$ *** $p < 0.001$, **** $p < 0.0001$, determined by one-way ANOVA

To ensure the effect of reduced invasion and adherence in the presence of the peptides was due to the peptide itself engaging the host receptors, not due to the peptide causing detrimental effects on the bacteria and the host, the viabilities throughout the assay were determined for both the OK-F6 cells and the *P. gingivalis* bacteria. In the presence of the highest concentrations of each peptide (50 μg/ml), no significant change in the viability can be seen in either the oral epithelial cells or the bacteria, confirming that the results observed are due to the action of the peptide.

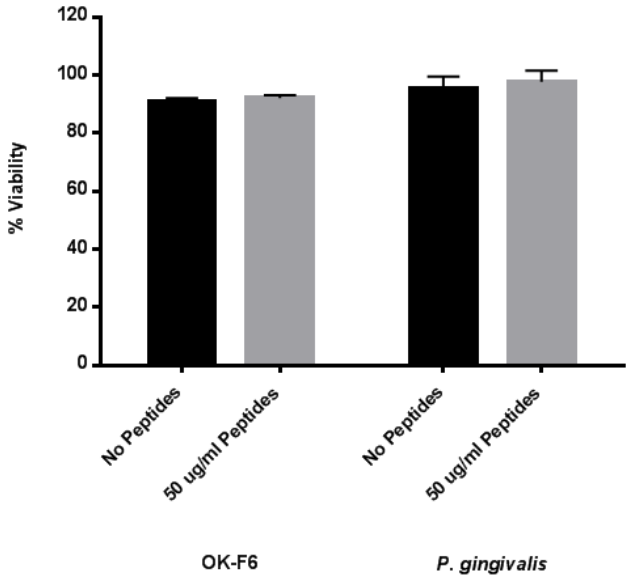

Figure 4.25 Viability of OK-F6 and *P. gingivalis* in the presence of the peptides. Peptides were applied to OK-F6 cells and *P. gingivalis* cells in the conditions that would be found during the standard antibiotic protection assay. Viability of OK-F6 cells was determined by recovering the cells and determining the number of live and dead cells stained with Trypan blue and the percentage viable cells calculated. The viability of *P. gingivalis* in the presence of peptides was determined by calculating the CFUs recovered after incubation with the peptide for the duration of the standard antibiotic protection assay and compared to the starting CFU count. No significant difference was observed between no peptides and the inclusion of peptides (n=3).

4.3.9 Peptide-Coating of Microspheres Directs Interaction with Oral Epithelial Cells

To further examine the host-cell interaction with the OmpA2 protein extracellular loops, the ability of the peptides to direct interaction of fluorescent inert latex beads with oral epithelial cells was determined. Yellow-green fluorescent microspheres which were coated in NeutrAvidin® for binding of the Biotin tag on the peptide were purchased from Life Technologies. The particular size of 1 µm was chosen for the microsphere size as this resembles the native size of *P. gingivalis* so the adherence of any microsphere via the OmpA2 peptides would partially mimic the adherence of a bacterium. Peptide-coated microspheres were then incubated with a monolayer of oral epithelial cells in a 96-well MTP and then washed thoroughly to remove any unbound microspheres and the fluorescence was read directly. BSA-coated microspheres were also included as a negative control for non-specific adherence as well as a scrambled peptide-coated microsphere, as shown in Figure 4.26.

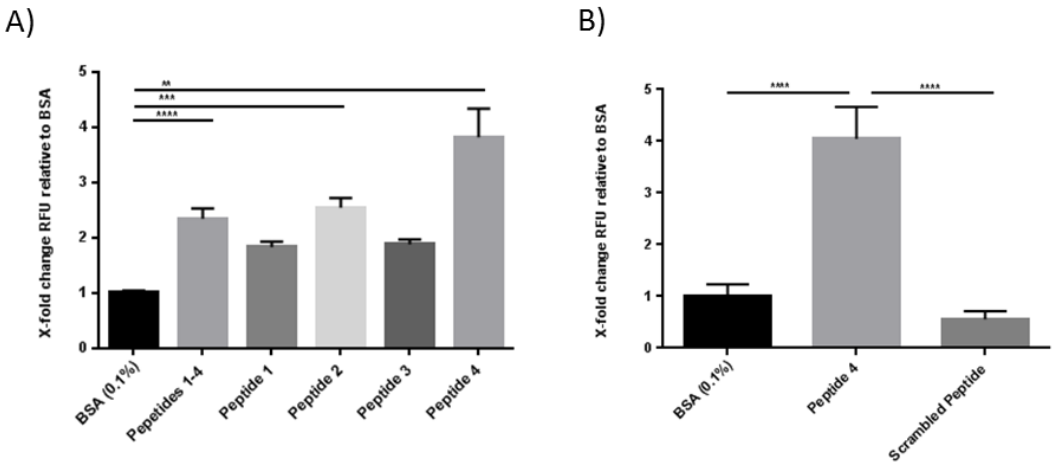

Figure 4.26 Fluorescence determination of peptide-coated Microspheres bound to OK-F6 cells. Microspheres coated in OmpA2 extracellular loop peptides were applied to monolayers of OK-F6 cells at a MOI of 1:100 and incubated at 37°C for 4 h before washing and the fluorescence levels determined. Increased fluorescence denotes the binding of the peptides to the oral epithelial cell monolayer, relative to the BSA-coated microsphere control. The scrambled peptide-coated microspheres were also examined as a control. Fluorescence was measured as the average of three biological repeats (of which had 3 technical repeats), with Error bars representing ± SEM. Statistical significance was accepted if $p < 0.05$. * $p < 0.05$ ** $p < 0.01$ *** $p < 0.001$, **** $p < 0.0001$, determined by One-way ANOVA.

All peptides demonstrate a clear increase the binding of the microspheres to the host cell, suggesting that a direct interaction between the extracellular loops of the OmpA2 protein and the oral epithelial cells. This increase in fluorescence was between 1.8- and 3.8- fold, with significance for peptide 2 ($p < 0.001$) and peptide 4 ($p < 0.01$) only. Similar to the modified standard antibiotic protection assays with the included peptide steps, peptide 4 shows the greatest effect. Interestingly, although no effect for combined peptides was observed when used in the standard antibiotic protection assays, an increase in binding to host cells was observed in this assay, with an increase in fluorescence of 2.3-fold ($p < 0.0001$). As peptide 4 showed the greatest increase in fluorescence, and therefore the greatest increase in host-cell interaction, the scrambled version (RINFMAGMPGFADTVGKAKQKF) of peptide 4 was used to determine if the binding of the extracellular loops to the host was specific. When compared to peptide 4, the scrambled peptide showed an 8-fold lower detection in fluorescence, and a 2-fold decrease in fluorescence when compared to the BSA-coated microspheres (Figure 4.26B), suggesting the interaction of peptide 4 with the host cell is specific to the sequence.

4.3.10 Immunofluorescence of OmpA2 Extracellular Loops Interaction with Oral Epithelial cells

As peptide 4 had shown the greatest effect in binding to the host both in interruption of wild-type *P. gingivalis* binding coupled to an increase in fluorescence when binding to a monolayer of host cells, immunofluorescence studies were undertaken to determine any direct binding of the peptide 4-coated beads to the host cell. To visualise the binding of the peptide-coated microspheres to the host epithelial cell, a monolayer of cells was seeded onto coverslips in a 24-well MTP. Peptide-coated microspheres were incubated with the cells before thorough washing to remove any unbound microspheres. The cells and any adhered beads were fixed with paraformaldehyde and cell membranes stained using WGA-Texas Red® conjugated fluorescent antibody. Figure 4.27 demonstrates an increased binding of peptide 4-coated microspheres to the cells.

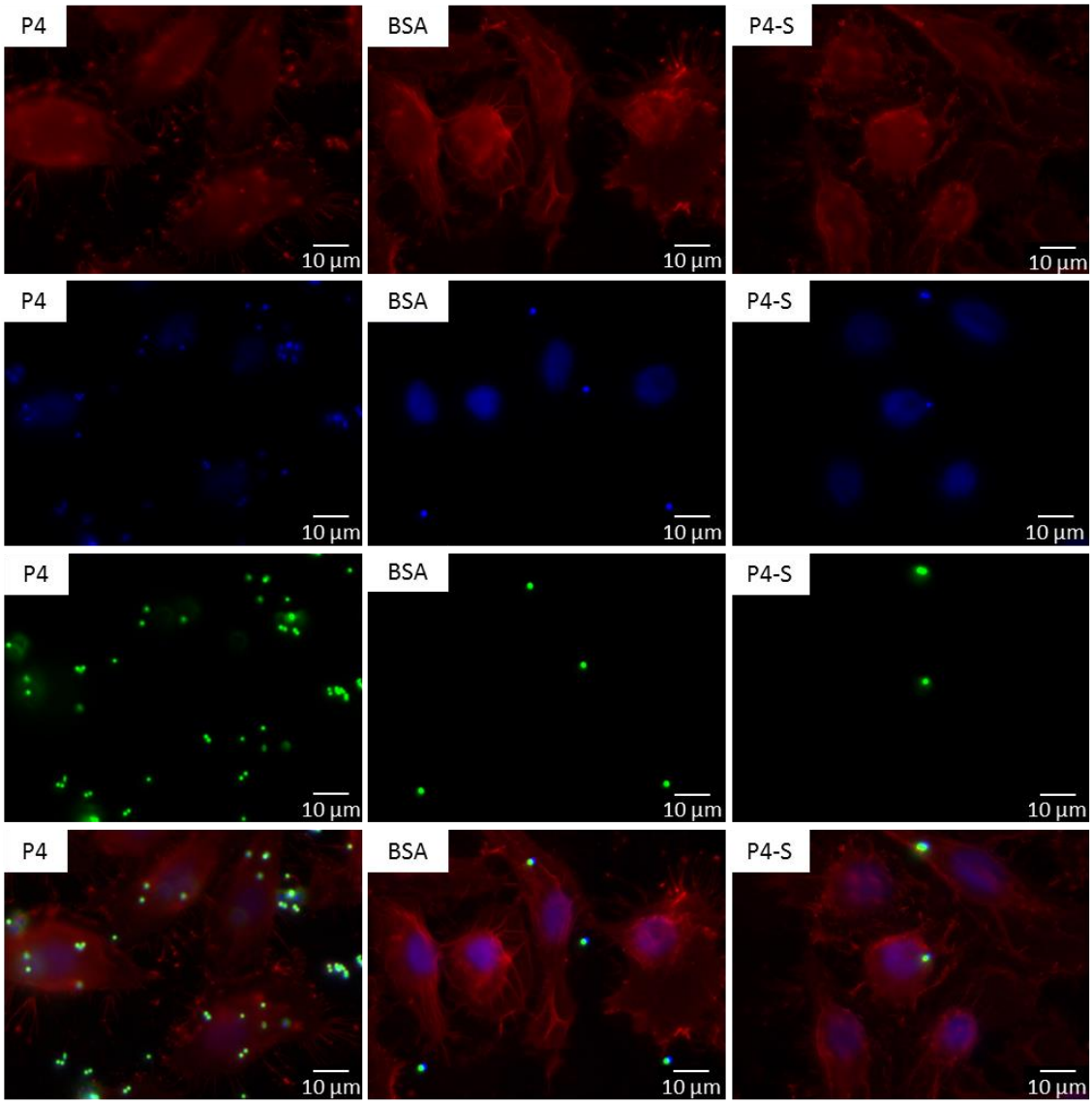

Figure 4.27 Immunofluorescence imaging of peptide-bound microspheres interaction with oral epithelial cells. Peptide 4-bound microspheres were examined for interaction (P4), compared to BSA-coated (BSA) and scrambled peptide-coated (P4-S) microsphere controls. AlexaFluor® 488 (green) shows peptide-bound Microspheres, WGA-Texas Red® (red) shows cell membranes and DAPI (blue) shows cell nuclei. Scale bars are indicated in the lower right hand corner.

These images show clearly a significant increase in the number of microspheres bound to the host cell when coated in peptide 4 compared to BSA and scrambled peptide bound microspheres. This indicates that the peptide 4 is sufficient to allow direct binding of the microsphere to the host, and therefore suggests the OmpA2 protein is sufficient at binding to the host directly. When the number of microspheres bound to the host in each condition is determined, there is an increase of 6-fold with the microspheres coated in peptide 4,

compared to BSA-coated microspheres (Figure 4.28). An even greater increase is observed compared to scrambled peptide-coated microspheres, in compliance with the fluorescence data already observed.

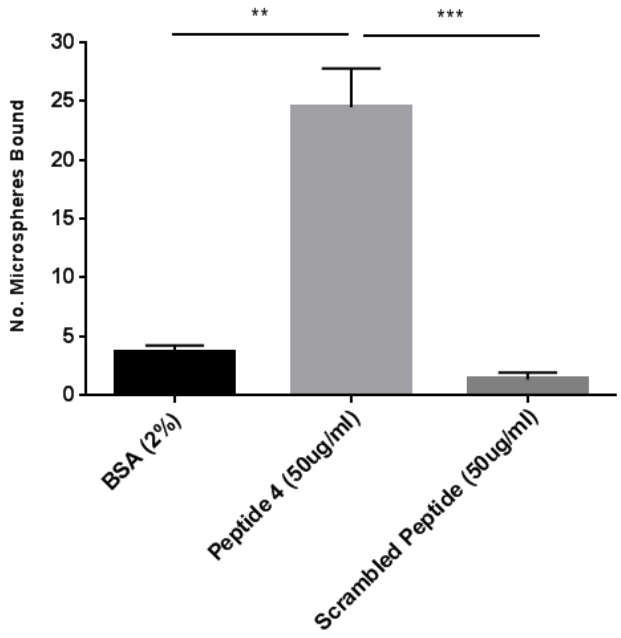

Figure 4.28 Enumerated peptide-coated microspheres interaction with OK-F6 cells. The number of microspheres bound to OK-F6 cells was calculated as the average from images from three technical repeats. Error bars represent ±SEM, and statistical significance was accepted if $p < 0.05$. ** $p < 0.01$ *** $p < 0.005$, determined by students' *t*-test

These data suggest that all four extracellular loops of OmpA2 are sufficient for host-cell interaction, and particularly peptide 4 is capable of directing binding of inert molecules to the host cell. Together, this suggests that there is a direct interaction between the OmpA2 extracellular loops and molecules found on the surface of the human oral epithelial cells.

4.4 Discussion

As outlined in section 4.1, OmpA is an integral outer membrane protein, predicted to be found on all Gram-negative bacterial membranes (Beher *et al.*, 1980). The OmpA protein has the predicted structure of a conserved N-terminal β-barrel, displaying extracellular loops between each β-sheet, and a C-terminal peptidoglycan-associated domain (Schulz, 2000). Large variations are observed in the extracellular loops (Pautsch and Schulz, 1998), however the β-barrel appears conserved, indicating strong selection pressure (Wang,

2002). This chapter has investigated the role of *P. gingivalis* OmpA in its interaction with the host, and in particular, the role of the extracellular surface loops in this interaction.

To characterise the relationship between the OmpA protein and its biological function, one of the fundamental steps is the purification of the protein. The standard method of protein purification relies on overexpression of the protein, lysis of the expression cells, binding the protein to a matrix, washing the matrix and finally elution of the protein. Many variables exist within these basic steps to increase the purity and yield of the protein, and were explored in depth in this chapter to attempt to purify pure and soluble OmpA protein.

Initially, recombinant OmpA was overexpressed using a polyhistidine-tag for purification. The His-tag is one of the most widely used affinity tags, allowing one-step purification of the protein through immobilised metal-ion affinity chromatography (IMAC) (Hage, 1999). The imidazole side chain of the histidine amino acids have a high affinity for the immobilised chelated metals (Ni^{2+}) on a nitrilotriatic acid (NTA) ligand support (Porath, 1992), which immobilises the protein on the Ni^{2+}-NTA resin where it can be recovered to a high level of purity using an imidazole eluent. The use of a His-tag for purification was initially chosen as it is a small tag that can be used under native and denaturing conditions (Porath, 1992) and although the idea cannot be completely excluded, the His tag is unlikely to interfere with the protein activity and therefore does not need to be removed for downstream applications (Terpe, 2006). The gene encoding OmpA1 and OmpA2 protein was provided already in a plasmid that would produce a His-tagged protein upon expression, and the OmpA1 and OmpA2 protein were successfully expressed to a very high yield, as seen within Figure 4.1. However, due to the high concentrations of protein produced during overexpression in *E. coli* coupled to the unfavourable conditions in the cytoplasm, hydrophobic proteins (e.g. the β-barrel of the OmpA protein) often partially fold before aggregating in dimers and multimers (Hong Lu *et al.*, 2001). This lead to the overexpressed OmpA protein forming inclusion bodies and therefore produced insoluble protein. It was possible to recover the insoluble OmpA protein through solubilisation of pellet using high concentrations of urea; however solubilisation of the protein leads to the need of dialysis to remove the solubilising reagent. Dialysis of the OmpA1 and OmpA2 protein lead to further protein aggregation and precipitation, which resulted in an unfolded and inactive protein which was therefore redundant for any downstream interaction studies.

Other purification protein tags can be employed to increase the solubility of the protein, such as fusion to glutathione-S-transferase (GST) or maltose-binding protein (MBP) (Lichty *et al.,* 2005; Nilsson *et al.*, 1997). Such fusion tags are popular as they act both to increase the solubility of the recombinant protein as well as acting as an affinity tag to allow one-step purification (Frangioni and Neel, 1993). This is beneficial over other fusion tags such as thioredoxin (TRX) or ubiquitin (Ub) which require an additional affinity tag for purification of the protein (Marblestone *et al.*, 2006). As the study by Marblestone *et al* (2006) demonstrated little difference in increased solubility between one-step purification fusion tags (MBP and GST), GST was chosen for fusion to the OmpA1 and –A2 protein for purification. GST is a 26 kDa protein originating from *Schistosoma japonicum*, first described by Smith *et al* (1986) and then subsequently inserted into a pGEX-vector for use as a recombinant protein affinity tag (Smith *et al.*, 1986; Smith and Johnson, 1988). The GST tag is not only useful for easy detection of the protein in downstream studies, but it can help to protect against intracellular cleavage by host cell proteases (Arnau *et al.*, 2006) and helps to stabilise the recombinant protein and increase its solubility (Terpe, 2006), and has been shown to successfully increase solubility in a number of cases (Dümmler *et al.*, 2005; Kim & Lee 2008; Phansopa *et al.,* 2015).

In the case of increasing solubility for the OmpA1 and OmpA2 proteins in this study, the use of the GST-fusion tag increased solubility only marginally. After dialysing the protein, only the GST-OmpA2 remained partially soluble, and after combining and concentrating the soluble fractions, a minimal amount of protein remained. This soluble protein was enough to perform interaction studies with the host cell with technical repeats. Both of these image sets using CellMask™ and WGA-Texas Red® membrane stains demonstrated the ability of the OmpA2 protein to adhere to the host cell, providing encouraging results that the OmpA2 protein subunit is involved in *P. gingivalis* interaction with the host epithelial cells, as previously indicated in the *ompA* mutants in Chapter 3. However due to the technical difficulties with the OmpA purification, the interaction studies in this chapter utilised peptides of the extracellular loops instead of purified protein.

Dialysis is needed after the purification of the protein to remove the solubilising and elution reagents and to refold the protein. Protein refolding is a process that leads to a conformational change from a disordered and flexible state in the denaturant conditions, to a folded and compact state in an aqueous buffer (Tsumoto *et al.*, 2003). Ideally, by removal of the denaturing solution the aqueous buffer should force the protein to collapse into the

compact structure; however this often leads to misfolding and aggregation, as seen with the OmpA1 and OmpA2 proteins here. Once the urea was removed from the protein elutions in dialysis, the OmpA proteins had no flexibility to refold correctly and precipitated becoming insoluble again. This was the case for the His-tagged proteins, and the OmpA protein remained insoluble after dialysis and therefore could not be used in any further experimental analysis.

As the insolubility after dialysis appeared to be the major hindrance in protein purification, various methods of dialysis were trialled to determine a method which would increase the likelihood of soluble protein after dialysis. Initially, stepwise dialysis was attempted which involved the gradual decrease in the concentration of urea to create intermediate levels of folding whilst still allowing protein flexibility and solubility until complete folding has occurred (Maeda *et al.*, 1995; Tsumoto *et al.,* 2003). This involved decreasing the concentration of Urea from 8 M to 0 M Urea in the dialysis buffer over the space of 24 hours, from 8 M to 6 M, then 4 M and 2 M before all urea was removed completely so in theory the protein would be soluble (Tsumoto *et al.*, 2010). Unfortunately, this method of dialysis was unsuccessful and the protein precipitated after dialysis.

As previously detailed, reviews of the literature indicated proteins are likely to aggregate when a high concentration of them is reached (Kiefhaber *et al.*, 1991; Lebendiker and Danieli, 2014), lending favour to the idea of reducing the temperature whilst proteins are expressed to reduce expression and therefore the potential for aggregating (Schein, 1989; Vasina, 1997). This idea was then taken further into the aggregation of the protein determined in the dialysis, and therefore that the high concentration of protein during dialysis increases the likelihood of protein aggregation and precipitation. This method to increase solubility post dialysis provided some success as protein was detected in the soluble fraction after dialysis. However, even after increasing the protein concentration through a Vivaspin® column, the concentration was still too low to provide a viable method for purification of soluble OmpA protein for downstream experiments.

Another method of dialysis that was trialled to increase solubility was to include the amino acids L-arginine and L-glutamate in the dialysis buffer. The theory behind this was explained by Golovanov *et al* (2004) which demonstrated a 9-fold increase in solubility of the protein after dialysis in the presence of 50 mM L-glutamate and L-arginine (Golovanov *et al.*, 2004). The amino acids are thought to perform a similar role to stepwise dialysis by suppressing the aggregation of refolding intermediate proteins, leading to an increased yield of overall

correctly folded protein (Hong Lu *et al.*, 2001). Arginine is a positively charged amino acid, and alone is effective at increasing protein solubility but is needed at a much higher concentration (Clark, 2001; Hamada *et al.*, 2009). Glutamate, a negatively charged amino acid, was previously found to increase aggregation of lysozyme after dilution out of 8 M urea, but suppresses aggregation after the addition of thermal stress (Shiraki *et al.*, 2002). When applied together, the charges of these amino acids are thought to interact with oppositely charged groups on the surface of the protein, whilst the aliphatic region of the R group side chains are thought to cover the hydrophobic regions of the protein, reducing the "stickiness" which is thought to cause the aggregation of the protein (Golovanov *et al.*, 2004). Golovanov *et al* showed that together, the concentrations of L-arginine and L-glutamine can be reduced to 50 mM and still be effective at increasing the stabilisation of the proteins of interest, and therefore the method was applied in the dialysis in this chapter. The addition of the L-arginine and L-glutamine alone had no effect on the solubility of the protein during dialysis, and when coupled to stepwise dialysis, no soluble protein was observed.

Additives to the purification buffers exert their effects through either the enhancement of the native stability of the protein, or by destabilising the aggregates formed during overexpression (Bondos and Bicknell, 2003). The list of additives to the protein purification buffers and to the dialysis buffers is extensive and an impractical list to conquer (Bagby *et al.*, 2001; Clark, 2001; Hamada *et al.*, 2009) some of which is shown in Table 4.3, and to date, no single standard model exists to provide the perfect conditions for protein solubility and refolding. Alternatively, the protein could have been exported to the periplasm during expression which is usually used for proteins needing the correct formation of disulphide bonds (Bessette *et al.*, 1999) or for especially toxic proteins (Saida *et al.*, 2006), but has been shown to increase purification of insoluble proteins (Rosano *et al.*, 2014; Dow *et al.*, 2015). However, this method is not always possible for all proteins, and periplasmic protease proteins can lead to proteolysis, resulting in fragmented and redundant proteins (Niazi and Brown, 2015). This is something that was not attempted in this body of work due to the progression into the structural models being produced, but will be kept in mind for future protein purifications. Due to the insolubility of the protein and impracticality of investigating every method to produce soluble proteins, alternative methods to study the interaction between OmpA and the host cells were explored.

Table 4.3 Collation of the most widely used additives for protein purification enhancement

Additive	Property	Reference
Tween 20 / 80	Detergent	(Kerwin *et al.*, 1998; Kreilgaard *et al.*, 1998)
Nonidet P-40	Detergent	(Zoueva *et al.*, 2002)
Glycine	Amino Acid	(H Lu *et al.*, 2001)
L-arginine, L- glutamate	Amino Acid	(Golovanov *et al.*, 2004)
Sucrose	Sugar	(Kerwin *et al.*, 1998; Webb *et al.*, 2001)
Glucose, Lactose	Sugar	(Arakawa and Timasheff, 1982)
Ethylene glycol, xylitol, mannitol, inositol, sorbitol	Sugar alcohol	(Gekko and Morikawa, 1981)
Glycerol	Sugar alcohol	(Gekko and Timasheff, 1981)
$MgSo_4$, $(NH_4)_2SO_4$, Na_2SO_4, Cs_2SO_4	Kosmotope (order creator)	(Neagu *et al.*, 2001)
NaCl, KCl	Weak kosmotrope	(Neagu *et al.*, 2001)
$CaCl_2$, $MgCl_2$, LiCl, RbCl, NaSCN, NaI, $NaClO_4$, NaBr	Chaotrope (disorder creator)	(Neagu *et al.*, 2001)
Urea	Chaotrope (disorder creator)	(H Lu *et al.*, 2001; Edwin *et al.*, 2002)

As there was no success in purifying soluble protein, the structures of the OmpA protein subunits were determined using online software protein prediction tools. Both OmpA1 and OmpA2 displayed the typical structure of an OmpA protein (Pautsch and Schulz, 1998; Pautsch and Schulz, 2000), with an N-terminal 8-stranded β-barrel and a C-terminal peptidoglycan-associated globular domain. Processing the structure through multiple structure prediction tools gave highly similar results, all indicating this same structure. Orientation software programmes such as TMPRED indicated the orientation of the subunit in the membrane and identified surface exposed loops which would be potentially involved in the interaction with the host. The sequence of these loops in the protein subunit was strongly indicated when both Phyre2 and RaptorX predicted the same placement in the protein sequence for the extracellular loops. Actual structure demonstration through crystallisation would be clearly beneficial, especially to confirm the location of these loops, however due to the insoluble nature of the protein, this is not practical. However, there is high confidence in the structure prediction by both homology studies (Iwami *et al.*, 2007) and the high confidence (99.6 - 100%) in the model assigned by the Phyre2 software.

The extracellular loops of the OmpA2 protein were utilised in invasion assays and demonstrated that these loops are sufficient and specific in the interaction with the host. Invasion and adhesion of wild-type *P. gingivalis* was interrupted in the presence of these loops, which was not observed in the presence of a completely scrambled peptide of peptide loop 4. Additionally, when bound to fluorescent microspheres the synthetic peptides were capable of directing interaction of these inert microspheres with human epithelial cells. This again was not seen when the microspheres were coated in with BSA or the Biotin-tagged scrambled peptide, reinforcing the specific interaction seen with the extracellular loops of OmpA2.

The interaction of the extracellular loops with the host cell display a novel finding for *P. gingivalis* but have been shown in a range of human pathogens. The extracellular loops of the meningitis-causing strain of *E. coli* (K1) have been shown to be important in the invasion of brain endothelial cells in a number of cases (Prasadarao, *et al.,* 1996; Maruvada & Kim 2011), but more specifically, pathogenicity is reduced when mutations are introduced into loops 1 and 2 (Mittal and Prasadarao, 2011). The loops are not only needed for adherence and invasion, but further studies in *E. coli* K1 show a mutation in the extracellular loops lead to reduced survival in dendritic cells and macrophages (Mittal *et al.*, 2011). This would be an interesting line of investigation in future work of this study, to determine if the predicted extracellular loops of *P. gingivalis* interact with other cell lines, such as endothelial cells or cells associated with the immune system. The human pathogen known for causing Q fever, *Coxiella burnetii,* also demonstrates an interaction with the host specifically attributed to the extracellular loops, with a significant loss of internalisation into lung epithelial cells with the deletion of loop 1, suggesting a direct interaction with the host cell receptors, and its role is primarily to interact with a cognate receptor at the surface of the host (Martinez *et al.*, 2014). These studies suggest an integral importance for the extracellular loops in the interaction with human cells, but these observations are not limited to human pathogens. Work explored by Weiss *et al* (2008) demonstrated that with the introduction of recombinant *E. coli* K1 OmpA can convert a usually symbiotic relationship between *Sodalis glossindius* and its host, the tsetse fly (*Glossina morsitans*) to a pathogenic one. This body of work also used comparisons of the extracellular loops of the pathogenic *E. coli* and symbiotic *S. glossindius* to determine the substitutions and insertions in the sequence for loop 1 which were not observed in the OmpA found associated with the pathogenic *E. coli* (Weiss *et al.*, 2008).

Combining the previous studies in the extracellular loops of other pathogen bacteria to the novel data generated from the extracellular loops of the OmpA2 protein of *P. gingivalis* in this results chapter, these demonstrate a role for the OmpA extracellular loops in the interaction of bacteria and the host, which contributes to the idea that this may be a widespread mechanism of host cell interaction.

The data presented in this chapter demonstrates evidence that the OmpA protein, specifically the OmpA2 subunit, is directly involved in the interaction with the host. The question still remains as to what the potential cognate receptor on the host would be. Studies attempting to identify the *P. gingivalis* OmpA host cell receptor are limited. In the case of endothelial cell invasion by *P. gingivalis,* evidence was provided by Komatsu *et al* (2012) that OmpA may interact with these cells via E-selectin (Komatsu *et al.*, 2012). However, there is only weak expression of E-selectin on epithelial cells so this may not be the case (Pietrzak *et al.*, 1996).

The host cell receptor for *E. coli* OmpA with the most evidential support is Gp96, a cell surface glycoprotein related to heat shock proteins (Prasadarao *et al.*, 1996). Multiple studies have shown the *E. coli* K1 meningitis-causing OmpA mediated interactions with brain endothelial cells (BMECs) via the Gp96 receptor (Prasadarao, 2002; Prasadarao *et al.*, 2003), but more specifically, further studies demonstrated the extracellular loops 1 and 2 in particular were important in gp96 receptor interaction (Mittal and Prasadarao, 2011; Mittal *et al.*, 2011).

The receptor for OmpA has also been implicated in the strains of *E. coli* (AIEC strains, specifically LF82) that contribute to Crohn's disease, the chronic intestinal diseases developed due to abnormal inflammatory responses to intestinal microbiota in humans (Strober *et al.*, 2007; Xavier and Podolsky, 2007). Using pull down assays, OmpA was shown to bind Gp96, and an Δ*ompA* mutant showed reduced invasion levels. This reduction in invasion was restored to wild-type level in the Δ*ompA* mutant when the intestinal epithelial cells were pre-treated with enriched OMVs containing OmpA (Rolhion *et al.*, 2010; Rolhion *et al.*, 2011), demonstrating a direct engagement of the gp96 receptor by OmpA of *E.coli* K1.

Gp96 appears to be a popular receptor for host-pathogen interactions, with many bacteria utilising it for adherence and subsequent entry to the cell, including OmpA-mediated interaction in *E. coli* as discussed previously, *Staphylococcus aureus* Bap-Gp96 interactions

(Valle *et al.*, 2012) and *Listeria monocytogenes* Vip surface factor-mediated interaction (Cabanes *et al.*, 2005) to name a few. Gp96 is highly expressed in intestinal epithelial cells (Rolhion *et al.*, 2010; Rolhion *et al.*, 2011) and in brain endothelial cells (Prasadarao, 2002; Mittal and Prasadarao, 2011), which supports the idea that it is the potential cognate receptor on the host in those cases; however there is little evidence that oral epithelial cells express this receptor or that *P. gingivalis* utilises it.

There is therefore the potential to utilise these peptides generated from the extracellular loops of the OmpA2 protein to perform binding assays to identify the host cell receptor for the *P. gingivalis* OmpA protein. This would involve immobilising the peptides on Avidin-coated resin and capturing interacting partners from epithelial cell lysates passed over the resin, with mass spectrometry to identify the partners. It would also be interesting to mutate the loops of the OmpA2 protein to investigate a loss of interaction with the host to confirm the role of the OmpA2 protein, and whether these extracellular loops are as important when the whole protein is present *in vivo*. Further analysis of the extracellular loops interaction with the host would be to investigate if there is any interaction with other cell types. Considering *P. gingivalis* interacts with endothelial cells (Deshpande and Khan, 1998; Deshpande *et al.*, 1998), and more recently has been shown to interact with these cells via the OmpA protein (Komatsu *et al.,* 2012), it would be interesting to determine if these extracellular loops are involved in the interaction with other cell types through repeating the peptide inclusive standard antibiotic protection assays with different cell types.

Further analysis of these peptides would provide the potential to utilise them as new therapeutic agents to aid the prevention of the onset of chronic periodontal diseases caused by *P. gingivalis*.

4.5 Summary

In conclusion, whilst not achieving the purification of a high yield of overexpressed OmpA protein, these data presented here have identified extracellular surface regions of the OmpA2 protein subunit and have shown direct interaction with the host cell through multiple assays. These data therefore have indicated a potential role for these peptides and suggest a possible role for the use of these surface protein derived peptide loops in a therapeutic role as anti-adhesive peptides to prevent *P. gingivalis*–caused periodontal disease.

Chapter 5

Preliminary Characterisation of the Putative OmpH/Skp Locus of *P. gingivalis*

5.1 Introduction

The outer membrane proteins from Gram negative bacteria are synthesised in the cytoplasm and then must be translocated across the inner membrane to the periplasm in an unfolded state (Manting and Driessen, 2000; Driessen *et al.*, 2001). Chaperone proteins are needed to assist the translocation of proteins across the periplasm, and to either then assist the folding of the protein or to deliver them to a folding system which will then insert the protein into the outer membrane (Missiakas *et al.*, 1996; Missiakas *et al.*, 1997; Danese and Silhavy, 1998). Multiple chaperone proteins have been identified and extensively studied, which can be seen later in Table 5.1.

The seventeen kilodalton protein (Skp), also known as OmpH or HlpA, is a homotrimeric periplasmic chaperone protein that specifically interacts with unfolded outer membrane protein intermediates to maintain the solubility and stability during the passage across the periplasm (Laura Hirvas *et al.*, 1990; Missiakas *et al.*, 1996). More recently, two Skp-like genes have been identified in *P. gingivalis*, named *ompH1* and *ompH2* which were found as part of the "signature set" of genes upregulated in the hyperinvasive subset of the *P. gingivalis* population (Suwannakul *et al.*, 2010). Currently, very little is known about the OmpH proteins of *P. gingivalis*, but these genes are predicted to function as a chaperone protein for delivering proteins to the Bam complex, an outer membrane assembly unit, as indeed they are thought to be in other organisms, with most studies being conducted in *E.coli*. The Bam complex (BamABCDE) is responsible for folding the β-barrel of outer membrane proteins, with BamA (also known as Omp85) being the central component conserved across all Gram-negative species (Hagan *et al.*, 2011). This complex, based on evidence from other organisms such as *E. coli* is therefore potentially involved in the assembly of the OmpA heterotrimer in *P. gingivalis*. (Patel *et al.*, 2013). A schematic representation of the Bam/Omp85 complex and the putative role of the OmpH-proteins is illustrated in Figure 5.1, based on evidence from *E. coli* Bam/OmpH secretion. The OmpH chaperone receives the unfolded protein from the Sec-secretion system, and translocates it across the periplasm in an unfolded state before delivery to the Bam complex where the protein is folded, modified and inserted into the outer membrane.

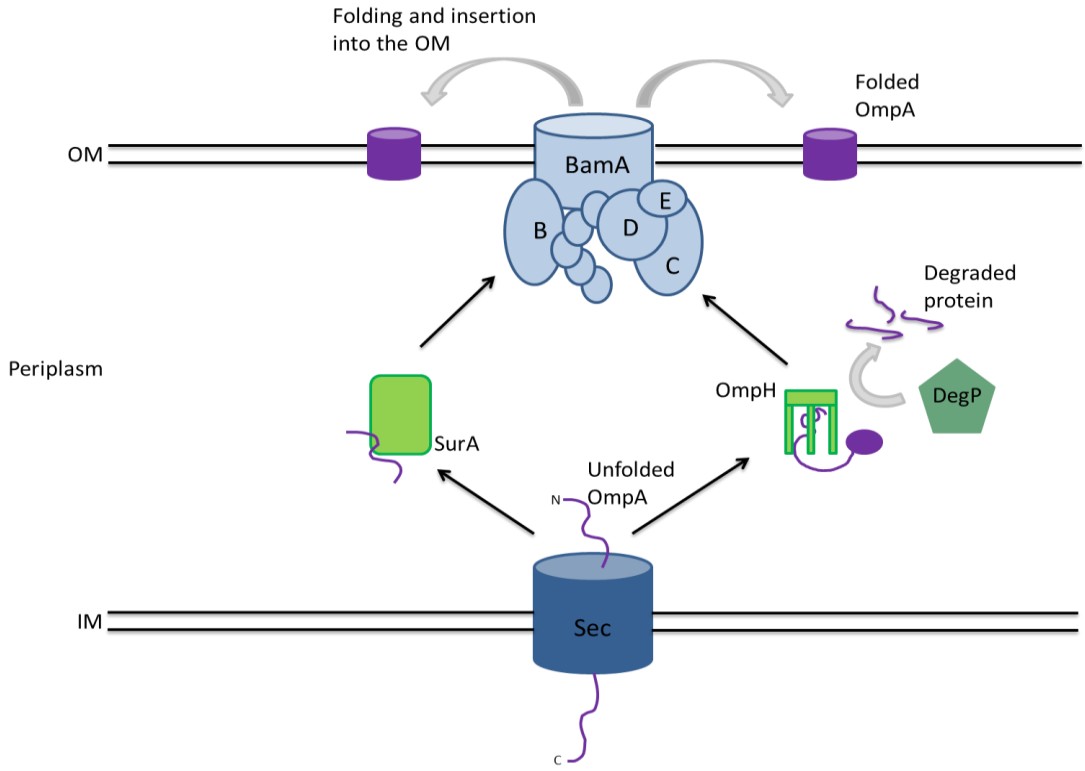

Figure 5.1. Schematic representation of the OmpH chaperone delivery of protein to the Bam complex. OmpH and SurA receive unfolded proteins from the Sec secretion system on the inner membrane (IM) and delivers the protein to the Bam complex in the outer membrane (OM) where they are processed, folded and inserted into the outer membrane.

The chaperoning of proteins across the periplasmic space is an important but complex process, and unsurprisingly contains multiple proteins for successful translocation and processing of the protein to be inserted into the outer membrane. The initial step in characterising the OmpH proteins and their role in protein chaperoning in *P. gingivalis* was to determine how they fit into a larger system and determining the similarity of the processes in comparison to a well understood chaperone system, such as the one found in *E. coli.* A comparison of the presence of well-known chaperone proteins in *E. coli* and associated proteins to *P. gingivalis* can be seen in Table 5.1.

Table 5.1 Common chaperone and related proteins found in *E. coli* and *P. gingivalis* for comparison

Protein in *E. coli*	**Role**	**Name in *P. gingivalis***
SurA	Major chaperone and PPIase involved in the biogenesis of OMPs (e.g. LamB, OmpA, OmpC, OmpF), assisting with folding as well as chaperoning. (Lazar and Kolter, 1996; Rouvière and Gross, 1996)	PG0415
DegP	Predominantly a protease and a heat shock protein activated by high temperatures (Lipinska *et al.*, 1989; Georgopoulos, 1990), but has chaperone activity at low temperatures (Skorko-Glonek *et al.*, 2007)	PG0593 – HtrA
FkpA	Chaperone and PPIase, specifically involved in the folding of LptD (LPS-assembly protein) and FhuA (outer membrane transporter for ferrichrome-iron) (Ramm and Pluckthun, 2000; Schwalm *et al.*, 2013)	PG0708
Skp	Chaperone involved in the biogenesis of OMPs (e.g. OmpF, OmpA), member of the holdase family of proteins (preventing protein aggregation) (Chen and Henning, 1996; Missiakas *et al.*, 1996; De Cock *et al.*, 1999)	PG0192/3 – OmpH
SecA	Part of the Sec secretion pathway, needed to secrete proteins across the cytoplasmic membrane in an unfolded state (Oliver and Beckwith, 1982; Akimaru *et al.*, 1991)	PG0514

BamA (YaeT)	Part of the BamABCDE complex, an outer membrane pore-forming assembly factor complex. (Voulhoux *et al.*, 2003; Wu *et al.*, 2005; Webb *et al.*, 2012)	PG0191 – Omp85
LolA	Lipoprotein-specific periplasmic carrier - Directly transfers lipoproteins from cytoplasmic (inner) membrane to the outer membrane (Matsuyama *et al.*, 1995)	Not found
HdeA	Highly flexible chaperone allowing binding to multiple targets to prevent aggregation, also involved in stress response and acid-resistance (Tapley *et al.*, 2009)	Not found
DsbA	Periplasmic folding catalyst, required for the formation of double bonds (Bardwell *et al.*, 1991)	Not found
Spy	Chaperone involved in suppressing protein aggregation and aids protein refolding (Quan *et al.*, 2011)	Not found

E. coli proteins were investigated for the presence in *P. gingivalis* using a standard protein BLAST against the *P. gingivalis* ATCC 33277 genome. If no homologues were identified, protein sequences were then submitted to cDART to determine any conserved domain architectural similarities, of which proteins that had no homologous presence in BLAST also had no conserved domains in *P. gingivalis* and therefore denoted “not found”.

In *E. coli*, outer membrane proteins are translated in the cytoplasm and targeted for secretion via the Sec system, where they are translocated across the inner membrane to the periplasmic space (Thome and Müller, 1991). The chaperone protein SurA is expected to act as a chaperone/folding catalyst, which assists with folding of outer membrane proteins immediately after export through the Sec system (Missiakas *et al.*, 1996; Missiakas *et al.*, 1997) before delivery to the Bam complex for processing and insertion into the outer membrane (Webb *et al.*, 2012). The predominant role for DegP is as a protease enzyme,

working alongside the SurA chaperone, whereby it degrades unfolded proteins in the periplasm (Strauch and Beckwith, 1988). It also has an essential role in survival of *E. coli* at elevated temperatures (Lipinska *et al.*, 1989). DegP also displays a minor role acting as a holdase-type chaperone at low temperatures (<28°C), by preventing the aggregation of certain substrates (Skorko-Glonek *et al.*, 2007) and preventing their degradation by other proteases during the transport across the periplasm (Krojer *et al.*, 2008). The *P. gingivalis* genome contains homologues of all of these proteins found in the major chaperone system.

FkpA has been shown to act as a periplasmic chaperone to prevent aggregation of proteins (Saul *et al.*, 2004), and has been recently shown to act cooperatively with Skp and SurA in the folding of LptD and FhuA (both outer membrane proteins) (Schwalm *et al.*, 2013). Skp itself has been shown to act as a holdase, preventing the aggregation of proteins rather than playing an active role in the folding of the outer membrane proteins (Walton and Sousa, 2004), and has already been shown to be important in the chaperoning of over 30 envelope proteins (Jarchow *et al.*, 2008). As the deletion of the *skp* gene shows only diminution of outer membrane proteins in *E. coli* rather than a complete loss from the outer membrane, it is expected to act as a minor chaperone (Chen and Henning, 1996).

5.2 Aims

Previous work by Suwannakul *et al* (2010) demonstrated that a particular set of genes that are differentially regulated in a hyperinvasive subset of the *P. gingivalis* population. It was theorised that these genes are involved in either the invasion process or in the survival of the bacterium within the host. Of particular notice was the identification of the Skp-related OmpH protein of *P. gingivalis* as being potentially important in the interaction with the host, therefore this chapter will focus bioinformatics investigation on this particular chaperone protein, followed by characterisation of the Δ*ompH* mutant and investigation into the OmpH proteins and their effect on *P. gingivalis* virulence and interaction with the host. As previous work in *E. coli* has demonstrated evidence that OmpA is chaperoned by the OmpH protein (Chen and Henning, 1996; Schäfer *et al.*, 1999; Patel *et al.*, 2009; Walton *et al.*, 2009), the link between OmpH and OmpA in *P. gingivalis* will also be investigated in this chapter.

5.3 Results

5.3.1 Bioinformatic Analysis of OmpH

The two *ompH1* and *ompH2* genes (also known as PGN_0300 and PGN_0301 or PG0192 and PG0193) are predicted to potentially form an operon with coding sequences PGN_0296 – PGN_0299 upstream of the *ompH* genes (Taguchi *et al.*, 2016), as seen in Figure 5.2.

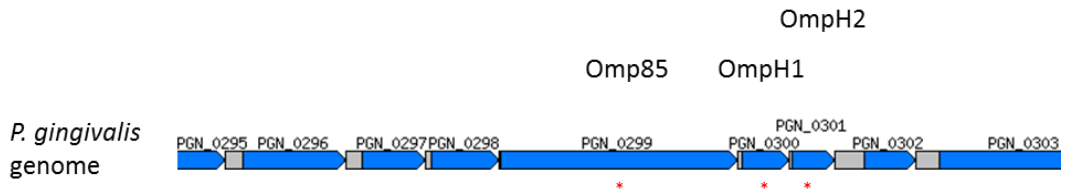

Figure 5.2 Location of the *ompH1* and *ompH2* genes in the *P. gingivalis* genome. The two genes are located downstream of the BamA β-barrel assembly outer membrane protein (Omp85), indicated by the *.

Protein family (Pfam) analysis of the amino acid sequences of OmpH1 and –H2 subunits of *P. gingivalis* show significant matches to the OmpH-like family of proteins, although the identity of the sequences to *E. coli* Skp is relatively low (26.17% and 20.89% for OmpH1 and –H2 respectively). The two *P. gingivalis* OmpH subunits also displays relatively low sequence homology to each other, at only 22.2% similarity.

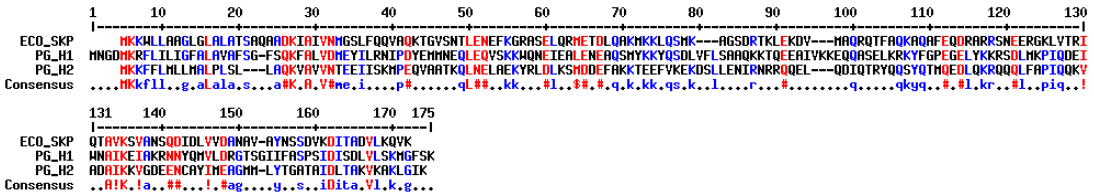

Figure 5.3 Alignment of *E. coli* Skp with *P. gingivalis* OmpH1 and H2 proteins. Red indicates high consensus between sequences, with blue indicating low consensus. The consensus sequence is listed below the three protein sequences and demonstrates a low sequence homology between *E. coli* and *P. gingivalis* Skp and OmpH proteins.

The amino acid sequences of the individual OmpH subunits were further analysed through transmembrane structure prediction software programmes to determine the topology of the protein. Using DAS software (http://www.sbc.su.se/~miklos/DAS/) both the OmpH1

and OmpH2 subunits were predicted to possess a transmembrane helix at the N-terminal end (Phe_8 – Ser_{23} for OmpH1 and Leu_6 – Lys_{21} for OmpH2), following a signal sequence. Using another software tool, TMpred, produced results that complied with this, with OmpH1 showing a transmembrane helix from residues 8-27 and OmpH2 at residues 6-21. This suggests that a small section of these proteins may be anchored in the membrane of *P. gingivalis*, with the rest spanning the periplasm. However, when using TMHMM software, only OmpH1 demonstrates the presence of a transmembrane α-helix, as previously reported by Taguchi *et al* (2016). The prediction of the protein structure of OmpH1 and OmpH2 singular subunits using Phyre2 suggests a similar protein structure as observed for *E. coli* Skp, which has been suggested as forming a "jellyfish"- type architecture, with a body-domain and long α-helices forming the tentacles, as shown in Figure 5.4. The Skp proteins of *E. coli* have been shown to form a homotrimer (Walton and Sousa, 2004; Korndörfer *et al.*, 2004), which contributes to the function of Skp.

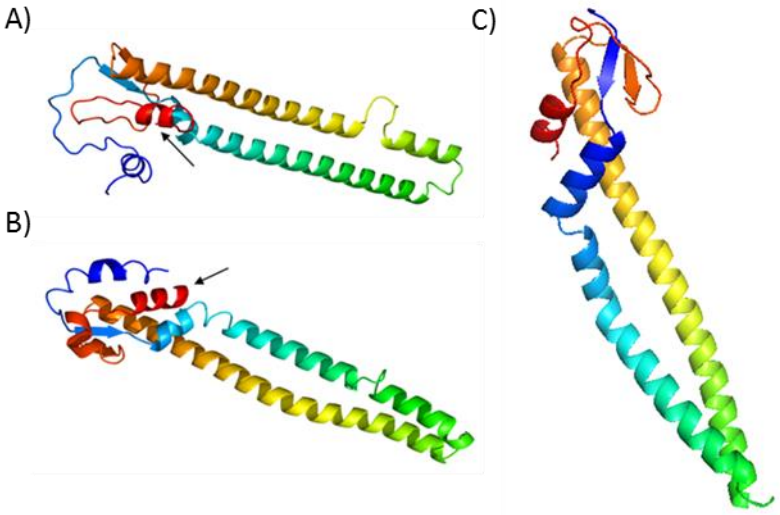

Figure 5.4 Protein structure prediction of *P. gingivalis* OmpH1, OmpH2 and *E. coli* Skp. *P. gingivalis* OmpH1 (A) and -H2 (B) structure predictions using Phyre2 (black arrows indicating the predicted transmembrane α-helix), and *E. coli* Skp (C) from crystal structure determination.

This trimeric structure formed by *E.coli* Skp has been suggested as a necessity for binding the β-barrel of outer membrane proteins deep into the cavity of the trimer, with the "tentacles" wrapping around the chaperoned protein to prevent aggregation and stabilise

the protein during the translocation across the periplasm (Walton *et al.*, 2009), and may be the case for *P. gingivalis* OmpH due to their structural similarities, although the trimeric formation of OmpH has not yet been investigated.

5.3.2 Generation of an *ompH1H2* Mutant

As the *ompH1, -H2* genes are expected to form a complex, both genes were deleted to determine the effects of the loss of the entire protein on the *P. gingivalis* outer membrane and virulence. The *ompH1H2* mutant was generated to study the effects on *P. gingivalis* biology and its ability to interact with human cells. Similar to the attempt to generate the Δ*ompA1* mutant, the assembly of a knock out construct through PCR assembly yielded no triplet construct, despite the many PCR conditions attempted. Therefore, a knock out construct was designed with two flanking regions of 1000 bp upstream and downstream of the OmpH1H2 coding region, and with the erythromycin resistance gene inserted at the corresponding ATG start codon of *ompH1*, and the TAA stop codon at the stop codon of *ompH2* to knock out the whole OmpH1H2 protein, before synthesis through GeneArt™.

The coding sequences upstream and downstream the *ompH* operon were also analysed to determine if there would be any read-through effects caused by the deletion of the operon. Upstream of *ompH1* encodes Omp85 (also known as YaeT or BamA, see Fig. 5.2.) which is an integral member of the BamABCDE complex involved in the assembly of β-barrels in the outer membrane, and is an essential gene. Disruption of this gene during the deletion of OmpH would result in non-viable cells and therefore this is not a concern as no triple mutants of *ompH1H2* and *omp85* would be produced. Downstream of the *ompH* operon contains a 327 bp non-coding region before encoding a transposase unrelated to the *ompH* operon, so no read-through effects were predicted to be observed in the deletion of the operon.

The synthesised knock out construct was initially blunt-end cloned into pJET1.2/blunt vector for storage, and transformed into DH5α for amplification. Plasmids were isolated from positive colonies selected on LB plates supplemented with ampicillin. Positive plasmids for the insert were then used for transformation into wild-type *P. gingivalis* 33277 through all four methods (plate-to-plate, plate-to-liquid, liquid-to-plate and liquid-to-liquid) as previously described in materials and methods 2.6.4.

The different methods of transformation were assessed for their efficiency, as previously described in the generation of Δ*ompA1* and Δ*ompA2* mutants in Chapter 3.3.2. Again,

overall the natural competency method proved to generate more colonies than the electrocompetency method. However, the overall efficiency was minimal, with multiple transformation attempts yielding no colonies. As many attempts at transformation produced no colonies, the methods were dissected further.

The original electroporation involves the growth of a large liquid broth (20 ml) before preparation of the cells, electroporation and then the cells plated onto plain BA plates for 24 h before transferral to erythromycin-containing plates for selection. The original natural competency method involved inoculating 1 ml BHI with bacteria obtained from a 3-day old plate to OD_{600} ~2.0 before adding DNA and plating on plain BA plates for 24 h before transferring to erythromycin-containing plates. General laboratory observation demonstrated the *P. gingivalis* cultures appeared to grow better in liquid broth than plates, so this was incorporated into the design of the new transformation methods. The origin of the starting cultures for transformation by natural competency was investigated to determine if *P. gingivalis* taken from either 3-day old plates or liquid cultures would produce a higher yield of mutants, whilst the 24 h recovery incubation post DNA transformation was investigated on plain BA plates and liquid BHI with supplements to determine which would produce more mutants for both electrocompetency and natural competency. In all methods, after the 24 h recovery in BHI broth or BA plates, the *P. gingivalis* was transferred to erythromycin-containing BA plates for 2 weeks for the growth of *P. gingivalis* mutants. Two different cultures were set up for each method and the efficiency of the method was determined as an average number of colonies observed on the erythromycin-containing plates after 2 weeks incubation. The different methods under investigation can be seen diagrammatically in Figure 5.5.

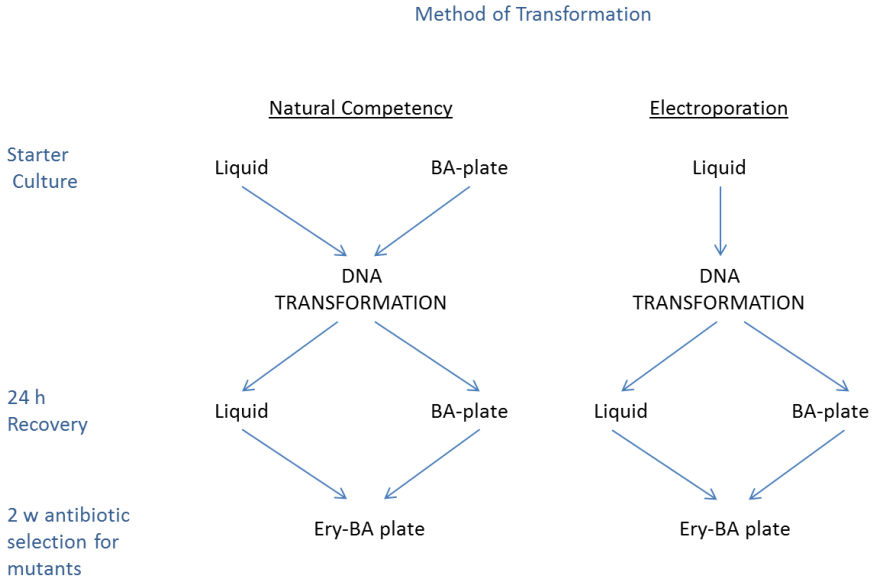

Figure 5.5 Schematic representation of the optimisation of *P. gingivalis* transformation methods. The transformation of *P. gingivalis* is performed via two main methods, natural competency and electroporation, with optimisation of these methods detailed in this Figure.

Electroporation yielded no mutants in either condition, similar to the creation of the Δ*ompA* mutants. Natural competency yielded mutant colonies in 3 out of the four conditions, and if the starting culture was from a liquid culture rather than a plate, a greater number of colonies were observed on the erythromycin-containing BA plates, and even more colonies were observed if the recovery 24 h was in a liquid culture, as seen in Table 5.2.

Table 5.2 Transformation efficiency of each method of transformation for *P. gingivalis*

Method of transformation	**Colonies μg^{-1}**
Electroporation – liquid 24 h recovery	0
Electroporation – plate 24 h recovery	0
Natural competency - plate-to-plate	0
Natural competency - plate-to-liquid	1.2
Natural competency - liquid-to-plate	13.6
Natural competency - liquid-to-liquid	24.4

The concentration of DNA in all methods was between 250-270 ng / µl, so the efficiency of transformation was expressed as the number of colonies produced per overall DNA input concentration.

DNA from several colonies in each condition was purified and PCRs were carried out using various combinations of primers from Table 2.8 to determine the successful homologous recombination of the erythromycin resistance cassette into the *P. gingivalis* genome, thereby knocking out the *ompH* operon. Analysis of PCR products on agarose gel indicated multiple positive colonies, with one shown in Figure 5.6.

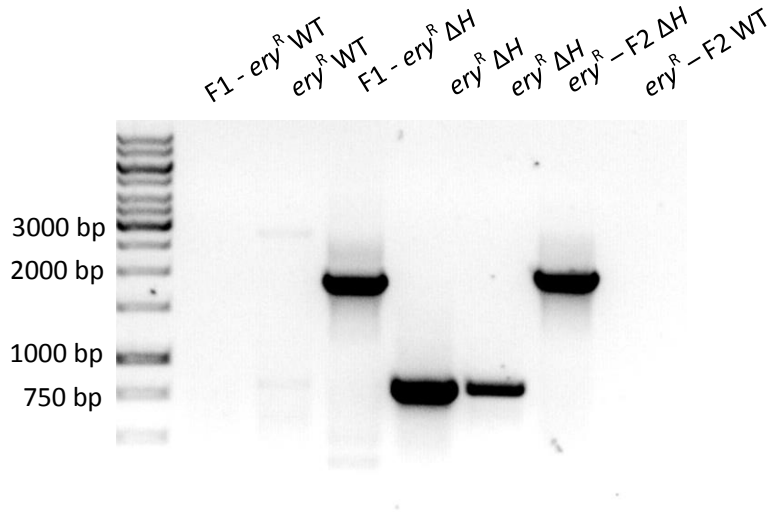

Figure 5.6 PCR analysis of the generation of a Δ*ompH1H2* mutant. DNA was isolated from *P. gingivalis ery*^{R} colonies growing on erythromycin-containing BA plates using the Wizard® Genomic DNA Purification Kit (Promega). Multiple combinations of primers were used to assess the deletion of the *ompH* operon. F1-*ery*^{R} primers generate the flanking region upstream and the erythromycin cassette (1800 bp), ery^{R} primers generate the erythromycin cassette (800 bp) and *ery*^{R} – F2 generate the erythromycin cassette and the downstream flanking region (1800 bp). DNA was extracted from both wild-type (WT) *P. gingivalis* and the mutants in question (ΔH). No bands were observed in the wild-type DNA-containing PCRs as they do not possess an erythromycin gene, whereas all PCRs were positive for the mutant at the correct sizes.

DNA products from the PCR were analysed using sequencing to determine correct mutation of the *ompH* operon and confirmed that all colonies tested contained deletion of the *ompH1 and ompH2* genes with replacement by the *ery*^{R} cassette. These also appeared to be identical so one was selected for further analysis in this chapter.

5.3.3 Morphological analysis of Δ*ompH1H2*

The first and most obvious observation of the Δ*ompH1H2* mutant was the morphology of the colonies. The colonies observed on the erythromycin-containing plates after transformation appeared much larger than wild-type *P. gingivalis*, as shown in Figure 5.7. These colonies also appeared to be brown and glossy, rather than the small black colonies usually seen with wild-type *P. gingivalis*.

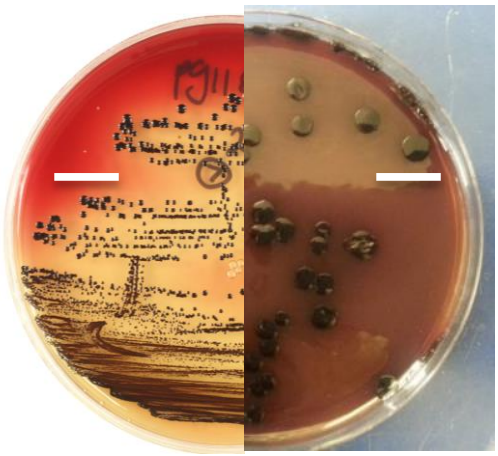

Figure 5.7 Δ*ompH1H2* mutant morphology. Wild-type (left) colonies appear as small black-pigmented colonies compared to the large, brown colonies observed for Δ*ompH1H2* (right). The white scale bar represents 1.5 cm, indicating a vast difference in size between the two.

After replating these colonies for further growth, it was also observed that the Δ*ompH1H2* mutant grows much slower on BA-plates, and takes an increased length of time to darken whilst still retaining the glossy appearance, as shown in Figure 5.8.

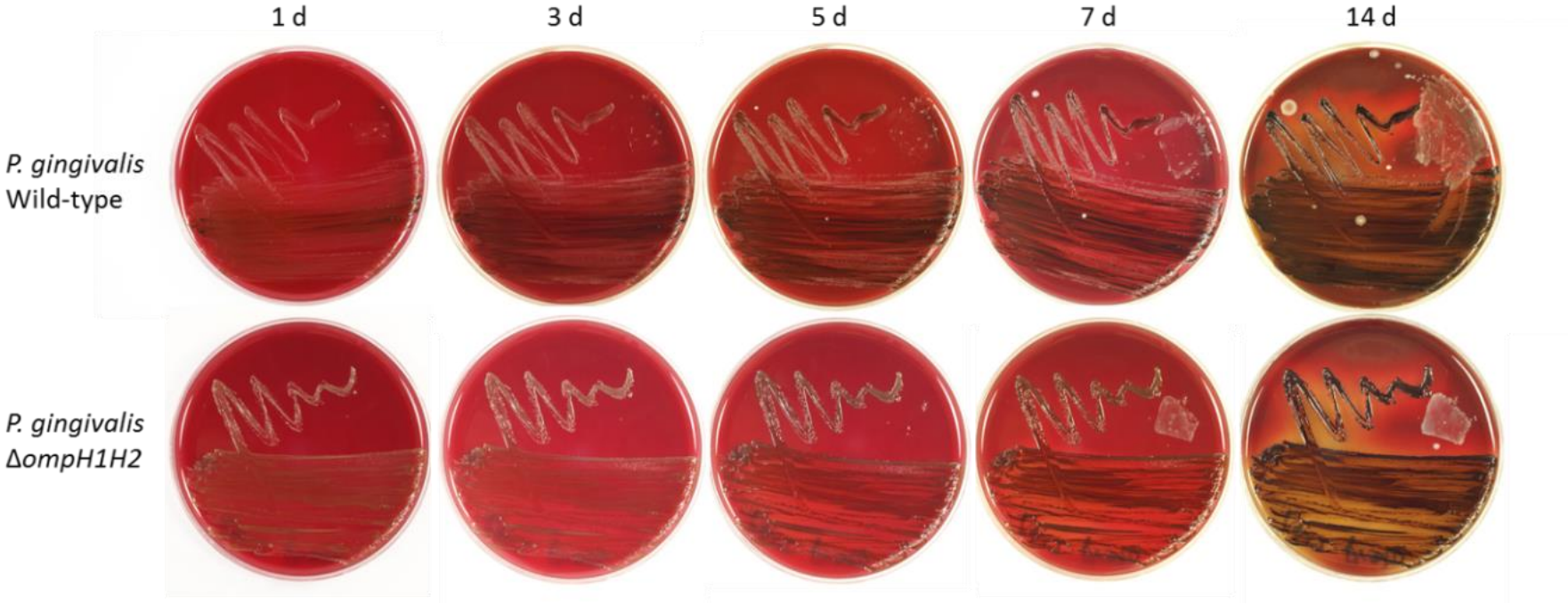

Figure 5.8 Time lapse of growth of *P. gingivalis* wild-type and Δ*ompH1H2* mutant. Plates were photographed every other day (d) until 7 days, and then again after another week (14 d). Each plate was removed from the anaerobic cabinet to be photographed in a non-sterile environment, therefore plates contain contamination from other microorganisms, however this did not affect the growth so was no major concern.

Wild-type colonies turn black after 3 days, but more apparently so after 5 days. The Δ*ompH1H2* colonies remain brown and glossy until 14 days, where they apparently darken but still remain glossy, indicating a potential change to the surface characteristics due to the loss of the OmpH protein.

5.3.4 Protein Profiling of the Δ*ompH1H2* Mutant

As the initial morphological study of the Δ*ompH1H2* colonies demonstrates a potentially altered surface profile it could be possible that the outer membrane protein profile was altered. This can he hypothesised since colony pigmentation in particular is known to be defined in *P. gingivalis* by the action of secreted and membrane associated proteins such as gingipains. Therefore, the proteins in the outer membrane affected by the loss of OmpH were investigated further. A general observation of the outer membrane proteins was investigated through the purification of the outer membrane as detailed in Materials and Methods 2.7.5, and analysed on an SDS-PAGE gel, as seen in Figure 5.9

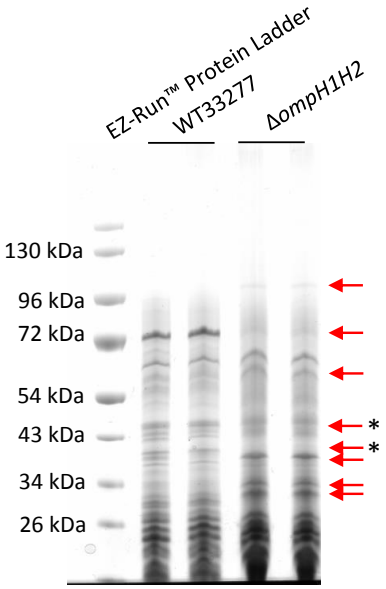

Figure 5.9 SDS-PAGE analysis of purified outer membranes of wild-type and Δ*ompH1H2* *P. gingivalis.* Liquid cultures were grown and adjusted to OD_{600} 1.0 before the membranes purified by differential detergent centrifugation before being applied to the SDS-PAGE 4-15% pre-cast gradient gel. DTT was applied to the SDS-loading buffer and samples boiled before loading so proteins were denatured in this analysis. Particularly obvious differences between the wild-type and Δ*ompH1H2* membrane proteome are highlighted with red arrows.

The SDS-PAGE analysis demonstrates a significant alteration to the outer membrane in the Δ*ompH1H2* mutant compared to the wild-type. Many proteins appear to be absent from the outer membrane, suggesting that these proteins might be clients of the OmpH chaperone. While speculative, the sizes of proteins of interest are around ~41 kDa (potentially OmpA), or ~48 kDa (potentially the gingipains), which are marked with an asterisk on the gel arrow. However, in multiple instances there appears to be proteins found in the sample which are not present in the wild-type. These proteins may be present in these samples due to aggregation of pre-processed proteins (i.e. because they are not chaperoned to the outer membrane for processing) and pelleting during centrifugation, and therefore they appear in the outer membrane sample preparation. Further analysis of these proteins would be necessary to identify which proteins are no longer in the outer membrane and therefore indicative of being chaperoned by the OmpH proteins.

As previous studies have identified *E. coli* Skp as being involved in the assembly of OmpA (Bulieris *et al.*, 2003; Patel *et al.*, 2009; Qu *et al.*, 2009; Walton *et al.*, 2009), coupled to the potential loss of the protein band in the Δ*ompH1H2* outer membrane preparation at ~41 kDa in Figure 5.10 and OmpA being a major protein of interest in this project, the appearance of OmpA in the outer membrane in Δ*ompH1H2* mutants was probed using Western blotting. The OmpA antibody was previously used to probe for the presence of OmpA in the outer membrane of the Δ*ompA* single and double mutants in Chapter 3 (Fig. 3.8), and a similar protocol was followed here for Δ*ompH1H2* mutants. Figure 5.10 demonstrates the SDS-PAGE analysis of the outer membrane preparations and the Western blot corresponding to the SDS-PAGE gel.

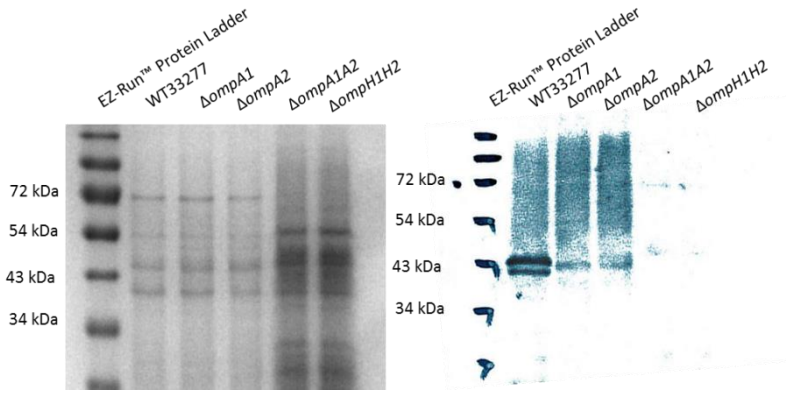

Figure 5.10 SDS-PAGE (A) and anti-OmpA Western blot (B) of outer membrane preparations from wild-type *P. gingivalis* and Δ*ompA* and Δ*ompH* mutants. Outer membrane preparations were prepared as previously described and analysed on an SDS-PAGE gel (A) alongside probing for the OmpA protein using an anti-OmpA antibody (1:1000) (B).

Previous attempts at SDS-PAGE analysis of membrane preparations from the Δ*ompA1A2* and Δ*ompH1H2* double mutants often show a fainter band marking on the gel, so twice as much protein was loaded to ensure any protein being detected in the Western blot. Ultimately, no protein band was observed in the corresponding anti-OmpA Western blot in the Δ*ompA1A2* and Δ*ompH1H2* membrane preparation samples, indicating the possibility of OmpA being a client of the OmpH chaperone in *P. gingivalis*.

5.3.5 Assessment of the Integrity of the Outer Membrane in the Δ*ompH1H2* Mutant: Imaging and Vesicle Counts

As the *P. gingivalis* OmpH chaperone protein is likely to translocate proteins across the periplasm to the outer membrane, outer membrane integrity assays were carried out to determine the effects of the loss of the chaperone protein on the integrity of the outer membrane. The outer membrane integrity and morphology was determined through two methods, transmission electron microscopy (TEM), as was performed for the *ompA* mutant morphology (which led to assessment of the outer membrane vesicles) and also through thiazole orange membrane integrity assays.

TEM was carried out as previously described in Materials and Methods 2.8.5, and checked for contamination through Gram-staining. Pure cultures of wild-type *P. gingivalis* and

Δ*ompH1H2* were prepared and sectioned for TEM. Images generated can be seen in Figure 5.11.

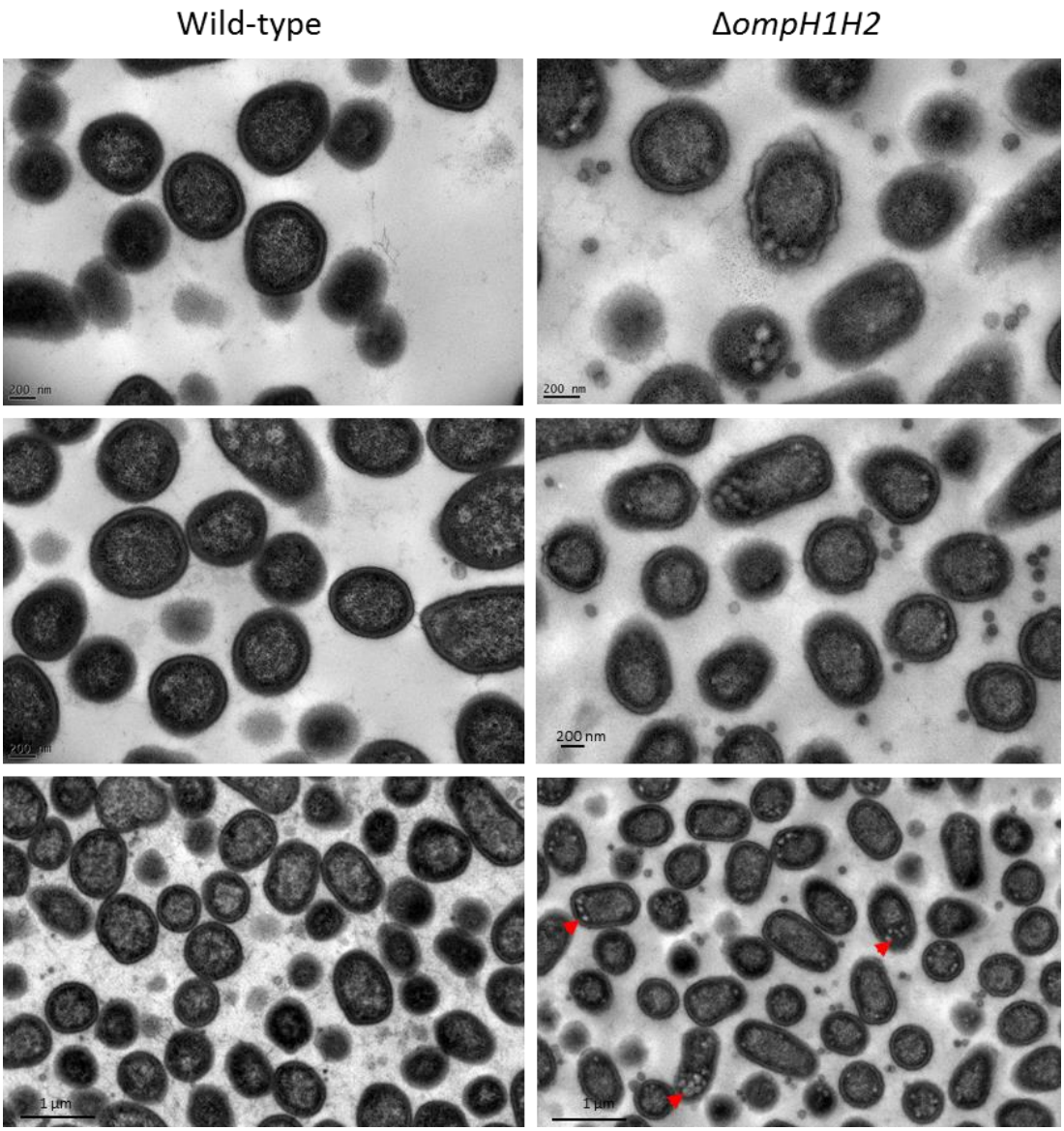

Figure 5.11. *P. gingivalis* wild-type and Δ*ompH1H2* membrane morphology assessed via TEM imaging. Wild-type (left) and Δ*ompH1H2* (right) images were taken at various magnifications, and represented by the scale bars at the bottom left of each image. Red arrows indicate cells of interest with significantly altered morphology.

From the TEM images, it is immediately apparent differences are observed between the wild-type and Δ*ompH1H2* strains in the number of vesicles observed with the Δ*ompH1H2* mutant appears to produce a higher number of vesicles than the wild-type. Alongside the increase in extracellular vesicles, the Δ*ompH1H2* mutant also appears to have a similarly

wavy membrane morphology in a significant proportion of the cells as observed previously in the Δ*ompA* mutants, although in this instance this occurs in a higher proportion of the population than previously observed, between 20-25% of the population compared to 3-4% seen for *ompA* mutants. Interesting to note were the cells indicated by the red arrows, which appear to have vesicle-like structures intracellularly.

As the number of vesicles produced in the Δ*ompH1H2* mutant appeared much larger, the number of vesicles produced by both the wild-type and the mutant was assessed using the qNANO as previously described. The count and the size of the vesicles can be seen in Figure 5.12.

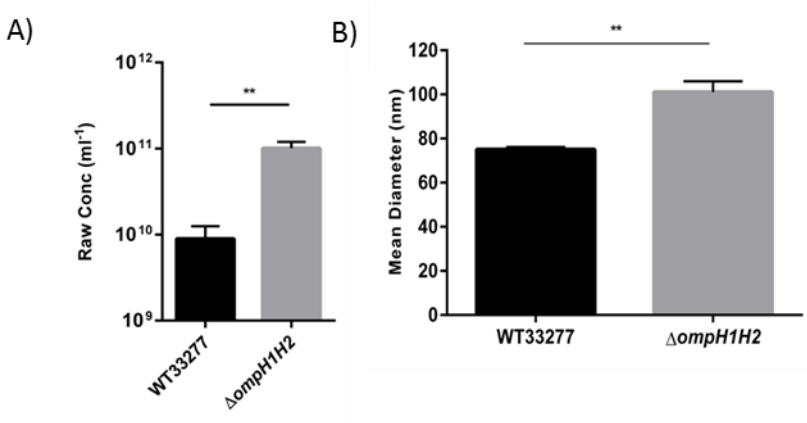

Figure 5.12 Assessment of OMVs of *P. gingivalis* wild-type and Δ*ompH1H2* mutant. Figure (A) demonstrates the raw count of vesicles (adjusted to the bacterial OD and calculated per ml of bacteria), whilst (B) compares the size of the vesicles observed. Vesicles were isolated from overnight liquid cultures as previously described and the raw count observed expressed on a log scale. Error bars represent ± SEM, and significance was assigned if $p < 0.05$ as determined by student's *t*-test. ** $p < 0.01$ (n=3).

The raw count demonstrates that the Δ*ompH1H2* mutant produced 10-fold more vesicles than the wild-type mutant (Fig. 5.12A, log scale). The average size of the vesicles produced is significantly larger (25%) than the wild-type, as shown in Figure 5.12B, where there appears to be a significant size shift in the vesicle diameter compared to the wild-type, suggesting a greater disturbance in the membrane integrity.

Together these data support the idea that the OmpH proteins are important chaperone proteins found in *P. gingivalis*, and the clients of these chaperones may be important in maintaining the integrity of the bacterium's membrane.

5.3.6 Assessment of the Integrity of the Outer Membrane in the Δ*ompH1H2* Mutant: Assessment of Permeability Using a Fluorescent Dye.

The second method utilised to study the membrane integrity of the Δ*ompH1H2* mutant was using thiazole orange coupled to stress-inducing conditions. Thiazole orange (TO) is a synthetic dye made up of two aromatic ring systems connected via a bond which, when bound to nucleic acids, becomes restricted causing an intense fluorescence (Nygren *et al.*, 1999). The most common uses for TO are in the detection of DNA in flow cytometry, especially in detecting reticulocytes (Lee *et al.*, 1986) or in general use for detection of DNA in gel electrophoresis (Rye *et al.*, 1992). For this investigation, TO was adapted as a detector for the permeability of the bacterial membranes, as an increase in fluorescence would indicate a higher permeability in the membranes, indicative of a lesser membrane integrity.

Liquid cultures of *P. gingivalis* were grown according to materials and methods 2.4.2, and the cells washed thoroughly in phosphate buffer to remove any extracellular DNA from lysed cells. In order to test membrane integrity the cells were tested for exclusion of the dye using 2-conditions, namely a low (0.001 % SDS) and high (0.025 % SDS) levels of detergent induced membrane stress. These were applied to the cells, and the rate of uptake of TO into the cells was measured for the wild-type and Δ*ompH1H2* mutant. The background rate of fluorescence was measured for 10 s before the TO dye was added and the change in fluorescence measured as a fluorescence trace (Fig. 5.13A). The rate of fluorescence uptake was determined from the trace, and plotted as the rate of uptake of TO (Fig. 5.13B) between the wild-type and Δ*ompH1H2* mutant in normal and stressed conditions.

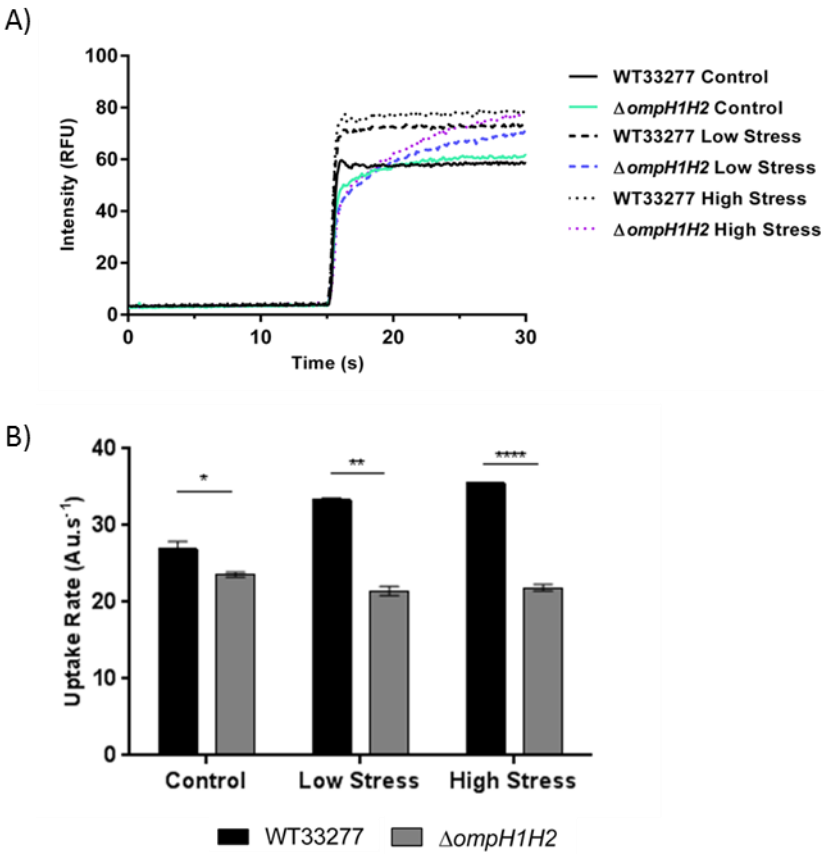

Figure 5.13 Membrane integrity assay using Thiazole Orange. Fluorescence of the wild-type and Δ*ompH1H2* mutant cells was followed during the addition of the thiazole orange (A), whereby the sharp increase in fluorescence intensity corresponds to the addition of TO at 15 s. Figure (B) demonstrates the rate of TO uptake for wild-type and Δ*ompH1H2* mutant cells (n=3). Error bars represent ±SEM, with significance assigned if $p < 0.05$ as determined by student's *t*-test. * $p < 0.05$. ** $p < 0.01$, **** $p < 0.0001$.

The fluorescence trace shows an increase in fluorescence in both strains when the stress agent (SDS) is applied to the cells, however it also shows a slower increase in fluorescence for the Δ*ompH1H2* mutant than the wild-type cells, in both non-stressed and stressed conditions. As the membranes of the Δ*ompH1H2* mutant were expected to be weaker and therefore would let more TO dye into the cells, this was the opposite of what was expected. In the original hypothesis that the membrane integrity would be weaker in the Δ*ompH1H2* mutant, this should demonstrate a higher rate of TO uptake in the mutant. However, what is actually observed is that the Δ*ompH1H2* mutant displays a significantly lower rate of uptake of the fluorescent dye. This may indicate that the OmpH chaperone delivers a protein to the outer membrane that is involved in the translocation of substrates across the

membrane into the cells, and the loss of the chaperone has removed this possible transporter from the membrane.

5.3.7 Assessment of Virulence Factor Production in the Δ*ompH1H2* Mutant

To attempt to determine the clients of the OmpH chaperone protein, various proteinaceous virulence factors of the Δ*ompH1H2* mutant were investigated. The sialidases of *P. gingivalis* were previously described as being important in the virulence of the bacterium in Chapter 3.3.3.4, so the activity of these enzymes was studied here. Sialidase activity of the whole cells were assessed as previously described in Materials and Methods 2.8.9.3, and determined as a fold-change compared to wild-type activity, as seen in Figure 5.14.

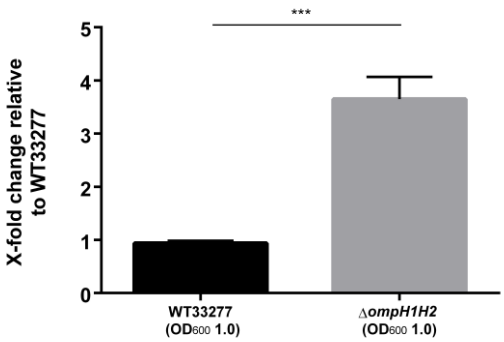

Figure 5.14 Sialidase activity of wild-type and Δ*ompH1H2 P. gingivalis*. Whole cell sialidase assays were assessed on liquid cultures of the two *P. gingivalis* strains as previously described in Materials and Methods 2.8.9.3. Sialidase activity of the Δ*ompH1H2* mutant was determined as a fold-change relative to wild-type (=1). Error bars represent ±SEM, with significance assigned if $p < 0.05$ as determined by student's *t*-test. *** $p < 0.001$.

Similar to the sialidase activity of the Δ*ompA* mutants, the sialidase activity of the Δ*ompH1H2* mutant was four-fold higher than the wild-type *P. gingivalis*. This coupled to the increase in the number of vesicles as seen in here in section 5.14, and the increase in vesicle numbers observed for the Δ*ompA1A2* mutant in Results Chapter 3.3.3.2 may suggest a greater number of sialidase enzymes being found on the vesicles, which often contain proteins from the outer membrane. This increase in sialidase activity also suggests that the sialidase protein is unlikely to be translocated across to the outer membrane by the OmpH chaperone.

As previously described, the gingipains are major virulence factors of *P. gingivalis*, and are highly active extracellular and surface proteinases. Recently, the gingipains have been shown to contain a C-terminal domain (CTD) which targets them for secretion through the Sec apparatus and the PorSS secretion system (the type IX secretion system), where they are processed and inserted into the cell surface or secreted into the extracellular space (Glew *et al.*, 2012; Sato *et al.*, 2013). The gingipain activity in the Δ*ompH1H2* mutant was investigated here, to determine if the secretion of the gingipains is affected by the loss of the OmpH chaperone.

Gingipain activity was assessed as previously described in Materials and Methods 2.8.9, and the activity of the whole cells was determined for both Rgp and Kgp-gingipains, as shown in Figure 5.15.

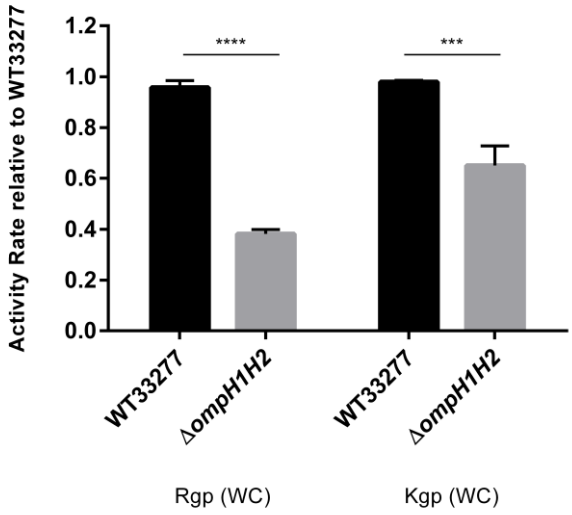

Figure 5.15 Whole cell Rgp and Kgp gingipain activity of wild-type and Δ*ompH1H2* *P. gingivalis*. Liquid cultures of *P. gingivalis* strains were grown and adjusted to OD_{600} 1.0 and the appropriate substrate added for Rgp or Kgp before the activity read over 30 mins. The rate of activity was determined by subtracting the Abs_{405nm} value at 1 min from 6 min when the rate of activity was still linear and plotted as a relative value compared to the rate of wild-type (=1). Significance was assigned if $p < 0.05$ as determined by student's *t*-test. *** $p < 0.001$, **** $p < 0.0001$ (n=3).

Whole cell gingipain activity was reduced 2.5- and 1.5-fold for Rgp and Kgp activity respectively. This reduction in activity suggests that the gingipain pre-proteins are transported across the periplasm by the OmpH chaperone proteins before being processed

and inserted into the outer membrane and this data potentially identifies a client of the OmpH chaperone, although further investigation is required.

5.3.8 Assessment of General Virulence of the Δ*ompH1H2* Mutant

As the importance of OmpH in the ability for *P. gingivalis* to interact with the host cell was originally indicated by the 4-fold upregulation in expression of the *ompH* genes in the hyperinvasive subset of the *P. gingivalis* population by Suwannakul *et al* (2010), the invasive and adhesive capabilities of Δ*ompH1H2 P. gingivalis* mutant was assessed in this study using standard antibiotic protection assays as previously described.

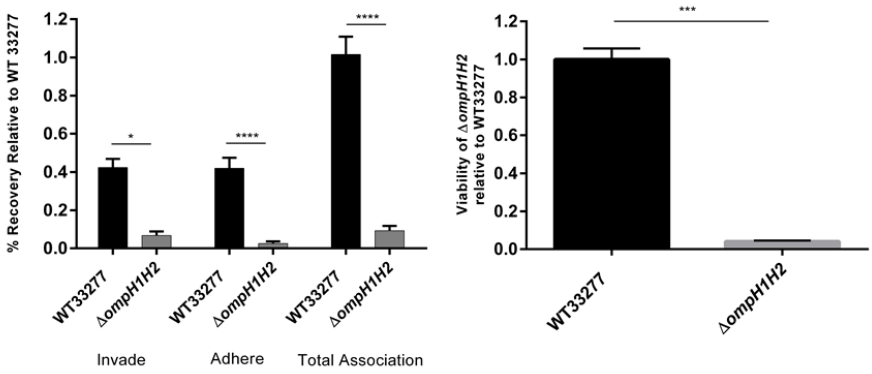

Figure 5.16 Standard antibiotic protection assay of wild-type *P. gingivalis* and Δ*ompH1H2* mutant. Standard antibiotic protection assay (A) was carried out as previously described. Bacterial strains were incubated with OK-F6 cells at 1:100 MOI and viable counts were taken for each strain and the number of bacteria recovered was determined as a % of the viable count. Invasion was defined as the percentage of the bacterial inoculum protected from metronidazole killing, whereas total association denotes the number of bacteria that adhere to and invade the OK-F6 cells. Adherence was determined by subtracting invasion CFUs from the total associated. Each % Recovery was corrected to the wild-type *P. gingivalis* total association (=1). The overall viability of the two strains was determined in (B) by calculating the bacterial counts at the end of the standard antibiotic assay and determining these as a percentage of the counts used to infect the cells, and made relative to the wild-type viability (=1). Error bars ± SEM. Statistical significance was defined by * $p < 0.05$, *** $p < 0.001$ and **** $p < 0.0001$, determined by students' *t*-test.

The ability of the Δ*ompH1H2* mutant to adhere to the cells has been almost completely abrogated, whilst the invasive capabilities are also significantly reduced. This was expected due to the changes to the outer membrane proteome, and indicates the OmpH chaperone protein is responsible for translocating proteins to the outer membrane involved in the

interaction with the host cell. The adherence and invasive capabilities resemble what is seen for the Δ*ompA1A2* double mutant, and considering there is a loss of detectable OmpA in the outer membrane preps (Fig. 5.10), this loss in the ability to adhere to an invade the host may be due to the loss of OmpA, supporting the idea the OmpA of *P. gingivalis* is a client of the OmpH chaperone, however, this would need further investigation to confirm.

The viability of the Δ*ompH1H2* mutant was significantly lower compared to the wild-type during the standard antibiotic protection assay, and this was expected as the outer membrane has been significantly altered in the Δ*ompH1H2* mutant. As the values for adherence, invasion and total association are determined as a percentage of the overall viability of that strain, this should not have had any masking effects on the values produced for invasion and adherence.

As the ability for *P. gingivalis* to form a biofilm is a key virulence factor, the biofilm forming capabilities of the Δ*ompH1H2* mutant was also determined. Biofilms were grown for 72 h in a 96-well polystyrene plate as previously described, and the overall growth was determined before analysis of the biofilm commenced. In 6 out of 9 experimental repeats, the overall growth of the Δ*ompH1H2* mutant was much lower than the wild-type, suggesting the effects of the loss of the OmpH chaperone proteins impedes the growth of the bacteria, which may influence the biofilm formation. The three experimental repeats that had similar levels of overall growth (biofilm and planktonic) were analysed for the biofilm formation through Crystal Violet staining and extraction, alongside visual imaging, as seen in Figure 5.17.

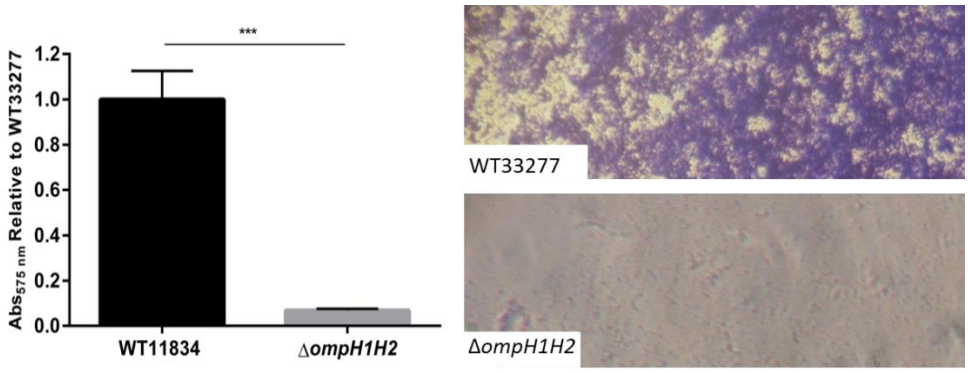

Figure 5.17 Biofilm formation of wild-type *P. gingivalis* and the Δ*ompH1H2* mutant. Biofilms were grown for 72 hours before the planktonic cells were removed and the resulting biofilm stained with 1% Crystal Violet. Biofilms were imaged under x400 magnification, and the Crystal Violet extracted using ethanol, and the Abs_{575} determined. The absorbance of the Crystal violet for the Δ*ompH1H2* mutant was determined relative to wild-type Crystal Violet extraction absorbance (=1). Error bars ± SEM. Statistical significance was defined by *** $p < 0.001$ as determined by students' *t*-test.

The ability of the Δ*ompH1H2* mutant to form a biofilm is greatly reduced, similar to what was previously observed for the Δ*ompA1A2* mutant. The mutant appears to no longer adhere to the plate well, and biofilm formation is visually abrogated. When the Crystal Violet was extracted, the quantifiable amount of biofilm that the Δ*ompH1H2* mutant formed was 14-fold less than the wild-type. This indicates that proteins in the outer membrane needed for biofilm formation may be chaperoned by the OmpH proteins, but similarly, as the biofilm in the Δ*ompA1A2* mutant was reduced 8.8-fold, this apparent loss of biofilm in the Δ*ompH1H2* mutant may be due in part to the loss of the OmpA protein.

These data together suggest that the OmpH protein is essential in chaperoning proteins involved in the virulence of the bacteria.

5.4 Discussion

In Gram negative bacteria, around one in five of the proteins transcribed are targeted for the outer membrane (Goemans *et al.*, 2014). Newly synthesised proteins destined for the outer membrane through the Sec machinery need a chaperone protein to escort them through the periplasm to reach the outer membrane (Hagan *et al.*, 2011). As these proteins enter the periplasm in an unfolded state, they are much more likely to aggregate in the aqueous environment, and therefore folding pathways exist to prevent the aggregation and

also assist the folding of these outer membrane proteins (Entzminger *et al.*, 2012). These chaperone pathways have been studied at great length in *E. coli*, with the major chaperone pathway involving the SurA protein and the secondary pathway consisting of the Skp and DegP proteins (Sklar *et al.*, 2007). Analysis of Gram-negative genomes using the SEED analysis tool, applied to the national microbial pathogen data resource database (http://www.nmpdr.org/FIG/wiki/view.cgi) which is supported by protein entries from KEGG, NCBI, UniProt etc., demonstrates the appearance of these three proteins in a vast number of bacteria, with nearly all Gram-negative genome entries containing the SurA protein, and slightly fewer containing the Skp and DegP proteins demonstrating these proteins are widely used for protein chaperoning across the periplasm.

Bioinformatics analysis of *P. gingivalis* demonstrated all three of these chaperone-related proteins are observed in *P. gingivalis* (Skp – PG0192/3 or OmpH1/2; SurA – PG0415; DegP – PG0593) indicating a similar pathway to *E. coli* for the delivery proteins through the Sec pathway to the outer membrane across the periplasmic compartment. The importance of the OmpH of *P. gingivalis* was identified previously by Suwannakul *et al* (2010), who observed a signature set of genes that are differentially regulated in a hyperinvasive subset of the *P. gingivalis* population (Suwannakul *et al.*, 2010). Within this set of genes, *PG0193* (OmpH2) was upregulated 4-fold in the highly invasive subset, indicating an involvement in delivering proteins to the outer membrane that are involved in adherence to and invasion of the host cell.

Outer membrane proteins found upregulated in this signature gene set include *PG0063* and *PG1058*, both putative outer membrane proteins with no assigned function yet. As these proteins are upregulated 6.3- and 4.65-fold in the hyperinvasive population of *P. gingivalis* (Suwannakul *et al.*, 2010), they may be involved in the adhesion and invasion of the host and may be clients of the OmpH chaperone. Another outer membrane protein upregulated in this gene set is the TonB-dependant receptor, *hmuR*, which is a hemin-binding protein (Simpson *et al.*, 2000), and may be important in scavenging in the hemin-limiting environment inside the host cell.

The function of these outer membrane proteins and their relation to the invasion of the host is an exciting area to investigate further in future work on this project. Creation of null mutants in these genes has already begun, but due to time constraints, no further analysis has occurred. Through these mutants, investigation of their ability to invade the host cell could potentially provide new insights into proteins needed for host cell interaction and

therefore potentially allude to new therapeutic targets to combat *P.* gingivalis-associated periodontal disease.

The creation of the Δ*ompH1H2* mutant proved to be unsuccessful for a number of attempts, and therefore allowed some optimisation of the methods of *P. gingivalis* transformation found in the literature. The traditional method of mutagenesis of *P. gingivalis* involves introducing the DNA via electroporation (Yoshimoto *et al.*, 1993), however this method involves multiple time-consuming steps, increasing the amount of aerobic exposure the bacterium has, followed by reduction in viability with the electric pulse and reducing the efficiency of this method. More recently, a mutagenesis method was developed which exploits the natural competency found in the *P. gingivalis* bacterium (Tribble *et al.,* 2012), which limits the aerobic exposure and eliminates the need for the electric pulse, resulting in a higher number of viable cells for DNA uptake. Although this natural competency method was successful for the creation of Δ*ompA1* and Δ*ompA2* mutants, initial attempts at the creation of Δ*ompH1H2* proved ineffective.

As the electrocompetency method requires a high number of bacteria to begin with, liquid cultures of wild-type *P. gingivalis* were used for the electroporation as previously described. Optimisation of the method involved the post-introduction of the DNA incubation as either in a liquid culture or on a BA-plate, before transferral to an erythromycin-containing plate for generation of the mutants. Optimisation of the natural competency transformation method involved the preparation of the wild-type *P. gingivalis* starter cultures from either a liquid culture or from a 3-day old BA plate, and after the introduction of the DNA, incubating for 24 hours either on in a fresh BHI broth or on a BA-plate before transferral to erythromycin-containing BA-plates. Successful mutant colonies were only produced using starter cultures from a liquid origin in the natural competency, and no colonies were observed in the electrocompetency. Liquid starter cultures were also more successful at generating colonies for the knock out mutagenesis of *ompA1* and *ompA2* mutants, showing a development and optimisation of existing mutagenesis methods of *P. gingivalis.*

General characterisation of the Δ*ompH1H2* mutant demonstrated an altered colony phenotype when growing on BA-plates, with a much larger colony size and a glossy appearance. The colonies also required a longer growth period to turn from brown to black, potentially indicating a potential client of the OmpH chaperone related to hemin-acquisition. When the outer membrane protein profiles of the wild-type bacteria to the

Δ*ompH1H2* mutant were compared, an obvious difference in protein banding was observed between the two which suggests the OmpH protein is involved in the chaperoning of multiple outer membrane proteins. Further analysis of the outer membrane proteins affected by the loss of the OmpH protein involved the probing for the OmpA protein specifically, as many papers have previously reported the loss of OmpA in an *E. coli skp* mutation (Chen and Henning, 1996; Missiakas *et al.*, 1996; Schäfer *et al.*, 1999; Bulieris *et al.*, 2003). Using an anti-OmpA antibody, no OmpA protein was observed in the purified outer membranes of *P. gingivalis* Δ*ompH1H2*, suggesting this protein is translocated across the periplasmic space via the OmpH chaperone.

As mentioned previously folding and insertion of OmpA in *E. coli* has been shown to be assisted by Skp/OmpH, but there also is a requirement for LPS in the insertion of the protein into the membrane. Previous studies have shown the folding of OmpA into phospholipid bilayers occurs (Surrey and Jähnig, 1995; Surrey *et al.*, 1996) but the kinetics of this folding are relatively slow. The Skp/OmpH protein is capable of binding OmpA and keeping it unfolded, but this inhibits the folding of the protein and insertion into the membrane. The Skp-OmpA complex therefore interacts with the LPS and the Bam complex to facilitate OmpA insertion into the membrane where folding can occur (Bulieris *et al.*, 2003). It would be interesting to determine if this is the case for *P. gingivalis* OmpH/OmpA interactions.

When the bacteria were visualised through TEM, the most striking difference in the phenotype of the Δ*ompH1H2* mutant was the presence of intracellular vesicle-like structures. At present we have no idea what these might be but it is tempting to hypothesise that these might be inclusion bodies containing proteins that have been targeted for secretion to the outer membrane but remain stuck in the cytoplasm where they potentially aggregate and appear as these structures in the cell. Another apparent difference between wild-type and Δ*ompH1H2* was the vast increase in vesicle production, which was supported by performing vesicle counts with the qNANO. This increase in the number of vesicles is likely due to the loss of integral outer membrane proteins that would usually anchor the outer membrane to the peptidoglycan layer. One of these proteins lost is likely to be the OmpA protein, as this hypervesiculation was observed in the Δ*ompA1A2* mutant in Chapter 3.3.3.2 as well as in previous studies (Nagano *et al.*, 2005), coupled to the loss of detectable OmpA in the purified outer membranes of Δ*ompH1H2* when probed with anti-OmpA antibody during Western blotting.

Due to the apparent loss of significant proteins from the outer membrane, leading to hypervesiculation and the "wavy" membranes observed in the TEMs, the integrity of the membrane was assessed using a dye that increases in fluorescence when encountering DNA, i.e. a higher level of fluorescence would be observed if the cell membrane integrity was limited by the loss of outer membrane proteins. Surprisingly, there was no difference in the membrane integrity between the wild-type cells and the Δ*ompH1H2* mutant, even when stress to the membrane was applied. Indeed the opposite was observed, whereby instead of seeing a higher rate of uptake of the dye in the mutant, it was observed that the dye entered the mutant cells at a lower rate. This was hypothesised to be due to the loss of a protein transporter on the outer membrane of the cell so less of the dye is transported into the cell, although this is unconfirmed experimentally. Future work on the identification of the proteins that are chaperoned by the OmpH protein may reveal outer membrane protein transporters that would explain this phenomenon.

During the course of this part of my work a paper was published (Taguchi *et al.*, 2016) where the authors had produced a mutant of the *ompH1* gene and assessed its phenotype. This work originally identified only the OmpH1 protein subunit (not OmpH2) to contain a transmembrane helix, but only assessed this through one prediction software programme. However, bioinformatics analysis of both subunits through 3 different programmes suggested that both subunits contained an α-helix transmembrane domain in two out of three cases. Taguchi *et al*., only created an Δ*ompH1* strain and suggested that Δ*ompH2* was an essential gene as a viable mutant could not be made. However in the case of the work presented here, this seems not to be the case as an entire Δ*ompH1H2* mutant has been created (Taguchi *et al.*, 2016). Taguchi *et al* also identified the co-transcribed operon that *ompH* is encoded by, containing genes *PGN_0296*, *PGN_0297*, *PGN_0298*, *PGN_0299* (which bioinformatic analysis in this work identified it as Omp85, or BamA, which is also found in the Skp-encoding operon of *E. coli*), and the two *ompH* genes (*PGN_0300* and *PGN_0301*).

Taguchi *et al* also provided a general characterisation of the phenotype found in the Δ*ompH1* mutant. Cell lysates and outer membrane preparations showed a much less dramatic alteration in the outer membrane protein profile than seen in the double Δ*ompH1H2* mutant that is observed in this work, suggesting that the OmpH2 protein may have a much larger client set of proteins to be chaperoned to the outer membrane than OmpH1, or that the two OmpH protein subunits work as a complex to chaperone a large

number of proteins to the outer membrane. Identification of the client set of protein for OmpH is a major part of the future work of this project, and it would be interesting to determine if OmpH1 and OmpH2 had a different set of specific proteins, or if it relies on both OmpH1 and OmpH2 protein subunits to be present in a complex. The phenotypic analysis by Taguchi *et al* also demonstrated a loss in pigmentation and haemagglutination which lead to the possibility that the presence of properly processed gingipains had been lost due to the *ompH1* mutation. Work in this chapter also concurred with this loss in gingipain activity, showing similar levels of reduction. Taguchi *et al* related the reduction in gingipains to the presence of a C-terminal domain in the gingipain proteins which targets it to the PorSS pathway of secretion (Seers *et al.*, 2006). MALDI-TOF analysis in their study of the Δ*ompH1* culture supernatants demonstrated the presence of several immature forms of CTD-containing proteins amongst others, suggesting that the OmpH protein may act as the chaperone protein for the PorSS pathway of secretion (Taguchi *et al.*, 2016). Homologs of the OmpH protein exist in various Gram–negative bacteria, as previously discussed (Chapter 1.6.13.), including *B. fragilis* which does not have a PorSS system (Narita *et al.,* 2014), and the fact that proteins such as OmpA do not possess a CTD but (as shown in this study) but appear to be a client of the OmpH chaperone complex suggest that it is likely that the OmpH chaperone complex doesn't act solely as the chaperone for the PorSS pathway but more as a general non-specific chaperone.

Future work would involve the confirmation of the OmpA protein being a client of the OmpH chaperone, as observations here have indicated it is. Using anti-OmpA antibody used in this study, future experiments could investigate the presence of OmpA on the surface of Δ*ompH1H2 P. gingivalis* using fluorescence microscopy, to allow a native visualisation of what is expected from the lack of protein on the Western blot. Previous studies have shown that the aggregation of overexpressed *E. coli* OmpA is prevented in the presence of buffers containing Skp trimers, which are then assessed using size exclusion chromatography to demonstrate a 1:1 binding between Skp and OmpA (Walton *et al.*, 2009), which could be applied to the OmpA and OmpH proteins of *P. gingivalis* to determine binding. As the study by Walton *et al* also demonstrates the β-barrel of the OmpA protein is bound inside the cavity of the trimeric Skp to prevent aggregation (Walton *et al.*, 2009), the deletion of certain sections of the *P. gingivalis* OmpA protein could be investigated to determine initially if OmpH binds OmpA, and also if it acts via similar mechanisms.

Further investigation into the characterisation of the Δ*ompH1H2* mutant involved the investigation of the virulence of the bacteria through biofilm formation and standard antibiotic protection assays. The loss of the OmpH chaperone protein in *P. gingivalis* has led to a significant reduction in the ability for *P. gingivalis* to form a biofilm, an essential part of the formation of dental plaque, and this ability of *P. gingivalis* to form a biofilm allows the contribution of the bacterium to shift the balance of microflora in dental plaque from a healthy to disease associated state when major ecological pressures arise (Marsh, 2003), leading to periodontitis. This loss in biofilm formation would remove the contribution of *P. gingivalis* in the progression of the imbalance of bacteria to the disease associated state, and reduce the severity of the disease, as *P. gingivalis* has been ascribed a keystone pathogen of periodontal disease (Hajishengallis *et al.*, 2012). Identification of the proteins that are chaperoned by OmpH would allow investigations into the proteins involved in the biofilm formation, and therefore contribute to the understanding of the ability of *P. gingivalis* to cause disease and potentially identify therapeutic targets to block biofilm formation and reduce the capacity for disease.

The Δ*ompH1H2* bacteria also had a significant reduction in the ability to adhere to and invade the host cell, an essential virulence factor in the progression of periodontal disease. The invasion of the host is critical for *P. gingivalis* to remain hidden from the host immune system whilst replicating intracellularly and persisting to lead to a chronic infection (Hajishengallis, 2010). The loss of the OmpH protein led to a greatly significant reduction in the ability for the bacteria to adhere to the host cells and a major reduction in the invasion of the host, indicating proteins chaperoned by OmpH to the outer membrane are essential in the ability for *P. gingivalis* to interact with the host.

With this loss of biofilm and invasive capabilities in mind, it would therefore be ideal to identify the proteins that are affected by the loss of OmpH, which would lead to the identification of the proteins that are chaperoned by OmpH. This would be performed using purified outer membranes of both wild-type and Δ*ompH1H2* and investigating which proteins differ using mass spectrometry. This work was started during this project but due a lack of time, it could not be investigated fully. Alternatively, affinity chromatography with immobilised OmpH could be employed to ascertain the clients of the OmpH chaperone protein, and identify the proteins of interest by mass spectrometry identification of the altered proteins identified by SDS-PAGE. This work was begin during this project, with the identification of a few potential candidates on the SDS-PAGE seen in Figure 5.9, however,

these were only observations and need to be identified fully in future work. Once the proteins that interact with the OmpH chaperone are identified, they would be investigated for their function on the outer membrane and could then be used as a target for therapeutic agents. This could eventually lead to the design of an agent to specifically target *P. gingivalis* as it is considered to be the keystone pathogen of periodontal disease (Hajishengallis *et al.*, 2012), leaving the rest of the healthy-related microflora viable and maintaining the homeostasis within the oral cavity.

5.5 Summary

In conclusion, this chapter has enforced the hypothesis that OmpH has a role in the chaperoning of proteins to the outer membrane and the deletion of the OmpH proteins leads to a distinctly different phenotype due to the loss of integral outer membrane proteins. This chapter has determined a significantly altered outer membrane protein profile, and identified the loss of multiple outer membrane proteins which opens up the exciting opportunity to identify these proteins that act as clients of the OmpH chaperone. This chapter has also potentially identified OmpA and gingipains as proteins that are chaperoned by the OmpH protein, as demonstrated by a loss of detectable OmpA on the outer membrane of the Δ*ompH1H2* mutant and a reduction in the gingipain activity. This chapter demonstrated a significant loss of virulence in the Δ*ompH1H2* mutant and therefore identification of proteins lost from the outer membrane could lead to exciting new possibilities for potential therapeutic drug targets to combat periodontal disease.

Chapter 6

Discussion & Future Prospects

6.1 Summary of Major Findings

The work described in this thesis has provided a deeper understanding of the molecular mechanisms behind *P. gingivalis* major outer membrane protein, OmpA, and its interaction with the host, followed by a preliminary characterisation of the putative periplasmic chaperone, OmpH.

Unpublished data from Suwannakul *et al* (2010) demonstrated an upregulation of the *ompA1* and *ompA2* genes in a hyperinvasive population of *P. gingivalis* (Suwannakul *et al.*, 2010), indicating the potential involvement of the OmpA protein in adherence and invasion of the host cell. This data also identified a set of genes that were differentially regulated in this hyperinvasive subset of the population, which identified the putative OmpH chaperone protein as being upregulated four-fold, signifying potential importance in invasion, and thus produced the basis for the third chapter investigation.

The hypothesis behind the importance of OmpA was developed through the apparent involvement of OmpA in adherence and invasion of the host for several species, including *E.coli* K1 (Prasadarao *et al.*, 1996; Shin *et al.*, 2005), *N. gonorrhoeae* (Serino *et al.*, 2007), and indeed with *P. gingivalis* OmpA involvement in endothelial cell invasion (Komatsu *et al.*, 2012). This coupled with the fact that surface exposed proteins are potentially the first line of interaction with human surfaces and cells means the importance of understanding their molecular biology is key to understanding the basis of host-pathogen interactions and in this cases periodontal disease. As the health of the oral cavity is an extremely complicated balance of host and bacterial factors, this study into investigating the disease-causing bacterium at the molecular level and determining specific proteins involved would allow a the design of particular therapeutic agents to for a targeted defence against the pathogen, reversing dysbiosis and repopulating the commensal bacteria to return once again to a healthy periodontium.

As a prelude to a final discussion I have summarised the major findings from each part of the thesis.

6.1.1 Chapter 3: Role of the *ompA* Gene Cluster in Host-Cell Interactions and Biofilm Formation

This chapter focussed on the effects of the deletion of the *ompA1A2* operon and its individual *ompA1* and *ompA2* genes. The following major results and conclusions were drawn:

- In determining an effective mutagenesis method for *P. gingivalis*, electrocompetency and natural competency techniques were employed to introduce DNA for the creation of the *ompA1* and *ompA2* mutants. Natural competency demonstrated a significantly higher number of colonies produced per µg of DNA used, regardless of the origin of the DNA (plasmid or linear). As this method of transformation proved to be much more efficient, it was therefore implemented in the laboratory as a standard method of transformation for oral anaerobic bacterial mutagenesis and is used by many of the group members.
- TEM was used to study the effects of the deletion of the OmpA protein from the outer membrane. This demonstrated an instability of the membranes with the loss of the protein, with "wavy" membranes observed in a small number of the population. As the structure of the OmpA protein involves a β-barrel located in the outer membrane, linked to a peptidoglycan-associated domain, this loss of an outer membrane protein that would anchor the outer membrane to the bacterial cell, creating this membrane instability. The TEM images also displayed the presence of outer membrane vesicles, of which a significantly higher number were produced in the *ompA1A2* mutant, and a slight increase in the *ompA1* and *ompA2* mutants. This supports the idea that the OmpA protein plays an important role in the stability of the *P. gingivalis* membrane, and agrees with similar data shown by others (Iwami *et al.*, 2007).
- The ability of *P. gingivalis* to form a biofilm is an important virulence factor, as this ability contributes to the formation of biofilms on tooth structures, leading to the accumulation of dental plaque. Biofilm formation was assessed to understand the role of OmpA in adherence to surfaces, as well as itself. In all mutants, the biofilm appeared to be more fragile, however a marked decrease in the ability of the *ompA2* and *ompA1A2* mutants to form a biofilm was observed, both through qualitative and quantitative means. As the *ompA1A2* mutant shows a vast difference in all aspects analysed throughout this thesis (membrane profile, membrane stability, vesicles, enzymatic assays etc.), it was interesting to observe a similar lack of biofilm formation in the *ompA2* mutant, which portrayed the first indication that this protein subunit may have a greater role within the OmpA protein complex in interactions with its environment.
- This is the first time that the OmpA protein has been shown to be involved in the interactions with oral epithelial cells, and in particular the data presented in this

thesis show a specific and significant role for the OmpA2 protein subunit. Through standard antibiotic protection assays, the ability of *P. gingivalis* wild-type and *ompA* mutants to adhere and invade oral epithelial cells was assessed. Whilst the *ompA1* and *ompA2* mutants showed a 50 % reduction in adherence, whilst the *ompA1A2* mutant lost almost all ability to adhere to the cell. Interestingly, the intracellular count of *ompA2* mutants resembled the *ompA1A2* mutant with a significant reduction in the invasive capability whilst Δ*ompA1* intracellular numbers were closer to wild-type. This result indicates that the OmpA2 protein the dominant subunit involved in the events leading to internalisation, whilst both subunits are required for effective adherence.

- As the deletion of *ompA2* appeared to show a greater effect in both biofilm and host cell interaction, a complement of this mutant was used to confirm the loss of biofilm formation and interaction with the host was due to the loss of the protein, not any downstream effects. The Δ*ompA2* + pT-COW-*A2* complement partially but significantly rescued the biofilm formation phenotype, whilst fully rescued the adherence and invasion phenotype, confirming the importance of the OmpA2 subunit in these virulence factors.

6.1.2 Chapter 4: Molecular Mechanism of OmpA Interaction with Host Epithelial Cells.

This chapter focussed on the purification of the OmpA protein to determine the molecular mechanisms behind its interaction with the host cell. Despite numerous attempts at purifying soluble OmpA, including using solubilising agents, the use of binding proteins, truncated protein purification, making additions to the dialysis buffer, protein remained insoluble and therefore other methods of determining the molecular mechanism behind the host cell interactions were studied.

- The structures of the OmpA proteins were determined using online prediction software, yielding a structure with high homology to the OmpA proteins found in *E. coli* and *Klebsiella pneumoniae*, with the classic two-domain structure of a β-barrel and a peptidoglycan-associated globular domain. This structure also indicated the presence of extracellular surface loops, which due to the predicted orientation of the protein; these would be exposed on the outside of the *P. gingivalis* cell. The hypothesis developed that these loops would be the part of the protein exposed and therefore involved in the interaction with the host cell.

- The extracellular loops were synthesised and used in place of recombinant OmpA protein in further experimental analysis. These loops, when included in a standard antibiotic protection assay with wild-type *P. gingivalis* successfully interrupted the adherence and invasion of the bacteria, indicating that these loops are binding to the host cell receptors, and efficiently preventing the binding of *P. gingivalis.*
- Peptide 4 was especially effective at preventing the adherence and invasion of *P. gingivalis* to host cells, so a scrambled peptide was designed against this sequence, which when included in standard antibiotic protection assays as a negative control, showed no interruption of *P. gingivalis* interaction with the host, indicating a strong and specific interaction of peptide 4 of OmpA2 with human cells.
- The synthesised peptides were designed with an N-terminal Biotin tag, which was used to bind the peptides to fluorescent microspheres. These peptide-coated microspheres were applied to monolayers of oral epithelial cells and the binding of the peptides to the cells analysed, which displayed a significant level of all peptides binding to the host cells, with peptide 4 displaying the greatest increase in binding, especially when compared to the control scrambled peptide.
- These data together demonstrate the peptides are sufficient to allow direct binding to the host, and therefore greatly imply that there is a direct binding between OmpA2 and the host cell. This data also supports the hypothesis that the reduced invasion phenotype in Chapter 3 of the Δ*ompA2* mutant is due specifically to the lack of the OmpA2 protein subunits.

6.1.3 Chapter 5: Preliminary Characterisation of the Putative OmpH/Skp Locus of *P. gingivalis.*

This chapter focussed on the characterisation of the putative outer membrane protein chaperone, OmpH, a protein whose gene transcript had previously been shown to be upregulated in *P. gingivalis* cells with a 'hyperinvasive' phenotype. The following major results and conclusions were drawn:

- The generation of an *ompH1H2* mutant allowed further development of the mutagenesis method of *P. gingivalis.* This involved the optimisation of the starting cultures and 24 hour incubation after the introduction of the DNA for both electroporation and natural competency methods. The optimisation of the method confirmed the efficiency of the natural competency versus electroporation, however within the natural competency method, liquid cultures proved to be the

most efficient mutagenesis method. This further optimisation over that in chapter 3, has been further implemented as general lab practice for anaerobic bacterial mutagenesis within the Stafford group at The School of Clinical Dentistry.

- Initial studies of the *ompH1H2* mutant demonstrated a much larger colony size and a glossy, brown phenotype, suggesting an alteration to the outer membrane protein profile. This was confirmed through purification of the outer membrane proteins and analysis on SDS-PAGE gels, showing multiple absent protein bands, which at this stage have yet to be identified.
- TEM imaging of the *ompH1H2* mutant was performed, where a much higher proportion of the mutant population displayed the "wavy" membranes, indicating a higher level of membrane instability with the loss of various outer membrane proteins. This instability was supported by the significant increase in vesicle production observed in the mutant.
- The presence of specific proteins was analysed through Western blot, which demonstrated the loss of the OmpA protein and the fimbrial proteins in the *ompH1H2* mutant, indicating that these proteins may be clients of the OmpH chaperone system. The presence of other outer membrane proteins such as the sialidases and the gingipains were analysed through enzymatic assays. Sialidase activity was increased to similar levels observed for *ompA1A2* mutants in chapter 3, which again were hypothesised to be due to the increase in the production of outer membrane vesicles. The gingipain activity, however, was significantly reduced in the *omH1H2* mutant, suggesting that these proteins are also potential clients of the OmpH chaperone.
- Similar to the *ompA1A2* mutant phenotype in Chapter 3, the *ompH1H2* mutant showed a complete abrogation of the ability to form a biofilm, with almost no bacteria adherent to the polystyrene plate surface. This loss of adherence was also observed in the standard antibiotic protection assay, whereby the mutant could no longer adhere to the oral epithelial cells, and very few were observed intracellularly. This data indicates that the outer membrane protein clients of the OmpH chaperone are crucial to the ability of *P. gingivalis* to interact with the host cell, and therefore to its ability to contribute to periodontal disease.

6.2 Host Cell Interaction of *P. gingivalis* with Human Cells: OmpA Surface Loops at the Host-Interface

The data presented in this thesis has contributed to our understanding of the molecular determinants of host-cell interactions by *P. gingivalis* where previous studies have focussed chiefly on gingipains (Chen *et al.*, 2001; Chen and Duncan, 2004), fimbriae (Hamada *et al.*, 1994; Weinberg *et al.*, 1997; Njoroge *et al.*, 1997) and haemagglutinin type proteins (Chen *et al.*, 2001; Song *et al.,* 2005; Bélanger *et al.*, 2012).

Specifically, my work has elucidated that the OmpA protein complex plays a key role in adhering to and invading the host epithelial cells, independent of existing mechanisms of host-cell interaction as shown by no change in the fimbriae expression and gingipain activities in the *ompA1* and *ompA2* mutants. This work has also provided novel data demonstrating the particular importance of the OmpA2 protein subunit extracellular loops in this interaction. However, one of the major aims when this work began was to eventually identify the host cellular target that OmpA interacts with. Due to the pitfalls of production of soluble outer membrane proteins, such as OmpA, this particular focal point of the project was never reached. Previous reporting into the identification of the host cell receptor engaged by *P. gingivalis* OmpA indicate a potential interaction with E-selectin on the cell surface of endothelial cells (Komatsu *et al.*, 2012), however there is no evidence for this being the case for epithelial cells, and the presence of E-selectin on epithelial cells remains unclear (Moughal *et al.*, 1992; Pietrzak *et al.*, 1996). The OmpA of *E. coli* K1 has been shown to potentially interact with the gp96 receptor (Prasadarao *et al.*, 1996), with the extracellular loops being of particular importance in this interaction (Mittal and Prasadarao, 2011; Mittal *et al.*, 2011). The extracellular loops of *E. coli* OmpA show little homology to the extracellular loops determined in this project, however the observation that the peptides interrupted wild-type *P. gingivalis* from adhering and invading the host cell provides potential that these peptides could be used to identify the epithelial cell receptor for *P. gingivalis* OmpA. This would be achieved through immobilising the peptides on Avidin-coated resin by binding the biotin tag, and running host cell lysates over them, capturing any binding between host cell proteins and the OmpA2 extracellular loop peptides. Binding partners would then be purified and identified through mass spectrometry; however time constraints on this project have left this only as promising future work.

Identification of the host cell target would lead to the investigation of the molecular mechanisms behind invasion of the cell. Invasion of *P. gingivalis* using the fimbriae has been well documented, whereby the fimbriae engage the $\alpha_5\beta_1$ integrins on the epithelial cell surface, leading to a kinase signalling cascade being triggered and the rearrangement of the cytoskeleton (Yilmaz, 2003). If similar host cell targets were identified for the OmpA protein, this would indicate a similar mechanism of invasion. Alternatively without the identification of the host cell target, future work to investigate if this molecular mechanism is also triggered by the OmpA protein binding could be performed using fluorescent tagging of the actin filaments to determine if the cytoskeleton is rearranged in a similar fashion to the fimbrial FimA binding trigger.

6.3 Periodontal Disease: A Targeted Approach?

As this research has highlighted a role for OmpA in the adherence and invasion of the host, it is therefore a possibility to target this particular protein for therapeutic treatment development. This approach to targeted treatment of periodontal disease is a highly significant area for exploratory study, as the oral cavity contains a plethora of bacterial species with only a certain few that contribute to disease (Socransky *et al.*, 1998; Aas *et al.*, 2005; Pennisi, 2005). The identification of the OmpA protein in the influence of the disease progression of the host by *P. gingivalis* coupled to the hypothesis of *P. gingivalis* being the keystone pathogen of periodontal disease (Hajishengallis *et al.*, 2012), this targeted treatment is a realistic possibility of tackling the ever burdening issue of periodontal disease. As OmpA-like proteins can be found in all Gram-negatives (Beher *et al.*, 1980), and Gram-negative bacteria have been implicated in the dysbiosis imbalance of the oral cavity and are heavily present in periodontal disease, using the OmpA as a target in periodontal treatment may allow a specific combat of the disease-causing periodontal pathogens. It would be interesting to determine the structural similarities of the OmpA proteins in the red complex bacteria, and any similarities of their extracellular loops for this specific approach. This area of future research is also interesting given that anti-OmpA1A2 protein serum can also bind the OmpA protein of *T. forsythia* (designated TF1331) (Imai *et al.*, 2005; Veith *et al.*, 2009; Abe *et al.*, 2011), another oral pathogen found in severe cases of periodontal disease, this OmpA-targeted approach may have further benefits in patient treatment.

The identification of the extracellular surface regions of OmpA2, leading to the generation of peptides yielded very exciting data on the ability of these extracellular loops to directly

bind the host cells and interrupt *P. gingivalis* interacting with the host. The possibility remains to further investigate these peptides, in altering the sequence to favour binding, or to identify particular residues necessary for the binding and eventually to allow development of novel anti-adhesive therapeutic agents to prevent *P. gingivalis* binding efficiently to the host. As adherence is one of the first steps of host colonisation, this would be advantageous as it could provide a block to a specific interaction between *P. gingivalis* (and possibly other periodontal pathogens binding through OmpA) and the host to prevent the adherence and invasion and therefore the progression to chronic periodontitis. Anti-gingipain peptides have been previously developed for therapeutic use, specifically a study by Genco *et al* (1998) used the N-terminal sequence of the catalytic domain of the gingipain R1 which conferred resistance in mice against *P. gingivalis* infection (Genco *et al.*, 1998), suggesting a possibility to use these peptides as therapeutic agents. Caution with the use of peptides in therapeutics would have to be considered as except for a general toxicity study in Figure 4.25, no data has been observed for the immunogenic effects of the OmpA peptides used in this study in the host. Traditionally, therapeutic peptides show poor physical stability and have a short half-life (Fosgerau and Hoffmann, 2015). However, if these peptides are incorporated into a topical preventative treatment such as a toothpaste, gel or a mouthwash, this would circumvent the short half-life but may also stimulate immunity, though this may prove to be potentially interesting in terms of vaccines.

Previous reports have used the keystone-pathogen hypothesis to theorise that a vaccination of *P. gingivalis*-specific extracellular structures would reduce periodontal disease progression. Indeed, analysis of 14 clinical strains and isolates demonstrated a high level of conservation between *P. gingivalis* strains (Ross *et al.*, 2001) so recombinant versions of OmpA proteins were used as a vaccine and provided protection in murine models (Ross *et al.*, 2004). The protein provided some protection against development of oral lesions in the mouse model but showed no reduction in alveolar bone loss when orally challenged (Jong and van der Reijden, 2010), and therefore provides only partial protection against the development of periodontal disease. Issues with the OmpA protein solubility still remain, and would provide a great impracticality to use the whole or large sections of the OmpA protein as the sole determinant in the vaccine. Future work into the extracellular peptides of OmpA2 identified in this study may involve the investigation into generating an immune response from the peptides, and determine if they would be an appropriate vaccine candidate.

Outer membrane protein of *P. gingivalis* have been previously investigated as vaccine candidates, with moderate success (Maeba *et al.*, 2005; Liu *et al.*, 2010; Cai *et al.*, 2013). The use of various outer membrane proteins in these studies showed protection against alveolar bone loss, both through introduction as an injection or nasally, and especially proved effective when introduced with a modified cholera toxin (Cai *et al.*, 2013), displaying a potential path for using OmpA as a vaccine candidate.

To use the peptides as a potential vaccine, the effects on the host immune system would have to be thoroughly investigated. Previous studies of the effect of OmpA, using the *Klebsiella pneumoniae* protein, on the host innate immune response have shown an importance of OmpA as a bacterial ligand which binds to and triggers internalisation by dendritic cells and macrophages, which activates them in a TLR2-dependant manner (Jeannin *et al.*, 2002). The OmpA protein is then recognised by various scavenger receptors, resulting in the production in PTX3 (a pentraxin-related protein) which binds to OmpA and in turn, increases the inflammatory response (Mantovani *et al.*, 2008). Investigations into the host cell response to OmpA2 alone and the extracellular peptides would therefore be critically important in determining if they would be suitable as a vaccine candidate. However, if it is possible to elicit a similar host response using only the peptides, this will elucidate potential epitopes in vaccine development, or be used in a combination with the OmpA protein to create a more effective vaccination to influence dysbiosis and result in a "re-biosis" of the oral microbiome (Curtis, 2015).

6.4 The Role of OmpH Chaperone: Implications for Surface Proteome Involvement in *P. gingivalis* Biology

The data presented in the final results chapter of this thesis gave a general characterisation to the relatively unknown OmpH protein of *P. gingivalis.* This protein was alluded to as being important in invasion when identified as an upregulated protein in a signature set of genes in the hyperinvasive subset of the *P. gingivalis* population (Suwannakul *et al.*, 2010). It is currently unclear whether the OmpH1H2 protein complex functions as a trimer of OmpH1 and OmpH2 proteins, and in what composition (e.g. like OmpA is in a 2:1 heterotrimeric structure of OmpA1:OmpA2) as this has not yet been determined. As little knowledge exists of the OmpH protein of *P. gingivalis*, a full knock out of the protein was created, with the intention to study the single mutations later. General analysis of a mutant lacking this chaperone indicated that strains lacking the OmpH complex have significantly altered physiology, with abrogated growth characteristics, colony morphology, biofilm

growth and viability in certain media conditions (e.g. tissue culture media during standard antibiotic protection assays). These observations can be explained largely in terms of its role as a periplasmic chaperone of outer membrane proteins. The *ompH* mutant in my work displays a drastically altered outer membrane protein profile, which is in stark contrast to the work of Taguchi *et al.,* who described the phenotype of a mutant lacking only OmpH1, which largely seemed to lack proteins whose secretion to the OM is dependent on the Type IX PorSS system, including gingipains (Taguchi *et al.*, 2016). It would therefore be an interesting prospect to complement the *ompH1H2* mutant with the OmpH2 protein to determine if the mutant then behaves like the *ompH1* single mutant demonstrated in the Taguchi *et al* work, i.e. the two subunits may have different client bases. The difference in the two mutants' membrane profiles indicates the potential greater role for OmpH2 in the chaperoning of proteins, as a greater number of proteins are lost in the mutant lacking the entire operon, but may also indicate that it has a role in stabilisation of the potential OmpH1H2 complex. Analysis of the single mutants would form a large part of the ongoing work from this project.

Although it is tempting to speculate that loss in virulence factors, such as the ability to form a biofilm, to adhere to and invade host cells, etc. is due at least in part to the loss of the OmpA protein in the *ompH1H2* mutant as both mutants display very similar phenotypes. However, it is very difficult to dissect the effect of the OmpA protein missing in the outer membrane from the overall effect of all of the proteins lost from the outer membrane of the *ompH1H2* mutant. It would therefore be very interesting for future work to determine which proteins are affected by the loss of the OmpH chaperone. This chapter has potentially identified three of these, the two gingipains, Kgp and Rgp (which were also identified by Taguchi *et al*), and the OmpA protein (a novel finding in this research) however further identification of outer membrane proteins that are clients of the OmpH protein would help to establish new proteins of *P. gingivalis* outer membrane that potentially could act as therapeutic targets for drugs to prevent the progression of periodontal disease. Some of these clients have been hinted at by the work performed by Taguchi *et al*, (2016) however this is still preliminary work as little is still known about *P. gingivalis* OmpH and therefore there is a great deal more to be defined and discovered.

6.5 Conclusion

This body of work has identified a role for the OmpA in *P. gingivalis* virulence, contributing to the ability for the bacterium to form a biofilm as well as enabling the interaction with the host. In particular, these findings have demonstrated an increased role for the OmpA2 subunit in the host cell interactions, with particular importance of the extracellular surface regions of the protein. There is promising potential to develop the extracellular loops derived from the peptides into potential anti-adhesive therapeutic agents or vaccines, whilst also using OmpA as a potential target for treatment of periodontal disease. This thesis has also developed a greater understanding of the OmpH chaperone protein of *P. gingivalis* and has provided evidence that the OmpA protein is a client of this chaperone system. The identification of other clients of OmpH would allow the further identification of targets for periodontal disease therapeutics. A schematic of how these proteins complement each other and fit into the larger picture of *P. gingivalis* interaction with the host can be seen in Figure 6.1.

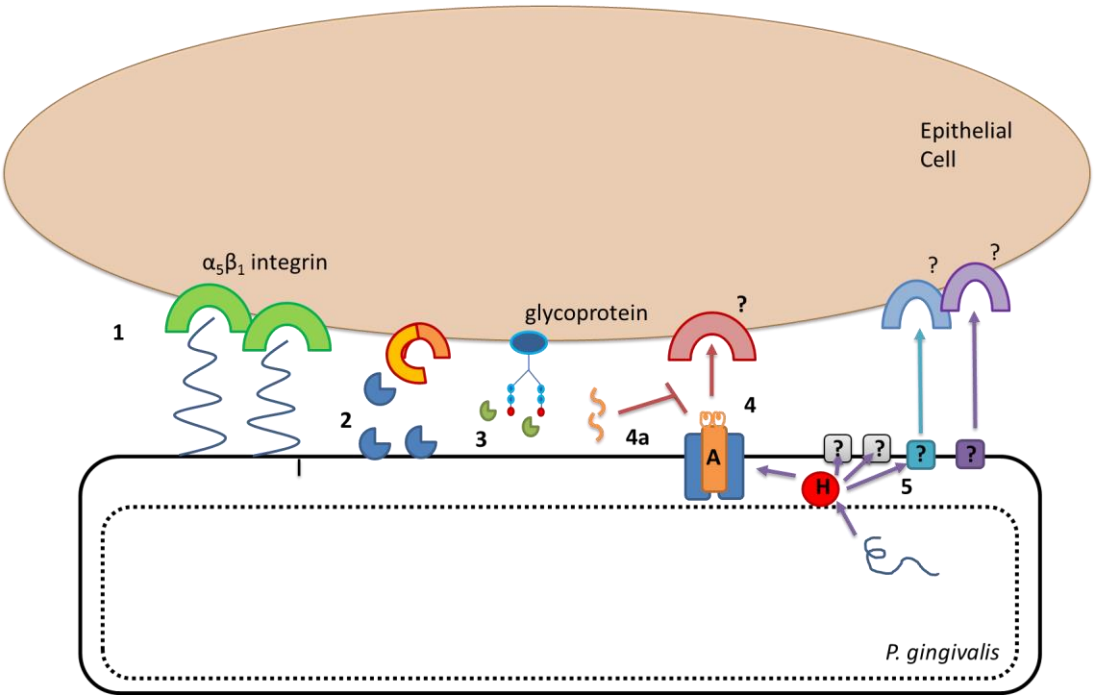

Figure 6.1. Schematic diagram representing the surface proteins of *P. gingivalis* and their interactions with the host epithelial cell. The major mechanisms of adherence and invasion are indicated, with the addition of OmpH as a chaperone of the outer membrane proteins. The fimbriae (1) bind to the $\alpha_5\beta_1$ integrins, triggering a signalling cascade causing cytoskeleton rearrangement and internalisation of the bacteria. The gingipains (2) modify and cleave host cell receptors to reveal cryptotopes and allow *P. gingivalis* adherence. Similarly, the sialidases (3) cleave the terminal sialic acid to increase *P. gingivalis* adherence to the host. The OmpA protein (4), specifically the OmpA2 subunit's extracellular loops are involved in the binding of an unknown host cell receptor, and mediating invasion of the bacterium. The peptides designed to resemble these OmpA2 loops successfully reduce this adherence (4a). The OmpH protein (5) chaperones proteins to the outer membrane of the *P. gingivalis* cell, of which potentially include the OmpA protein, the fimbriae, and the gingipains, and other important proteins necessary for successful adherence and invasion of the host oral epithelial cells.

Given that none of the mutations in these proteins needed for host cell interaction completely abrogate the ability of the bacteria to invade the host, merely that they severely reduce the capability, it would suggest that they are all needed in some form for maximal efficiency of host cell interaction and work synergistically. Particular mechanisms may be needed in different points of the adherence and invasion cycle, for example, gingipains are needed in adherence but not in invasion (Chen *et al.*, 2001; Suwannakul *et al.*, 2010), and they may be needed to reveal the receptors necessary for other molecular determinants to bind to facilitate invasion. It is evident from this study that OmpA plays a role in the host

cell interaction; however it should be seen with caution as an actual *in vivo* situation would employ a whole subset of virulence factors that would stimulate the cell in multiple different ways that a single virulence factor such as OmpA would not. It would be thoroughly interesting for future work to determine which are expressed at particular points of the host interaction cycle, and under what conditions they are necessary, and ultimately how the OmpA protein fits into this. In addition to this, periodontal disease is not the work of a single species; it is likely due to the interaction of *P. gingivalis* with multiple oral species and the host-related factors to thrive and cause disease, and therefore the effect of the OmpA protein in a multi-species environment would be an interesting area for follow up.

With numerous studies already performed to determine the mechanism of virulence behind *P. gingivalis* and the cellular interaction with the host, there is still a substantial amount more work to be done. This study has hypothesised and confirmed the importance of OmpA in this interaction, and further exploration of this area will hopefully greatly contribute to the overall understanding of *P. gingivalis* virulence, and eventually lead to the development of effective therapies for controlling chronic *P. gingivalis* infections and help to prevent periodontal disease.

References

Aas, J.A., Paster, B.J., Stokes, L.N., Olsen, I., and Dewhirst, F.E. (2005) Defining the Normal Bacterial Flora of the Oral Cavity. *J Clin Microbiol* **43**: 5721–5732.

Abaibou, H., Chen, Z., Olango, G.J.O.N., Liu, Y.I., Edwards, J., and Fletcher, H.M. (2001) vimA Gene Downstream of recA Is Involved in Virulence Modulation in *Porphyromonas gingivalis* W83. *Infect Immun* **69**: 325–335.

Abe, T., Murakami, Y., Nagano, K., Hasegawa, Y., Moriguchi, K., Ohno, N., *et al.* (2011) OmpA-like protein influences cell shape and adhesive activity of *Tannerella forsythia*. *Mol Oral Microbiol* **26**: 374–387.

Agbor, T.A., and McCormick, B.A. (2011) *Salmonella* effectors: important players modulating host cell function during infection. *Cell Microbiol* **13**: 1858–1869.

Akcalı, A., Huck, O., Buduneli, N., Davideau, J.-L., Köse, T., and Tenenbaum, H. (2014) Exposure of *Porphyromonas gingivalis* to cortisol increases bacterial growth. *Arch Oral Biol* **59**: 30–34.

Akimaru, J., Matsuyama, S., Tokuda, H., and Mizushima, S. (1991) Reconstitution of a protein translocation system containing purified SecY, SecE, and SecA from *Escherichia coli*. *Proc Natl Acad Sci U S A* **88**: 6545–9.

AlJehani, Y.A. (2014) Risk factors of periodontal disease: review of the literature. *Int J Dent* **2014**: 1-9.

Amano, A., Nakagawa, I., Okahashi, N., and Hamada, N. (2004) Variations of *Porphyromonas gingivalis* fimbriae in relation to microbial pathogenesis. *J Periodontal Res* **39**: 136–42.

Andrian, E., Grenier, D., and Rouabhia, M. (2006) *Porphyromonas gingivalis*-Epithelial Cell Interactions in Periodontitis. *J Dent Res* **85**: 392–403.

Arakawa, T., and Timasheff, S.N. (1982) Stabilization of protein structure by sugars. *Biochemistry* **21**: 6536–6544.

Arendorf, T.M., Bredekamp, B., Cloete, C. A, and Sauer, G. (1998) Oral manifestations of HIV infection in 600 South African patients. *J Oral Pathol Med* **27**: 176–9.

Arnau, J., Lauritzen, C., Petersen, G.E., and Pedersen, J. (2006) Current strategies for the use of affinity tags and tag removal for the purification of recombinant proteins. *Protein Expr Purif* **48**: 1–13.

Aruni, W., Vanterpool, E., Osbourne, D., Roy, F., Muthiah, A., Dou, Y., and Fletcher, H.M. (2011) Sialidase and sialoglycoproteases can modulate virulence in *Porphyromonas gingivalis*. *Infect Immun* **79**: 2779–91.

Azghani, A.O., Idell, S., Bains, M., and Hancock, R.E.W. (2002) *Pseudomonas aeruginosa* outer membrane protein F is an adhesin in bacterial binding to lung epithelial cells in culture. *Microb Pathog* **33**: 109–114.

Baek, K.J., Ji, S., Kim, Y.C., and Choi, Y. (2015) Association of the invasion ability of *Porphyromonas gingivalis* with the severity of periodontitis. *Virulence* **6**: 274–81.

Bagby, S., Tong, K.I., and Ikura, M. (2001) Optimization of protein solubility and stability for protein nuclear magnetic resonance. *Methods Enzymol* **339**: 20-41.

Bakri, I., Douglas, C.W.I., and Rawlinson, A. (2013) The effects of stress on periodontal treatment: a longitudinal investigation using clinical and biological markers. *J Clin Periodontol* **40**: 955–61.

Bao, K., Belibasakis, G.N., Thurnheer, T., Aduse-Opoku, J., Curtis, M. A, and Bostanci, N. (2014) Role of *Porphyromonas gingivalis* gingipains in multi-species biofilm formation. *BMC Microbiol* **14**: 258.

Bardwell, J.C., McGovern, K., and Beckwith, J. (1991) Identification of a protein required for disulfide bond formation in vivo. *Cell* **67**: 581–589.

Barken, K.B., Pamp, S.J., Yang, L., Gjermansen, M., Bertrand, J.J., Klausen, M., *et al.* (2008) Roles of type IV pili, flagellum-mediated motility and extracellular DNA in the formation of mature multicellular structures in *Pseudomonas aeruginosa* biofilms. *Environ Microbiol* **10**: 2331–2343.

Barrios, A.F.G., Zuo, R., Ren, D., and Wood, T.K. (2006) Hha, YbaJ, and OmpA Regulate *Escherichia coli* K12 Biofilm Formation and Conjugation Plasmids Abolish Motility. *Biotechnol Bioeng* **93**: 188–200.

Bartold, P.M., and Narayanan, A.S. (2006) Molecular and cell biology of healthy and diseased periodontal tissues. *Periodontol 2000* **40**: 29–49.

Basset, C., Holton, J., O'Mahony, R., and Roitt, I. (2003) Innate immunity and pathogen–host interaction. *Vaccine* **21**: S12–S23.

Beachy, E. H. 1981. Bacterial adherence, p. 1–4. In L. Switalski, M. Hook, and E. H. Beachy (ed.), Molecular mechanisms of microbial adhesion. Springer-Verlag, Inc., New York, N.Y.

Bearfield, C., Davenport, E.S., Sivapathasundaram, V., and Allaker, R.P. (2002) Possible association between amniotic fluid micro-organism infection and microflora in the mouth. *BJOG* **109**: 527–33.

Beck, J., Garcia, R., Heiss, G., Vokonas, P.S., and Offenbacher, S. (1996) Periodontal disease and cardiovascular disease. *J Periodontol* **67**: 1123–37.

Beck, J.D., Koch, G.G., Rozier, R.G., and Tudor, G.E. (1990) Prevalence and risk indicators for periodontal attachment loss in a population of older community-dwelling blacks and whites. *J Periodontol* **61**: 521–8.

Beher, M.G., Schnaitman, C. a., and Pugsley, a. P. (1980) Major heat-modifiable outer membrane protein in gram-negative bacteria: comparison with the OmpA protein of *Escherichia coli*. *J Bacteriol* **143**: 906–913.

Bélanger, M., Kozarov, E., Song, H., Whitlock, J., and Progulske-Fox, A. (2012) Both the unique and repeat regions of the *Porphyromonas gingivalis* hemagglutinin A are involved in adhesion and invasion of host cells. *Anaerobe* **18**: 128–134.

Belton, C.M., Izutsu, K.T., Goodwin, P.C., Park, Y., and Lamont, R.J. (1999) Fluorescence image analysis of the association between *Porphyromonas gingivalis* and gingival epithelial cells. *Cell Microbiol* **1**: 215–23.

Berezow, A.B., and Darveau, R.P. (2012) Microbial Shift and Periodontitis. *Periodontol 2000* **55**(1): 36–47.

Bergström, J. (2004) Tobacco smoking and chronic destructive periodontal disease. *Odontology* **92**: 1–8.

Bermejo-Fenoll, A., and Sánchez-Pérez, A. (2004) Necrotising periodontal diseases. *Med Oral Patol Oral Cir Bucal* **9 Suppl**: 114–9; 108–14.

Bessette, P.H., Aslund, F., Beckwith, J., and Georgiou, G. (1999) Efficient folding of proteins with multiple disulfide bonds in the *Escherichia coli* cytoplasm. *Proc Natl Acad Sci* **96**: 13703–13708.

Biosciences, A. (2001) The recombinant protein handbook. *Methods* 107.

Bliska, J.B., Galán, J.E., and Falkow, S. (1993) Signal transduction in the mammalian cell during bacterial attachment and entry. *Cell* **73**: 903–20.

Bondos, S.E., and Bicknell, A. (2003) Detection and prevention of protein aggregation before, during, and after purification. *Anal Biochem* **316**: 223–231.

Borgnakke, W.S., Ylöstalo, P. V, Taylor, G.W., and Genco, R.J. (2013) Effect of periodontal disease on diabetes: systematic review of epidemiologic observational evidence. *J Clin Periodontol* **40 Suppl 1**: S135–52.

Bos, M.P., Robert, V., and Tommassen, J. (2007) Biogenesis of the Gram-Negative Bacterial Outer Membrane. *Annu Rev Microbiol* **61**: 191–214.

Bos, M.P., and Tommassen, J. (2004) Biogenesis of the Gram-negative bacterial outer membrane. *Curr Opin Microbiol* **7**: 610–616.

Botto, M., Kirschfink, M., Macor, P., Pickering, M.C., Würzner, R., and Tedesco, F. (2009) Complement in human diseases: Lessons from complement deficiencies. *Mol Immunol* **46**: 2774–2783.

Bradshaw, D.J., Homer, K.A., Marsh, P.D., and Beighton, D. (1994) Metabolic cooperation in oral microbial communities during growth on mucin. *Microbiology* **140**: 3407–3412.

Bradshaw, D.J., Marsh, P.D., Watson, G.K., and Allison, C. (1998) Role of *Fusobacterium nucleatum* and coaggregation in anaerobe survival in planktonic and biofilm oral microbial communities during aeration. *Infect Immun* **66**: 4729–32.

Bramanti, T.E., and Holt, S.C. (1991) Roles of porphyrins and host iron transport proteins in regulation of growth of *Porphyromonas gingivalis* W50. *J Bacteriol* **173**: 7330–9.

Branda, S.S., Vik, Å., Friedman, L., and Kolter, R. (2005) Biofilms: the matrix revisited. *Trends Microbiol* **13**: 20–26.

Bremer, E., Cole, S.T., Hindennach, I., Henning, U., Beck, E., Kurz, C., and Schaller, H. (1982) Export of a protein into the outer membrane of *Escherichia coli* K12. Stable incorporation of the ompA protein requires less than 193 amino-terminal amino-acid residues. *Eur J Biochem* **122**: 223–231.

Brown, L.J., Johns, A.B., and Wall, T.P. (2002) The economics of periodontal. *Periodontol 2000* **29**: 223–234.

Brunner, J., Scheres, N., Idrissi, N.B. El, Deng, D.M., Laine, M.L., Winkelhoff, A.J. van, and Crielaard, W. (2010) The capsule of *Porphyromonas gingivalis* reduces the immune response of human gingival fibroblasts. *BMC Microbiol* **10**: 5.

Bryzek, D., Ksiazek, M., Bielecka, E., Karim, A.Y., Potempa, B., Staniec, D., *et al.* (2014) A pathogenic trace of *Tannerella forsythia* - shedding of soluble fully active tumor necrosis factor α from the macrophage surface by karilysin. *Mol Oral Microbiol* **29**: 294–306.

Bulieris, P. V., Behrens, S., Holst, O., and Kleinschmidt, J.H. (2003) Folding and insertion of the outer membrane protein OmpA is assisted by the chaperone Skp and by lipopolysaccharide. *J Biol Chem* **278**: 9092–9099.

Cabanes, D., Sousa, S., Cebriá, A., Lecuit, M., García-del Portillo, F., and Cossart, P. (2005) Gp96 is a receptor for a novel *Listeria monocytogenes* virulence factor, Vip, a surface protein. *EMBO J* **24**: 2827–38.

Cacalano, G., Kays, M., Saiman, L., and Prince, a (1992) Production of the *Pseudomonas aeruginosa* neuraminidase is increased under hyperosmolar conditions and is regulated by genes involved in alginate expression. *J Clin Invest* **89**: 1866–74.

Cai, Y., Kurita-Ochiai, T., Kobayashi, R., Hashizume, T., and Yamamoto, M. (2013) Nasal immunization with the 40-kDa outer membrane protein of *Porphyromonas gingivalis* plus cholera toxin induces protective immunity in aged mice. *J Oral Sci* **55**: 107–14.

Caroff, M., and Karibian, D. (2003) Structure of bacterial lipopolysaccharides. *Carbohydr Res* **338**: 2431–2447.

Cekici, A., Kantarci, A., Hasturk, H., and Dyke, T.E. Van (2014) Inflammatory and immune pathways in the pathogenesis of periodontal disease. *Periodontol 2000* **64**: 57–80.

Cells, E., Maier, T., Smith, K.S., and Adams, D.F. (1819) Differential Attachment of Oral Treponemes to Monolayers of epithelial cells. *J Periodontol* **68**(10): 1010–1018.

Chalifour, A., Jeannin, P., Gauchat, J.-F., Blaecke, A., Malissard, M., N'Guyen, T., *et al.* (2004) Direct bacterial protein PAMP recognition by human NK cells involves TLRs and triggers alpha-defensin production. *Blood* **104**: 1778–83.

Chen, R., and Henning, U. (1996) A periplasmic protein (Skp) of Escherichia coli selectively binds a class of outer membrane proteins. *Mol Microbiol* **19**: 1287–1294.

Chen, T., and Duncan, M.J. (2004) Gingipain adhesin domains mediate *Porphyromonas gingivalis* adherence to epithelial cells. *Microb Pathog* **36**: 205–9.

Chen, T., Nakayama, K., Belliveau, L., and Duncan, M.J. (2001) *Porphyromonas gingivalis* gingipains and adhesion to epithelial cells. *Infect Immun* **69**: 3048–3056.

Chen, Y.-Y., Peng, B., Yang, Q., Glew, M.D., Veith, P.D., Cross, K.J., *et al.* (2011) The outer membrane protein LptO is essential for the O-deacylation of LPS and the co-ordinated secretion and attachment of A-LPS and CTD proteins in *Porphyromonas gingivalis*. *Mol Microbiol* **79**: 1380–401.

Chi, B., Qi, M., and Kuramitsu, H.K. (2003) Role of dentilisin in *Treponema denticola* epithelial cell layer penetration. *Res Microbiol* **154**: 637–643.

Chicurel, M. (2000) Slimebusters. *Nature* **408**: 284–286.

Christensen, G.D., Simpson, W. a, Younger, J.J., Baddour, L.M., Barrett, F.F., Melton, D.M., and Beachey, E.H. (1985) Adherence of coagulase-negative *Staphylococci* to plastic tissue

culture plates: a quantitative model for the adherence of *Staphylococci* to medical devices. *J Clin Microbiol* **22**: 996–1006.

Igboin, C.O., Tordoff, K.P., Moeschberger, M.L., Griffen, A. L. and Leys, E.J. (2011) *Porphyromonas gingivalis*-Host Interactions in a *Drosophila melanogaster* Model. *Infect Immun* **79**: 449.

Chukkapalli, S.S., Velsko, I.M., Rivera-Kweh, M.F., Zheng, D., Lucas, A.R., and Kesavalu, L. (2015) Polymicrobial Oral Infection with Four Periodontal Bacteria Orchestrates a Distinct Inflammatory Response and Atherosclerosis in ApoE null Mice. *PLOS One*. 1-17.

Clark, E.D. (2001) Protein refolding for industrial processes. *Curr Opin Biotechnol* **12**: 202–7.

Cock, H. De, Schäfer, U., Potgeter, M., Demel, R., Müller, M., and Tommassen, J. (1999) Affinity of the periplasmic chaperone Skp of *Escherichia coli* for phospholipids, lipopolysaccharides and non-native outer membrane proteins. Role of Skp in the biogenesis of outer membrane protein. *Eur J Biochem* **259**: 96–103.

Conlon, B.P., Rowe, S.E., and Lewis, K. (2015) Persister Cells in Biofilm Associated Infections.*Advances in Experimental Medicing and Biology* **831**:1-9

Connolly, E., Millhouse, E., Doyle, R., Culshaw, S., Ramage, G., and Moran, G.P. (2016) The *Porphyromonas gingivalis* haemagglutinins HagB and HagC are major mediators of adhesion and biofilm formation. *Mol Oral Microbiol*. *Published ahead of print.*

Cook, G.S. (1998) Biofilm formation by *Porphyromonas gingivalis* and *Streptococcus gordonii*. *J Periodontal Res* **33**(6): 323–327.

Corey, L.A., Nance, W.E., Hofstede, P., and Schenkeinf, H.A. (1993) Self-Reported Periodontal Disease in a Virginia Twin Population. *J Periodontol* **64**: 1205–1208.

Corfield, T. (1992) Bacterial Sialidases - Roles in Pathogenicity and Nutrition. *Glycobiology* **2**: 509–521.

Corpet, F. (1988) Multiple sequence alignment with hierarchical clustering. *Nucl Acids Res* **16**: 10881–10890.

Coutard, B., Danchin, E.G.J., Oubelaid, R., Canard, B., and Bignon, C. (2012) Single pH buffer refolding screen for protein from inclusion bodies. *Protein Expr Purif* **82**: 352–359.

Curtis, M. A, Zenobia, C., and Darveau, R.P. (2011) The relationship of the oral microbiotia to periodontal health and disease. *Cell Host Microbe* **10**: 302–6.

Curtis, M (2015). Dysbiosis of the periodontal microbiome: Cause vs consequence? Conference paper at: *PgLondon15*, June 23-25, 2015, London, UK.

Danese, P.N., and Silhavy, T.J. (1998) Targeting and assembly of periplasmic and outer-membrane proteins in *Escherichia coli*. *Annu Rev Genet* **32**: 59–94.

Darveau, R.P., Belton, C.M., Reife, R.A., and Lamont, R.J. (1998) Local chemokine paralysis, a novel pathogenic mechanism for *Porphyromonas gingivalis*. *Infect Immun* **66**: 1660–5.

Darveau, R.P., Cunningham, M.D., Bailey, T., Seachord, C., Ratcliffe, K., Bainbridge, B., *et al.* (1995) Ability of bacteria associated with chronic inflammatory disease to stimulate E-selectin expression and promote neutrophil adhesion. *Infect Immun* **63**: 1311–7.

Darveau, R.P., Pham, T.T., Lemley, K., Reife, R.A., Bainbridge, B.W., Coats, S.R., *et al.* (2004) *Porphyromonas gingivalis* Lipopolysaccharide Contains Multiple Lipid A Species That Functionally Interact with Both Toll-Like Receptors 2 and 4. **72**: 5041–5051.

Deatherage, B.L., Lara, J.C., Bergsbaken, T., Barrett, S.L.R., Lara, S., and Cookson, B.T. (2010) Biogenesis of Bacterial Membrane Vesicles. **72**: 1395–1407.

Delemarche, C., Manoha, F., Behar, G., Houlgatte, R., Hellman, U., and Wroblewsji, H. (1995) Characterization of the *Pasteurella multocida* skp and firA genes. *Gene* **161**: 39–43.

Deshpande, R.G., Khan, M.B., and Genco, C. A (1998) Invasion of aortic and heart endothelial cells by *Porphyromonas gingivalis*. *Infect Immun* **66**(11): 5337–43.

Díaz, L., Hoare, A., Soto, C., Bugueño, I., Silva, N., Dutzan, N., *et al.* (2015) Changes in lipopolysaccharide profile of *Porphyromonas gingivalis* clinical isolates correlate with changes in colony morphology and polymyxin B resistance. *Anaerobe* **33**: 25–32.

Dickson, M. a, Hahn, W.C., Ino, Y., Ronfard, V., Wu, J.Y., Weinberg, R. a, *et al.* (2000) Human keratinocytes that express hTERT and also bypass a p16(INK4a)-enforced mechanism that

limits life span become immortal yet retain normal growth and differentiation characteristics. *Mol Cell Biol* **20**: 1436–47.

Diego, I. de, Veillard, F., Sztukowska, M.N., Guevara, T., Potempa, B., Pomowski, A., *et al.* (2014) Structure and Mechanism of Cysteine Peptidase Gingipain K (Kgp), a Major Virulence Factor of *Porphyromonas gingivalis* in Periodontitis. *J Biol Chem* **289**: 32291–32302.

Diego, I. de, Veillard, F.T., Guevara, T., Potempa, B., Sztukowska, M., Potempa, J., and Gomis-Rüth, F.X. (2013) *Porphyromonas gingivalis* virulence factor gingipain RgpB shows a unique zymogenic mechanism for cysteine peptidases. *J Biol Chem* **288**: 14287–96.

Dierickx, K., Pauwels, M., Laine, M.L., Eldere, J. Van, Cassiman, J.-J., Winkelhoff, A.J. van, *et al.* (2003) Adhesion of *Porphyromonas gingivalis* serotypes to pocket epithelium. *J Periodontol* **74**: 844–8.

Dissick, A., Redman, R.S., Jones, M., Rangan, B. V., Reimold, A., Griffiths, G.R., *et al.* (2010) Association of Periodontitis With Rheumatoid Arthritis: A Pilot Study. *J Periodontol* **81**: 223–230.

Dolgilevich, S., Rafferty, B., Luchinskaya, D., and Kozarov, E. (2011) Genomic comparison of invasive and rare non-invasive strains reveals *Porphyromonas gingivalis* genetic polymorphisms. *J Oral Microbiol* **3**: 1-11.

Dorn, B.R., Burks, J.N., Seifert, K.N., and Progulske-Fox, A. (2000) Invasion of endothelial and epithelial cells by strains of *Porphyromonas gingivalis*. *FEMS Microbiol Lett* **187**: 139–144.

Douglas, C.W.I., Naylor, K., Phansopa, C., Frey, A.M., Farmilo, T., and Stafford, G.P. (2014) *Advances in Bacterial Pathogen Biology*. First Edition. Elsiever, p. 295-298.

Dow, B.A., Tatulian, S.A., and Davidson, V.L. (2015) Use of the amicyanin signal sequence for efficient periplasmic expression in *E. coli* of a human antibody light chain variable domain. *Protein Expr Purif* **108**: 9–12.

Driessen, a J.M., Manting, E.H., and Does, C. van der (2001) The structural basis of protein targeting and translocation in bacteria. *Nat Struct Biol* **8**: 492–498.

Dümmler, A., Lawrence, A.-M., and Marco, A. de (2005) Simplified screening for the detection of soluble fusion constructs expressed in *E. coli* using a modular set of vectors. *Microb Cell Fact* **4**: 34.

Dumon-Seignovert, L., Cariot, G., and Vuillard, L. (2004) The toxicity of recombinant proteins in *Escherichia coli*: a comparison of overexpression in BL21(DE3), C41(DE3), and C43(DE3). *Protein Expr Purification* **37**: 203–206.

Duncan, M.J., Nakao, S., Skobe, Z., and Xie, H. (1993) Interactions of *Porphyromonas gingivalis* with epithelial cells. *Infect Immun* **61**: 2260–5.

Dzink, J.L., Socransky, S.S., and Haffajee, A.D. (1988) The predominant cultivable microbiota of active and inactive lesions of destructive periodontal diseases. *J Clin Periodontol* **15**: 316–23.

Ebersole, J.L., Cappelli, D., Holt, S.C., Singer, R.E., and Filloon, T. (2000) Gingival crevicular fluid inflammatory mediators and bacteriology of gingivitis in nonhuman primates related to susceptibility to periodontitis. *Oral Microbiol Immunol* **15**: 19–26.

Edwin, F., Valkya Sharma, Y., and Jagannadham, M. V (2002) Stabilization of Molten Globule State of Papain by Urea. *Biochem Biophys Res Commun* **290**: 1441–1446.

Egli, C., Leung, W.K., Muller, K.H., Hancock, R.E.W., and McBride, B.C. (1993) Pore-forming properties of the major 53-kilodalton surface antigen from the outer sheath of *Treponema denticola*. *Infect Immun* **61**: 1694–1699.

Eley, B.M. (1999) Antibacterial agents in the control of supragingival plaque — a review. *Br Dent J* **186**: 286–296.

Emrich, L.J., Shlossman, M., and Genco, R.J. (1991) Periodontal disease in non-insulin-dependent diabetes mellitus. *J Periodontol* **62**: 123–31.

Enersen, M., Nakano, K., and Amano, A. (2013) *Porphyromonas gingivalis* fimbriae. *J Oral Microbiol* **5**: 1–10.

Entzminger, K.C., Chang, C., Myhre, R.O., Mccallum, K.C., and Maynard, J.A. (2012) The Skp chaperone helps fold soluble proteins in vitro by inhibiting aggregation. *Biochemis* **51**: 4822–4834.

Fairman, J.W., Noinaj, N., and Buchanan, S.K. (2011) The structural biology of β-barrel membrane proteins: a summary of recent reports. *Curr Opin Struct Biol* **21**: 523–531.

Feldner, B.D., Reinhardt, R.A., Garbin, C.P., Seymour, G.J., and Casey, J.H. (1994) Histological evaluation of interleukin-1 beta and collagen in gingival tissue from untreated adult periodontitis. *J Periodontal Res* **29**: 54–61.

Fenno, J.C. (2012) *Treponema denticola* interactions with host proteins. *J Oral Microbiol* **4**: 1-13.

Filoche, S., Wong, L., and Sissons, C.H. (2010) Oral biofilms: emerging concepts in microbial ecology. *J Dent Res* **89**: 8–18.

Fito-Boncompte, L., Chapalain, A., Bouffartigues, E., Chaker, H., Lesouhaitier, O., Gicquel, G., *et al.* (2011) Full Virulence of *Pseudomonas aeruginosa* Requires OprF. *Infect Immun* **79**: 1176–1186.

Flemming, H.-C., Neu, T.R., and Wozniak, D.J. (2007) The EPS Matrix: The House of Biofilm Cells. *J Bacteriol* **189**: 7945–7947.

Fosgerau, K., and Hoffmann, T. (2015) Peptide therapeutics: current status and future directions. *Drug Discov Today* **20**: 122–128.

Frangioni, J. V, and Neel, B.G. (1993) Solubilization and purification of enzymatically active glutathione S-transferase (pGEX) fusion proteins. *Anal Biochem* **210**: 179–87.

Gaetti-Jardim, E., Marcelino, S.L., Feitosa, A.C.R., Romito, G. a, and Avila-Campos, M.J. (2009) Quantitative detection of periodontopathic bacteria in atherosclerotic plaques from coronary arteries. *J Med Microbiol* **58**: 1568–75.

Gaffen, S.L., and Hajishengallis, G. (2009) A New Inflammatory Cytokine on the Block: Re-thinking Periodontal Disease and the Th1/Th2 Paradigm in the Context of Th17 Cells and IL-17. *J Dent Res* **87**: 817–828.

Gaibani, P., Caroli, F., Nucci, C., and Sambri, V. (2010) Major surface protein complex of *Treponema denticola* induces the production of tumor necrosis factor alpha, interleukin-1 beta, interleukin-6 and matrix metalloproteinase 9 by primary human peripheral blood monocytes. *J Periodontal Res* **45**: 361–6.

Galen, J.E., Ketley, J.M., Fasano, A., Richardson, S.H., Wasserman, S.S., and Kaperl, J.B. (1992) Role of *Vibrio cholerae* Neuraminidase in the Function of Cholera Toxin. **60**.

Gardner, R.G., Russell, J.B., Wilson, D.B., Wang, G.R., and Shoemaker, N.B. (1996) Use of a modified *Bacteroides-Prevotella* shuttle vector to transfer a reconstructed beta-1,4-D-endoglucanase gene into *Bacteroides uniformi*s and P*revotella ruminicola*. *Appl Environ Microbiol* **62**: 196–202.

GE Healthcare (2010) Strategies for Protein Purif ication Handbook. 167.

Gekko, K., and Morikawa, T. (1981) Preferential hydration of bovine serum albumin in polyhydric alcohol-water mixtures. *J Biochem* **90**: 39–50

Gekko, K., and Timasheff, S.N. (1981) Mechanism of protein stabilization by glycerol: preferential hydration in glycerol-water mixtures. *Biochemistry* **20**: 4667–76.

Genco, C.A., Odusanya, B.M., Potempa, J., Mikolajczyk-Pawlinska, J., and Travis, J. (1998) A peptide domain on gingipain R which confers immunity against *Porphyromonas gingivalis* infection in mice. *Infect Immun* **66**: 4108–14.

Genco, R.J., and Borgnakke, W.S. (2013) Risk factors for periodontal disease. *Periodontol 2000* **62**: 59–94.

Genco, R.J., Ho, A.W., Grossi, S.G., Dunford, R.G., and Tedesco, L.A. (2002) Relationship of stress, distress and inadequate coping behaviors to periodontal disease. *J Periodontol* **70**: 100–101.

Georgopoulos, C. (1990) HtrA (DegP) Protein, Essential for *E. coli* Survival at High Temperatures, is an Endopeptidase. *J Bacteriol* **172**: 1791–1797.

Gibbs, R.S. (2001) The relationship between infections and adverse pregnancy outcomes: an overview. *Ann Periodontol* **6**: 153–63.

Gilbert, N.M., Lewis, W.G., and Lewis, A.L. (2013) Clinical features of bacterial vaginosis in a murine model of vaginal infection with *Gardnerella vaginalis*. *PLoS One* **8**: e59539.

Glew, M.D., Veith, P.D., Peng, B., Chen, Y.-Y., Gorasia, D.G., Yang, Q., *et al.* (2012) PG0026 is the C-terminal signal peptidase of a novel secretion system of *Porphyromonas gingivalis*. *J Biol Chem* **287**: 24605–17.

Glick, M., Muzyka, B.C., Lurie, D., and Salkin, L.M. (1994) Oral manifestations associated with HIV-related disease as markers for immune suppression and AIDS. *Oral Surg Oral Med Oral Pathol* **77**: 344–9.

Goemans, C., Denoncin, K., and Collet, J.F. (2014) Folding mechanisms of periplasmic proteins. *Biochim Biophys Acta - Mol Cell Res* **1843**: 1517–1528.

Golovanov, A.P., Hautbergue, G.M., Wilson, S. A, and Lian, L.-Y. (2004) A simple method for improving protein solubility and long-term stability. *J Am Chem Soc* **126**: 8933–9.

Gonzales, J.R., Groeger, S., Johansson, A., and Meyle, J. (2014) T helper cells from aggressive periodontitis patients produce higher levels of interleukin-1 beta and interleukin-6 in interaction with *Porphyromonas gingivalis. Clin Oral Investig* **18**: 1835–1843.

Gore, E.A., Sanders, J.J., Pandey, J.P., Palesch, Y., and Galbraith, G.M. (1998) Interleukin-1beta+3953 allele 2: association with disease status in adult periodontitis. *J Clin Periodontol* **25**: 781–5.

Goulas, T., Ferrer, I.G., Hutcherson, J.A., Potempa, B.A., Potempa, J., Scott, D.A., and Gomis-Rüth, F.X. (2015) Structure of RagB, a major immunodominant outer-membrane surface receptor antigen of *Porphyromonas gingivalis*. *Mol Oral Microbiol*. *Published ahead of print.*

Greenstein, G., and Hart, Thomas, C. (2002) Haim-Munk syndrome and Papillon-Lefevre syndrome are allelic mutations in cathepsin C. *J Periodontololgy* **73**: 232–247.

Grenier, D., Chao, G., and McBride, B.C. (1989) Characterization of sodium dodecyl sulfate-stable *Bacteroides gingivalis* proteases by polyacrylamide gel electrophoresis. *Infect Immun* **57**: 95–9.

Griffen, A.L., Beall, C.J., Campbell, J.H., Firestone, N.D., Kumar, P.S., Yang, Z.K., *et al.* (2011) Distinct and complex bacterial profiles in human periodontitis and health revealed by 16S pyrosequencing. *ISME J* **6**: 1176–1185.

Grossi, S.G., and Genco, R.J. (1998) Periodontal disease and diabetes mellitus: a two-way relationship. *Ann Periodontol* **3**: 51–61.

Guo, Y., Nguyen, K., and Potempa, J. (2010) Dichotomy of gingipains action as virulence factors: from cleaving substrates with the precision of a surgeons knife to a meat chopper-like brutal degradation of proteins. *Periodontol 2000* **54**: 15–44.

György, B., Tóth, E., Tarcsa, E., Falus, A., and Buzás, E.I. (2006) Citrullination: A post-translational modification in health and disease. *Int J Biochem Cell Biol* **38**: 1662–1677.

Haapasalo, M., Singh, U., Uitto, V.-J., and McBride, B.C. (1991) Sulfhydryl-dependent binding of *Treponema denticola* to laminin and other proteins. *InfectImmun* **59**: 4230–4237.

Hagan, C.L., Silhavy, T.J., and Kahne, D. (2011) β-Barrel Membrane Protein Assembly by the Bam Complex. *Annu Rev Biochem* **80**: 189–210.

Hage, D.S. (1999) Affinity chromatography: a review of clinical applications. *Clin Chem* **45**: 593–615.

Hajishengallis, G. (2010) *Porphyromonas gingivalis*-Host Interactions: Open War or Intelligent Guerilla Tactics? *Microbes Infect* **11**: 637–645.

Hajishengallis, G. (2014) Periodontitis: from microbial immune subversion to systemic inflammation. *Nat Rev Immunol* **15**: 30–44.

Hajishengallis, G. (2015) Periodontitis: from microbial immune subversion to systemic inflammation. *Nat Rev Immunol* **15**: 30–44.

Hajishengallis, G., Darveau, R.P., and Curtis, M. A (2012) The keystone-pathogen hypothesis. *Nat Rev Microbiol* **10**: 717–25.

Hajishengallis, G., and Lamont, R.J. (2012) Beyond the red complex and into more complexity: the polymicrobial synergy and dysbiosis (PSD) model of periodontal disease etiology. *Mol Oral Microbiol* **27**: 409–19.

Hajishengallis, G., Liang, S., Payne, M. a, Hashim, A., Jotwani, R., Eskan, M. a, *et al.* (2011) Low-abundance biofilm species orchestrates inflammatory periodontal disease through the commensal microbiota and complement. *Cell Host Microbe* **10**: 497–506.

Hamada, H., Arakawa, T., and Shiraki, K. (2009) Effect of additives on protein aggregation. *Curr Pharm Biotechnol* **10**: 400–407.

Hamada, N., Watanabe, K., Sasakawa, C., Yoshikawa, M., Yoshimura, F., and Umemoto, T. (1994) Construction and characterization of a fimA mutant of *Porphyromonas gingivalis*. *Infect Immun* **62**: 1696–704.

Han, N., Whitlock, J., and Progulske-Fox, A. (1996) The hemagglutinin gene A (hagA) of *Porphyromonas gingivalis* 381 contains four large, contiguous, direct repeats. *Infect Immun* **64**: 4000–4007.

Han, Y.W., Redline, R.W., Li, M., Yin, L., Hill, G.B., and McCormick, T.S. (2004) *Fusobacterium nucleatum* induces premature and term stillbirths in pregnant mice: implication of oral bacteria in preterm birth. *Infect Immun* **72**: 2272–9.

Han, Y.W., Shi, W., Huang, G.T., Kinder Haake, S., Park, N.H., Kuramitsu, H., and Genco, R.J. (2000) Interactions between periodontal bacteria and human oral epithelial cells: *Fusobacterium nucleatum* adheres to and invades epithelial cells. *Infect Immun* **68**: 3140–6.

Haraguchi, A., Miura, M., Fujise, O., Hamachi, T., and Nishimura, F. (2014) *Porphyromonas gingivalis* gingipain is involved in the detachment and aggregation of *Aggregatibacter actinomycetemcomitans* biofilm. *Mol Oral Microbiol* **29**: 131–143.

Harms, N., Koningstein, G., Dontje, W., Muller, M., Oudega, B., Luirink, J., and Cock, H. de (2001) The Early Interaction of the Outer Membrane Protein PhoE with the Periplasmic Chaperone Skp Occurs at the Cytoplasmic Membrane. *J Biol Chem* **276**: 18804–18811.

Hart, T.C., Hart, P.S., Michalec, M.D., Zhang, Y., Firatli, E., Dyke, T.E. Van, *et al.* (2000) Haim-Munk syndrome and Papillon-Lefevre syndrome are allelic mutations in cathepsin C. *J Med Genet* **37**: 88–94.

Hasan, A., and Palmer, R.M. (2014) A clinical guide to periodontology: Pathology of periodontal disease. *BDJ* **216**: 457–461.

Hasegawa, Y., Iwami, J., Sato, K., Park, Y., Nishikawa, K., Atsumi, T., *et al.* (2009) Anchoring and length regulation of *Porphyromonas gingivalis* Mfa1 fimbriae by the downstream gene product Mfa2. *Microbiology* **155**: 3333–47.

Hashimoto, M., Ogawa, S., Asai, Y., Takai, Y., and Ogawa, T. (2003) Binding of *Porphyromonas gingivalis* fimbriae to *Treponema denticola* dentilisin. *FEMS Microbiol Lett* **226**: 267–271.

Hassell, T.M., and Harris, E.L. (1995) Genetic Influences In Caries And Periodontal Diseases. *Crit Rev Oral Biol Med* **6**: 319–342.

Hassett, D.J., Cuppoletti, J., Trapnell, B., Lymar, S. V, Rowe, J.J., Yoon, S.S., *et al.* (2002) Anaerobic metabolism and quorum sensing by *Pseudomonas aeruginosa* biofilms in chronically infected cystic fibrosis airways: rethinking antibiotic treatment strategies and drug targets. *Adv Drug Deliv Rev* **54**: 1425–43.

Hayashi, S., Yamada, H., Fukui, M., Ito, H., and Sata, M. (2015) Correlation Between Arteriosclerosis and Periodontal Condition Assessed by Lactoferrin and α1-Antitrypsin Levels in Gingival Crevicular Fluid. *Int Heart J* **56**: 639–643.

Hirsch, R., Deng, H., and Laohachai, M.N. (2012) Azithromycin in periodontal treatment: more than an antibiotic. *J Periodontal Res* **47**: 137–48.

Hirt, R.P., Harriman, N., Kajava, A. V, and Embley, T.M. (2002) A novel potential surface protein in *Trichomonas vaginalis* contains a leucine-rich repeat shared by micro-organisms from all three domains of life. *Mol Biochem Parasitol* **125**: 195–9.

Hirvas, L., Coleman, J., Koski, P., and Vaara, M. (1990) Bacterial “histone-like protein I” (HLP-I) is an outer membrane constituent? *FEBS Lett* **262**: 123–126.

Hirvas, L., Koski, P., and Vaara, M. (1991) The ompH Gene of *Yersinia enterocolitica*: Cloning, Sequencing, Expression, and Comparison with Known *Enterobacterial ompH* Sequences. *J Bacteriol* **173**: 1223–1229.

Ho, M.-H., Chen, C.-H., Goodwin, J.S., Wang, B.-Y., and Xie, H. (2015) Functional Advantages of *Porphyromonas gingivalis* Vesicles. *PLoS One. Published ahead of print.*

Hochuli, E., Dobeli, H., and Schacher, A. (1987) New Metal Chelate Adsorbent Selective For Proteins And Peptides Containing Neigh Bouring Histidine Residues. *J Chromatogr* **411**: 177–184.

Hojo, K., Nagaoka, S., Ohshima, T., and Maeda, N. (2009) Bacterial interactions in dental biofilm development. *J Dent Res* **88**: 982–90.

Holt, S.C., Kesavalu, L., Walker, S., and Genco, C. a (1999) Virulence factors of *Porphyromonas gingivalis*. *Periodontol 2000* **20**: 168–238.

Honma, K., Kuramitsu, H.K., Genco, R.J., and Sharma, A. (2001) Development of a gene inactivation system for *Bacteroides forsythu*s: construction and characterization of a BspA mutant. *Infect Immun* **69**: 4686–90.

Honma, K., Mishima, E., and Sharma, A. (2011) Role of tannerella forsythia nanh sialidase in epithelial cell attachment. *Infect Immun* **79**: 393–401.

Hosogi, Y., and Duncan, M.J. (2005) Gene Expression in *Porphyromonas gingivalis* after Contact with Human Epithelial Cells. **73**: 2327–2335.

How, K.Y., Song, K.P. and Chan, K.G. (2016) *Porphyromonas gingivalis*: An Overview of Periodontopathic Pathogen below the Gumline. *Front Microbiol* **7**(53): 1-14.

Howell, T.H., Ridker, P.M., Ajani, U. a, Hennekens, C.H., and Christen, W.G. (2001) Periodontal disease and risk of subsequent cardiovascular disease in U.S. male physicians. *J Am Coll Cardiol* **37**: 445–50.

Huang, R., Li, M., and Gregory, R.L. (2011) Bacterial interactions in dental biofilm. *Virulence* **2**: 435–44.

Hugoson, A., Laurell, L., and Lundgren, D. (1992) Frequency distribution of individuals aged 20-70 years according to severity of periodontal disease experience in 1973 and 1983. *J Clin Periodontol* **19**: 227–32.

Hujoel, P.P., Drangsholt, M., Spiekerman, C., and DeRouen, T. A (2000) Periodontal disease and coronary heart disease risk. *JAMA* **284**: 1406–10.

Hutcherson, J.A., Bagaitkar, J., Nagano, K., Yoshimura, F., Wang, H., and Scott, D.A. (2015) *Porphyromonas gingivalis* RagB is a proinflammatory signal transducer and activator of transcription 4 agonist. *Mol Oral Microbiol* **30**: 242–252.

Ikegami, A., Honma, K., Sharma, A., and Kuramitsu, H.K. (2004) Multiple Functions of the Leucine-Rich Repeat Protein LrrA of *Treponema denticola. Society* **72**: 4619–4627.

Imai, M., Murakami, Y., Nagano, K., Nakamura, H., and Yoshimura, F. (2005) Major outer membrane proteins from *Porphyromonas gingivalis*: strain variation, distribution, and clinical significance in periradicular lesions. *Eur J Oral Sci* **113**: 391–9.

Ito, R., Ishihara, K., Shoji, M., Nakayama, K., and Okuda, K. (2010) Hemagglutinin/Adhesin domains of *Porphyromonas gingivalis* play key roles in coaggregation with *Treponema denticola*. *FEMS Immunol Med Microbiol* **60**: 251–260.

Iwami, J., Murakami, Y., Nagano, K., Nakamura, H., and Yoshimura, F. (2007) Further evidence that major outer membrane proteins homologous to OmpA in *Porphyromonas gingivalis* stabilize bacterial cells. *Oral Microbiol Immunol* **22**: 356–360.

Jarchow, S., Lück, C., Görg, A., and Skerra, A. (2008) Identification of potential substrate proteins for the periplasmic *Escherichia coli* chaperone Skp. *Proteomics* **8**: 4987–4994.

Jeannin, P., Magistrelli, G., Goetsch, L., Haeuw, J.F., Thieblemont, N., Bonnefoy, J.Y., and Delneste, Y. (2002) Outer membrane protein A (OmpA): a new pathogen-associated molecular pattern that interacts with antigen presenting cells—impact on vaccine strategies. *Vaccine* **20**: 23–27.

Johnson, J.D., Chen, R., Lenton, P.A., Zhang, G., Hinrichs, J.E., and Rudney, J.D. (2008) Persistence of extracrevicular bacterial reservoirs after treatment of aggressive periodontitis. *J Periodontol* **79**: 2305–12.

Johnson, N.W., Griffiths, G.S., Wilton, J.M., Maiden, M.F., Curtis, M.A., Gillett, I.R., *et al.* (1988) Detection of high-risk groups and individuals for periodontal diseases. Evidence for the existence of high-risk groups and individuals and approaches to their detection. *J Clin Periodontol* **15**: 276–82.

Jong, R.A.M., and Reijden, W.A. van der (2010) Feasibility and therapeutic strategies of vaccines against *Porphyromonas gingivalis. Expert Rev Vaccines* **9**: 193–208.

Kadono, H., Kido, J., and Kataoka, M. (1999) Inhibition of Osteoblastic Cell Differentiation by Lipopolysaccharide Extract from Porphyromonas gingivalis. *Infect Immun* **67**(6):2841-2846.

Kato, H., Taguchi, Y., Tominaga, K., Umeda, M., and Tanaka, A. (2014) *Porphyromonas gingivalis* LPS inhibits osteoblastic differentiation and promotes pro-inflammatory cytokine production in human periodontal ligament stem cells. *Arch Oral Biol* **59**: 167–175.

Katz, J., Sambandam, V., Wu, J.H., Suzanne, M., Balkovetz, D.F., and Michalek, S.M. (2000) Characterization of *Porphyromonas gingivalis* -Induced Degradation of Epithelial Cell Junctional Complexes. *Infect Immun* **68**: 1441–1449.

Kenny, B., Devinney, R., Stein, M., Reinscheid, D.J., Frey, E.A., and Brett, B. (1997) Enteropathogenic *E. coli (EPEC)* Transfers Its Receptor for Intimate Adherence into Mammalian Cells. *Cell* **91**: 511–520.

Kerwin, B. A., Heller, M.C., Levin, S.H., and Randolph, T.W. (1998) Effects of tween 80 and sucrose on acute short-term stability and long- term storage at -20°C of a recombinant hemoglobin. *J Pharm Sci* **87**: 1062–1068.

Kesavalu, L., Sathishkumar, S., Bakthavatchalu, V., Matthews, C., Dawson, D., Steffen, M., and Ebersole, J.L. (2007) Rat model of polymicrobial infection, immunity, and alveolar bone resorption in periodontal disease. *Infect Immun* **75**: 1704–12.

Kiefhaber, T., Rudolph, R., Kohler, H.H., and Buchner, J. (1991) Protein aggregation in vitro and in vivo: a quantitative model of the kinetic competition between folding and aggregation. *Biotechnology* **9**: 825–9.

Kim, S., and Lee, S.B. (2008) Soluble expression of archaeal proteins in *Escherichia coli* by using fusion-partners. *Protein Expr Purif* **62**: 116–119.

Kim, T.-S., Obst, C., Zehaczek, S., and Geenen, C. (2008) Detection of bone loss with different X-ray techniques in periodontal patients. *J Periodontol* **79**: 1141–9.

Kinane, D.F., and Hart, T.C. (2003) Genes And Gene Polymorphisms Associated With Periodontal Disease. *Crit Rev Oral Biol Med* **14**: 430–449.

Kiyonobu Honma, Mishima, E., and Sharma, A. (2011) Role of *Tannerella forsythia* NanH Sialidase in Epithelial Cell Attachment. *Infect Immun* **79**: 393–401.

Klareskog, L., Rönnelid, J., Lundberg, K., Padyukov, L., and Alfredsson, L. (2008) Immunity to Citrullinated Proteins in Rheumatoid Arthritis. *Annu Rev Immunol* **26**: 651–675.

Klose, M., Schwarz, H., MacIntyre, S., Freudl, R., Eschbach, M.L., and Henning, U. (1988) Internal deletions in the gene for an *Escherichia coli* outer membrane protein define an area possibly important for recognition of the outer membrane by this polypeptide. *J Biol Chem* **263**: 13291–13296.

Koebnik, R. (1999) Structural and functional roles of the surface-exposed loops of the beta-barrel membrane protein OmpA from *Escherichia coli. J Bacteriol* **181**: 3688–3694.

Koebnik, R., Locher, K.P., and Gelder, P. Van (2000) Structure and function of bacterial outer membrane proteins: barrels in a nutshell. *Mol Microbiol* **37**: 239–253.

Kolenbrander, P.E., Andersen, R.N., Blehert, D.S., Egland, P.G., Foster, J.S., and Palmer, R.J. (2002) Communication among oral bacteria. *Microbiol Mol Biol Rev* **66**: 486–505.

Kolenbrander, P.E., Palmer, R.J., Rickard, A.H., Jakubovics, N.S., Chalmers, N.I., and Diaz, P.I. (2006) Bacterial interactions and successions during plaque development. *Periodontol 2000* **42**: 47–79.

Komatsu, T., Nagano, K., Sugiura, S., Hagiwara, M., Tanigawa, N., Abiko, Y., *et al.* (2012) E-selectin mediates *Porphyromonas gingivalis* adherence to human endothelial cells. *Infect Immun* **80**: 2570–2576.

Kontani, M., Ono, H., Shibata, H., Okamura, Y., Tanaka, T., Fujiwara, T., *et al.* (1996) Cysteine protease of *Porphyromonas gingivalis* 381 enhances binding of fimbriae to cultured human fibroblasts and matrix proteins. *Infect Immun* **64**: 756–762.

Korndörfer, I.P., Dommel, M.K., and Skerra, A. (2004a) Structure of the periplasmic chaperone Skp suggests functional similarity with cytosolic chaperones despite differing architecture. *Nat Struct Mol Biol* **11**: 1015–1020.

Koski, P., Rhen, M., Kantele, J., and Vaara, M. (1989) Isolation, cloning, and primary structure of a cationic 16-kDa outer membrane protein of *Salmonella typhimurium. J Biol Chem* **264**: 18973–80.

Kostic, A.D., Chun, E., Robertson, L., Glickman, J.N., Gallini, C.A., Michaud, M., *et al.* (2013) Fusobacterium nucleatum Potentiates Intestinal Tumorigenesis and Modulates the Tumor-Immune Microenvironment. *Cell Host Microbe* **14**(2):207-215.

Kozarov, E., Sweier, D., Shelburne, C., Progulske-Fox, A., and Lopatin, D. (2006) Detection of bacterial DNA in atheromatous plaques by quantitative PCR. *Microbes Infect* **8**: 687–93.

Kozarov, E. V., Dorn, B.R., Shelburne, C.E., Dunn, W.A., and Progulske-Fox, A. (2005) Human Atherosclerotic Plaque Contains Viable Invasive Actinobacillus actinomycetemcomitans and Porphyromonas gingivalis. *Arterioscler Thromb Vasc Biol* **25**: e17–e18.

Kozarov, E., Whitlock, J., Dong, H., Carrasco, E., and Progulske-Fox, a. (1998) The number of direct repeats in hagA is variable among *Porphyromonas gingivalis* strains. *Infect Immun* **66**: 4721–4725.

Koziel, J., Mydel, P., and Potempa, J. (2014) The Link Between Periodontal Disease and Rheumatoid Arthritis: An Updated Review. *Curr Rheumatol Rep.* **16**(3):408

Kreilgaard, L., Jones, L.S., Randolph, T.W., Frokjaer, S., Flink, J.M., Manning, M.C., and Carpenter, J.F. (1998) Effect of tween 20 on freeze-thawing- and agitation-induced aggregation of recombinant human factor XIII. *J Pharm Sci* **87**(12):1597-603.

Krojer, T., Sawa, J., Schäfer, E., Saibil, H.R., Ehrmann, M., and Clausen, T. (2008) Structural basis for the regulated protease and chaperone function of DegP. *Nature* **453**: 885–890.

Kuboniwa, M., Hasegawa, Y., Mao, S., Shizukuishi, S., Amano, A., Lamont, R.J., and Yilmaz, O. (2008) *P. gingivalis* accelerates gingival epithelial cell progression through the cell cycle. *Microbes Infect* **10**: 122–8.

Kuboniwa, M., Hendrickson, E.L., Xia, Q., Wang, T., Xie, H., Hackett, M., and Lamont, R.J. (2009) Proteomics of *Porphyromonas gingivalis* within a model oral microbial community. *BMC Microbiol* **9**: 98.

Kuehn, M.J., and Kesty, N.C. (2005) Bacterial outer membrane vesicles and the host – pathogen interaction. *Genes Dev* 2645–2655.

Kuramitsu, H.K., He, X., Lux, R., Anderson, M.H., and Shi, W. (2007) Interspecies interactions within oral microbial communities. *Microbiol Mol Biol Rev* **71**: 653–70.

Kuramitsu, H.K., Qi, M., Kang, I.C., and Chen, W. (2001) Role for periodontal bacteria in cardiovascular diseases. *Ann Periodontol* **6**: 41–47.

Kurniyati, K., Zhang, W., Zhang, K., and Li, C. (2013) A surface-exposed neuraminidase affects complement resistance and virulence of the oral spirochaete *Treponema denticola*. *Mol Microbiol* **89**: 842–856.

Kuroiwa, A., Hisatsune, A., Isohama, Y., and Katsuki, H. (2009) Bacterial neuraminidase increases IL-8 production in lung epithelial cells via NF-kappaB-dependent pathway. *Biochem Biophys Res Commun* **379**: 754–9.

Laine, M.L., Appelmelk, B.J., and Winkelhoff, A.J. van (1997) Prevalence and distribution of six capsular serotypes of *Porphyromonas gingivalis* in periodontitis patients. *J Dent Res* **76**: 1840–4.

Lamont, R.J., Chan, a, Belton, C.M., Izutsu, K.T., Vasel, D., and Weinberg, A (1995) *Porphyromonas gingivalis* invasion of gingival epithelial cells. *Infect Immun* **63**: 3878–85.

Lamont, R.J., El-Sabaeny, A., Park, Y., Cook, G.S., Costerton, J.W., and Demuth, D.R. (2002) Role of the *Streptococcus gordonii* SspB protein in the development of *Porphyromonas gingivalis* biofilms on streptococcal substrates. *Microbiology* **148**: 1627–36.

Lamont, R.J., and Jenkinson, H.F. (1998) Life below the gum line: pathogenic mechanisms of *Porphyromonas gingivalis*. *Microbiol Mol Biol Rev* **62**: 1244–63.

Lamont, R.J., and Jenkinson, H.F. (2000) Subgingival colonization by *Porphyromonas gingivalis*. *Oral Microbiol Immunol* **15**: 341–349.

Lamont, R.J., and Jenkinson, H.F. (2000) Subgingival colonization by *Porphyromonas gingivalis. Oral Microbiol Immunol* **15**: 341–349.

Lamont, R.J., Oda, D., Persson, R., and Persson, G. (1992) Short communication Interaction of *Porphyromonas gingivalis* with gingival epithelial cells maintained in culture. *Oral Microbiol Immunol* 364–367.

Lawrence, T., and Gilroy, D.W. (2007) Chronic inflammation: a failure of resolution? *Int J Exp Pathol* **88**: 85–94.

Lazar, S., and Kolter, R. (1996) SurA assists the folding of *Escherichia coli* outer membrane proteins. *J Bacteriol* **178**: 1770–1773.

Lebeaux, D., Ghigo, J.-M., and Beloin, C. (2014) Biofilm-related infections: bridging the gap between clinical management and fundamental aspects of recalcitrance toward antibiotics. *Microbiol Mol Biol Rev* **78**: 510–43.

Lebendiker, M., and Danieli, T. (2014) Production of prone-to-aggregate proteins. *FEBS Lett* **588**: 236–246.

Lee, L.G., Chen, C.H., and Chiu, L. a (1986) Thiazole orange: a new dye for reticulocyte analysis. *Cytometry* **7**: 508–17.

Lee, S.H., Kim, J.S., Jun, H.-K., Lee, H.-R., Lee, D., and Choi, B.-K. (2009) The Major Outer Membrane Protein of a Periodontopathogen Induces IFN- and IFN-Stimulated Genes in Monocytes via Lipid Raft and TANK-Binding Kinase 1/IFN Regulatory Factor-3. *J Immunol* **182**: 5823–5835.

Lee, S.W., Sabet, M., Um, H.-S., Yang, J., Kim, H.C., and Zhu, W. (2006) Identification and characterization of the genes encoding a unique surface (S-) layer of *Tannerella forsythia*. *Gene* **371**: 102–11.

Lépine, G., Ellen, R.P., Ellen, R.P., and Le, G. (1996) Construction and preliminary characterization of three hemagglutinin mutants of Porphyromonas gingivalis . These include : Construction and Preliminary Characterization of Three Hemagglutinin Mutants of Porphyromonas gingivalis. **64**: 1467–1472.

Li, C., Kurniyati, Hu, B., Bian, J., Sun, J., Zhang, W., *et al.* (2012) Abrogation of neuraminidase reduces biofilm formation, capsule biosynthesis, and virulence of *Porphyromonas gingivalis*. *Infect Immun* **80**: 3–13.

Li, X., Kolltveit, K.M., Tronstad, L., and Olsen, I. (2000) Systemic diseases caused by oral infection. *Clin Microbiol Rev* **13**: 547–58.

Lichty, J.J., Malecki, J.L., Agnew, H.D., Michelson-Horowitz, D.J., and Tan, S. (2005) Comparison of affinity tags for protein purification. *Protein Expr Purif* **41**: 98–105.

Lin, X., Wu, J., and Xie, H. (2006) *Porphyromonas gingivalis* minor fimbriae are required for cell-cell interactions. *Infect Immun* **74**: 6011–5.

Lipinska, B., Fayet, O., Baird, L., and Georgopoulos, C. (1989) Identification, characterization, and mapping of the *Escherichia coli* htrA gene, whose product is essential for bacterial growth only at elevated temperatures. *J Bacteriol* **171**: 1574–1584.

Listgarten, M.A., Lai, C.H., and Young, V. (1993) Microbial composition and pattern of antibiotic resistance in subgingival microbial samples from patients with refractory periodontitis. *J Periodontol* **64**: 155–61.

Liu, C., Hashizume, T., Kurita-Ochiai, T., Fujihashi, K., and Yamamoto, M. (2010) Oral immunization with *Porphyromonas gingivalis* outer membrane protein and CpGoligodeoxynucleotides elicits T helper 1 and 2 cytokines for enhanced protective immunity. *Mol Oral Microbiol* **25**: 178–89.

Liu, H., Redline, R.W., and Han, Y.W. (2007) Fusobacterium nucleatum Induces Fetal Death in Mice via Stimulation of TLR4-Mediated Placental Inflammatory Response. *J Immunol* **179**: 2501–2508.

Llobet, E., March, C., Gimnez, P., and Bengoechea, J. a. (2009) *Klebsiella pneumoniae* OmpA confers resistance to antimicrobial peptides. *Antimicrob Agents Chemother* **53**: 298–302.

Locker, D., and Leake, J.L. (1993) Periodontal attachment loss in independently living older adults in Ontario, Canada. *J Public Health Dent* **53**: 6–11.

Lockhart, P.B., Bolger, A.F., Papapanou, P.N., Osinbowale, O., Trevisan, M., Levison, M.E., *et al.* (2012) Periodontal disease and atherosclerotic vascular disease: Does the evidence support an independent association?: A scientific statement from the American heart association. *Circulation* **125**: 2520–2544.

Löe, H., Anerud, A., Boysen, H., and Morrison, E. (1986) Natural history of periodontal disease in man. Rapid, moderate and no loss of attachment in Sri Lankan laborers 14 to 46 years of age. *J Clin Periodontol* **13**: 431–45.

Loesche, W.J., and Grossman, N.S. (2001) Periodontal Disease as a Specific, albeit Chronic, Infection: Diagnosis and Treatment. *Clin Mocrobiol Rev* **14**: 727–752.

Lu, H., Zhang, H., Wang, Q., Yuan, H., He, W., Zhao, Z., and Li, Y. (2001) Purification, refolding of hybrid hIFNγ-kringle 5 expressed in *Escherichia coli*. *Curr Microbiol* **42**: 211–216.

Ma, Q., and Wood, T.K. (2009) OmpA influences *Escherichia coli* biofilm formation by repressing cellulose production through the CpxRA two-component system. *Environ Microbiol* **11**: 2735–2746.

Mackenzie, R.S., Millard, H. an De, Aiguier, J.E., Beardwood, J.T., Rhein, M.L., Niles, J.G., *et al.* (1963) Interrelated effects of diabetes, arteriosclerosis and calculus on alveolar bone loss. *J Am Dent Assoc* **66**: 191–198.

Madianos, P.N., Papapanou, P.N., Nannmark, U., Dahlén, G., and Sandros, J. (1996) *Porphyromonas gingivalis* FDC381 multiplies and persists within human oral epithelial cells *in vitro*. *Infect Immun* **64**: 660–664.

Maeba, S., Otake, S., Namikoshi, J., Shibata, Y., Hayakawa, M., Abiko, Y., and Yamamoto, M. (2005) Transcutaneous immunization with a 40-kDa outer membrane protein of *Porphyromonas gingivalis* induces specific antibodies which inhibit coaggregation by *P. gingivalis*. *Vaccine* **23**: 2513–2521.

Maeda, K., Nagata, H., Yamamoto, Y., Tanaka, M., Tanaka, J., Minamino, N., and Shizukuishi, S. (2004) Glyceraldehyde-3-Phosphate Dehydrogenase of *Streptococcus oralis* Functions as a Coadhesin for *Porphyromonas gingivalis* Major Fimbriae. **72**: 1341–1348.

Maeda, Y., Koga, H., and Yamada, H. (1995) Effective renaturation of reduced lysozyme by gentle removal of urea. *Protein* **8**: 201–205.

Malek, R., Fisher, J.G., Caleca, a, Stinson, M., Oss, C.J. van, Lee, J.Y., *et al.* (1994) Inactivation of the *Porphyromonas gingivalis* fimA gene blocks periodontal damage in gnotobiotic rats. *J Bacteriol* **176**: 1052–9.

Manting, E.H., and Driessen, A.J.M. (2000) *Escherichia coli* translocase: The unravelling of a molecular machine. *Mol Microbiol* **37**: 226–238.

Mantovani, A., Garlanda, C., Doni, A., and Bottazzi, B. (2008) Pentraxins in Innate Immunity: From C-Reactive Protein to the Long Pentraxin PTX3. *J Clin Immunol* **28**: 1–13.

Mao, S., Park, Y., Hasegawa, Y., Tribble, G.D., James, C.E., Handfield, M., *et al.* (2007) Intrinsic apoptotic pathways of gingival epithelial cells modulated by *Porphyromonas gingivalis*. *Cell Microbiol* **9**: 1997–2007.

Marblestone, J.G., Edavettal, S.C., Lim, Y., Lim, P., Zuo, X., and Butt, T.R. (2006) Comparison of SUMO fusion technology with traditional gene fusion systems: enhanced expression and solubility with SUMO. *Protein Sci* **15**: 182–9.

Marcus, A J., and Hajjar, D.P. (1993) Vascular transcellular signaling. *J Lipid Res* **34**: 2017–31.

Marsh, P.D. (2003) Are dental diseases examples of ecological catastrophes? *Microbiology* **149**: 279–294.

Marsh, P.D. (2006) Dental plaque as a biofilm and a microbial community - implications for health and disease. *BMC Oral Health* **6 Suppl 1**: S14.

Martinez, E., Cantet, F., Fava, L., Norville, I., and Bonazzi, M. (2014) Identification of OmpA , a Coxiella burnetii Protein Involved in Host Cell Invasion , by Multi-Phenotypic High-Content Screening. *PLoS Pathogens* **10**: 1-22.

Maruvada, R., and Kim, K.S. (2011) Extracellular loops of the *Eschericia coli* outer membrane protein A contribute to the pathogenesis of meningitis. *J Infect Dis* **203**: 131–140.

Masi, M., and Pagès, J.-M. (2013) Structure, Function and Regulation of Outer Membrane Proteins Involved in Drug Transport in Enterobactericeae: the OmpF/C – TolC Case. *Open Microbiol J* **7**: 22-33.

Mathers, D. a, Leung, W.K., Fenno, J.C., Hong, Y., and McBride, B.C. (1996) The major surface protein complex of *Treponema denticola* depolarizes and induces ion channels in HeLa cell membranes. *Infect Immun* **64**: 2904–10.

Matsuyama, S., Tajima, T., and Tokuda, H. (1995) A novel periplasmic carrier protein involved in the sorting and transport of *Escherichia coli* lipoproteins destined for the outer membrane. *Embo J* **14**: 3365–3372.

McCoy, A.N., Araújo-Pérez, F., Azcárate-Peril, A., Yeh, J.J., Sandler, R.S., Keku, T.O., *et al.* (2013) *Fusobacterium* Is Associated with Colorectal Adenomas. *PLoS One* **8**: 1-8.

Mcdevitt, M.J., Wang, H.-Y., Knobelman, C., Newman, M.G., Giovine, F.S. Di, Timms, J., *et al.* (2000) Interleukin-1 Genetic Association With Periodontitis in Clinical Practice. *J Periodontol* **7171**: 156–163.

Mcwilliam, H., Li, W., Uludag, M., Squizzato, S., Park, Y.M., Buso, N., *et al.* (2013) Analysis Tool Web Services from the EMBL-EBI. *Nucleic Acids Res* **41**: 597–600.

Medzhitov, R. (2007) Recognition of microorganisms and activation of the immune response. *Nature* **449**: 819–826.

Meier, C., Oelschlaeger, T.A., Merkert, H., Korhonen, T.K., Meier, C., Oelschlaeger, T.A., and Merkert, H. (1996) Ability of *Escherichia coli* isolates that cause meningitis in newborns to invade epithelial and endothelial cells. *Infect Immun* **64**(7): 2391-2399.

Michalowicz, B.S., Aeppli, D., Virag, J.G., Klump, D.G., Hinrichs, J.E., Segal, N.L., *et al.* (1991) Periodontal Findings in Adult Twins. *J Periodontol* **62**: 293–299.

Mikolajczyk-Pawlinska, J., Travis, J., and Potempa, J. (1998) Modulation of interleukin-8 activity by gingipains from *Porphyromonas gingivalis:* implications for pathogenicity of periodontal disease. *FEBS Lett* **440**: 282–6.

Miroux, B., and Walker, J.E. (1996) Over-production of proteins in *Escherichia coli*: mutant hosts that allow synthesis of some membrane proteins and globular proteins at high levels. *J Mol Biol* **260**: 289–98.

Missiakas, D., Betton, J.M., and Raina, S. (1996) New components of protein folding in extracytoplasmic compartments of *Escherichia coli* SurA, FkpA and Skp/OmpH. *Mol Microbiol* **21**: 871–884.

Missiakas, D., Raina, S., and Missiakas, D. (1997) Protein folding in the bacterial periplasm. *J Bacteriol* **179**: 2465–2471.

Mittal, R., Krishnan, S., Gonzalez-Gomez, I., and Prasadarao, N. V (2011) Deciphering the roles of outer membrane protein A extracellular loops in the pathogenesis of Escherichia coli K1 meningitis. *J Biol Chem* **286**: 2183–93.

Mittal, R., and Prasadarao, N. V (2011) gp96 expression in neutrophils is critical for the onset of *Escherichia coli* K1 (RS218) meningitis. *Nat Commun* **2**: 552.

Moore, P. A, Weyant, R.J., Mongelluzzo, M.B., Myers, D.E., Rossie, K., Guggenheimer, J., *et al.* (1999) Type 1 diabetes mellitus and oral health: assessment of periodontal disease. *J Periodontol* **70**: 409–17.

Mot, R. De, and Vanderleyden, J. (1994) The C-terminal sequence conservation betweenOmpA-related outer membrane proteins and MotB suggests a common function in both Gram-positive and Gram-negative bacteria, possibly in theinteraction of these domains with peptidogiycan. *Mol Microbiol* **12**: 333–334.

Moughal, N.A., Adonogianaki, E., Thornhill, M.H., and Kinane, D.F. (1992) Endothelial cell leukocyte adhesion molecule-1 (ELAM-1) and intercellular adhesion molecule-1 (ICAM-1) expression in gingival tissue during health and experimentally-induced gingivitis. *J Periodontal Res* **27**: 623–30.

Murakami, Y., Hasegawa, Y., and Nagano, K. (2014) Characterization of Wheat Germ Agglutinin Lectin-Reactive Glycosylated OmpA-Like Proteins Derived from *Porphyromonas gingivalis.* **82**: 4563–4571.

Murakami, Y., Imai, M., Nakamura, H., and Yoshimura, F. (2002) Separation of the outer membrane and identification of major outer membrane proteins from *Porphyromonas gingivalis. Eur J Oral Sci* **110**: 157–62.

Murray, P. A, and Patters, M.R. (1980) Gingival crevice neutrophil function in periodontal lesions. *J Periodontal Res* **15**: 463–9.

Nagano, K., Murakami, Y., Nishikawa, K., Sakakibara, J., Shimozato, K., and Yoshimura, F. (2007) Characterization of RagA and RagB in *Porphyromonas gingivalis*: study using gene-deletion mutants. *J Med Microbiol* **56**: 1536–48.

Nagano, K., Murakami, Y., Nishikawa, K., Sakakibara, J., Shimozato, K., and Yoshimura, F. (2007) Characterization of RagA and RagB in *Porphyromonas gingivalis*: study using gene-deletion mutants. *J Med Microbiol* **56**: 1536–1548.

Nagano, K., Read, E.K., Murakami, Y., Masuda, T., Noguchi, T., and Yoshimura, F. (2005) Trimeric Structure of Major Outer Membrane Proteins Homologous to OmpA in *Porphyromonas gingivalis*. **187**: 902–911.

Nakagawa, I., Amano, A., Kuboniwa, M., Nakamura, T., Kawabata, S., and Hamada, S. (2002) Functional Differences among FimA Variants of *Porphyromonas gingivalis* and Their Effects on Adhesion to and Invasion of Human Epithelial Cells. **70**: 277–285.

Nakano, K., Inaba, H., Nomura, R., Nemoto, H., Takeda, M., Yoshioka, H., *et al.* (2006) Detection of cariogenic *Streptococcus mutans* in extirpated heart valve and atheromatous plaque specimens. *J Clin Microbiol* **44**: 3313–7.

Nakao, R., Takashiba, S., Kosono, S., Yoshida, M., Watanabe, H., Ohnishi, M., and Senpuku, H. (2014) Effect of *Porphyromonas gingivalis* outer membrane vesicles on gingipain-mediated detachment of cultured oral epithelial cells and immune responses. *Microbes Infect* **16**: 6–16.

Nakayama, K., Yoshimura, F., Kadowaki, T., and Yamamoto, K. (1996) Involvement of arginine-specific cysteine proteinase (Arg-gingipain) in fimbriation of *Porphyromonas gingivalis*. *J Bacteriol* **178**: 2818–2824.

Nakhjiri, S.F., Park, Y., Yilmaz, O., Chung, W.O., Watanabe, K., El-Sabaeny, a, *et al.* (2001) Inhibition of epithelial cell apoptosis by *Porphyromonas gingivalis. FEMS Microbiol Lett* **200**: 145–9.

Nath, S.G., and Raveendran, R. (2013) Microbial dysbiosis in periodontitis. *J Indian Soc Periodontol* **17**: 543–5.

Neagu, A., Neagu, M., and Dér, A. (2001) Fluctuations and the Hofmeister effect. *Biophys J* **81**: 1285–94.

Niazi, S.K., and Brown, J.L. (2015) *Fundamentals of Modern Bioprocessing*. First., CRC Press, London.

Nikaido, H. (2003) Molecular basis of bacterial outer membrane permeability revisited. *Microbiol Mol Biol Rev* **67**: 593–656.

Nilsson J., Stahl S., J. Lundeberg, Uhlen M., N.P. (1997) Affinity fusion strategies for detection, purification, and immobilization of recombinant proteins. *Protein Expr Purif* **11 1-16 10**: 1–16.

Nishiyama, S.I., Murakami, Y., Nagata, H., Shizukuishi, S., Kawagishi, I., and Yoshimura, F. (2007) Involvement of minor components associated with the FimA fimbriae of *Porphyromonas gingivalis* in adhesive functions. *Microbiology* **153**: 1916–1925.

Njoroge, T., Genco, R.J., Sojar, H.T., Hamada, N., and Genco, C. a (1997) A role for fimbriae in *Porphyromonas gingivalis* invasion of oral epithelial cells. *Infect Immun* **65**: 1980–4.

Nygren, J., Svanvik, N., and Kubista, M. (1999) Interactions between the fluorescent dye thiazole orange and DNA. *Biopolymers* **46**: 39–51.

O'Toole, G.A., and Kolter, R. (1998) Flagellar and twitching motility are necessary for *Pseudomonas aeruginosa* biofilm development. *Mol Microbiol* **30**: 295–304.

Ogawa, T., and Yagi, T. (2010) Bioactive mechanism of *Porphyromonas gingivalis* lipid A. *Periodontol 2000* **54**: 71–77.

Okahashi, N., Inaba, H., Nakagawa, I., Yamamura, T., Kuboniwa, M., Nakayama, K., *et al.* (2004) Porphyromonas gingivalis Induces Receptor Activator of NF-κB Ligand Expression in Osteoblasts through the Activator Protein 1 Pathway. **72**: 1706–1714.

Oliver, D.B., and Beckwith, J. (1982) Identification of a new gene *secA* and gene product involved in the secretion of envelope proteins in *Escherichia coli*. **150**(2): 686–691.

Orme, R., Douglas, C.W.I., Rimmer, S., and Webb, M. (2006) Proteomic analysis of *Escherichia coli* biofilms reveals the overexpression of the outer membrane protein OmpA. *Proteomics* **6**: 4269–4277.

Papapanou, P.N., Sandros, J., Lindberg, K, Duncan, M.J., Niederman, R., and Nannmark, U. (1994) *Porphyromonas gingivalis* may multiply and advance within stratified human junctional epithelium in vitro. *J Periodont Res* **29**: 374–375.

Papapanou, P.N., and Wennström, J.L. (1989) Radiographic and clinical assessments of destructive periodontal disease. *J Clin Periodontol* **16**: 609–12.

Park, Y., and Lamont, R.J. (1998) Contact-dependent protein secretion in *Porphyromonas gingivalis*. *Infect Immun* **66**: 4777–4782.

Park, Y., Simionato, M.R., Sekiya, K., Murakami, Y., James, D., Chen, W., *et al.* (2005) Short Fimbriae of *Porphyromonas gingivalis a*nd Their Role in Coadhesion with *Streptococcus gordonii*. **73**: 3983–3989.

Patel, G.J., Behrens-Kneip, S., Holst, O., and Kleinschmidt, J.H. (2009) The periplasmic chaperone Skp facilitates targeting, insertion, and folding of OmpA into lipid membranes with a negative membrane surface potential. *Biochemistry* **48**: 10235–10245.

Patel, G.J., Rg, J., and Kleinschmidt, H. (2013) The Lipid Bilayer-Inserted Membrane Protein BamA of *Escherichia coli* Facilitates Insertion and Folding of Outer Membrane Protein A from Its Complex with Skp. *Biochemistry* **52**: 3974–3986.

Pautsch, a, and Schulz, G.E. (2000) High-resolution structure of the OmpA membrane domain. *J Mol Biol* **298**: 273–82.

Pautsch, A., and Schulz, G.E. (1998) Structure of the outer membrane protein A transmembrane domain. *Nat Struct Biol* **5**: 1013–7.

Pennisi, E. (2005) A mouthful of microbes. *Science* **307**: 1899–901.

Peruzzo, D.C., Benatti, B.B., Ambrosano, G.M.B., Nogueira-Filho, G.R., Sallum, E.A., Casati, M.Z., and Nociti, F.H. (2007) A Systematic Review of Stress and Psychological Factors as Possible Risk Factors for Periodontal Disease. *J Periodontol* **78**: 1491–1504.

Peters, S.R., Valdez, M., Riviere, G., and Thomas, D.D. (1999) Adherence to and penetration through endothelial cells by oral treponemes. *Oral Microbiol Immnol* **14**: 379–383.

Petersen, P.E., and Ogawa, H. (2012) The global burden of periodontal disease: towards integration with chronic disease prevention and control. *Periodontol 2000* **60**: 15–39.

Phansopa, C., Kozak, R.P., Phing Liew, L., Frey, A.M., Farmilo, T., Parker, J.L., *et al.* (2015) Characterization of a Sialate O--acetyl esterase (NanS) from the oral pathogen Tannerella forsythia that enhances sialic acid release by NanH, its cognate sialidase. *Biochem J* **472**(2):157-167.

Philo, J., and Arakawa, T. (2009) Mechanisms of Protein Aggregation. *Curr Pharm Biotechnol* **10**: 348–351.

Pickering, M.C., Botto, M., Taylor, P.R., Lachmann, P.J., and Walport, M.J. (2000) Systemic lupus erythematosus, complement deficiency, and apoptosis. *Adv Immunol* **76**: 227–324.

Pierce Thermo Scientific (2010) Remove detergent from protein samples - Tech TIP #19. **0747**:3.

Pietrzak, E.R., Savage, N.W., Aldred, M.J., and Walsh, L.J. (1996) Expression of the E-selectin gene in human gingival epithelial tissue. *J oral Pathol Med* **25**: 320–324.

Pietrzak, E.R., Savage, N.W., and Walsh, L.J. (1996) Human gingival keratinocytes express E-selectin (CD62E). *Oral Dis* **2**: 11–7.

Pihlstrom, B.L., Michalowicz, B.S., and Johnson, N.W. (2005) Periodontal diseases. *Lancet* **366**: 1809–20.

Pizarro-Cerdá, J., and Cossart, P. (2006) Bacterial Adhesion and Entry into Host Cells. *Cell* **124**: 715–727.

Pizzo, G., Guiglia, R., Russo, L. Lo, and Campisi, G. (2010) Dentistry and internal medicine: from the focal infection theory to the periodontal medicine concept. *Eur J Intern Med* **21**: 496–502.

Pociot, F., Mølvig, J., Wogensen, L., Worsaae, H., and Nerup, J. (1992) A TaqI polymorphism in the human interleukin-1 beta (IL-1 beta) gene correlates with IL-1 beta secretion in vitro. *Eur J Clin Invest* **22**: 396–402.

Poklepovic, T., Worthington, H. V, Johnson, T.M., Sambunjak, D., Imai, P., Clarkson, J.E., and Tugwell, P. (2013) Interdental brushing for the prevention and control of periodontal diseases and dental caries in adults. *Cochrane database Syst Rev* CD009857.

Pöllänen, M., Paino, A., and Ihalin, R. (2013) Environmental Stimuli Shape Biofilm Formation and the Virulence of Periodontal Pathogens. *Int J Mol Sci* **14**: 17221–17237.

Porath, J. (1992) Immobilized metal ion affinity chromatography. *Protein Expr Purif* **3**: 263–281.

Potempa, J., Sroka, A., Imamura, T., and Travis, J. (2003) Gingipains, the Major Cysteine Proteinases and Virulence Factors of *Porphyromonas gingivalis:* Structure, Function and Assembly of Multidomain Protein Complexes. *Curr Protein Pept Sci* **4**: 397–407.

Prasadarao, N. V (2002) Identification of *Escherichia coli* outer membrane protein A receptor on human brain microvascular endothelial cells. *InfectImmun* **70**: 4556–4563.

Prasadarao, N. V, Blom, A.M., Villoutreix, B.O., and Linsangan, L.C. (2002) A novel interaction of outer membrane protein A with C4b binding protein mediates serum resistance of *Escherichia coli* K1. *J Immunol* **169**: 6352–60.

Prasadarao, N. V, Srivastava, P.K., Rudrabhatla, R.S., Kim, K.S., Huang, S., and Sukumaran, S.K. (2003) Cloning and Expression of the *Escherichia coli* K1 Outer Membrane Protein A Receptor , a gp96 Homologue. *Society* **71**: 1680–1688.

Prasadarao, N. V, Wass, C. a, Weiser, J.N., Stins, M.F., Huang, S.H., and Kim, K.S. (1996) Outer membrane protein A of *Escherichia coli* contributes to invasion of brain microvascular endothelial cells. *Infect Immun* **64**: 146–53.

Prasadarao, N. V, Wass, C.A., and Kim, K.S. (1996) Endothelial cell GlcNAc [beta],1-4GlcNAc epitopes for outer membrane protein A enhance traversal of *Escherichia coli* across the blood-brain barrier. *Infect Immun* **64**: 154–160.

Preber, H., and Bergström, J. (1990) Effect of cigarette smoking on periodontal healing following surgical therapy. *J Clin Periodontol* **17**: 324–8.

Preshaw, P.M., Alba, A.L., Herrera, D., Jepsen, S., Konstantinidis, A., Makrilakis, K., and Taylor, R. (2012) Periodontitis and diabetes: a two-way relationship. *Diabetologia* **55**: 21–31.

Prieto-langarica, A. (2013) A Cellular Automata Model of Infection Control on Medical Implants. *Appl Appl Math* **6**: 1–10.

Prigent-Combaret, C., Vidal, O., Dorel, C., and Lejeune, P. (1999) Abiotic surface sensing and biofilm-dependent regulation of gene expression in *Escherichia coli*. *J Bacteriol* **181**: 5993–6002.

Qu, J., Behrens-Kneip, S., Holst, O., and Kleinschmidt, J.H. (2009) Binding regions of outer membrane protein A in complexes with the periplasmic chaperone Skp. A site-directed fluorescence study. *Biochemistry* **48**: 4926–4936.

Qu, J., Mayer, C., Behrens, S., Holst, O., and Kleinschmidt, J.H. (2007) The Trimeric Periplasmic Chaperone Skp of *Escherichia coli* Forms 1:1 Complexes with Outer Membrane Proteins via Hydrophobic and Electrostatic Interactions. *J Mol Biol* **374**: 91–105.

Quan, S., Koldewey, P., Tapley, T., Kirsch, N., Ruane, K.M., Pfizenmaier, J., *et al.* (2011) Genetic selection designed to stabilize proteins uncovers a chaperone called Spy. *Nat Struct Mol Biol* **18**: 262–269.

Quirke, A.-M., Lugli, E.B., Wegner, N., Hamilton, B.C., Charles, P., Chowdhury, M., *et al.* (2014) Heightened immune response to autocitrullinated *Porphyromonas gingivalis* peptidylarginine deiminase: a potential mechanism for breaching immunologic tolerance in rheumatoid arthritis. *Ann Rheum Dis* **73**: 263–9.

Radford, A. P. (1970) Biological detergents. *Bmj* **4**: 181–182.

Rafferty, B., Jönsson, D., Kalachikov, S., Demmer, R.T., Nowygrod, R., Elkind, M.S. V, *et al.* (2011) Impact of monocytic cells on recovery of uncultivable bacteria from atherosclerotic lesions. *J Intern Med* **270**: 273–80.

Ramm, K., and Pluckthun, A (2000) The Periplasmic *Escherichia coli* Peptidylprolyl cis, trans-Isomerase FkpA. *J Biol Chem* **275**: 17106–17113.

Rangarajan, M., Aduse-Opoku, J., Paramonov, N., Hashim, A., Bostanci, N., Fraser, O.P., *et al.* (2008) Identification of a second lipopolysaccharide in *Porphyromonas gingivalis* W50. *J Bacteriol* **190**: 2920–32.

Rasamiravaka, T., Labtani, Q., Duez, P., Jaziri, M. El, Rasamiravaka, T., Labtani, Q., *et al.* (2015) The Formation of Biofilms by *Pseudomonas aeruginosa* : A Review of the Natural and Synthetic Compounds Interfering with Control Mechanisms. *Biomed Res Int* **2015**: 1–17.

Rath, S., Mukherjee, M., Kaushik, R., Sen, S., and Kumar, M. (2014) Periodontal pathogens in atheromatous plaque. *Indian J Pathol Microbiol* **57**: 259.

Razak, P.A., Richard, K.M.J., Thankachan, R.P., Hafiz, K.A.A., Kumar, K.N., and Sameer, K.M. (2014) Geriatric oral health: a review article. *J Int oral Heal JIOH* **6**: 110–6.

Reynolds, E.S. (1963) The Use Of Lead Citrate At High pH As An Electron-Opaque Stain In Electron Microscopy. *J Cell Biol* **17**: 208-212.

Ribet, D., and Cossart, P. (2015) How bacterial pathogens colonize their hosts and invade deeper tissues. *Microbes Infect* **17**: 173–183.

Rizzitello, A.E., Harper, J.R., and Silhavy, T.J. (2001) Genetic evidence for parallel pathways of chaperone activity in the periplasm of *Escherichia coli. J Bacteriol* **183**: 6794–800.

Robinson, P. (1992) Periodontal disease and HIV infection. *J Clin Periodontol* **19**: 609–614.

Rôças, I.N., Siqueira, J.F., Santos, K.R., and Coelho, a M. (2001) "Red complex" (*Bacteroides forsythus, Porphyromonas gingivalis,* and *Treponema denticola*) in endodontic infections: a molecular approach. *Oral Surg Oral Med Oral Pathol Oral Radiol Endod* **91**: 468–71.

Roitt, I., Delves, P., and Martin, S. (2011) *Innate immunity.* Molecular Biology of the Cell, 1st Edition. Garland Science, pp. 3–16.

Rolhion, N., Barnich, N., Bringer, M.-A., Glasser, A.-L., Ranc, J., Hébuterne, X., *et al.* (2010) Abnormally expressed ER stress response chaperone Gp96 in CD favours adherent-invasive *Escherichia coli* invasion. *Gut* **59**: 1355–1362.

Rolhion, N., Hofman, P., and Darfeuille-Michaud, A. (2011) The endoplasmic reticulum stress response chaperone: Gp96, a host receptor for crohn disease-associated adherent-invasive *Escherichia coli. Gut Microbes* **2**: 115-119.

Rollauer, S.E., Sooreshjani, M.A., Noinaj, N., Buchanan, S.K., Gan, L., Chen, S., *et al.* (2015) Outer membrane protein biogenesis in Gram-negative bacteria. *Philos Trans R Soc Lond B Biol Sci* **370**: 404–411.

Romero, R., Chaiworapongsa, T., Kuivaniemi, H., and Tromp, G. (2004) Bacterial vaginosis, the inflammatory response and the risk of preterm birth: A role for genetic epidemiology in the prevention of preterm birth. *Am J Obstet Gynecol* **190**: 1509–1519.

Rosan, B., and Lamont, R.J. (2000) Dental plaque formation. *Microbes Infect* **2**: 1599–607.

Rosano, G.L., Ceccarelli, E.A., Neubauer, P., Bruno-Barcena, J.M., and Schweder, T. (2014) Recombinant protein expression in *Escherichia coli:* advances and challenges. *Front Micrbiol* **5**: 172

Rosen, G., Genzler, T., and Sela, M.N. (2008) Coaggregation of *Treponema denticola* with *Porphyromonas gingivalis* and *Fusobacterium nucleatum* is mediated by the major outer sheath protein of *Treponema denticola. FEMS Microbiol Lett* **289**: 59–66.

Rosen, G., and Sela, M.N. (2006) Coaggregation of *Porphyromonas gingivalis* and *Fusobacterium nucleatum* PK 1594 is mediated by capsular polysaccharide and lipopolysaccharide. *FEMS Microbiol Lett* **256**: 304–10.

Rosenberger, C.M., and Finlay, B.B. (2003) Phagocyte sabotage: disruption of macrophage signalling by bacterial pathogens. *Nat Rev Mol Cell Biol* **4**: 385–96.

Ross, B.C., Czajkowski, L., Hocking, D., Margetts, M., Webb, E., Rothel, L., *et al.* (2001) Identification of vaccine candidate antigens from a genomic analysis of *Porphyromonas gingivalis*. *Vaccine* **19**: 4135–4142.

Ross, B.C., Czajkowski, L., Vandenberg, K.L., Camuglia, S., Woods, J., Agius, C., *et al.* (2004) Characterization of two outer membrane protein antigens of *Porphyromonas gingivalis* that are protective in a murine lesion model. *Oral Microbiol Immunol* **19**: 6–15.

Rosselin, M., Virlogeux-Payant, I., Roy, C., Bottreau, E., Sizaret, P.-Y., Mijouin, L., *et al.* (2010) Rck of *Salmonella enterica*, subspecies *enterica serovar Enteritidis*, mediates Zipper-like internalization. *Cell Res* **20**: 647–664.

Rouvière, P.E., and Gross, C. A. (1996) SurA, a periplasmic protein with peptidyl-prolyl isomerase activity, participates in the assembly of outer membrane porins. *Genes Dev* **10**: 3170–3182.

Roy, S., Honma, K., Ian Douglas, C.W., Sharma, A., and Stafford, G.P. (2011) Role of sialidase in glycoprotein utilization by *Tannerella forsythia*. *Microbiology* **157**: 3195–3202.

Rubinstein, M.R., Wang, X., Liu, W., Hao, Y., Cai, G., and Han, Y.W. (2013) *Fusobacterium nucleatum* Promotes Colorectal Carcinogenesis by Modulating E-Cadherin/β-Catenin Signaling via its FadA Adhesin. *Cell Host Microbe* **14**: 195–206.

Rudney, J.D., and Chen, R. (2006) The vital status of human buccal epithelial cells and the bacteria associated with them. *Arch Oral Biol* **51**: 291–298.

Rudney, J.D., Chen, R., and Sedgewick, G.J. (2001) Intracellular Actinobacillus actinomycetemcomitans and Porphyromonas gingivalis in Buccal Epithelial Cells Collected from Human Subjects. *Infect Immun* **69**: 2700–2707.

Rudney, J.D., Chen, R., and Sedgewick, G.J. (2005) *Actinobacillus actinomycetemcomitans, Porphyromonas gingivalis*, and *Tannerella forsythensis* are components of a polymicrobial intracellular flora within human buccal cells. *J Dent Res* **84**: 59–63.

Rye, H.S., Yue, S., Wemmer, D.E., Quesada, M. A, Haugland, R.P., Mathies, R. A, and Giazer, A.N. (1992) bis-intercalating asymmetric cyanine dyes: properties and applications. *Nucleic Acids Res* **20**: 2803–2812.

Sabet, M., Lee, S.-W., Nauman, R.K., Sims, T., and Um, H.S. (2003) The surface (S-) layer is a virulence factor of *Bacteroides forsythus*. *Microbiology* **149**: 3617–27.

Saida, F., Uzan, M., Odaert, B., and Bontems, F. (2006) Expression of Highly Toxic Genes in *E. coli:* Special Strategies and Genetic Tools. *Curr Protein Pept Sci* **7**: 47–56.

Saiki, K., and Konishi, K. (2012) Strategies for targeting the gingipain secretion system of *Porphyromonas gingivalis*. *J Oral Biosci* **54**: 155–159.

Saito, A., Inagaki, S., and Ishihara, K. (2009) Differential ability of periodontopathic bacteria to modulate invasion of human gingival epithelial cells by *Porphyromonas gingivalis*. *Microb Pathog* **47**: 329–33.

Saito, S., Hiratsuka, K., Hayakawa, M., Takiguchi, H., and Abiko, Y. (1997) Inhibition of *Porphyromonas gingivalis* colonizing factor between *actinomyces viscosus* ATCC 19246 by monoclonal antibodies against recombinant 40-kDa outer-membrane protein. *Gen Pharmacol Vasc Syst* **28**: 675–680.

Sakakibara, J., Nagano, K., Murakami, Y., Higuchi, N., Nakamura, H., Shimozato, K., and Yoshimura, F. (2007) Loss of adherence ability to human gingival epithelial cells in S-layer protein-deficient mutants of *Tannerella forsythensis*. *Microbiology* **153**: 866–76.

Salvi, G.E., Lawrence, H.P., Offenbacher, S., and Beck, J.D. (1997) Influence of risk factors on the pathogenesis of periodontitis. *Periodontol 2000* **14**: 173–201.

Salyers, a a, Bonheyo, G., and Shoemaker, N.B. (2000) Starting a new genetic system: lessons from bacteroides. *Methods* **20**: 35–46.

Sambunjak, D., Nickerson, J.W., Poklepovic, T., Johnson, T.M., Imai, P., Tugwell, P., and Worthington, H. V (2011) Flossing for the management of periodontal diseases and dental caries in adults. *Cochrane database Syst Rev* CD008829.

Sammartino, M., Sardi, J. de C.O., Duque, C., Höfling, J.F., and Gonçalves, R.B. (2010) The role of immune system in the development of periodontal disease: a brief review. *J Dent Sci* **25**: 300–305.

Sato, K., Naito, M., Yukitake, H., Hirakawa, H., Shoji, M., McBride, M.J., *et al.* (2010) A protein secretion system linked to *bacteroidete* gliding motility and pathogenesis. *Proc Natl Acad Sci U S A* **107**: 276–81.

Sato, K., Sakai, E., Veith, P.D., Shoji, M., Kikuchi, Y., Yukitake, H., *et al.* (2005) Identification of a new membrane-associated protein that influences transport/maturation of gingipains and adhesins of *Porphyromonas gingivalis*. *J Biol Chem* **280**: 8668–77.

Sato, K., Yukitake, H., Narita, Y., Shoji, M., Naito, M., and Nakayama, K. (2013) Identification of *Porphyromonas gingivalis* proteins secreted by the Por secretion system. *FEMS Microbiol Lett* **338**: 68–76.

Saul, F. A., Ari, J.P., Vulliez-le Normand, B., Kahn, R., Betton, J.M., and Bentley, G. A, (2004) Structural and Functional Studies of FkpA from *Escherichia coli*, a cis/trans Peptidyl-prolyl Isomerase with Chaperone Activity. *J Mol Biol* **335**: 595–608.

Sbordone, L., Ramaglia, L., Barone, A, Ciaglia, R.N., and Iacono, V.J. (1998) Periodontal status and subgingival microbiota of insulin-dependent juvenile diabetics: a 3-year longitudinal study. *J Periodontol* **69**: 120–8.

Schäfer, U., Beck, K., and Müller, M. (1999) Skp, a molecular chaperone of Gram-negative bacteria, is required for the formation of soluble periplasmic intermediates of outer membrane proteins. *J Biol Chem* **274**: 24567–24574.

Schein, C.H. (1989) Production of Soluble Recombinant Proteins in Bacteria. *Nat Biotechnol* **7**: 1141–1149.

Schenkein, H.A., and Loos, B.G. (2013) Inflammatory mechanisms linking periodontal diseases to cardiovascular diseases. *J Clin Periodontol* **40**: S51–S69.

Schulz, G.E. (2000) beta-Barrel membrane proteins. *Curr Opin Struct Biol* **10**: 443–7.

Schulz, G.E. (2002) The structure of bacterial outer membrane proteins. *Biochim Biophys Acta* **1565**: 308–17.

Schwalm, J., Mahoney, T.F., Soltes, G.R., and Silhavy, T.J. (2013) Role for Skp in LptD assembly in *Escherichia coli. J Bacteriol* **195**: 3734–3742.

Seddon, A.M., Curnow, P., and Booth, P.J. (2004) Membrane proteins, lipids and detergents: Not just a soap opera. *Biochim Biophys Acta - Biomembr* **1666**: 105–117.

Sedlacek, M.J., and Walker, C. (2007) Antibiotic resistance in an in vitro subgingival biofilm model. *Oral Microbiol Immunol* **22**: 333–339.

Seers, C. a, Slakeski, N., Veith, P.D., Nikolof, T., Chen, Y.-Y., Dashper, S.G., and Reynolds, E.C. (2006) The RgpB C-terminal domain has a role in attachment of RgpB to the outer membrane and belongs to a novel C-terminal-domain family found in *Porphyromonas gingivalis*. *J Bacteriol* **188**: 6376–86.

Serino, L., Nesta, B., Leuzzi, R., Fontana, M.R., Monaci, E., Mocca, B.T., *et al.* (2007) Identification of a new OmpA-like protein in *Neisseria gonorrhoeae* involved in the binding to human epithelial cells and *in vivo* colonization. *Mol Microbiol* **64**: 1391–403.

Settem, R.P., El-Hassan, A.T., Honma, K., Stafford, G.P., and Sharma, A. (2012) *Fusobacterium nucleatum* and *Tannerella forsythia* Induce Synergistic Alveolar Bone Loss in a Mouse Periodontitis Model. *Infect Immun* **80**: 2436–2443.

Sharma, A. (2010) Virulence mechanisms of *Tannerella forsythia*. *Periodontol 2000* **54**: 106–16.

Sharma, A., Honma, K., Evans, R.T., Hruby, D.E., and Genco, R.J. (2001) Oral Immunization with Recombinant *Streptococcus gordonii* Expressing *Porphyromonas gingivali*s FimA Domains. **69**: 2928–2934.

Sharma, A., Inagaki, S., Sigurdson, W., and Kuramitsu, H.K. (2005) Synergy between *Tannerella forsythia* and *Fusobacterium nucleatum* in biofilm formation. *Oral Microbiol Immunol* **20**: 39–42.

Sharma, A., Sojar, H.T., Glurich, I., Honma, K., Kuramitsu, H.K., and Genco, R.J. (1998) Cloning, expression, and sequencing of a cell surface antigen containing a leucine-rich repeat motif from *Bacteroides forsythus* ATCC 43037. *Infect Immun* **66**: 5703–10.

Shin, S., Lu, G., Cai, M., and Kim, K.-S. (2005) *Escherichia coli* outer membrane protein A adheres to human brain microvascular endothelial cells. *Biochem Biophys Res Commun* **330**: 1199–1204.

Shiraki, K., Kudou, M., Fujiwara, S., Imanaka, T., and Takagi, M. (2002) Biophysical effect of amino acids on the prevention of protein aggregation. *J Biochem* **132**: 591–595.

Shoji, M., Naito, M., Yukitake, H., Sato, K., Sakai, E., Ohara, N., and Nakayama, K. (2004) The major structural components of two cell surface filaments of *Porphyromonas gingivalis* are matured through lipoprotein precursors. *Mol Microbiol* **52**: 1513–25.

Shoji, M., Ratnayake, D.B., Shi, Y., Kadowaki, T., Yamamoto, K., Yoshimura, F., *et al.* (2002) Construction and characterization of a nonpigmented mutant of *Porphyromonas gingivalis*: cell surface polysaccharide as an anchorage for gingipains. *Microbiology* **148**: 1183–91.

Simpson, W., Olczak, T., and Genco, C. A. (2000) Characterization and expression of HmuR, a TonB-dependent hemoglobin receptor of *Porphyromonas gingivalis. J Bacteriol* **182**: 5737–5748.

Singh, A., Wyant, T., Anaya-Bergman, C., Aduse-Opoku, J., Brunner, J., Laine, M.L., *et al.* (2011) The capsule of *Porphyromonas gingivalis* leads to a reduction in the host inflammatory response, evasion of phagocytosis, and increase in virulence. *Infect Immun* **79**: 4533–42.

Sklar, J.G., Wu, T., Kahne, D., and Silhavy, T.J. (2007) Defining the roles of the periplasmic chaperones SurA, Skp, and DegP in *Escherichia coli. Genes Dev* **21**: 2473–2484.

Skorko-Glonek, J., Laskowska, E., Sobiecka-Szkatula, A., and Lipinska, B. (2007) Characterization of the chaperone-like activity of HtrA (DegP) protein from *Escherichia coli* under the conditions of heat shock. *Arch Biochem Biophys* **464**: 80–89.

Slots, J., and Gibbons, R.J. (1978) Attachment of *Bacteroides melaninogenicus* subsp. *asaccharolyticus* to oral surfaces and its possible role in colonization of the mouth and of periodontal pockets. *Infect Immun* **19**: 254–264.

Smith, C.J. (1995) Genetic transformation of *Bacteroides spp.* using electroporation. *Methods Mol Biol* **47**: 161–169.

Smith, D.B., Davern, K.M., Board, P.G., Tiu, W.U., Garcia, E.G., and Mitchell, G.F. (1986) Mr 26,000 antigen of *Schistosoma japonicum* recognized by resistant WEHI 129/J mice is a parasite glutathione S-transferase. *Proc Natl Acad Sci U S A* **83**: 8703–8707.

Smith, D.B., and Johnson, K.S. (1988) Single-step purification of polypeptides expressed in *Escherichia coli* as fusions with glutathione S-transferase. *Gene* **67**: 31–40.

Smith, S.G.J., Mahon, V., Lambert, M. a, and Fagan, R.P. (2007) A molecular Swiss army knife: OmpA structure, function and expression. *FEMS Microbiol Lett* **273**: 1–11.

Socransky, S.S., Haffajee, A D., Cugini, M. a, Smith, C., and Kent, R.L. (1998) Microbial complexes in subgingival plaque. *J Clin Periodontol* **25**: 134–44.

Sojar, H.T., and Smith, D.F. (2012) *Porphyromonas gingivalis* fimbriae carbohydrate specificity assessment by glycomics. *FEMS Immunol Med Microbiol* **66**: 83–87.

Song, H., Bélanger, M., Whitlock, J., Kozarov, E., and Progulske-Fox, A. (2005) Hemagglutinin B Is Involved in the Adherence of *Porphyromonas gingivalis* to Human Coronary Artery Endothelial Cells. *Infect Immun* **73**: 7267–7273.

Song, H., Bélanger, M., Whitlock, J., Kozarov, E., Progulske-fox, A., and Be, M. (2005) Hemagglutinin B Is Involved in the Adherence of Porphyromonas gingivalis to Human Coronary Artery Endothelial Cells. *Society* **73**: 7267–7273.

Song, T., Mika, F., Lindmark, B., Liu, Z., Schild, S., Bishop, A., *et al.* (2008) A new *Vibrio cholerae* sRNA modulates colonization and affects release of outer membrane vesicles. *Mol Microbiol* **70**: 100–111.

Sonntag, I., Schwarz, H., and Hirota, Y. (1978) Cell envelope and shape of *Escherichia coli* : multiple mutants missing the outer membrane lipoprotein and other major outer membrane proteins. *J Bacteriol* **136**: 280–285.

Soong, G., Muir, A., Gomez, M.I., Waks, J., Reddy, B., Planet, P., *et al.* (2006) Bacterial neuraminidase facilitates mucosal infection by participating in biofilm production. *J Clin Invest* **116**: 2297–2305.

Sørensen, H.P., and Mortensen, K.K. (2005) Soluble expression of recombinant proteins in the cytoplasm of *Escherichia coli*. *Microb Cell Fact* **4**: 1.

Soskolne, W. a, and Klinger, a (2001) The relationship between periodontal diseases and diabetes: an overview. *Ann Periodontol* **6**: 91–8.

Spiess, C., Beil, A., and Ehrmann, M. (1999) A Temperature-Dependent Switch from Chaperone to Protease in a Widely Conserved Heat Shock Protein. *Cell* **97**: 339–347.

Stafford, P., Higham, J., Pinnock, A., Murdoch, C., Douglas, I., Stafford, G., and Lambert, D. (2013) Gingipain-dependent degradation of mTOR pathway proteins by the periodontal pathogen Porphyromonas gingivalis during invasion. *Mol Oral Microbiol* Online Article Only.

Steenbergen, T.J., Winkelhoff, A.J., and Graaff, J.D.E. (1984) Pathogenic synergy : mixed infections in the oral cavity. **50**: 789–798.

Strauch, K.L., and Beckwith, J. (1988) An *Escherichia coli* mutation preventing degradation of abnormal periplasmic proteins. *Proc Natl Acad Sci U S A* **85**: 1576–80.

Strober, W., Fuss, I., and Mannon, P. (2007) Science in medicine: The fundamental basis of inflammatory bowel disease. *J Clin Invest* **117**: 514–21.

Surrey, T., and Jähnig, F. (1995) Kinetics of Folding and Membrane Insertion of a β-Barrel Membrane Protein. *J Biol Chem* **270**: 28199–28203.

Surrey, T., Schmid, A., and Jähnig, F. (1996) Folding and Membrane Insertion of the Trimeric β-Barrel Protein OmpF. *Biochemistry* **35**: 2283–2288.

Sutherland, I.W. (2001) The biofilm matrix – an immobilized but dynamic microbial environment. *Trends Microbiol* **9**: 222–227.

Suwannakul, S., Stafford, G.P., Whawell, S. a, and Douglas, C.W.I. (2010) Identification of bistable populations of Porphyromonas gingivalis that differ in epithelial cell invasion. *Microbiology* **156**: 3052–64.

Suzuki, N., Yoneda, M., Hirofuji, T., Suzuki, N., Yoneda, M., and Hirofuji, T. (2013) Mixed Red-Complex Bacterial Infection in Periodontitis. *Int J Dent* **2013**: 1–6.

Syed, S.A., Mikinen, K.K., Mikinen, P.-L., Chen, C.-Y., and Muhammad, Z. (1993) Proteolytic and oxidoreductase activity of *Treponema denticola* ATCC 35405 grown in an aerobic and anaerobic gaseous environment. *MicrobioL Paris* **144**: 317–326.

Taguchi, Y., Sato, K., Yukitake, H., Inoue, T., Nakayama, M., Naito, M., *et al.* (2016) Involvement of an Skp-Like Protein, PGN_0300, in the Type IX Secretion System of Porphyromonas gingivalis. *Infect Immun* **84**: 230–240.

Takemoto, T., Kurihara, H., and Dahlen, G. (1997) Characterization of *Bacteroides forsythus* isolates. *J Clin Microbiol* **35**: 1378–81.

Tanner, A.C.R., and Izard, J. (2006) *Tannerella forsythia*, a periodontal pathogen entering the genomic era. *Periodontol 2000* **42**: 88–113.

Tapley, T.L., Körner, J.L., Barge, M.T., Hupfeld, J., Schauerte, J. a, Gafni, A., *et al.* (2009) Structural plasticity of an acid-activated chaperone allows promiscuous substrate binding. *Proc Natl Acad Sci U S A* **106**: 5557–5562.

Taylor, G., and Borgnakke, W. (2008) Periodontal disease: associations with diabetes, glycemic control and complications. *Oral Dis* **14**: 191–203.

Taylor, G.W. (2001) Bidirectional interrelationships between diabetes and periodontal diseases: an epidemiologic perspective. *Ann Periodontol* **6**: 99–112.

Telgi, R.L., Tandon, V., Tangade, P.S., Tirth, A., Kumar, S., and Yadav, V. (2013) Efficacy of nonsurgical periodontal therapy on glycaemic control in type II diabetic patients: a randomized controlled clinical trial. *J Periodontal Implant Sci* **43**: 177–82.

Teng, C.-H., Xie, Y., Shin, S., Cello, F. Di, Paul-Satyaseela, M., Cai, M., and Kim, K.S. (2006) Effects of ompA deletion on expression of type 1 fimbriae in *Escherichia coli* K1 strain RS218 and on the association of *E. coli* with human brain microvascular endothelial cells. *Infect Immun* **74**: 5609–16.

Terpe, K. (2006) Overview of bacterial expression systems for heterologous protein production: From molecular and biochemical fundamentals to commercial systems. *Appl Microbiol Biotechnol* **72**: 211–222.

Tezal, M., Grossi, S.G., Ho, A.W., and Genco, R.J. (2004) Alcohol consumption and periodontal disease. The Third National Health and Nutrition Examination Survey. *J Clin Periodontol* **31**: 484–8.

Theilade, E. (1986) The non-specific theory in microbial etiology of inflammatory peridontal diseases. *J Clin Periodontol* **13**: 905–911.

Theilade, E., Wright, W.H., Jensen, S.B., and Loe, H. (1966) Experimental gingivitis in man. *J Periodontal Res* **1**: 1–13.

Thome, B.M., and Müller, M. (1991) Skp is a periplasmic *Escherichia coli* protein requiring SecA and SecY for export. *Mol Microbiol* **5**: 2815–21.

Tokuda, M., Duncan, M., Cho, M.I., and Kuramitsu, H.K. (1996) Role of *Porphyromonas gingivalis* protease activity in colonization of oral surfaces. *Infect Immun* **64**: 4067–4073.

Tracey, K.J. (2002) The inflammatory reflex. *Nature* **420**: 853–859.

Travis, J., Pike, R., Imamura, T., and Potempa, J. (1997) *Porphyromons gingivalis* proteinases as virulence factors in the development of periodontitis. *J Periodontal Res* **32**: 120–125.

Tribble, G.D., and Lamont, R.J. (2010) Bacterial invasion of epithelial cells and spreading in periodontal tissue. *Periodontol 2000* **52**: 68–83.

Tribble, G.D., Rigney, T.W., Dao, D. V, Wong, C.T., Kerr, J.E., Taylor, B.E., Pacha, S., *et al.* (2012) Natural Competence Is a Major Mechanism for Horizontal DNA Transfer in the Oral Pathogen Porphyromonas gingivalis. **3**: 1–8.

Tsumoto, K., Arakawa, T., and Chen, L. (2010) Step-wise refolding of recombinant proteins. *Curr Pharm Biotechnol* **11**: 285–8.

Tsumoto, K., Ejima, D., Kumagai, I., and Arakawa, T. (2003) Practical considerations in refolding proteins from inclusion bodies. *Protein Expr Purif* **28**: 1–8.

Valle, J., Latasa, C., Gil, C., Toledo-Arana, A., Solano, C., Penadés, J.R., and Lasa, I. (2012) Bap, a Biofilm Matrix Protein of *Staphylococcus aureus* Prevents Cellular Internalization through Binding to GP96 Host Receptor. *PLoS Pathog* **8**: 1-15.

Vanterpool, E., Roy, F., Zhan, W., Sheets, S.M., Sangberg, L., and Fletcher, H.M. (2006) VimA is part of the maturation pathway for the major gingipains of *Porphyromonas gingivalis* W83. *Microbiology* **152**: 3383–9.

Vasina, J. A (1997) Expression of Aggregation-Prone Recombinant Proteins at Low Temperatures : A Comparative Study of the *Escherichia coli* cspA and tac Promoter Systems. **218**: 211–218.

Veith, P.D., Brien-simpson, N.M.O., Tan, Y., Djatmiko, D.C., Dashper, S.G., and Reynolds, E.C. (2009) Outer Membrane Proteome and Antigens of *Tannerella forsythia* research articles. 4279–4292.

Veith, P.D., Muhammad, N.A.N., Dashper, S.G., Likic, V.A., Gorasia, D.G., Chen, D., *et al.* (2013) Protein Substrates of a Novel Secretion System Are Numerous in the Bacteroidetes Phylum and Have in Common a Cleavable C-Terminal Secretion Signal, Extensive Post-Translational Modification, and Cell- Surface Attachment. *J Proteome Res* **12**(1):4449-61.

Veith, P.D., Talbo, G.H., Slakeski, N., and Reynolds, E.C. (2001) Identification of a novel heterodimeric outer membrane protein of Porphyromonas gingivalis by two-dimensional gel electrophoresis and peptide mass fingerprinting. *Eur J Biochem* **268**: 4748–57.

Velsko, I.M., Chukkapalli, S.S., Rivera, M.F., Lee, J.-Y., Chen, H., Zheng, D., *et al.* (2014) Active invasion of oral and aortic tissues by *Porphyromonas gingivalis* in mice causally links periodontitis and atherosclerosis. *PLoS One* **9**: e97811.

Vernal, R., León, R., Silva, A., Winkelhoff, A.J. van, Garcia-Sanz, J. a, and Sanz, M. (2009) Differential cytokine expression by human dendritic cells in response to different *Porphyromonas gingivalis* capsular serotypes. *J Clin Periodontol* **36**: 823–9.

Vicki Caligur (Sigma Aldrich) (2008). *Detergent Properties and Applications* (online). Available at: http://www.sigmaaldrich.com/technical-documents/articles/biofiles/detergent-properties.html.

Visser, M.B., and Ellen, R.P. (2011) New insights into the emerging role of oral spirochaetes in periodontal disease. *Clin Microbiol Infect* **17**: 502–512.

Voulhoux, R., Bos, M.P., Geurtsen, J., Mols, M., and Tommassen, J. (2003) Role of a highly conserved bacterial protein in outer membrane protein assembly. *Science* **299**: 262–265.

Walther, D.M., Rapaport, D., and Tommassen, J. (2009) Biogenesis of beta-barrel membrane proteins in bacteria and eukaryotes: evolutionary conservation and divergence. *Cell Mol Life Sci* **66**: 2789–804.

Walton, T. a, Sandoval, C.M., Fowler, C.A., Pardi, A., and Sousa, M.C. (2009) The cavity-chaperone Skp protects its substrate from aggregation but allows independent folding of substrate domains. *Proc Natl Acad Sci U S A* **106**: 1772–7.

Walton, T. a., and Sousa, M.C. (2004) Crystal structure of Skp, a prefoldin-like chaperone that protects soluble and membrane proteins from aggregation. *Mol Cell* **15**: 367–374.

Wang, X., Buhimschi, C.S., Temoin, S., Bhandari, V., Han, Y.W., and Buhimschi, I.A. (2013) Comparative Microbial Analysis of Paired Amniotic Fluid and Cord Blood from Pregnancies Complicated by Preterm Birth and Early-Onset Neonatal Sepsis. *PLoS One* 8(2): 1-8

Wang, Y. (2002) The Function of OmpA in *Escherichia coli. Biochem Biophys Res Commun* **292**: 396–401.

Wang, Y., Li, M., Stadler, S., Correll, S., Li, P., Wang, D., *et al.* (2009) Histone hypercitrullination mediates chromatin decondensation and neutrophil extracellular trap formation. *J Cell Biol* **184**: 205–13.

Watanabe, K., Yamaji, Y., and Umemoto, T. (1992) Correlation between cell-adherent activity and surface structure in *Porphyromonas gingivalis*. *Oral Microbiol Immunol* **7**: 357–363.

Webb, C.T., Heinz, E., and Lithgow, T. (2012) Evolution of the β-barrel assembly machinery. *Trends Microbiol* **20**: 612–620.

Webb, J.N., Webb, S.D., Cleland, J.L., Carpenter, J.F., and Randolph, T.W. (2001) Partial molar volume, surface area, and hydration changes for equilibrium unfolding and formation of aggregation transition state: High-pressure and cosolute studies on recombinant human IFN-γ. *Proc Natl Acad Sci* **98**: 7259–7264.

Wegner, N., Lundberg, K., Kinloch, A., Fisher, B., Malmström, V., Feldmann, M., and Venables, P.J. (2010) Autoimmunity to specific citrullinated proteins gives the first clues to the etiology of rheumatoid arthritis. *Immunol Rev* **233**: 34–54.

Weinberg, a, Belton, C.M., Park, Y., and Lamont, R.J. (1997) Role of fimbriae in *Porphyromonas gingivalis* invasion of gingival epithelial cells. *Infect Immun* **65**: 313–6.

Weiss, B.L., Wu, Y., Schwank, J.J., Tolwinski, N.S., and Aksoy, S. (2008) An insect symbiosis is influenced by bacterium-specific polymorphisms in outer-membrane protein A. *Proc Natl Acad Sci U S A* **105**: 15088–93.

Whitmore, S.E., and Lamont, R.J. (2014) Oral Bacteria and Cancer. *PLOS Pathog* **10**: 1–3.

Wimley, W.C. (2003) The versatile β-barrel membrane protein. *Curr Opin Struct Biol* **13**: 404–411.

Wu, T., Malinverni, J., Ruiz, N., Kim, S., Silhavy, T.J., and Kahne, D. (2005) Identification of a multicomponent complex required for outer membrane biogenesis in *Escherichia coli*. *Cell* **121**: 235–245.

Wyss, C., Moter, a., Choi, B.K., Dewhirst, F.E., Xue, Y., Schüpbach, P., *et al.* (2004) *Treponema putidum* sp. *nov.,* a medium-sized proteolytic spirochaete isolated from lesions

of human periodontitis and acute necrotizing ulcerative gingivitis. *Int J Syst Evol Microbiol* **54**: 1117–1122.

Xavier, R.J., and Podolsky, D.K. (2007) Unravelling the pathogenesis of inflammatory bowel disease. *Nature* **448**: 427–434.

Xia, Q., Wang, T., Taub, F., Park, Y., Capestany, C. a, Lamont, R.J., and Hackett, M. (2007) Quantitative proteomics of intracellular *Porphyromonas gingivalis*. *Proteomics* **7**: 4323–37.

Ximenez-Fyvie, L.A., Haffajee, A.D., and Socransky, S.S. (2000) Comparison of the microbiota of supra- and subgingival plaque in health and periodontitis. *J Clin Periodontol* **27**: 648–657.

Yamada, M., and Geiger, B. (1997) Molecular interactions in cell adhesion complexes. *Curr Opin Cell Biol* **9**: 76–85.

Yamada, M., Ikegami, A., and Kuramitsu, H.K. (2005) Synergistic biofilm formation by *Treponema denticola* and *Porphyromonas gingivalis*. *FEMS Microbiol Lett* **250**: 271–277.

Yilmaz, O. (2003) Gingival epithelial cell signalling and cytoskeletal responses to *Porphyromonas gingivalis* invasion. *Microbiology* **149**: 2417–2426.

Yilmaz, O. (2008) The chronicles of *Porphyromonas gingivalis:* the microbium, the human oral epithelium and their interplay. *Microbiology* **154**: 2897–2903.

Yilmaz, O., Watanabe, K., and Lamont, R.J. (2002) Involvement of integrins in fimbriae-mediated binding and invasion by *Porphyromonas gingivalis. Cell Microbiol* **4**: 305–14.

Yoshimoto, H., Takahashi, Y., Hamada, N., and Umemoto, T. (1993) Genetic transformation of *Porphyromonas gingivalis* by electroporation. *Oral Microbiol Immunol* **8**: 208–12.

Yoshimura, F., Murakami, Y., Nishikawa, K., Hasegawa, Y., and Surface, K.S. (2009) Surface components of *Porphyromonas gingivalis*. *J Periodontal Res* **44**(1): 1–12.

Yoshimura, F., Takahashi, K., Nodasaka, Y., and Suzuki, T. (1984) Purification and characterization of a novel type of fimbriae from the oral anaerobe *Bacteroides gingivalis*. *J Bacteriol* **160**: 949–57.

Yoshimura, F., Watanabe, K., Takasawa, T., Kawanami, M., and Kato, H. (1989) Purification and properties of a 75-kilodalton major protein, an immunodominant surface antigen, from the oral anaerobe *Bacteroides gingivalis. Infect Immun* **57**: 3646–52.

Zhang, D.-F., Li, H., Lin, X.-M., Wang, S.-Y., and Peng, X.-X. (2011) Characterization of outer membrane proteins of *Escherichia coli* in response to phenol stress. *Curr Microbiol* **62**: 777–83.

Zhang, T., Hashizume, T., Kurita-Ochiai, T., and Yamamoto, M. (2009) Sublingual vaccination with outer membrane protein of *Porphyromonas gingivalis* and Flt3 ligand elicits protective immunity in the oral cavity. *Biochem Biophys Res Commun* **390**(3): 937-41.

Zilm, P.S., Bagley, C.J., Rogers, A.H., Milne, I.R., and Gully, N.J. (2007) The proteomic profile of *Fusobacterium nucleatum* is regulated by growth pH. *Microbiology* **153**: 148–59.

Zoueva, O.P., Bailly, J.E., Nicholls, R., and Brown, E.G. (2002) Aggregation of influenza virus ribonucleocapsids at low pH. *Virus Res* **85**: 141–149.

Appendix

Appendix I

Sequence of Δ*ompA2* + pT-COW - *A2* complement insert:

GGATCTGCTTACGAAGTAATTATGCATACAGGGAAAAAATTACCGGAGAATCTTCTTTGCAGCTCTGCAGATACA
CCACATGAAAAGCTCTACGAGATTCGCCAAAGGAATTATTTCTCCCAAGCGTTTTATAATAATACTCTATAATAAA
AAGACTGTTATTTGTTTTTGATCAATGGCTTTTTGAGAGGAGAACTAACGCTTTTCTCTCCTAATTATTTGGCTGT
TCAAATTTCTTACATTACATTTGTGTAGCGAATAGGCTATTGGTAAACGTATAAAAATACACTTAGAAAAGTAAAA
CTATGAAAGCTAAATCTTTATTATTAGCACTTGCGGGTCTCGCATGCACATTCAGTGCAACAGCCCAAGAAGCTAC
TACACAGAACAAAGCAGGGATGCACACCGCATTCCAACGTGATAAGGCCTCCGATCATTGGTTCATTGACATTGCA
GGTGGAGCAGGTATGGCTCTCTCGGGATGGAATAATGATGTAGACTTTGTAGATCGTCTAAGTATCGTTCCTACTT
TCGGTATCGGTAAATGGCATGAGCCTTATTTCGGTACTCGTCTCCAATTCACAGGATTCGACATCTATGGATTCCC
GCAAGGGAGCAAGGAGCGTAACCACAATTACTTTGGAAACGCCCACCTTGACTTCATGTTCGATCTGACGAACTAT
TTCGGTGTATACCGTCCCAATCGTGTCTTCCATATCATCCCATGGGCAGGTATAGGATTTGGTTATAAATTCCATA
GCGAAAACGCCAATGGTGAAAAAGTAGGAAGTAAAGATGATATGACCGGAACAGTTAATGTCGGTTTGATGCTGAA
ATTCCGCCTATCAAGAGTCGTAGACTTCAATATTGAAGGACAAGCTTTTGCCGGAAAGATGAACTTTATCGGGACA
AAGAGAGGAAAAGCAGACTTCCCTGTAATGGCTACAGCAGGTCTAACGTTCAACCTTGGCAAGACAGAGTGGACAG
AAATTGTTCCTATGGACTATGCTTTGGTCAATGACCTGAACAACCAAATCAACTCACTTCGCGGTCAAGTGGAAGA
GTTGAGCCGTCGTCCTGTTTCATGCCCTGAATGCCCTGAGCCTACACAGCCTACAGTTACTCGTGTAGTCGTTGAC
AATGTGGTTTACTTCCGTATCAATAGTGCAAAGATTGATCGTAATCAAGAAATCAATGTTTACAATACAGCTGAAT
ATGCGAAGACCAACAACGCACCGATCAAGGTAGTAGGTTACGCTGACGAAAAAACCGGTACTGCGGCCTATAACAT
GAAGCTTTCAGAGCGTCGTGCAAAAGCGGTAGCCAAGATGCTTGAAAAGTATGGTGTTTCTGCGGATCGCATTACA
ATTGAATGGAAGGGCTCATCAGAGCAAATCTATGAAGAGAACGCTTGGAATCGTATTGTAGTAATGACTGCAGCGG
AATAAGTCGAC

The above details the sequence used to clone into pT-COW plasmid to generate a complement Δ*ompA2* strain. Highlighted in teal are the two restriction enzyme sites (*Bam*HI and *Sal*I respectively) used to insert the sequence into the pT-COW plasmid. The grey highlighted section displays the 300 bp sequence upstream of the *ompA1* gene which encodes the *ompA* operon promoter, whereas the section without highlighting denotes the *ompA2* gene used to complement the Δ*ompA2* mutant *in trans*.